Synthesis, Catalysis and Stoichiometric Reactivity of Mo Imido Complexes

Nicolas A. McLeod

BSc. in Chemistry

Chemistry

Thesis submitted to the Faculty of Graduate Studies

In the partial fulfillment of the requirements

For the MSc. degree in chemistry

Chemistry Department

Faculty of Mathematics and Science

Brock University

St. Catharines, Ontario

Abstract

The current thesis describes the syntheses, catalytic reactivity and mechanistic investigations of novel Mo(IV) and Mo(VI) imido systems. Attempts at preparing mixed bis(imido) Mo(IV) complexes of the type (RN)(R′N)Mo(PMe_3)$_n$ (n = 2 or 3) derived from the mono(imido) complexes (RN)Mo(PMe_3)$_3$(X_2) (R = ^{t}Bu (**1**) or Ar (**2**); X = Cl_2 or HCl, Ar=2,6-^{i}Pr$_2$C$_6$H$_3$) are also described. The addition of lithiated silylamides to **1** or **2** results in the unexpected formation of the C-H activated cyclometallated complexes (RN)Mo(PMe_3)$_2$(η^2-CH_2PMe_2)(X) (R = Ar, X = H (**3**); R = ^{t}Bu, X = Cl (**4**)). Complexes **3** and **4** were used in the activation of R′E-H bonds (E = Si, B, C, O, P; R′ = alkyl or aryl), which typically give products of addition across the M-C bond of the type (RN)Mo(PMe_3)$_3$(ER′)(X) (**4**). In the case of 2,6-dimethylphenol, subsequent heating of **4** (R = Ar, R′ = 2,6-$Me_2C_6H_3$, E = O) to 50 °C results in C-H activation to give the cyclometallated complex (ArN)Mo(PMe_3)$_3$(κ^2-*O*,*C*-OPh(Me)CH_2) (**5**). An alternative approach was developed in synthesizing the mixed imido complex (ArN)(^{t}BuN)Mo(PMe_3)(η^2-C_2H_4) (**6**) through EtMgBr reduction of (ArN)(^{t}BuN)$MoCl_2$(DME) in the presence of PMe_3. Complex **6** reacts with various hydro- and chlorosilanes to give β-agostic silylamido complexes and in one case, when Me_2SiHCl is the silane, leads to the silanimine complex (^{t}BuN)Mo(η^2-$SiMe_2$-NAr)(Et)(η^2-C_2H_4) (**7**).

Mechanistic studies on the formation of the Mo(VI) tris(silyl) complex (^{t}BuN)Mo(SiHPh)(H){(μ-N^{t}Bu)(SiHPh)}(PMe_3)$_2$ (**8**) were done from the addition of three equivalents of $PhSiH_3$ to (^{t}BuN)Mo(PMe_3)(η^2-C_2H_4), resulting in identification of β- and γ-agostic SiH$\cdots$Mo intermediates. The reactivity of complex **8** towards ethylene and nitriles was studied. In both cases coupling of unsaturated substrates with the Mo-Si bond of the metalacycle

was observed. In the case of nitriles, insertion into the 4-membered disilaazamolybdacycle results in complexes of the type (^{t}BuN)Mo{(κ^2-*Si*,*C*-SiHPh-N^{t}Bu-SiHPh-N=C(R)}(PMe_3)$_2$.

Catalytic hydrosilylation of carbonyls mediated by the β-agostic silylamido complex (ArN)$_2$Mo(η^3-N^{t}Bu-SiMe$_2$-H)(H) (**9**) was investigated. Stoichiometric reactions with organic substrates showed that catalysis with **9** does not proceed via the conventional insertion of substrate into the Mo-H bond.

.

Acknowledgements

I would like to first off acknowledge my supervisor, Dr. Georgii Nikonov for keeping me on-board and in-check for the last five years. I am grateful for the opportunity you gave me five years ago as an undergrad in allowing me to be a part of your group. I have gained an incredible amount of knowledge and life experience because of this and I thank you.

To my committee members at Brock University, Dr. Melanie Pilkington and Dr. Art van der Est, I appreciate your honesty and ability to keep me on track during the course of my work. I am grateful to Dr. Stuart Rothstein and Dr. Tony Yan for their assistance in the administrative aspect of things. To John and Jordan Vandenhoff of the glassblowing shop and both young and old Steve at the Machine Shop, I appreciate all the work you guys did for us especially during the hectic times during the move.

I have to thank and praise Razvan Simionescu (NMR technician) who has been instrumental in the culmination of this thesis. Thank you for the time and effort you devoted to instructing me how to better understand the world of NMR. I would also like to thank our crystallographer from the University of Ottawa; Dr. Ilya Korobkov.

I am particularly grateful to all my colleagues and friends at Brock that I have been privileged to work with and meet including: Dr. Andrey Khalimon, Dr. Dmitry Gutsulyuk, Dr. Oleg Shirobokov, Phil Farha, Sun Hwa (Tori) Lee (Toreelee! *Italian version*), Dr. Ksenyia Revunova, Sergey Vischenko, Terry Chu, Van Hung Mai, Courtney Boone, Emma Gavey, Dr. Roger Gumbau-Brisa, Drew Marquadrt, Vimal and Joshni, Zemane Bekele, Iraj, Shufen Xu, Michelle Eisner and if I missed anyone I apologize.

I have to thank all of my friends outside of school who have been patient with me all these years; you know who you are! I must thank Julie who has kept me sane and grounded all these years. I would also like to thank my family for their understanding and sacrifices throughout this time.

Table of Contents

Abbreviations

Å	Angstrom
Ar	2,6-diisopropyl phenyl
Ar′	2,6-dimethylphenyl
Ar″	3,5-dimethylphenyl
atm	atmosphere (1 atm = 1 bar, 760 mmHg)
b	broad (NMR)
Bn	benzyl
^{t}Bu	*tert*-butyl
cat.	catalyst
Cat	catechol
°C	degrees celsius
3c-2e	three centre - two electron bonding
Chapt.	chapter
COD	cyclooctadiene
COSY	Correlation Spectroscopy
Cp	η^5-cyclopentadiene (C_5H_5)
Cp′	η^5-C_5H_4Me
Cp*	η^5-C_5Me_5
Cy	Cyclohexyl
d	doublet (NMR)
DCD	Dewar-Chatt-Duncanson model
DCM	dichloromethane
DFT	density functional theory
DME	1,2-dimethoxyethane
DMSO	dimethyk sulphoxide
Et	ethyl
exc.	excess
h	hour
$\Delta H^{‡}$	enthalpy of activtaion
hal	halogen
HOMO	highest occupied molecular orbital
hv	light
Hz	Hertz
HSQC	Heteronuclear Single Quantum Coherence
HSQC JC	Heteronuclear Single Quantum Coherence J-Coupled
IHI	Interligand Hypervalent Interaction

J	coupling constant (NMR)
IR	infrared spectroscopy
KIE	Kinetic isotope effect
L_n	Ligand
LUMO	Lowest unoccupied molecular orbital
M	Metal centre
m	*meta-*
m	multiplet (NMR)
Me	methyl
Mes	mesityl
MO	molecular orbital
ND	neutron diffraction
NMR	nuclear magnetic resonance
NOE	nuclear Overhauser effect
o	*ortho-*
OA	oxidative addition
OTf	triflate
p	*para-*
p	pentet (NMR)
Ph	phenyl
PhMe	toluene
PMHS	polymethylhydrosiloxane
^{i}Pr	isopropyl
Py	pyridine
q	quartet
quant.	quantitative
RE	reductive elimination
RT	room temperature
s	singlet (NMR)
sat	satellite (NMR)
sept	septet (NMR)
$\Delta S^{\ddagger}$	entropy of activation
solv.	solvent
t	triplet (NMR)
tert-	tertiary
THF	tetrahydrofuran
TM	transition metal
TMS	trimethylsilyl
TMDS	tetramethyldisiloxane
Tol	tolyl

VT	variable temperature
vt	virtual triplet (NMR)
UV	ultraviolet
δ	chemical shift
Δ	heat

List of Figures

List of Schemes

List of Tables

I. Introduction

The study of non-classical interactions between transition metal centres and Si-H bonds began in the early 1980's despite already being known for about 15 years.[1-3] This is, in part, due to the essential discovery of dihydrogen σ-complexation introduced by Kubas *et al*. in 1984.[4] The use of dihydrogen σ-complexes in the activation of small molecules[5], sparked a resurgence in the silicon field. Nowadays, a wide range of non-classical Si-H interactions are known including silane σ- and agostic complexes[2], interligand hypervalent interactions (IHI)[6] and secondary interactions between a silicon and hydrogen atom or SISHA complexes.[7] Until recently, application of these complexes had been limited to only a few cases. In particular, Berry *et al.*[8] described the transformation of *β*-agostic hydride complex $Cp_2Zr(\eta^3\text{-}N^tBu\text{-}SiMe_2\text{-}H)(H)$ into the silanimine complex $Cp_2Zr(\eta^2\text{-}N^tBu\text{-}SiMe)(PMe_3)$ used for the activation of small molecules.

Interest of the Nikonov group in utilizing similar *β*-agostic silylamido complexes in small molecule activation and catalysis, stemmed from the discovery of a novel type of coupling between the imido group of group 5 metal imido transition metal complexes (i.e. CpM(NR)L, M = Ta, Nb) and the Si-H bond of silanes.[9] Extending this synthetic approach to the isolobal (bis)imido complexes of Mo led to the production of various *β*-agostic silylamido complexes of the type $(RN=)Mo(\eta^3\text{-}NR\text{-}SiR'_2\text{-}H)(Cl)(PMe_3)_2$ where R = 2,6-dimethylphenyl (Ar′), 2,6-diisopropylphenyl (Ar), ^{t}Bu and R′ being dependent on the type of chlorosilane used.[10,11] In particular, the addition of $PhSiH_3$ to the Mo(IV) complex $(ArN)_2Mo(PMe_3)_3$ generated the complex $(ArN)Mo(\eta^3\text{-}NAr\text{-}SiHPh\text{-}H)(SiH_2Ph)(PMe_3)$, used as a catalyst in the hydrosilylation of carbonyls which was shown to go through an important silanimine intermediate.[12] Further reactivity with the trichlorosilane and subsequent derivatization produced two new efficient

catalysts (ArN)Mo(PMe_3)$_3$(H)(Cl)[13,14] and (ArN)Mo(PMe_3)$_3$(SiH_2Ph)(H)[15] in the hydrosilylation and hydroboration of unsaturated substrates.

As part of this ongoing research programme, a section of this thesis will be devoted to the catalytic application and mechanistic investigation of the bis(imido) β-agostic silylamido complex (ArN)$_2$Mo(η^3-N^{t}Bu-$SiMe_2$-H). Alternatively, derivatization of novel mixed imido systems of the type (RN)(R′N)Mo(PMe_3)$_x$ (R ≠ R′; x = 2 or 3) through the reactivity of chloro- and hydrosilanes will also be discussed.

In an attempt to generate these mixed(imido) Mo(IV) phosphine complexes from the dichloride or hydrido chloride precursor (RN)Mo(PMe_3)$_3$(X)(Cl) (X = H or Cl), led to the serendipitous formation of the cyclometallated species (RN)Mo(PMe_3)$_2$(η^2-CH_2PMe_2)(X) (R = Ar, X = H; R = ^{t}Bu, X = Cl). Complexes of this type were tested in the E-H bond (E = Si, C, P, O) activation of various substrates and will be a major focus in this work.

Finally, the addition of excess $PhSiH_3$ and PMe_3 to the Mo(IV) complex (^{t}BuN)$_2$Mo(PMe_3)(L) (L = PMe_3, η^2-C_2H_4) has recently been found to cleanly generate the tris(silyl) complex (^{t}BuN)Mo(SiH_2Ph)(H){(μ-N^{t}Bu)(SiHPh)}(PMe_3)$_2$ featuring a four-membered bis(sila)azamolybdacycle. The final part of this thesis will focus on the mechanism of formation by monitoring this reaction by NMR at low temperature. As well, reactivity studies with organic substrates such as carbonyls, alkenes, alkynes and nitriles will be presented.

The following historical section will describe three major aspects of this thesis including β-agostic silylamido complexes, recent mechanisms of hydrosilylation of carbonyls mediated by Mo complexes and phosphine cyclometallation generating three-membered metallacycles.

II. Historical

II.1 Nonclassical Si-H···M Agostic Interactions in Transition Metal Complexes

Although the concept of non-classical Si-H--M bonds in transition metal complexes was proposed in the late 1960's,[2,3] it was accepted by the chemical community only after the σ-bond coordination of the H_2 ligand to tungsten and molybdenum was established by Kubas in 1984.[4] The coordination complex $[W(CO)_3(P^iPr_3)_2(H_2)]$[4] contains an H_2 ligand bound in a 3-centre 2-electron (3c-2e$^-$) fashion, similar to the trihydrogen cation **II-1**, methonium cation **II-2**, or polyborane compounds **II-3**. Representation of this type of complexation is indicated by an arrow stemming from the σ-bond, e.g. H-H, Si-H etc, and directed to the metal centre as is exemplified in compounds **II-1**, **II-2**, **II-4**, **II-5** and **II-6.** All complexes displaying coordination of σ-bonds will be drawn in this way.[3]

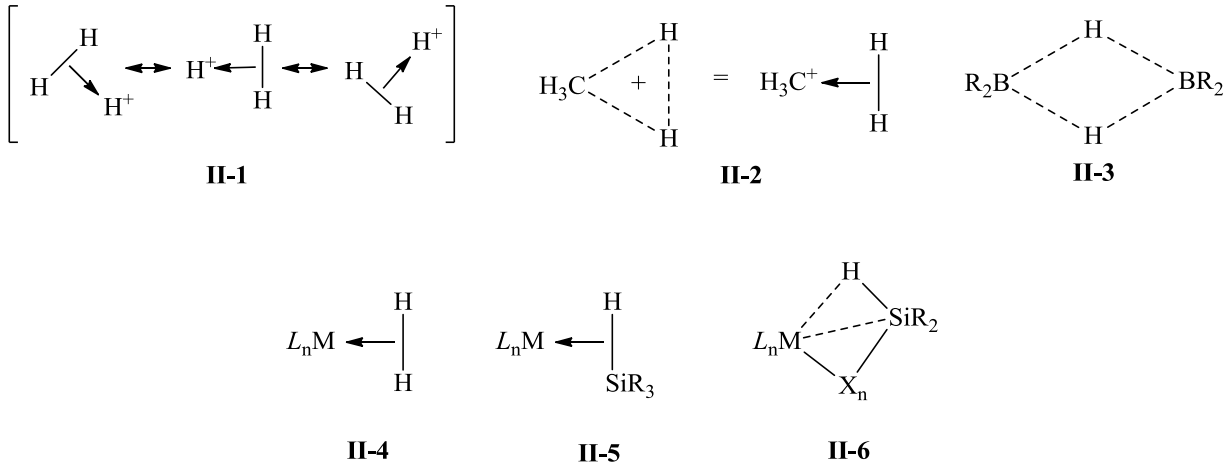

Figure 1- Non-classical 3c-2e- bonding for H_3^+, CH_5^+, polyboranes, H_2 ligands, silane σ-complexes and agostic complexes (X_n= number of atoms between metal and Si).

Non-classical bonding in agostic and silane σ-complexes is best represented by the Dewar-Chatt-Duncanson (DCD) model[5] (Figure 2) initially developed to describe bonding of

olefins to transition metal centres.[1,6] In the case of non-classical silane σ-complexes, the σ(Si-H) bonding orbital of the Si-H bond donates electron density into a vacant metal orbital of the appropriate symmetry. Likewise, metals containing d-electrons (d^n, $n \geq 1$) can donate electron density into a low-lying σ*(Si-H) antibonding orbital. This can be extended to agostic or silane σ-complexes in which the major difference lies in the bridge connecting the silane to the metal. In complex **II-6**, the length of this bridge is dependent on the number of atoms between the metal and the Si atom as well as the nature of the subsituent (Figure 1).

The major feature of silane σ-complexes is their ability to donate and accept electron density, to and from a metal centre (assuming the d configuration is d^n where $n \geq 1$, Figure 2). Silanes of the type R_3SiH typically have weaker Si-H bonds when compared to dihydrogen H_2, with a higher lying σ-bonding orbital and lower σ*-antibonding orbital. This fact makes silanes better σ-donors while at the same time better π-acids in that they are better able to accept electrons from a metal d orbital. Since backdonation is thought to be one of the most important factors determining the extent of Si-H oxidative addition, it is important to understand key factors which would reduce this component and minimize the extent to which the Si-H σ-bond is weakened. These include: i) first row transition metals have contracted d-orbitals and provide poor overlap with the Si-H ligand orbitals; ii) delocalization of d-electrons on strong π-accepting ligands (i.e. CO, CN); iii) the presence of strong σ-accepting ligands (i.e. Cl, Br); and iv) further contraction of d-orbitals due to high oxidation states can create a situation of poor overlap with Si-H orbitals. All these factors lead to diminished back-donation and hence the creation of a residual Si-H interaction. The length of the Si-H bond is also stretched upon coordination to the metal centre. The degree to which the bond is altered depends on many factors, including the nature of substituents on the Si atom. The coupling constant ($^1J_{Si\text{-}H}$) value is inevitably affected

and is decreased in almost every case upon σ-bond coordination compared to the respective free silanes.

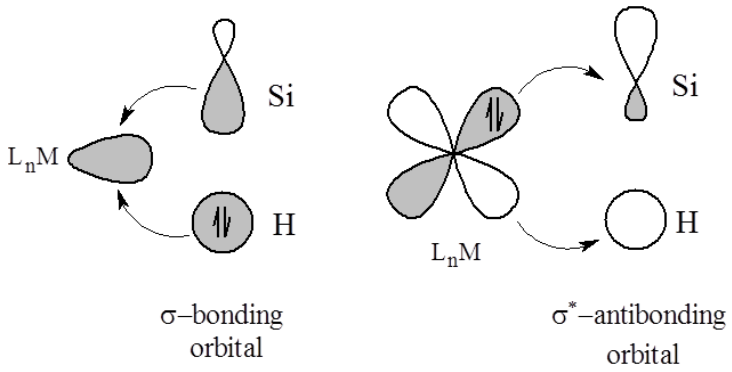

Figure 2- Dewar Chatt Duncanson (DCD) model for silane σ-complexes.

A great deal of work has been done with formal 2 centre - 2 electron bonds of silanes to metal centres ("classical bonds").[2] The oxidative addition pathway shows how a hydrosilane can add to a vacant site on a metal (Scheme 1) usually created by elimination of a small molecule, such as a hydrocarbon, H_2, HX or a two-electron donor (i.e. PR_3, olefin etc).

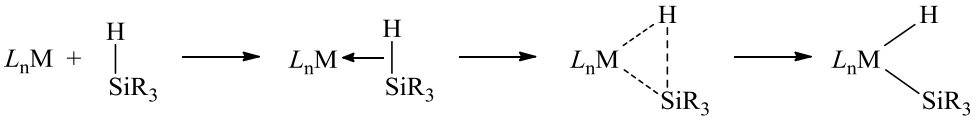

Scheme 1 - Oxidative addition pathway with classical and non-classical bonding shown.

The second step in Scheme 1 shows how the addition of a hydrosilane can become "arrested" or partially oxidatively added to a metal, then continues towards the classical bonding between independent hydride and SiR_3 fragments. Throughout the 1980's, coordination of Si-H bonds to metal complexes gained interest due to their potential in the activation of small molecules. The reactions of metals into silicon-hydrogen bonds are useful due to their role in catalytic hydrosilylation reactions.[16] Given below is an account of the first silane σ-complexes,

and the development of this field throughout the years.

The first structure to exhibit non-classical Si-H bonding was introduced by Graham *et al.* in 1969, with the dinuclear rhenium complex $[Re_2(\mu\text{-}H_2SiMe_2)(CO)_8]$ (**II-7**).[7] The major reason for suggesting the idea of residual Si-H interaction was the observation of an unusual triplet for the ^{1}H NMR signal of the CH_3 group, which displays a $^3J_{H\text{-}H}$ value of 1.5 Hz. Given that the $^3J_{H\text{-}H}$ value in free Me_2SiH_2 is quite small, 4.2 Hz, oxidative addition of Si-H bond to rhenium centres was accepted to result in disappearance of Si-H coupling. Further, X-ray data from the complex revealed a short Si-H distance of 1.57 Å, which was only slightly elongated in comparison with 1.48 Å observed in free hydrosilanes. With this small difference of only 0.09 Å, the value was taken as an additional manifestation of non-classical Si-H σ-bond. Although X-ray structure determination of the hydride positions had a low degree of accuracy, the data was accepted as true.[17,18]

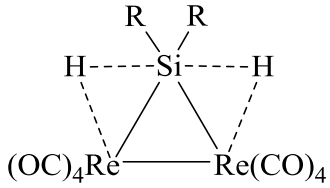

II-7

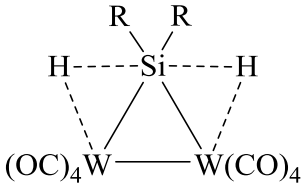

II-8

Soon after Graham's discovery, other complexes exhibiting a similar type of non-classical bonding emerged, including the analogous dinuclear tungsten complex $[W_2(\mu\text{-}H_2SiHMe_2)(CO)_8]$ (**II-8**). In 1971, Jetz and Graham[19] studied the effects of adding hydrosilanes to various metal centres, including Fe, Mn, Cr and Co. The results obtained were regarded as an oxidative addition of the silane across the metal with a hydride in one position and the SiR_3 in another (R= Cl, Ph), as is shown by **II-9**. However, it was later determined that there was an interaction between the Si and H atoms in the manganese complex **II-10**, deduced from analysis of the X-ray diffraction data.

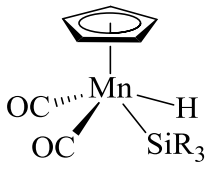

II-9

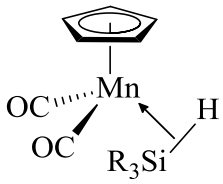

II-10

According to Schubert, in a review article published in 1990[20], identification of a 3c-2e$^-$ non-classical bond for structures similar to **II-10**, could be done by using the chemical, spectroscopic and structural data. The relative intensities of the CO stretches in the IR spectra showed the exclusive formation of a *cis* isomer, meaning the Si and H were in a close proximity to each other. Schubert suggested that if the hydrosilane were to oxidatively add across the metal and a dissociation of H were to occur, the resulting anionic manganese complex should give a *trans* arrangement of the CO ligands due to steric hindrance around the metal. However, it was found (by X-ray crystallography) that only the *cis* isomer was produced suggesting of a non-classical bond between Si-H and Mn.

Many silane σ-complexes have been structurally characterized by use of X-ray crystallography, which allows for determination of an approximate Si-H length.[2] The inaccuracy of X-ray diffraction studies towards the positions of hydrogen atoms in electronically dense environments (i.e. hydrides close to a metal centre)[3], presents a problem when trying to draw a border between a silane σ-complex and a classical hydridosilyl complex.

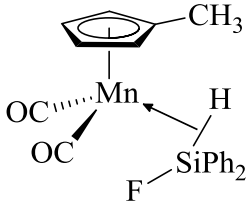

II-11

Neutron diffraction (ND) is much more accurate at determining the location of hydrogen atoms, compared to X-ray analysis. For example, in **II-11**[21] (the first silane σ-complex studied by

ND), the Mn-H distance was found to be to be 1.569(4) Å, located by ND analysis, which correlates well to other manganese ND determined hydride species, in particular $HMn(CO)_5$ (1.601(16) Å).[22] The Si-H distance was found to be 1.802(5) Å, which was less than the calculated non-bonding limit of 3.00 Å.[2] By comparison, the classical complex of $Re(CO)_5(SiH_3)$ showed a Si-H distance of 1.51 Å[23], meaning the slightly elongated Si-H distance (only 30-35 pm longer than covalent SiH bonds) in **II-11** must display some sort of interaction.[24] If a bonding interaction were ignored, the silicon geometry becomes highly distorted.[21]

Although IR, X-ray diffraction and ND analysis are useful when determining structures of silanes, the most powerful and practical method for distinguishing between classical and non-classical bonding in silane σ-complexes is NMR spectroscopy. In 1982, Corriu *et al.*[25] used NMR techniques to measure the coupling constants of complexes similar to **II-10**. They found that coupling constants of Si-H bonds coordinated to metal are higher than typically found values in classical hydridosilyl complexes ($^1J_{Si\text{-}H}$ = 3-10 Hz). Thus, for the complex Cp´Mn(η^2-$HSiPh_3$)$(CO)_2$ (where Cp´= η^5-$C_5H_4CH_3$), it was found that $^1J_{Si\text{-}H}$ was equal to 65-69 Hz, which is much lower than in free hydrosilanes (>180 Hz). This benchmark result enabled Schubert to introduce a minimum value of 10-20 Hz (for $^1J_{Si\text{-}H}$) that could be taken as a non-bonding point between Si and H, in a coordination sphere of a metal.[20] More recent results, including a PES (photo electron spectroscopy) study and Fenske-Hall calculations done in 1990 with the similar complex CpMn(η^2-$HSiR_3$)$(CO)_2$ (where R=H, Ph or alkyl), showed that the oxidative addition of silane is at an early stage, with the Mn being in the +1 oxidation state.[26] By altering the R groups at silicon to Cl atoms, a further state of oxidative addition is seen with $CpMn(H)(SiCl_3)(CO)_2$, which was found to be closer to the +3 oxidation state.[27] However, the $^1J_{Si\text{-}H}$ for this complex was 55 Hz, which is well above Schubert's non-bonding limit. To account for this discrepancy,

Nikonov suggested a revised DCD scheme[28] considering Bent's rule as an important factor.[29]

Bents rule states that more electronegative substituents prefer hybrid orbitals having less *s* character, and more electropositive substituents prefer hybrid orbitals having more *s* character.[29] Comparing the two systems of $CpMn(\eta^2\text{-}HSiR_3)(CO)$ (R=H, Ph or alkyl) and $CpMn(H)(SiCl_3)(CO)_2$, the inclusion of an $HSiCl_3$ moiety brings about a rehybrdization on the Si centre. In a sense, introducing a more electronegative substituent on Si gives more Si 3s character to the bond with the hydride and more 3p character to the chlorines. In turn, this lowers the energies of both the σ-bonding and σ*-antibonding orbitals of the Si-H bond. This inherently increases the degree of back-donation (localized on Si) from the metal to the σ*-antibonding orbital and decreases donation from the Si-H σ-bonding to the metal (bonding oribital now lower in energy). Taking into account all these factors, the large $^1J_{Si\text{-}H}$ value (55 Hz) observed in $CpMn(H)(SiCl_3)(CO)_2$ may imply non-classical bonding although the degree of oxidative addition may be larger when compared to $CpMn(\eta^2\text{-}HSiR_3)(CO)_2$. In this regard, the presence of a Si-H interaction with a metal may be probed by the $^1J_{Si\text{-}H}$ value but setting a threshold value may become complicated by other factors including the substituents on the metal and on silicon itself.[28]

Nevertheless, these cases are representative of a narrow range of $CpMn(CO)(L)(HSiR_3)$ complexes whereas more general conclusions can be made regarding the $^1J_{Si\text{-}H}$ value. For silane complexes exhibiting non-classical interactions between the Si-H bond and a metal, a range of 70-160 Hz is generally believed to be true.[3] This model can be extended to *β*-agostic silylamido complexes which differ only in the connectivity to the metal centre, when compared to silane σ-complexes. The next section will provide recent examples pertaining *β*-agostic silylamido complexes.

II.1.1 *β*-Agostic NSi-H···M Transition Metal Complexes

An agostic Si-H bond can be defined as a covalent intramolecular σ-bond in a close proximity to an electron deficient metal centre.[3] As mentioned earlier, Si-H agostic complexes are very similar to silane σ-complexes because of the 3c–2e$^-$ interaction between the Si-H fragment and the metal. Most agostic complexes act similar to a chelating ligand, where one end is bound directly to the metal but the other is bound in a non-classical fashion.

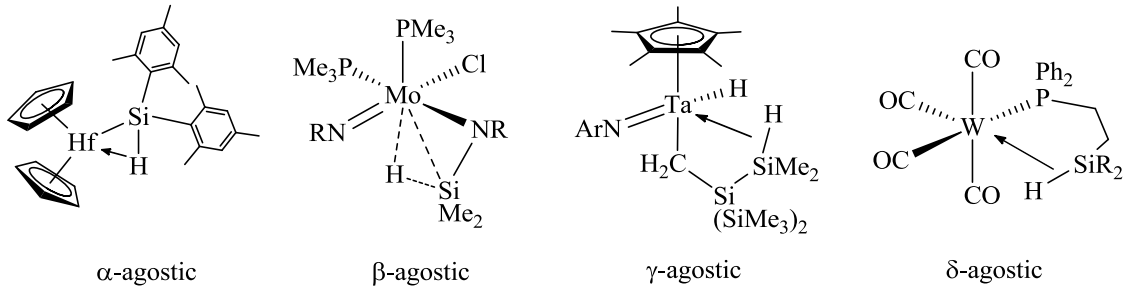

Figure 3 - Various lengths of the Si-H--M agostic bond.[10,30-32]

The type of agostic bond is determined by the type of bridging atom(s) attached to the metal and the length of the bridge separating Si from the metal (Figure 3). The length of the chains are denoted by greek symbols, where δ represents a three bond bridge from Si to the metal, γ represents a two bridge bond, β a one bridge bond and α has the Si directly bound to the metal, which is a relatively recent discovery.[3]

There is a wide range of *β*-agostic Si-H--M bonds in literature. Examples of the bridging M(η^3-X-Si--H$^{\cdots}$) atom include carbon, nitrogen or phosphorous. Only one example of a *β*-agostic phosphorous bridged system exists and was found by Driess *et al.* in 1992. The unusual silylated triphosphine ligand bound to a chromium centre exhibits agostic bonding between the Si-H bond and the metal centre. This was confirmed by a large $^1J_{\text{Si-H}}$ value of 135.7 Hz. The major focus of this thesis revolves around complexes containing a nitrogen bridge, which are termed *β*-agostic silylamido complexes.

The concept of bonding in silane σ-complexes, discussed above, can be extended to *β*-agostic silylamido complexes including the revised DCD scheme.[28] The only major difference would be the length of the Si-H bond, which tends to be shorter in agostic complexes when compared with silane σ-complexes. As for the $^{1}J_{Si\text{-}H}$ value, which is a common parameter used to distinguish classical and non-classical bonding situations, the values remain relatively the same. Most NSi-H--M have coupling constants greater than 100 Hz (larger than Schuberts limit of 10-20 Hz for non-bonded Si`s and H`s) but less than 180 Hz (approximately the $^{1}J_{Si\text{-}H}$ value for free hydrosilanes).[3]

One of the first agostic silylamido complexes was reported by Herrmann *et al.* in 1992.[33] The reaction between $ZrCl_4$ with $Li[N(SiHMe_2)_2]$ in diethyl ether provided the bimetallic species $[ZrCl(\mu\text{-}Cl)\{N(SiHMe_2)_2\}_2]_2$ (**II-12**) (Scheme 2). The Zr(IV) centre has the d^0 configuration and hence does not allows for back-donation into the σ*(Si-H) antibonding orbital, thus enabling, at least in principle, the formation of a non-classical bond. The Zr-N-Si angles were found to be highly distorted (102.8(2) °) compared to other Zr-N-Si angles in related complexes (i.e

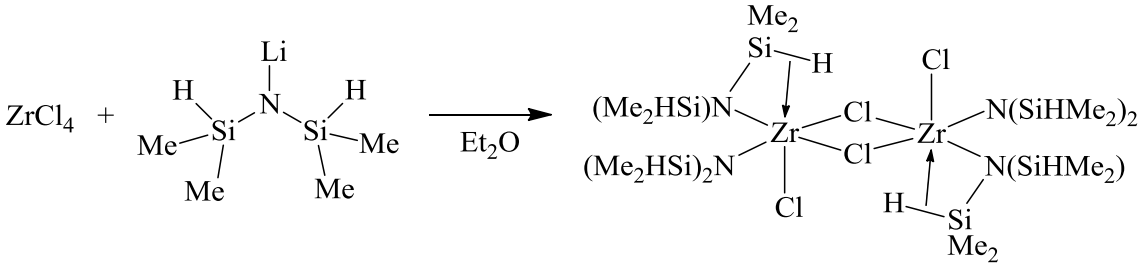

II-12

Scheme 2 - Preparation of $[ZrCl(\mu\text{-}Cl)\{N(SiHMe_2)_2\}_2]_2$ in Et_2O.

126.9(2)° and 116.0(5)° in $[Zr\{N(SiMe_3)_3\}_3(Cl)]$[34]; 126.7(4)° and 118.0(4)° in $[Zr\{N(SiMe_3)_3\}_3(Me)]$[35]). However, this distortion allows for a close contact between Zr and Si (2.943(1) Å). The Si-H stretch in the IR spectra revealed a band of 1948 cm^{-1}, which is lower than typical non-coordinated Si-H stretches (2080-2280 cm^{-1}). However, no conclusive NMR

evidence was provided at this point.

Two years later Berry *et al.* synthesized the *β*-agostic silylamido species $(Cp)_2Zr\{\eta^3$-$N(^tBu)$-$SiMe_2$-$H\}(H)$ (**II-13**) obtained by reacting $Li(N(^tBu)SiHMe_2)\cdot THF$ with $[Zr(Cp)_2(H)(Cl)]_n$.[8] Further reacting complex **II-13** with organic electrophiles such as CH_3Cl, CH_2Br_2, or CH_3I resulted in substitution of the hydride for the halo-derivatives $(Cp)_2Zr\{\eta^3$-$N(^tBu)$-$SiMe_2$-$H\}(X)$ (X = F (**II-14**), Cl (**II-15**), Br (**II-16**), I (**II-17**); Scheme 3a).[36] With zirconium in the +4 oxidation state, complexes **II-13** – **II-17** exhibit no back-donation from the metal into their Si-H antibonding orbitals, yet the data show that a definite non-classical 3c– $2e^-$ bond exists.

Compounds **II-13** – **II-17** exhibit $^1J_{Si\text{-}H}$ values between 113-136 Hz, well below that of the free silylated amine $HMe_2SiNH(^tBu)$ which has a $^1J_{Si\text{-}H}$ value of 192.6 Hz. All Si*H* ^{1}H-NMR shifts are located upfield (δ_{SiH} = 1.21, 2.84, 2.58, 2.24, 1.69 ppm for **II-13** to **III-17**, respectively) compared to the starting silylamide $Li(N(^tBu)SiHMe_2)\cdot THF$ (δ_{SiH} = 4.92 ppm). The IR spectrum exhibits a typical lowering or red shift (ν_{SiH} = 1912 – 1998 cm^{-1}) of the Si-H stretches compared to the precursor silylamide (ν_{SiH} = 2000 cm^{-1}). Berry *et al.* describes the variation of non-classical bonding (for **II-14 – II-17**) in a manner similar to the discussion of Lewis acidity of BX_3. In the series of BX_3 acids (where X=F, Cl, Br, I), BF_3 is the weakest, which can be attributed to strong π-donation from fluorine to a vacant p-orbital of boron. In the case of the zirconium complex (Scheme 3b), fluorine acts as the best π-donor to the metal, therefore the Si-H interaction is weakest. When there is no ancillary ligand to donate π-electron density to the metal, as is the case with the hydride starting material, the Si-H bond becomes the strongest.[36]

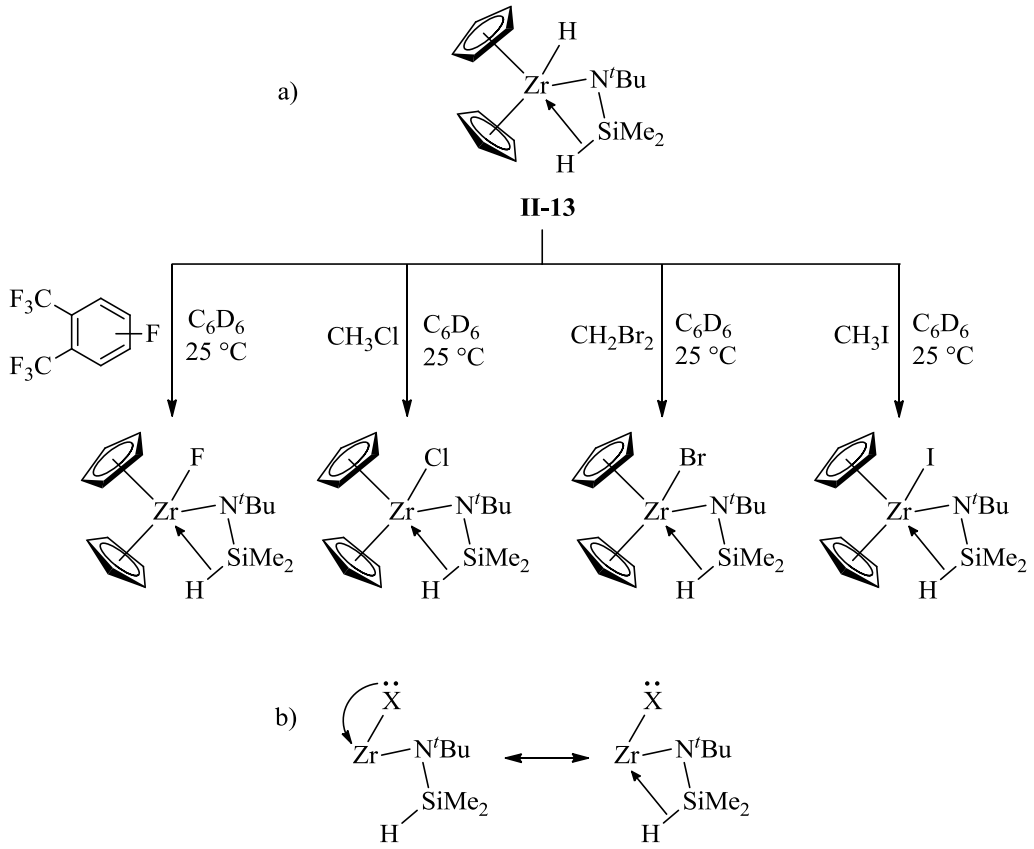

Scheme 3 - a) Substitution of **II-13** for various halides b) resonance form depicting donation into the metal from the halogen lone pair.

From 1997 to 2001, Anwander *et al.*[37-40] studied the effects of NSi-H--M agostic bonding to various d^0 lanthanide metal complexes of the type *ansa*-Cp′$_2$Ln(η^3-N(SiMe$_2$-H)$_2$) (where Cp′ denotes substituted cyclopentadienyl, ansa- fluorenyl and indenyl ligands). The IR frequencies of the agostic Si-H stretches ranged from 1833-1970 cm^{-1} for complexes similar to **II-18**, **II-19** and **II-20**. The $^1J_{Si-H}$ values for the agostically bound Si-H's were in the range of 133-155 Hz for the *ansa*-SiMe$_2$ bridged complexes **II-18** and **II-19**. The determination for the mono-agostic nature of non-linked bis(Cp*) complex **II-20** was suggested based on one small (99.7(1)°) and one large (124.9(1)°) Y-N-Si angle. [38]

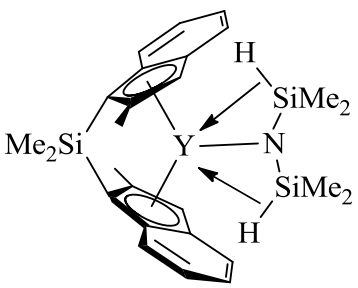

II-18

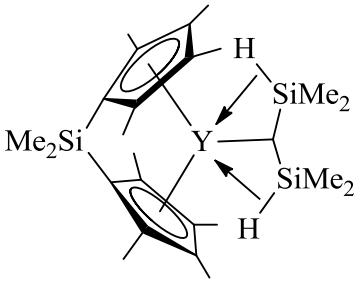

II-19

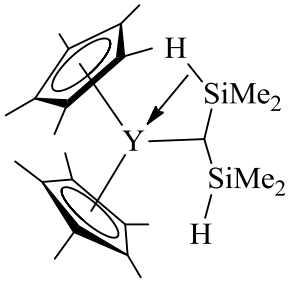

II-20

In 2001, Nikonov *et al.* produced the first example of a stretched NSi--H--M agostic bond.[9] From Scheme 4, it can be seen that the reaction between $Cp(RN=)Nb(PMe_3)_2$ (where R = 2,6-diisopropylphenyl or 2,6-dimethylphenyl) and $HSiClMe_2$, yields the agostic products $CpNb(\eta^3$- NR-$SiMe_2$-H)(Cl)(PMe_3) (R = Ar′ (**II–21**), Ar (**II-22**)). This reaction proceeds in two possible mechanistic pathways. The first route may proceed via an oxidative addition of the $HSiMe_2Cl$ over the phosphine dissociated complex $Cp(ArN=)Nb(PMe_3)$, which is known for many catalytic cycles. Further intramolecular attack by the lone pair on the imido nitrogen towards the Si-Cl bond could lead to an elimination of the chloride ligand, where it is then able to bind to the cationic complex forming the desired agostic complex. A second mechanism can occur via an initial attack of the imido group towards the silicon with the hydrogen shifting towards the metal centre to create a hydride. Further attack of the hydride to the silicon affords elimination of chloride which can once again bind to the cationic complex forming the agostic product. Both *cis* and *trans* products (**II-22** and **II-22′**; regarding PMe_3 to the hydride) were characterized by $^1J_{Si\text{-}H}$, IR, and X-ray crystallography. The coupling constants for **II-21** and **II-22** were found to be 116 Hz and 97 Hz respectively, falling within the range for Si-H σ-bond coordination. The lower values in the d^2 Nb complex **II-22** correlate well with the designation of a stretched or elongated agostic complex with elongation of the Si-H bond found from X-ray analysis. Alternatively, **II-21** can be classified as an unstretched β-agostic complex due to the

lengthening of the bond and higher $^{1}J_{Si\text{-}H}$ value. The Si-H IR stretches of all complexes were found to be lower than in their free silylated amine analogues.

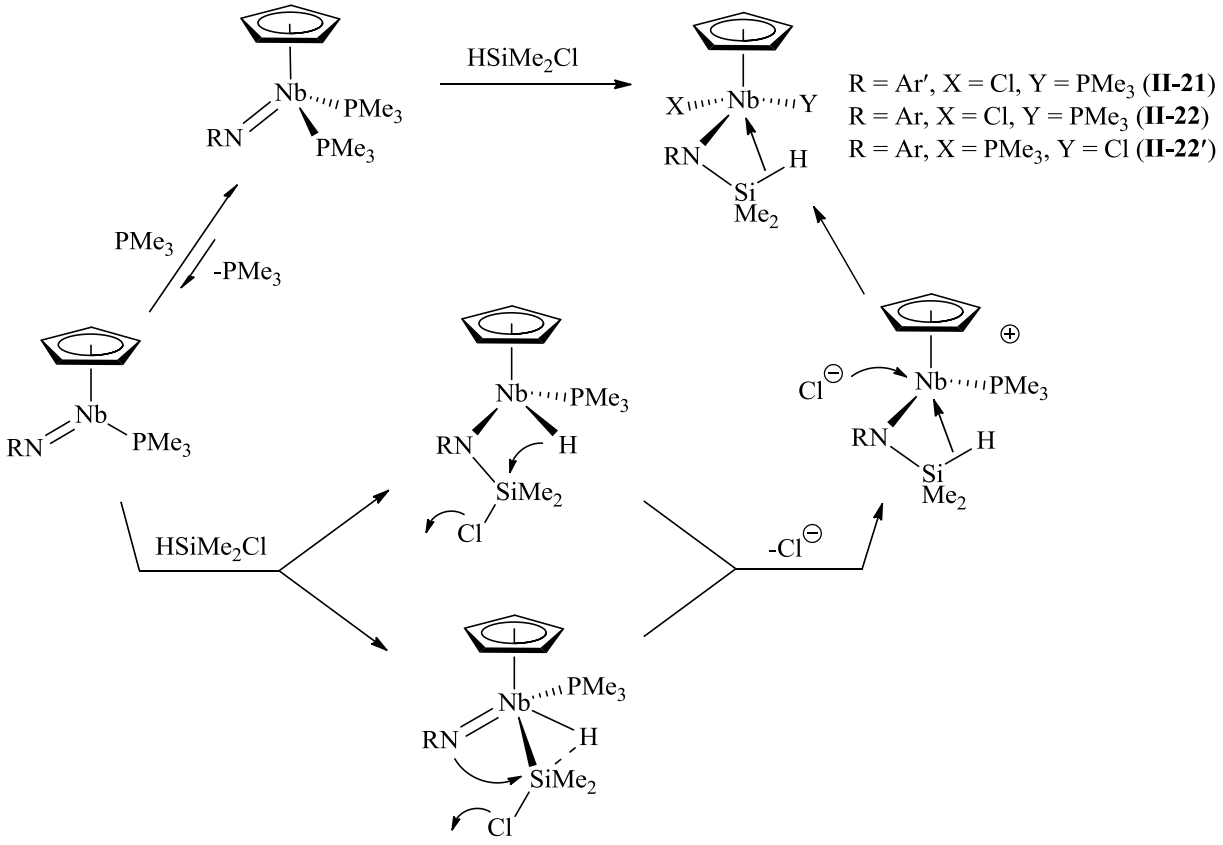

Scheme 4 - Reaction between Cp(RN=)Nb(PMe$_3$)$_2$ and HSiMe$_2$Cl yielding agostic silylamides **II-21**, **II-22** and **II-22′**.

The related family of isolobal group 6 Mo(IV) *β*-agostic silylamido complexes with the general formula (RN=)Mo(η^3-NR-SiR′$_2$-H)(Cl)(PMe$_3$)$_2$ (when R = ^{t}Bu, R′ = Me$_2$ (**II-23**), PhH (**II-24**), MeCl (**II-25**); R = Ar; R′ = Me$_2$ (**II-26**), MeCl (**II-27**); R = Ar′; R′ = Me$_2$ (**II-28**), MePh (**II-29**), MeCl (**II-30**)) were synthesized from the addition of mono- and dichloro silanes to (RN)$_2$Mo(PMe$_3$)$_x$ (R = Ar, Ar′, x = 3; R = ^{t}Bu, x = 2).[11] The $^{1}J_{Si\text{-}H}$ constants once again fall within the expected ranges for σ-bond complexation (93 Hz to 135 Hz). In complex **II-30**, which features a chlorine substituent at silicon, the Si-H bond was expected to become weaker and, therefore, elongated. However, the X-ray analysis, as well as a measurement of a high $^{1}J_{Si\text{-}H}$

value (135.6 Hz), established strengthening and shortening of the Si-H bond. In contrast, the Mo-H, Si-H and Si-Mo distances do not vary much at all, when comparing **II-28** to **II-30**. This discrepancy between theory and experiment can be rationalized in terms of the revised DCD scheme. This revised scheme takes into account that the chlorine substituent gives the Si-H bond more 3s character of Si making it a worse σ-donor, which explains the increase in the Si-H coupling when going from **II-28** to **II-30** (the $^{1}J_{\text{Si-H}}$ is proportional to the amount of 3s density). However, the introduction of Cl groups renders the Si centre more Lewis acidic, which increases the back-donation from Mo into the σ*(Si-H) anti-bonding orbital. This varies the Mo-Si and Mo-H distances because the σ(Si-H) bonding molecular orbital is localized closer to the H atom, and the σ*(Si-H) anti-bonding is closer to the Si atom, due to electronegativity differences.

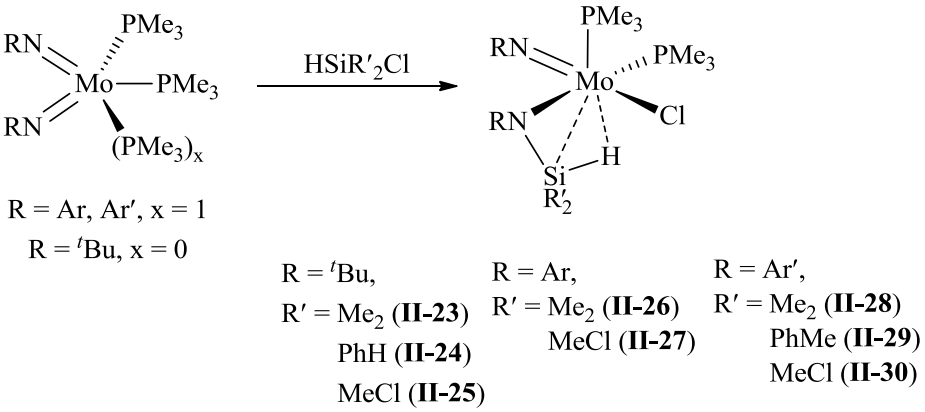

R = Ar, Ar′, x = 1
R = ^{t}Bu, x = 0

R = ^{t}Bu,
R′ = Me_2 (**II-23**)
PhH (**II-24**)
MeCl (**II-25**)

R = Ar,
R′ = Me_2 (**II-26**)
MeCl (**II-27**)

R = Ar′,
R′ = Me_2 (**II-28**)
PhMe (**II-29**)
MeCl (**II-30**)

Scheme 5 - Preparation of agostic complexes (RN=)Mo(η^3-NR-SiR′-H)(Cl)$(PMe_3)_2$ (**II-23** to **II-30**).

II.2 Hydrosilylation of Carbonyls Mediated by Transition Metal Complexes

The reduction of unsaturated organic substrates is an ongoing challenge for organic and inorganic chemists alike.[16] Typically, stoichiometric amounts of reducing agents, such as $LiAlH_4$ and $NaBH_4$, are used due their overall high rates of reactivity. However, these reagents are expensive, hazardous and toxic (e.g. $NaBH_4$). Alternative reduction methodologies are based on transition metal catalysts. Commonly used methods for reducing C=X (X = C, O, N, S, P) bonds include hydrogenation, hydrosilylation and hydroboration, each of which present specific advantages and disadvantages.[16] Hydrogenation is an attractive choice as it avoids unnecessary waste and is very cost effective. However, the use of highly pressurized hydrogen gas is dangerous and requires the use of special equipment, in particular when scale up is required. On the other hand, the application of hydroboration has its limits because of high cost of boranes and their sensitivity to air. For this reason, hydrosilylation has received great attention as it avoids the use of high pressures, uses cheap, air stable, and nontoxic reducing agents (i.e. PMHS, TMDS) and the resultant silylether products are protected forms of alcohols (Scheme 6). The latter is

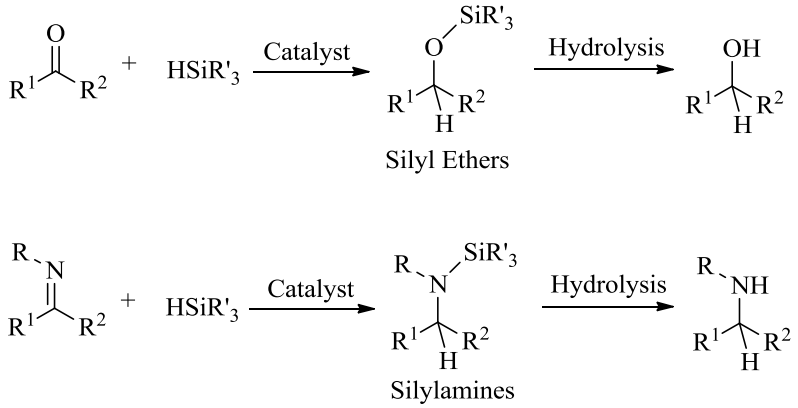

Scheme 6 – Products of hydrosilylation using carbonyls and imines to give silylethers or silylamines.

specifically intriguing when further derivatization is required, as can be the case in multistep natural product syntheses.

Transition metal hydrosilylation is nowadays extensively used in laboratory syntheses and industrial applications. The area of homogeneous hydrosilylation began in the late 1950's with discovery that chloroplatinic acid $H_2[PtCl_6]$ (Speir's catalyst) can catalyze the reduction of olefins using $MeSiHCl_2$.[41] Industrially, platinum catalysts (i.e. $Pt_2[(Me_2SiCH{=}CH_2)_2O]_3$, Karstedt's catalyst[42]) are usually used in the preparation of monomeric alkylsilanes, which can be hydrolyzed to produce various polymeric materials. It was not until 1972 when the reduction of carbonyls began to flourish with the work done by Ojima *et al.* using Wilkinsons catalyst $[RhCl(PPh_3)_3]$.[43,44] Since then the development of late transition metals, such as rhodium, ruthenium, palladium and platinum, has received the most attention. However, it is recognized that these metals suffer from high costs and increased toxicity. The development of early transition metals as catalysts has been widely exploited in recent years due to their associated low cost and environmentally benign nature. Mechanistic studies have aided in better understanding the required parameters needed for a catalyst to function efficiently. This ranges from the ligand design to the appropriate choice of metal. The following sections will briefly discuss recent studies on the mechanisms of hydrosilylation and the recent progress in hydrosilylation by molybdenum complexes.

II.2.1 Recent Mechanisms of Transition Metal Catalyzed Hydrosilylation of Carbonyls

Mechanistic studies of hydrosilylation were first conducted for alkene and cycloalkene substrates due to the initial discovery by Speirs in 1957. It is pertinent to include the general mechanism of alkene hydrosilylation in our discussion, as it further contributes to understanding the details of carbonyl hydrosilylation. In the late 60s, Chalk and Harrod developed a catalytic cycle which has been primarily used to describe many transition metal catalyzed reactions, despite their focus being primarily on platinum catalysts (i.e. $H_2[PtCl_6]$).[45] Scheme 11 depicts a typical catalytic cycle which involves oxidative addition (**A**) followed by coordination of the alkene (**B**) in the η^2-H_2C=CHR′ fashion.

The initial Chalk-Harrod mechanism describes a migratory insertion of the alkene into

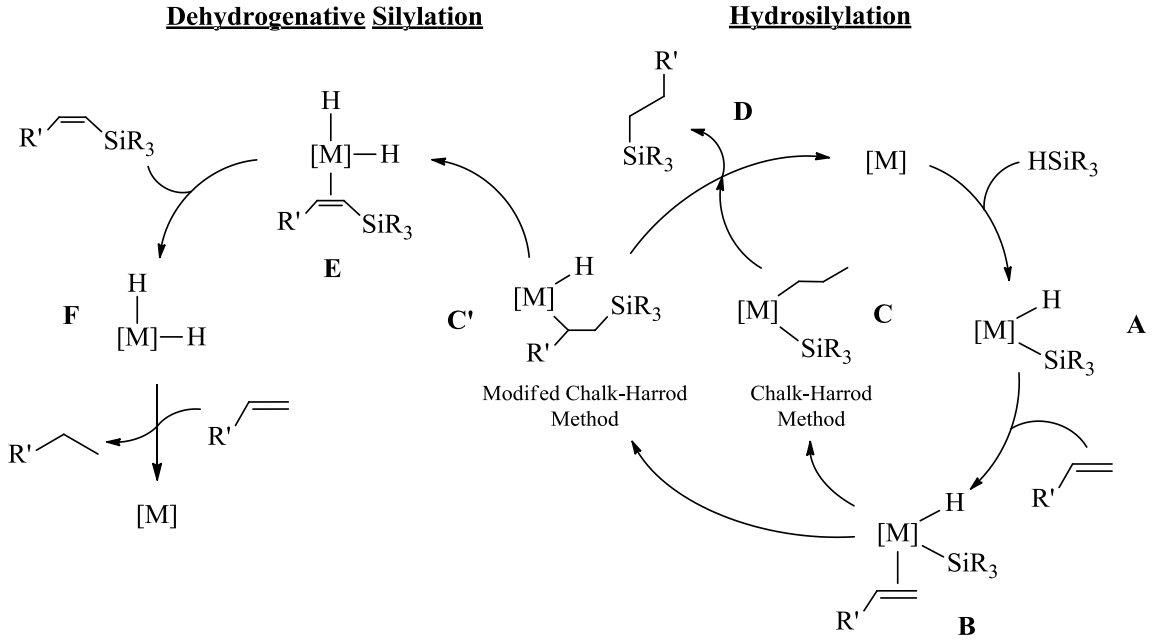

Scheme 7 – Chalk-Harrod and Modified Chalk-Harrod method for the transition metal catalyzed hydrosilylation (right side) and dehydrogenative silylation (left side) of alkenes.

the metal hydride bond (**C**) followed by reductive elimination to give the corresponding anti-Markovnikov addition product and regeneration of the starting metal complex (Scheme 7). However, in some cases generation of vinylsilanes, alkanes and isomerization products was observed, which could not be explained by this process. To address this issue, a modified Chalk-Harrod mechanism[46], involving alkene insertion into the M-Si bond (**C′**), was introduced by Wrighton *et al.* to account for these findings. In the latter scheme, steps **C′→D** involve dehydrogenative silylation which is produced from *β*-H elimination of the silylalkyl ligand to give a vinlylsilane. The resultant dihydride can react with another equivalent of substrate to give the corresponding alkane (**F**). Depending on the type of metal, ligand framework and stoichiometry of the reaction, preference for either hydrosilylation or dehydrogenative silylation can be induced.[47-49]

Like alkenes, hydrosilylation of carbonyls was suggested to go through a similar modified Chalk Harrod mechanism, proposed by Ojima *et al.* in 1972 for the Wilkinson's catalyst [$RhCl(PPh_3)_3$] (**II-31**).[43,44] The 1:1 addition of silane to carbonyl substrate in the presence of 0.5 mol % catalyst resulted in the successful conversion of simple aliphatic and aromatic carbonyl compounds into the corresponding silylethers. Based on stoichiometric reactions between complex and silane, Ojima proposed the initial step of the reaction to proceed through a Si-H oxidative addition generating the rhodium silyl hydride complex $(PPh_3)_2RhH(SiEt_3)Cl$ (**II-32**) and loss of one equivalent of triphenylphosphine (Scheme 8). Subsequent carbonyl coordination followed by migratory insertion into the M-Si bond gives the silylether and regeneration of the metal catalyst. This process was found to be applicable for many transition metal catalyzed hydrosilylation systems but within the last 20 years, a variety of new and intriguing mechanisms have been introduced.

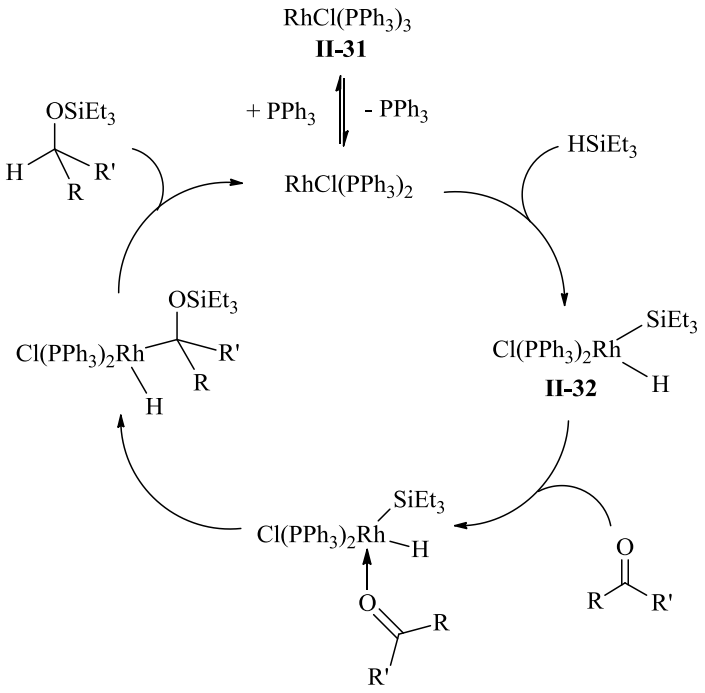

Scheme 8 – Ojima mechanism for the hydrosilylation of carbonyls using [$RhCl(PPh_3)_3$] (**II-31**).[43]

An in depth study on the hydrosilylation of α,β-unsaturated carbonyls using the rhodium catalyst [$(PPh_3)_4RhH$] (**II-33**) was performed by Chan *et al.* in 1995.[50] The use of diphenylsilane resulted in the selective 1,2-addition products whereas, the use of tertiary silanes (i.e. $PhMe_2SiH$, $(ClCH_2)Me_2SiH$, $(EtO)_3SiH$) gave selectively the 1,4-addition products. Based on 1:1 reactivity studies using secondary diphenylsilane (H_2SiPh_2) and dideuteriodiphenylsilane (D_2SiPh_2), a significant primary kinetic isotope effect (KIE) was observed (k_H/k_D = 2), suggesting the rate determining step to be the Si-H bond breaking across the carbon-oxygen double bond (C=O) followed by a hydride shift to give the respective silylether (Scheme 9, **A**). In contrast, tertiary silanes showed no significant KIE (k_H/k_D = 1) implying neither the Si-H nor M-H bond breaking step to be rate-limiting for this case. The proposed mechanistic cycle involves four steps beginning with oxidative addition of the Si-H bond to the Rh centre, followed by coordination of

the carbonyl to silicon centre. From here, the use of secondary silanes (pathway **A**, R = H) results in insertion directly into the Si-H bond to generate the rhodium silylether complex. Alternatively, insertion into the Rh-Si bond occurs with the use of prmary silanes followed by reductive elimination to give the respective silylether and regeneration of the catalyst.[50]

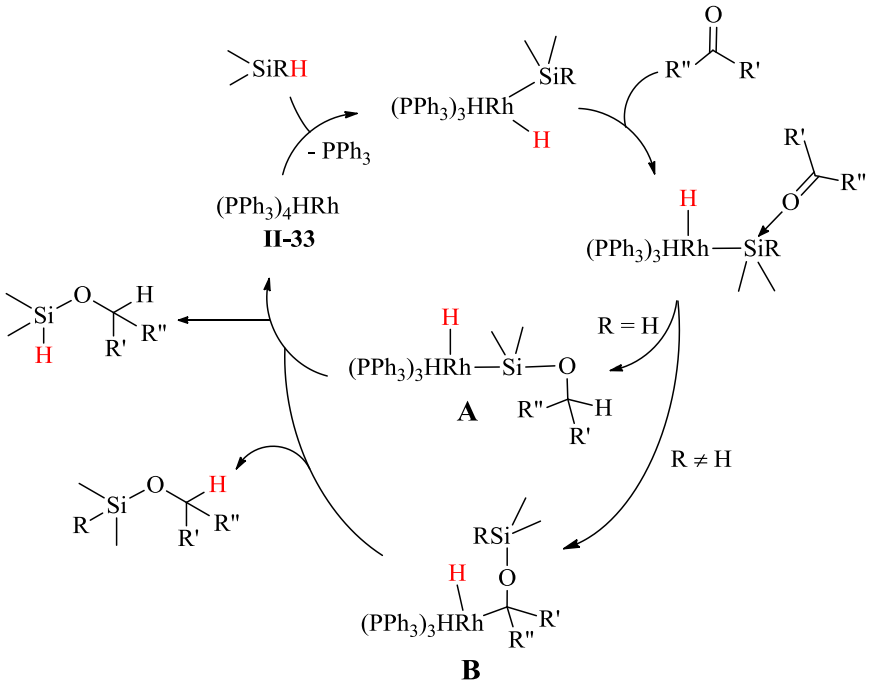

Scheme 9 – Initial mechanism of catalytic hydrosilylation using primary (**B**) and secondary (**A**) silanes, proposed by Chan *et al*.[50]

Chiral derivatives of titanocene were extensively studied by Buchwald and co-workers[51,52] in the mid 1990's in the enantioselective hydrosilylation of carbonyls. Their results showed that use of an additive (typically MeOH) greatly enhanced the rate of reaction mediated by (*R*,*R*)-(EBTHI)TiF_2 (**II-34,** EBTHI = ethylenebis(tetrahydroindenyl)) with $PhSiH_3$ or PMHS used as the hydride source. The mechanism shown in Scheme 10 was suggested based on their analysis. Initial generation of the titanium(III) hydride complex (*R*,*R*)-(EBTHI)$Ti^{III}H$ is accomplished through the addition of $PhSiH_3$ to **II-34**. Enantioselectivity is induced in the

following step with insertion of the carbonyl into the Ti^{III}-H bond to give a titanium alkoxy complex. The respective alcohol is then formed through coordination or σ-bond metathesis of the additive (MeOH) with the alkoxy ligand. The addition of silane then regenerates the hydride through a second proposed σ-bond metathesis step.[52] The current mechanism is based on their observations of the relative rate of their reactions with and without alcohol additives (MeOH). No in depth stoichiometric, kinetic or labelling studies were done to confirm this mechanism and, therefore, it is purely speculative.

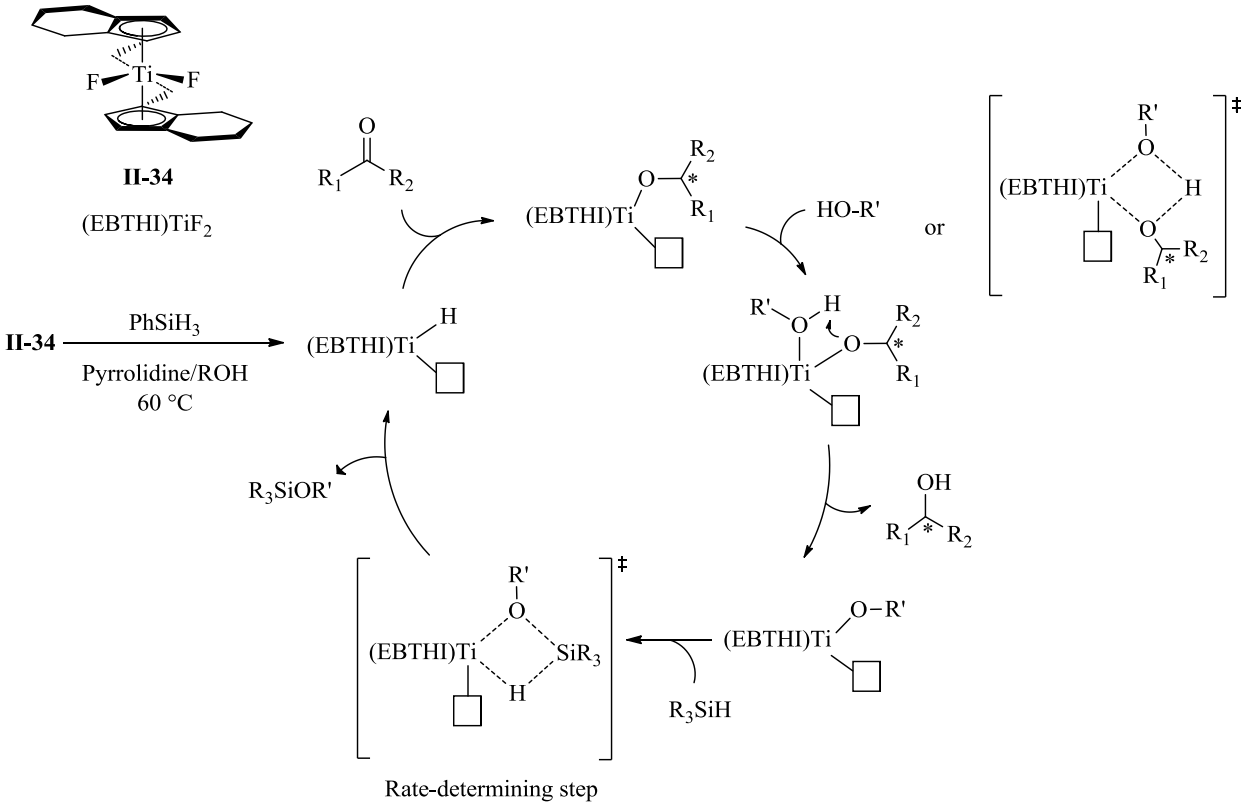

Scheme 10 – Proposed mechanism of enantioselective hydrosilylation of carbonyls using **II-34** and MeOH additive.

In 2003 - 2005, the groups of Toste and Abu-Omar investigated rhenium oxo complexes as catalysts for the hydrosilylation of carbonyls. Toste and co-workers initially found that

reacting the dioxo rhenium complex $(PPh_3)_2Re(O)_2I$ (**II-35**) at 2 mol % catalyst loading with Me_2PhSiH gives the respective silylether in moderate to high yields. The mechanism proposed (Scheme 11) involves initial addition of the silane across one of the rhenium oxo double bonds (Re=O) in a [2+2] fashion generating the siloxy hydride complex $(PPh_3)_2ReH(O)(OSiMe_2Ph)(I)$ (Scheme 11, **A**). This step does not depend on phosphine concentration. Then, complex $(PPh_3)_2ReH(O)(OSiMe_2Ph)(I)$ undergoes insertion of the carbonyl into the rhenium hydride bond. Kinetic studies showed that this step is inhibited by phosphine and, in fact, $1/k^{obs}$ shows a linear dependence on phosphine concentration, suggesting that phosphine dissociation precedes the carbonyl coordination (Scheme 11, **B**). Insertion into the Re-H bond followed by a formal reverse or *retro*-[2+2] reaction and PPh_3 re-coordination generates the silylether and regenerates the dioxo

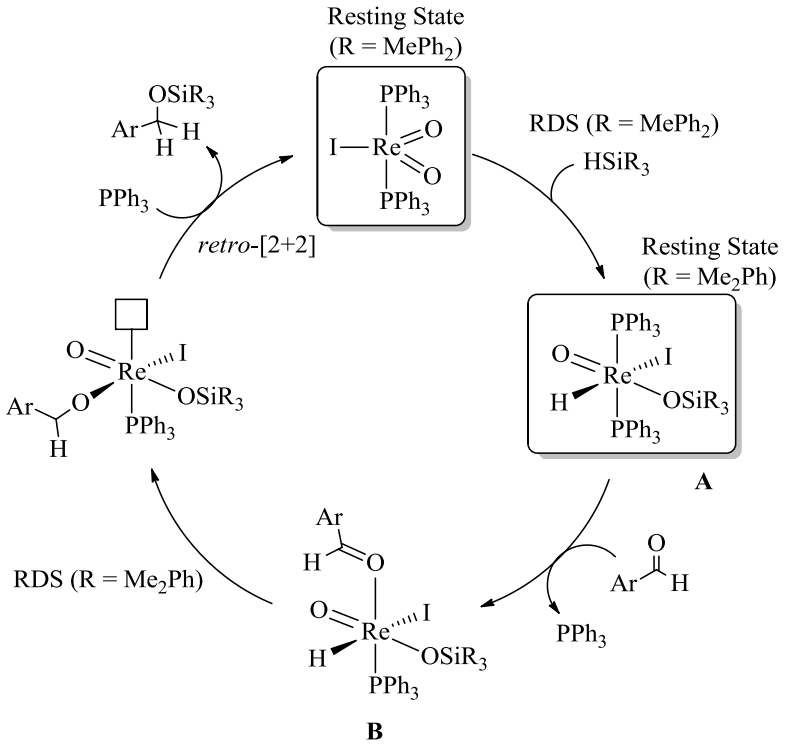

Scheme 11 – Toste mechanism for the hydrosilylation of carbonyls using $(PPh_3)_2Re(O)_2I$ (**II-35**)

as a catalyst. Different resting states and RDS's are shown for each type of silane used.

Re catalyst. Interestingly, the resting state and rate-determining steps (RDS) of the catalytic cycle are dependent on the type of tertiary silane used (i.e. Me_2PhSiH or $MePh_2SiH$).

Abu-Omar and co-workers studied the hydrosilylaition of carbonyls using the monooxorhenium(V) catalyst [Re(O)(hoz)$_2$(MeCN)][TFPB] (**II-36**)[53], similar to the work done by Toste only a few years earlier. However, their initial studies suggested a catalytic cycle that does not involve the addition of silane across the Re=O bond or oxidative addition of silane to the Re centre. Rather, loss of nitrile generates a vacant site allowing silane σ-cordination followed by silyl cation abstraction by the carbonyl generating a silyl oxonium ion, which is then attacked by the rhenium hydride to give the silylether. A similar mechanism, called ionic hydrosilylation, had been previously proposed by Bullock and co-workers. The salient features of this process are that hydrosilylation proceeds via heterolytic cleavage of the Si-H bond and does not involve the coordination of aldehyde or ketone to the metal center.[54] Interested in better understanding this mechanism, Abu-Omar *et al*. synthesized alternative trichloro Re complexes containing oxo (**II-37**), imido (**II-38**) and nitrido (**II-39**) moieties. Based on the faster rates of reactivity for imido complexes **II-38** opposed to the oxo Re complexes **II-36** and **II-37**, they concluded that addition of silane across the Re=X (X = N or O) does not take place. Stoichiometric reaction with Et_3SiH showed that the Re oxo hydride complex $Re(O)Cl_2(H)(PPh_3)_2$ (**II-40**) forms, presumably via metathesis with the Re-Cl bond. Insertion of benzaldehyde into Re-H gives the respective Re alkoxide complex $Re(O)Cl_2(OBn)(PPh_3)_2$ (**II-41**) which undergoes silylether formation upon addition of silane and regeneration of **II-40**. This sequence led to the suggestion of a simple catalytic cycle involving **II-40** and **II-41** as intermediates (Scheme 12A). However, kinetic simulations based on the measurements of rates

for individual steps afforded the overall rate which was much slower than the observed rate for PhCHO consumption, leading to a conclusion that complexes **II-40** and **II-41** are not active in the major catalytic cycle. Therefore, given on all the data obtained and based on process of elimination, a second mechanism was put-forth (Scheme 12B). In this mechanistic hypothesis, the silane adds to **II-37** or **II-38** resulting in Si-H σ-complex formed *cis* to the imido or oxo ligand. The formed silylium cation (Et_3Si^+) transfers to the substrate, which forms the respective

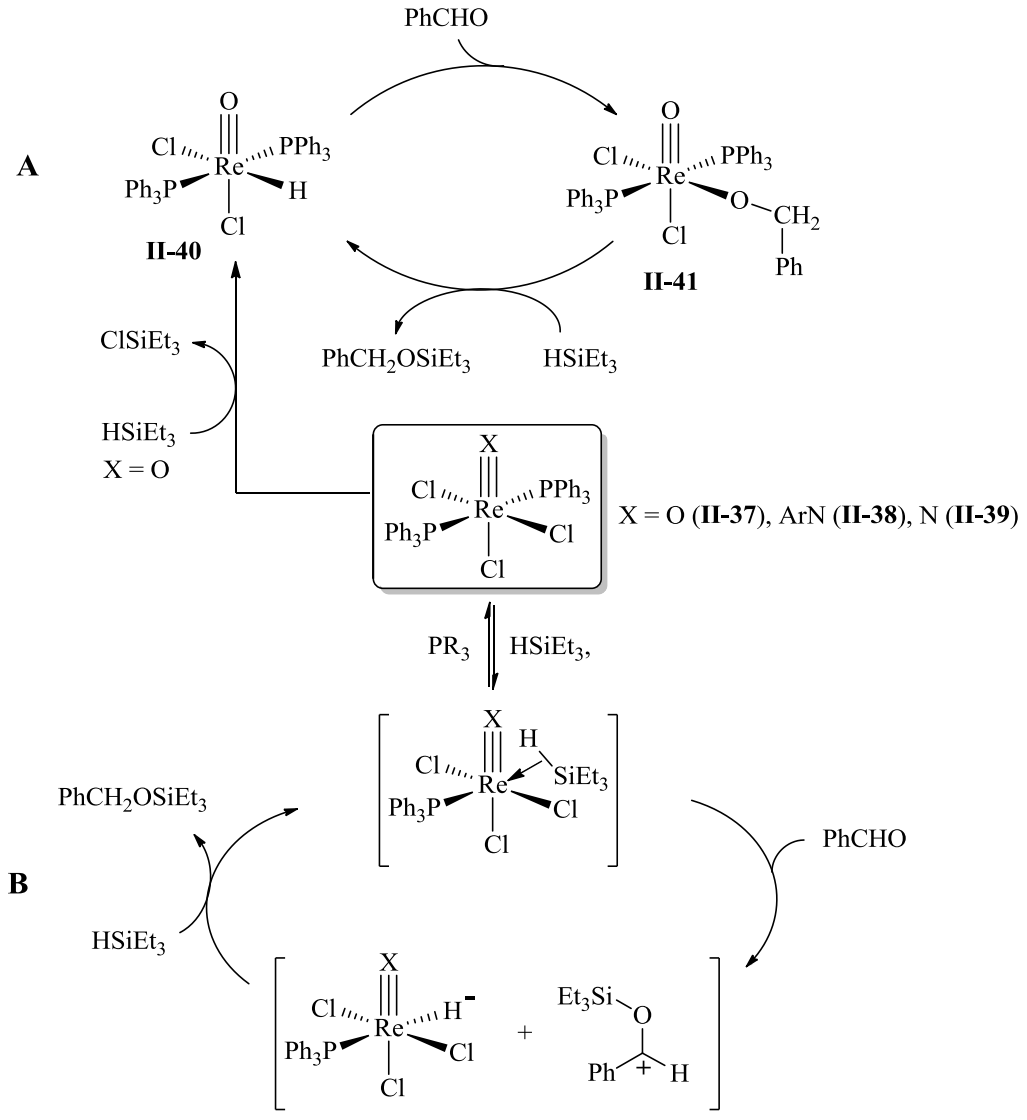

Scheme 12 – Abu-Omar`s initial (**A**) and revised (**B**) hydrosilylation mechanisms of aldehydes

silylether after H^- attack from the rhenium hydride. The addition of another equivalent of silane regenerates the silane σ-complex allowing this to become the active catalyst.[55]

In 2000, Bullock and co-workers developed cationic tungsten and molybdenum complexes of the type $[Cp(CO)_2(PR_3)M(\eta^1\text{-}O{=}CEt_2)][BAr_4^{F-}]$ (M = Mo or W) for their use as hydrogenation catalysts for the reduction of carbonyls.[54] An ionic mechanism of hydrogenation was proposed involving a cationic dihydride intermediate which initially transfers the acidic proton from the metal to the oxygen, generating the carbocation and a neutral complex. The neutral metal hydride then transfers the hydride to the protonated ketone giving the hydrogenated product and regenerating of the cationic catalyst (Scheme 13).[54] Similar complexes $[CpM(CO)_2(IMes)][B(C_6F_5)_4]$ (IMes = 1,3-bis(2,4,6-trimethylphenyl)-imidazol-2ylidene; M = Mo (**II-42**), W (**II-43**)) featuring N-heterocyclic carbenes instead of the phosphine ligands were tested in the hydrosilylation of carbonyls.[56] Bullock *et al.* found complex **II-43** to be a much better catalyst for the hydrosilylation of ketones using $HSiEt_3$ under solvent free conditions. In the presence of aliphatic substrates, precipitation of the resting state of the catalyst was observed. This precipitate could be isolated and reused in further catalytic runs (five cycles were tested). The precipitate was found to contain two cationic species $[CpW(CO)_2(IMes)(SiEt_3)H][B(C_6F_5)_4]$ (**II-44**) and $[CpW(CO)_2(IMes)(H)_2][B(C_6F_5)_4]$ (**II-45**). Based on these results, an ionic hydrosilylation mechanism was proposed and is shown in Scheme 13. The ketone complex $[CpW(CO)_2(IMes)(\eta^1\text{-}O{=}CEt_2)][B(C_6F_5)_4]$ (**II-46**) was shown to be abundant during the initial stages of the reaction and converts into either the dihydride (**II-45**) or silyl hydride complex (**II-44**) upon addition of either dihydrogen or silane, respectively. Complex **II-44** can react with an equivalent of substrate generating the silyloxy carbocation and a neutral hydride complex, which

can further react with an equivalent of silane to give the respective silylether and regenerate the cationic complex **II-44**.[56]

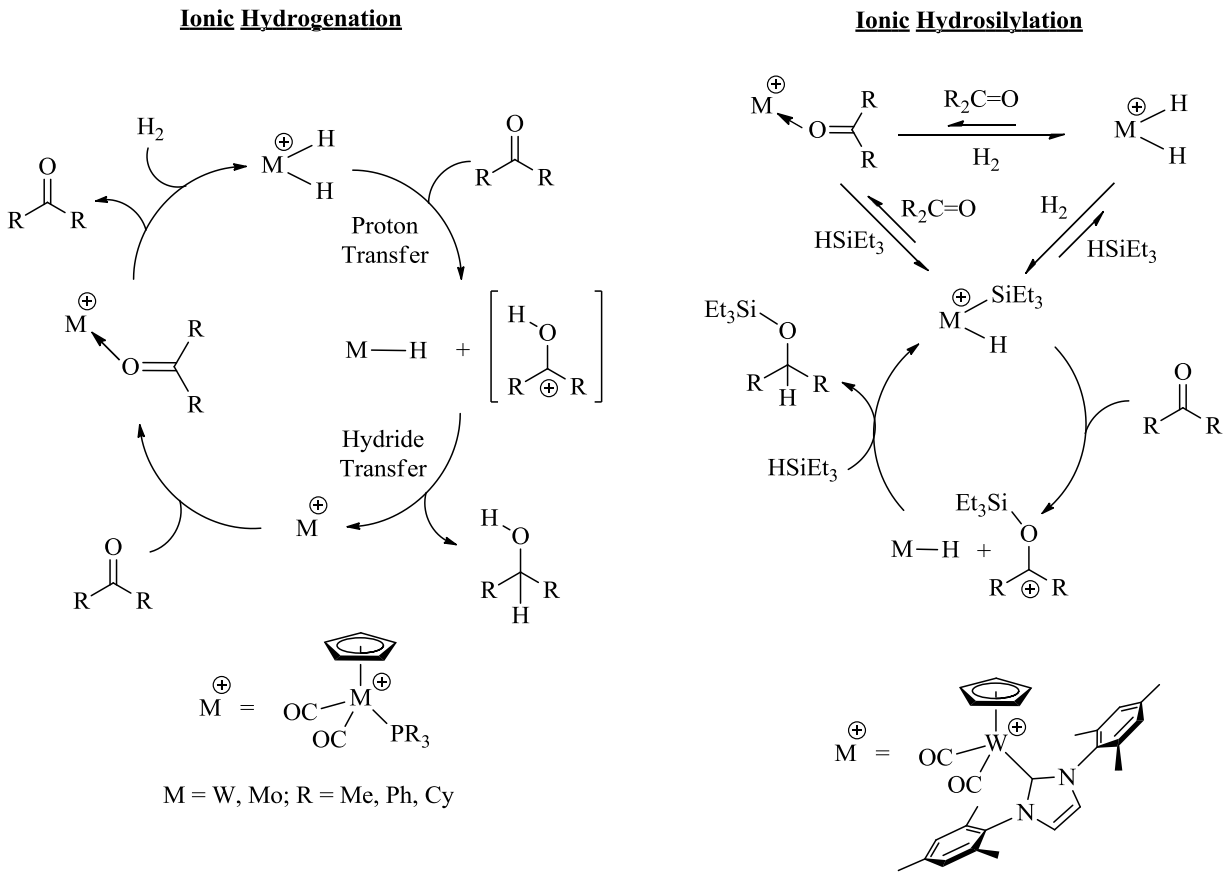

Scheme 13 - Bullock's ionic hydrogenation[54] and hydrosilylation[56] mechanism for the reduction of carbonyls.

II.2.2 Recent Advances in Hydrosilylation using Molybdenum Catalysts

In recent years, first row transition metals have received a great deal of attention as catalysts for the reduction of unsaturated small molecules such as simple carbonyls, alkenes and alkynes.[57,58] This is in part due to their low cost, environmentally benign nature and larger natural abundance compared to their second and third-row congeners. Interestingly, in spite of being the only second row transition metal met in biological systems[59], molybdenum complexes have received much less attention as catalysts for reduction reactions. Early examples of

hydrosilylation catalysts were based on low-valent Mo(0) complexes including $Mo(CO)_6$ (**II-47**)[60,61], the anionic bimetallic bridging hydride complex $[(CO)_5M(\mu\text{-}H)M(CO)_5][NEt_4]$ (**II-48**)[62], and the molybdenum oxadiene catalysts (**II-49**)[63] each used in the reduction of carbonyls and α,β-unsaturated ketones (Figure 4). Further advancement in the field had not been seen until 2005 when Royo and co-workers reported hydrosilylation catalysed by the dioxo molybdenum complex MoO_2Cl_2 (**II-50**).[64]

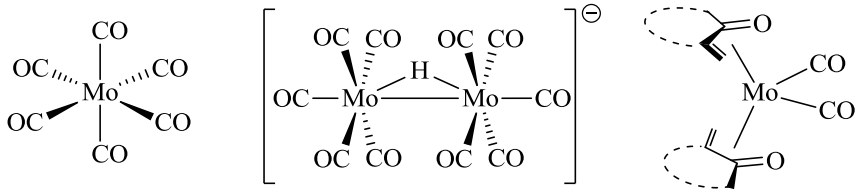

II-17 **II-18** **II-19**

Figure 4 – Early Mo(0) catalysts used in the hydrosilylation of carbonyl compounds.

Inspired by work done by Toste using Re dioxo complexes (Scheme 11), Royo *et al.* investigated a series of high-valent dioxo molybdenum(VI) complexes towards hydrosilylation of carbonyls, including **II-50**, $MoO_2(acac)_2$ (**II-51**), $CpMoO_2$ (**II-52**), $MoO_2(S_2CNEt_2)_2$ (**II-53**), $MoO_2(Mes)_2$ (**II-54**) and the organotin polymer $[(R_3Sn)_2MoO_4]$ (R = ^{n}Bu, ^{t}Bu, Me) (**II-55**).

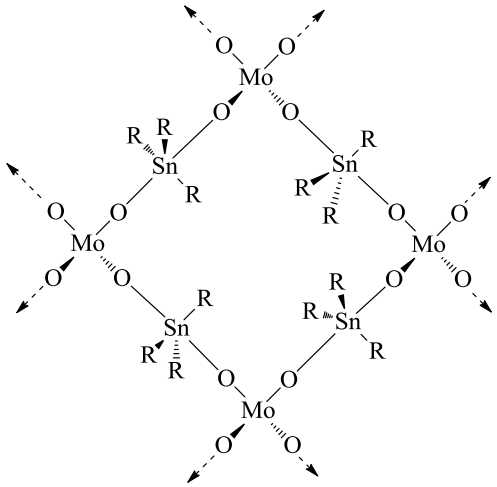

II-55

Complex **II-50** was found to be the most efficient. No intermediates were observed during catalysis, but the 1:1 reaction between $MoO_2Cl_2(NCBu^t)$ and $HSiMe_2Ph$ gave the dimeric complex $[MoO(OSiMe_2Ph)Cl_2]_2$. Based on this observation and in analogy with the mechanistic conclusions of Toste's group, Royo *et al.* proposed that the mechanistic cycle goes the intial [2+2] addition of silane across the Mo=O bond followed by a radical pathway. The implication of a radical mechanism was based on the increased catalytic activity in acetonitrile (known to facilitate radical processes), and inhibition by radical scavengers, such as Ph_2NH and 2,6-di-*tert*-butyl-4-methylphenol. As shown in Scheme 14, homolytic cleavage of the Mo-H bond in the presence of aldehyde or ketone takes place after silane addition, followed by a formal *retro*-[2+2] reaction generating the respective silylether and **II-50**. These results were also supported by two separate computational studies performed by Calhorda *et al.*[65] and Strassner *et al.*[66] Complex **II-50** was also used in the hydrosilylation of esters[67], imines[68], amides[69] and

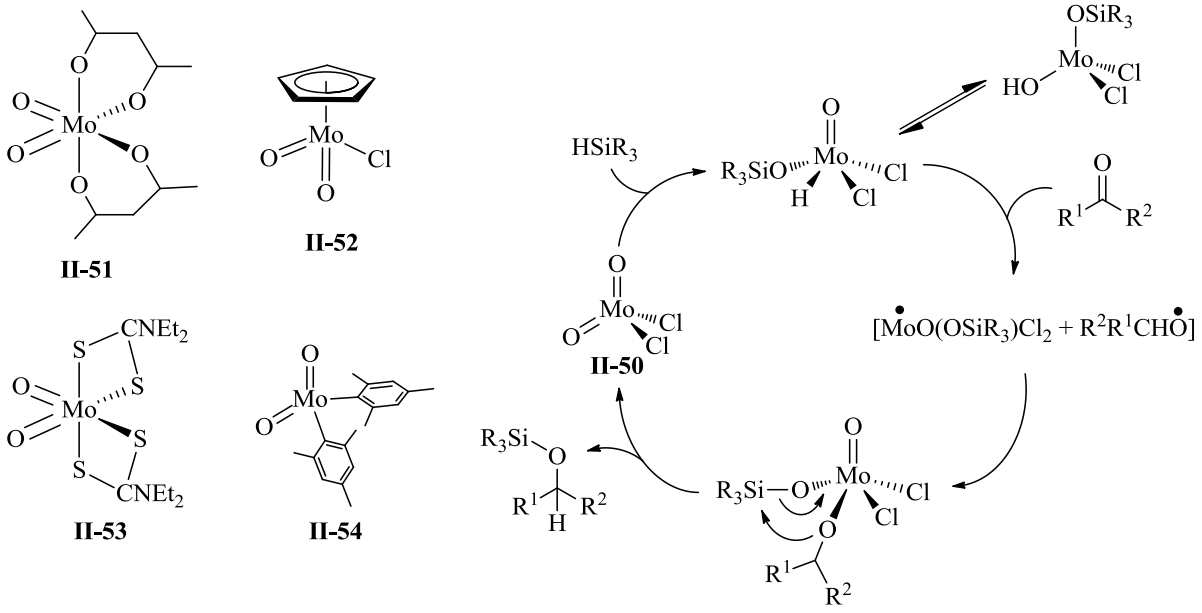

Scheme 14 – Mo(VI) dioxo complexes used by Royo in the catalytic hydrosilylation of carbonyls (left) along with proposed mechanism (right).

sulfoxides[70].

Interest by the Nikonov group in utilizing Mo imido complexes towards hydrosilylation of carbonyls was inspired by the reactivity studies between silanes and cyclopentadienyl/imido complexes of tantalum and bis(imido) complexes of molybdenum. Using chloro- and hydrosilanes, addition across the metal imido bond to give unclassical β-agostic silylamido complexes was observed. These species display 3-centre 2-electron interactions between the Si-H bond and the metal centre, such as (ArN)Mo(η^3-NAr-SiHPh-H)(SiH_2Ph)(PMe_3) (**II-56**) Since it had been postulated that key intermediates of hydrosilylation reactions display nonclassical Si-H coordination to metal centres[3,13], it was decided to test **II-56** as a catalyst in the hydrosilylation of unsaturated compounds.

The reduction of aldehydes, ketones, nitriles by silane and alcoholysis of $PhSiH_3$ gave their respective products in moderate to good yields.[12] A detailed investigation into the kinetic and stoichiometric reactivity of complex **II-56** with alkenes and silanes provided insight into the mechanism of hydrosilylation of ethylene. Unfortunately, the mechanism of carbonyl hydrosilylation remains elusive as stoichiometric and labelling studies did not provide much insight into a possible scheme. Scheme 15 shows the proposed cycle for ethylene hydrosilylation. The first step involves insertion of ethylene into the Si-H_{ag} bond *via* silanime formation to give the vinyl silane complex **II-57**. This step was supported by the preparative scale synthesis of **II-57** which was obtained directly from **II-56** by addition of excess ethylene. Addition of $PhSiH_3$ results in hydrogenation of the ethyl moiety on the silylamido fragment giving the agostic ethylene complex (ArN)Mo(SiH_2Ph)(η^2-C_2H_4)(η^3-NAr-SiEtPh-H). Ethylene can be substituted for PMe_3 followed by detachment of the silane product by silyl group exchange and regeneration of complex **II-56** (Scheme 15). This final step is highly unusual and

was postulated to take place via silane addition across the second Mo=N bond to give a bis(silylamido) species, followed by reversal Si-H elimination of the more substituted silane.

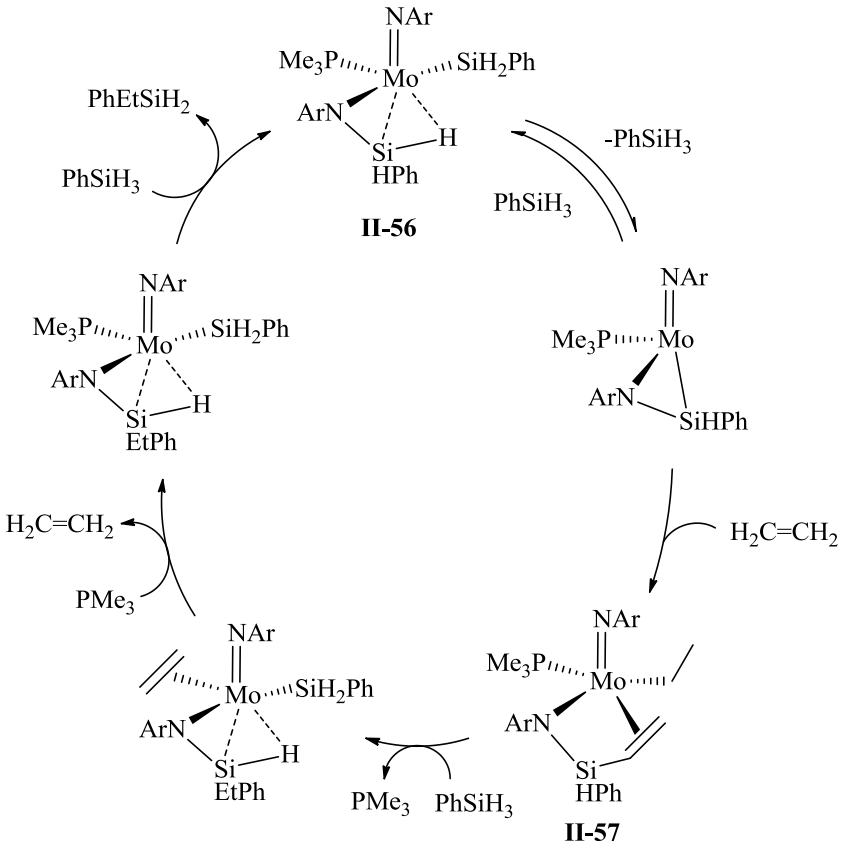

Scheme 15 – Hydrosilylation mechanism of ethylene using the *β*-agostic silylamido catalyst **II-56**.

Recently, Nikonov and co-workers investigated catalytic hydrosilylation of carbonyls using four related Mo(IV) complexes (ArN)Mo(PMe_3)$_3$(H)(Cl) (**II-58**), (R)(ArN)MoH(PMe_3) (R = Tp (**II-59**), Cp (**II-60**); Tp = tris(pyrazolyl) borate) and (ArN)Mo(PMe)$_3$(SiH_2Ph)(H) (**II-61**). In-depth mechanistic studies revealed unusual pathways devoid of both silane addition across the metal-imido bond and direct Si-H/ Mo-Cl bond metathesis as in the cases of Toste[71] and Abu-Omar[55], respectively (see Scheme 11 and Scheme 12). The mechanism of benzaldehyde hydrosilylation using complex **II-58** as a catalyst begins with initial PMe_3 dissociation of the

trans-to-hydride phosphine giving the unsaturated intermediate (ArN)Mo(PMe_3)$_2$(H)(Cl) which is quickly intercepted by the aldehyde to give complex **II-62** (Scheme 16A). Slow dissociation of a second phosphine and insertion of benzaldehyde gives the benzoxy complex **II-63**. Addition of $PhSiH_3$ regenerates the hydride complex by either oxidative addition of the Si-H bond to the metal, through formation of a silane σ-complex, or by heterolytic splitting of the silane on the Mo-O bond. This model was a good fit for benzaldehyde but when ketones, such as acetophenone or cyclohexanone. were used as substrates different observations were observed. For example, the 1:1:1 reaction between **II-58**, acetophenone and $PhSiD_3$ results in 80 % retention of **II-58** (i.e. 20 % deuteration in the hydride position) and PhCD(CH_3)OSiD_2Ph, indicating a possible non-hydride mechanism.[72]

Analogous labelling experiment was also applied to various other catalytic systems beginning with the tris(pyrazolyl) borate complex **II-59**. Initially, stoichiometric reactions with both silanes and aldehydes led to the conclusion of a typical mechanism involving aldehyde insertion into the Mo-H bond, heterolytic cleavage of silane on the Mo-OR bond, and regeneration of the catalyst. However, cyclohexanone insertion into the Mo-H bond requires longer reaction times (50 °C for many days), whereas catalysis occurs much faster (53 min. using cyclohexanone). The 1:1:1 reaction between **II-59**, PhCHO and $PhSiD_3$ results in retention of complex **II-59** and formation of PhCHDO-SiD_2Ph (Scheme 16B), indicating that the hydride from the complex is not transferred to the substrate as required by the conventional hydride mechanism. Explicit deuteration of only the substrate during both the labelling experiment and a catalytic run, suggests that carbonyl insertion into the Mo-H bond is not relevant to the catalytic cycle. The 1:1:1 addition of catalyst, substrate and deuterated silane was tested using other systems, including Toste's Re-oxo complex (O=)($PhMe_2SiO$)Re(PPh_3)$_2$(I)(H)[71], Abu-Omar's Re

hydride complex (O=)(PhMe$_2$SiO)Re(PPh$_3$)$_2$(I)(H)[55] and the Stryker reagent (Ph$_3$PCuH)$_6$ used by Lipshutz *et al.*, each of which showed retention of the respective hydride complex and deuteration of the silylether product. Thus, Lewis acid activation of the carbonyl was suggested as a simple mechanism avoiding hydride formation during the catalytic cycle.

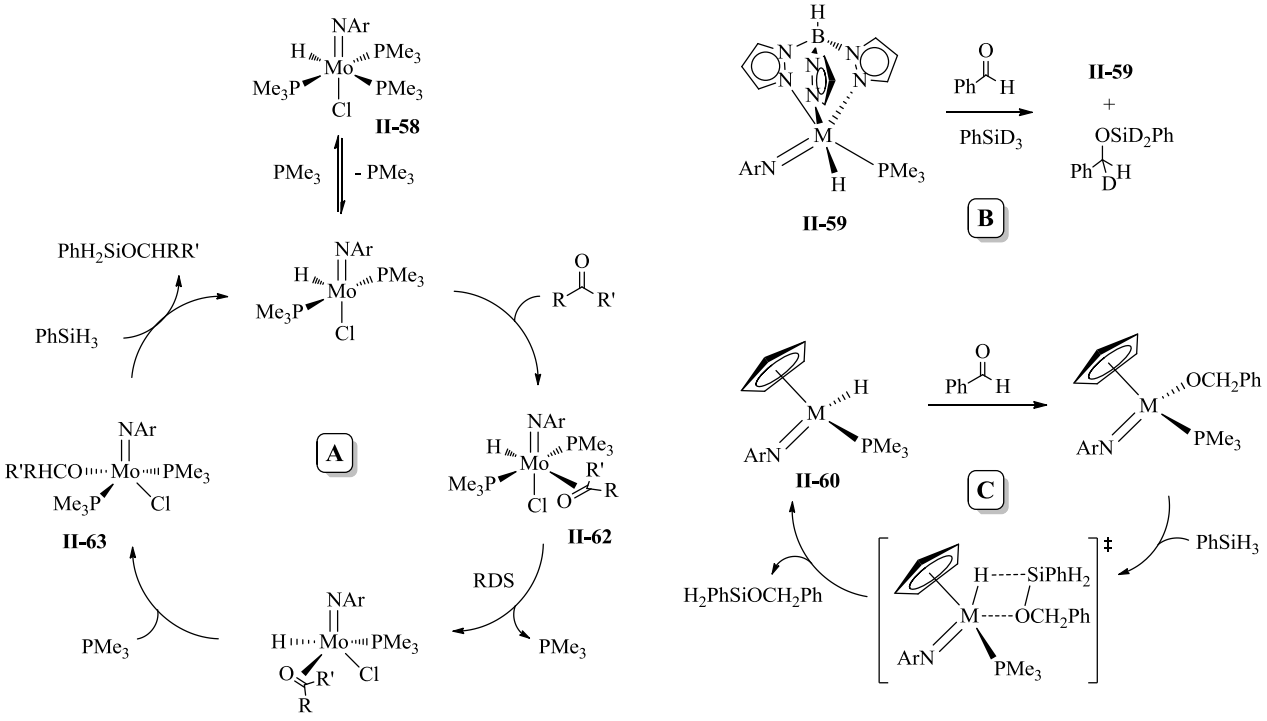

Scheme 16 – Mechanisms of carbonyl hydrosilylation mediated by (ArN)Mo(PMe$_3$)$_3$(H)(Cl) (**II-58**; **A**), (Cp)(ArN)Mo(PMe$_3$)(H) (**II-60**; **C**) and labelling experiment for the deduction of a non-hydride mechanism using (Tp)(ArN)Mo(PMe$_3$)(H) (**II-59**; **B**).

The related Cp hydrido derivative of complex **II-59**, (Cp)(ArN)MoH(PMe$_3$) (**II-60**), was also found to be an active catalyst in the hydrosilylation of carbonyls. However, mechanistic investigation led to the conclusion of the Mo-H playing a crucial role in the catalytic cycle. DFT calculations, kinetic analysis and stoichiometric reactivity aided in better understanding the mechanism shown in Scheme 16C. Addition of benzaldehyde to **II-60** proceeds without

phosphine dissociation and gives the insertion product (Cp)(ArN)Mo(OCH_2Ph)(PMe_3) which showed similar rates of catalysis to **II-60**. However, addition of $PhSiH_3$ to **II-59** gives (Cp)(ArN)Mo(SiH_2Ph)(PMe_3), which is not an active catalyst. DFT calculations aided in deducing a possible catalytic cycle. A simple mechanism involving carbonyl insertion into the Mo-H bond generates the alkoxy complex followed by σ-bond metathesis with silane to give the silylether product and regeneration of **II-60**.[73]

Finally, reacting complex **II-58** with $LiBH_4$ and $PhSiH_3$ gives the silyl hydride complex (ArN)Mo(PMe_3)$_3$(SiH_2Ph)(H) (**II-61**), which showed greater activity towards carbonyl hydrosilylation than complex **II-58**. Interestingly, different mechanisms were proposed for aldehydes and ketones based on their diverse stoichiometric reactivities. Ketones react with **II-61** to give the insertion product (ArN)Mo(PMe_3)$_2$(SiH_2Ph)(OR) (R = iPr, Cy) and no silylether production even when excess substrate was used. Alternatively, the addition of excess benzaldehyde quickly generates the silyl ether product ($PhHSi(OBn)_2$) and forms the complex (ArN)Mo(PMe_3)$_2$(η^2-O=CHPh)$_2$ (**II-64**) containing two side-on coordinated benzaldehyde ligands. $PhSiH_3$ addition to **II-64** gives the silyl hydride derivative **II-61**. DFT calculations on the model system (PhN)Mo(PMe_3)$_3$(SiH_2Me)(H) suggest the mechanistic pathways shown in Scheme 17. For ketones (Me_2C=O), initial PMe_3 dissociation gives **II-65**, followed by ketone insertion into the Mo-H bond to give the alkoxy silyl derivative **II-66.** Complex **II-66** undergoes heterolytic splitting of $PhSiH_3$ by the Mo-O bond to form the silyl ether adduct **II-67**, which dissociates the respective silyl ether product and regenerates complex **II-65** (Scheme 17; left). Aldehyde hydrosilylation begins with formation of the bis(aldehyde) complex (ArN)Mo(PMe_3)$_2$(η^2-O=CHPh)$_2$ (**II-64**) as seen from stoichiometric reactivity's. Dissociation of a second PMe_3 ligand stabilizes the system and allows for $PhSiH_3$ addition to give the η^1-silane intermediate **II-**

68. Rearrangement of complex **II-68** into the silyl alkoxy derivative **II-69** followed by PMe_3 addition gives the silyl ether complex **II-70**. Complex **II-70** regenerates complex **II-64** upon addition of another equivalent of benzaldehyde which liberates the silyl ether product (Scheme 17; right).[15]

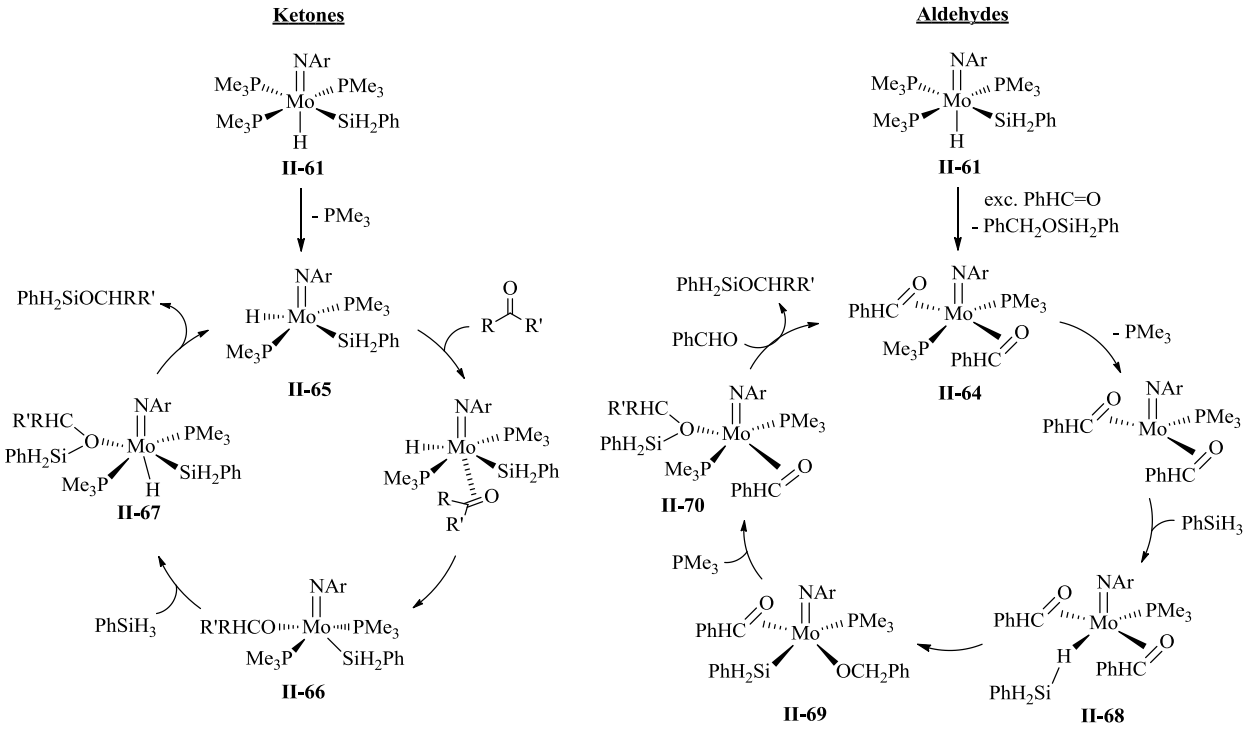

Scheme 17 – Hydrosilylation of ketones (left) and aldehydes (right) mediated by $(ArN)Mo(PMe_3)_3(SiH_2Ph)(H)$ (**II-61**).

II.3 Cyclometallation of Tertiary Phosphine Complexes

The term cyclometallation can be defined as a transition metal-mediated activation of a C-R (R = H, O, Si) bond to give a new metallacycle *via* a direct metal-carbon σ bond.[74] Intramolecular activation of the C-R group is preceded by initial coordination of a donor ligand such as N, O, or P. This is known as a heteroatom-assisted process (Scheme 18).[74,75] Therefore, the formation of a cyclic organo-transtion metal complex containing a metal-carbon σ-bond and a metal-donor atom is achieved under relatively mild conditions. Activation of both aliphatic and aromatic C-R bonds is common and an abundance of examples exist generating various sized ring structures. Ring sizes range from three to seven, with five being the most common. A large amount of research has been devoted to C-H bond activation and is of interest from a synthetic and industrial point of view. Many mechanisms involving catalytic conversions of hydrocarbon feedstock's into valuable products are believed to be dictated by similar cyclometallation processes.[76]

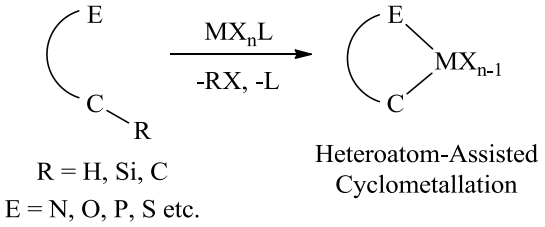

Scheme 18 – General schematic for the intramolecular heteroatom-assisted cyclometallation using transition metal complexes.

In particular, complexes containing phosphine donor atoms producing aryl carbon-metal σ-bonds, also called *ortho*-metallated complexes are of interest. These typically occur between a PPh_3 ligand and a specific metal centre, which produces a 4-membered metallacycle. An alternative example of *ortho*-metallated compounds are those containing pincer ligands, in

particular those of palladium with the general formula [PdX{1,3-$C_6H_3(CH_2PR_2)_2$}] (X = anionic ligands; R = multiple substituents), which are used for carbon-carbon bond forming processes such as Mizoroki-Heck, Suzuki and Stille type reactions.[77-79] Importantly, these phosphine metallated Pd(II) complexes (Figure 5; right) are thermally stable and were found to be better catalysts for the cross coupling of bulky aryl halides which typically need elevated temperatures to obtain products in high yields. Previous Pd(0) catalysts (Figure 5; left) were unable to achieve similar results.[77]

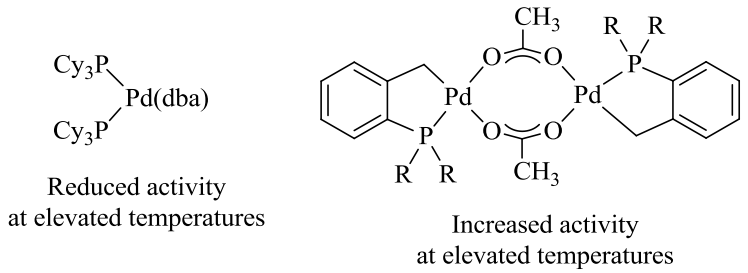

Figure 5 – Examples of Pd(0) (left) and Pd(II) complexes used at elevated temperatures for the Mizoroki-Heck, Suzuki and Stille type cross-coupling reactions.

Some of the first examples of *ortho*-metallated PPh_3 complexes were found in the late 1960's by three groups independently. Parshall observed deuterium exchange of all *ortho*-hydrogens for the $Co(H)N_2(PPh_3)_3$ complex and suggested that it goes *via* an *ortho*-metallation of each PPh_3 ligand at the Co centre.[80] Bennet and Milner described the *ortho*-metallated hydrido-iridium(III) complex upon heating of $[IrCl(PPh_3)_3]$ in inert solvents.[81] Likewise, Keim found that heating $[RhMe(PPh_3)_3]$ eliminates methane upon oxidative addition of the *ortho*-hydrogen on one PPh_3 ligand (Figure 6).[82]

Many other examples exist for almost all transition metals, which were structurally studied by X-ray diffraction analysis and spectroscopically characterized by NMR and IR spectroscopy. Much attention has been focused on late transition metals such as Ru, Os, Rh, Ir,

Pd, and Pt, with palladacycles being studied in greatest detail.

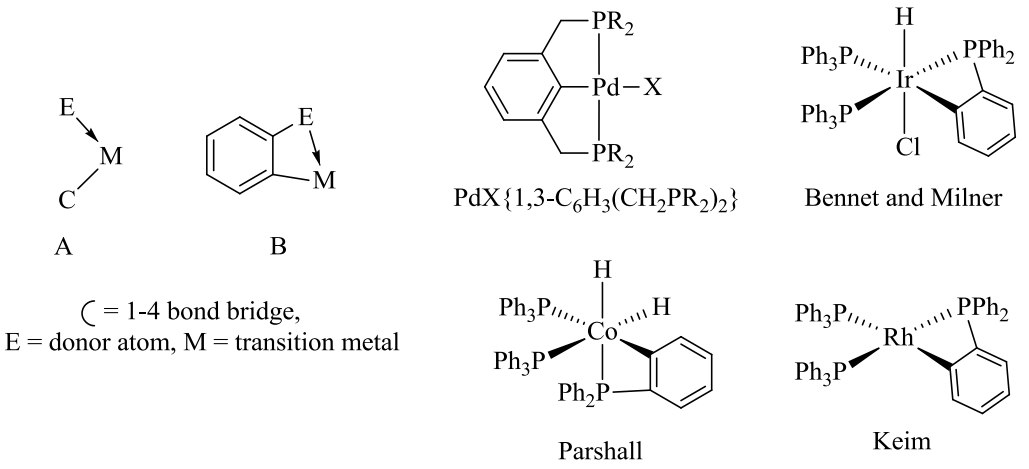

Figure 6 - Representation of different binding modes for cyclometallated complexes, and examples of *ortho*-metallated phosphine complexes.

From a synthetic point of view, thermal or photochemical activation of the *ortho* C-H bond of PPh_3 ligands is the simplest way to generate *ortho*-metallated complexes. Typically, migration of the *ortho*-hydrogen to the metal centre *via* oxidative addition is the first step to take place. Many studies, both computational and experimental, have proven the occurrence of an agostic C-H interaction[83,84], however direct population of the σ*-antibonding orbital of the C-H bond can induce a formal two-electron transfer from the metal to the ligands, thereby providing

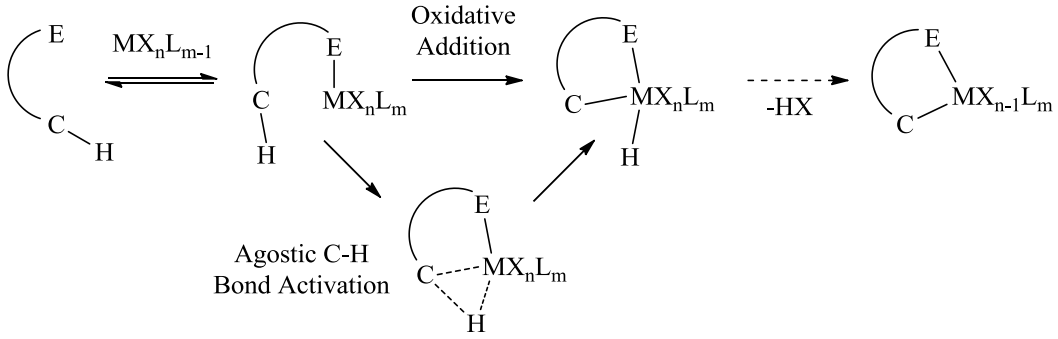

Scheme 19 – Proposed reaction pathway for the intramolecular cyclometallation of C-H bonds. direct oxidative addition with no intermediate formation.[81]

Despite the vast library of *ortho*-metallated phosphine complexes, a much more uncommon cyclometallation process is the formation of three-membered metallacycles, especially those containing a phosphorous heteroatom. In many cases, the donor group is trimethylphosphine (PMe_3), which initially coordinates to an electron rich metal centre which further induces *β*-C-H activation of the methyl group. However, this is not always the case as examples of α-C-H activation of a methyl group on 1,2-bis(dimethylphosphino)ethane (dmpe) exist, as well as α-C-H activation of of a methylene unit of triethylphosphine ligand. Interestingly, the first report of cyclometallation was initially founded by Chatt and Davidson in 1965 who observed the pyrolysis of $Ru(dmpe)_2(C_{10}H_9)$ (**II-71**) complex converts into a C-H activated three-membered metallacycle *via* the methyl group of the dmpe ligand.[85] This was initially characterized by IR analysis and classified as an intramolecular process, but almost a decade later the solid state structure was elucidated by X-ray crystallography and was determined to be a dimeric structure with two bridging P-CH_2 linkages between two Ru (II) centres. In spite of these subtle differences in mechanisms of activation, this provided a novel method for mild C-H activation.

Of the three membered metallacycles isolated thus far, oxidative addition is typically thought of as being the most viable pathway, consistent with similar mechanisms described for *ortho*-metallated species. In all cases, initial ligation of the donor atom (ie. PMe_3) to the metal centre is assumed or in some cases observed. Intramolecular activation of a C-H bond from a tertiary phosphine ligand then completes the cyle. However, in some cases addition of a base is used to promote deprotonation of an α-C-H hydrogen followed by subsequent attack of the resulting activated carbon towards a metal centre. The following sections will provide accounts of complexes containing of a phosphine donor group and an activated α-hydrogen from an

aliphatic carbon to produce a three-membered cyclometallated species. Interesting examples of reactivity have been shown across the metal-carbon bond or through the metal-hydride bond. These include reactions with electrophiles, such as methyl iodide (MeI), carbon disulfide, carbon dioxide, Ge-X and Pb-X (X = Cl, Br) bonds.[86] Categorization will be based on the respective transition metal groups (i.e. groups 3 through 10), with a large focus on the work done by Parkin *et al.* on the tungsten $W(PMe_3)_4(\eta^2\text{-}PMe_2CH_2)H$ complex.

II.3.1 Phosphine Cyclometallation: M-C-P Rings of Group 3 to 5 Metals

Cyclometalled phosphine complexes are extremely rare for early transition metals from groups 3 to 5, with only a few examples found in the literature. However, two examples of scandium and zirconium bearing phosphinomethyl groups ($M\text{-}CH_2PMe_2$) exist and provide some insight into the unfavourable formation of cyclometallated three membered rings. Bercaw and coworkers[87] attempted to obtain a better understanding of the mechanism of β-R (R = H, CH_3) elimination using the *ansa*-scandocene complex $OpSc(H)(PMe_3)$ ($Op = \{\eta^5\text{-}C_5Me_4)_2SiMe_2\}$) (**II-72**) leading to the discovery of an interesting degradation pathway and the generation of an phosphinomethyl complex. This reaserch was carried out in the context of studying olefin insertion into metal-carbon or metal-hydride bonds, which represents an important step in many polymerization processes. Reacting **II-72** with isobutene results in complete insertion of the olefin into the M-H bond to generate $OpSc\{CH_2CH(CH_3)_2\}(PMe_3)$ (**II-73**). Decomposition of **II-73** led to the production of the methyl complex $OpSc(CH_3)(PMe_3)$ (**II-74**), a variety of hydrocarbon byproducts as well as the alkenylphopsphine complex $OpSc(CH_2PMe_2)$ (**II-75**).[87] The authors suggested initial PMe_3 dissociation followed by insertion of isobutene into the Sc-H bond, and re-addition of PMe_3. This final addition of PMe_3 *via* C-H/Sc-C σ-bond metathesis is

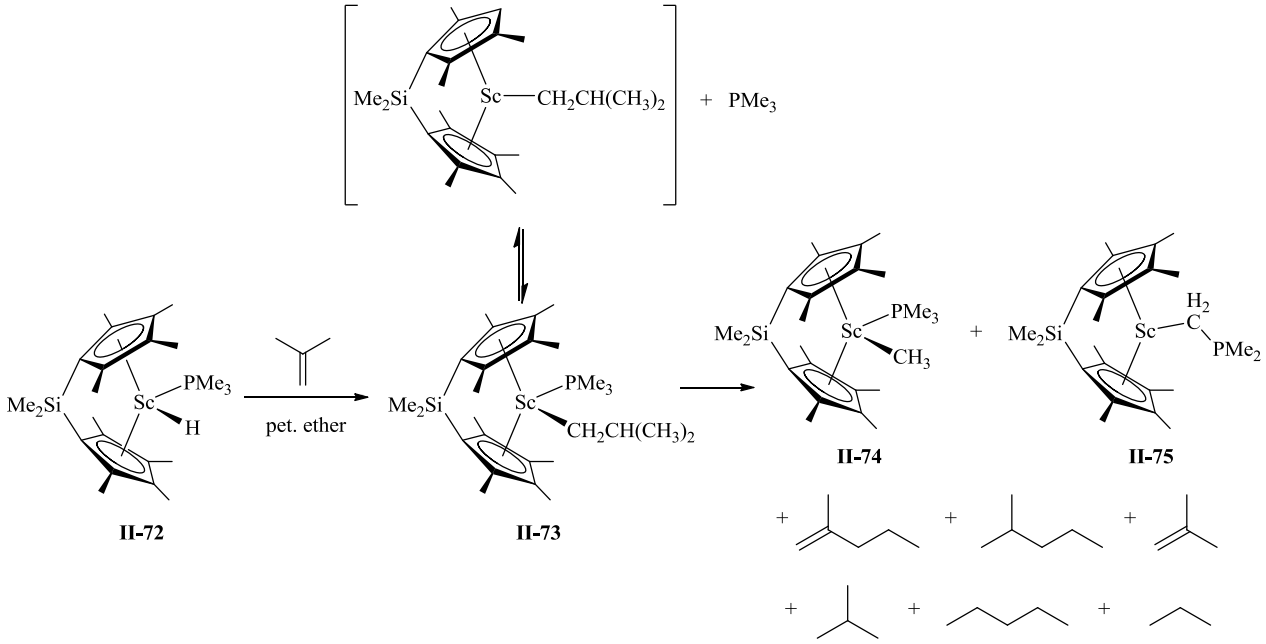

Scheme 20 - Synthesis of the cyclometallated complex **II-75**, alkyl chain byproducts and **II-74**.

the key step which generates all alkane and alkene byproducts. Although kinetic experiments could not sufficiently provide evidence for the mechanism, detailed NMR analysis gave some insight into the nature of the intermediates formed during the course of the reaction. Many of these intermediates were characterized as alkyl complexes with the general formula $OpSc(CH_2R)(PMe_3)$ (R = $(CH_2)_3(CH_3)$, $(CH_2)_4(CH_3)$, $CH(CH_3)(CH_2)_2(CH_3)$, $CH(CH_3)_2$). Addition of excess PMe_3 (11 equivalents) slows down the rate of formation of **II-74**, supporting the claim for equilibrium formation of all alkyl complexes in solution. Complex **II-75** gives rise to a diagnostic methylene doublet at 0.32 ppm (C_6D_6) in the ^{1}H-NMR spectrum coupled to phosphine with a $^2J_{H\text{-}P}$ value of 9.09 Hz. The methyl groups appear as one doublet with a smaller $^2J_{H\text{-}P}$ value of 5.96 Hz. Unfortunately, no further studies were done to provide evidence as to the nature of phosphine binding to the scandium centre.[87]

Conversely, the zirconocene phosphinomethyl complex $Cp_2Zr(Cl)CH_2PPh_2$ (**II-76**) has been studied in great detail, with a large amount of evidence to suggest a non-bonding situation

between the phosphine and metal centre. Shore and coworkers[88] initially synthesized compound **II-76** by reacting Cp_2ZrCl_2 with Ph_2PCH_2Li(TMEDA) at -78 °C, and were able to obtain a crystal structure for this complex showing a large 130 ° Zr-C-P angle and a long M-P distance of 3.75 Å. This seemed unusual due to the 16-electron nature of the d^0-Zr centre, which would seem to prefer phosphine coordination. An extensive molecular orbital study for $Cp_2Zr(Cl)CH_2PH_2$ showed the most energetically favourable complex to contain an η^2-coordinated P-C bond to the metal centre but once the steric effects of the two phenyl groups were employed, the η^1-coordination becomes the lowest energy structure. This was largely due to the steric influence of the phenyl groups, as well as some electronic contributions from the destabilized Zr-Cl π-antibonding interactions.[89] NMR analysis does not suggest phosphine coordination with the methylene protons appearing at δ = 1.68 ppm ($^2J_{H\text{-}P}$ = 2.9 Hz) in the ^{1}H-NMR, and a -1.8 ppm resonance in the ^{31}P-NMR spectrum typical for a simple tertiary phosphine. Interestingly, when **II-76** is treated with Na/Hg, ESR measurement provided evidence for a paramagnetic Zr (III) cyclometallated complex $Cp_2Zr(\eta^2\text{-}PPh_2CH_2)$ (**II-77**) that can be isolated as a pink solid. This displays a large doublet (a = 19.5 G, ^{31}P, I = ½, 100%) and an overlapping a doublet of septets (a = 13.5 G, ^{91}Zr, I = 5/2, 11.23 %) corresponding to a coordinated phosphine atom to the Zr centre in the ESR spectrum. Alternatively, complex **II-77** can be generated in solution (along with an equivalent of $Cp_2Zr(CH_2PPh)(H)$ by heating a THF solution to 60 °C for an extended period of time.[90] Due to the paramagnetic nature of this compound, NMR data were unobtainable; however 20% conversion to an NMR active dinuclear Zr complex **II-78** (Scheme 21) is obtained during reduction of **II-76**.[91] Similarly, monitoring the decomposition products showed the appearance of a dinuclear zirconium complex $[CpZr(MePPh_2)]_2[\mu\text{-}(\eta^1,\eta^5\text{-}C_5H_4)]_2$ (**II-79**) bridged by an η^1-coordinated Cp ring, formed *via* metathesis of the C-H bond to the Zr-C bond to

generate free $MePPh_2$.

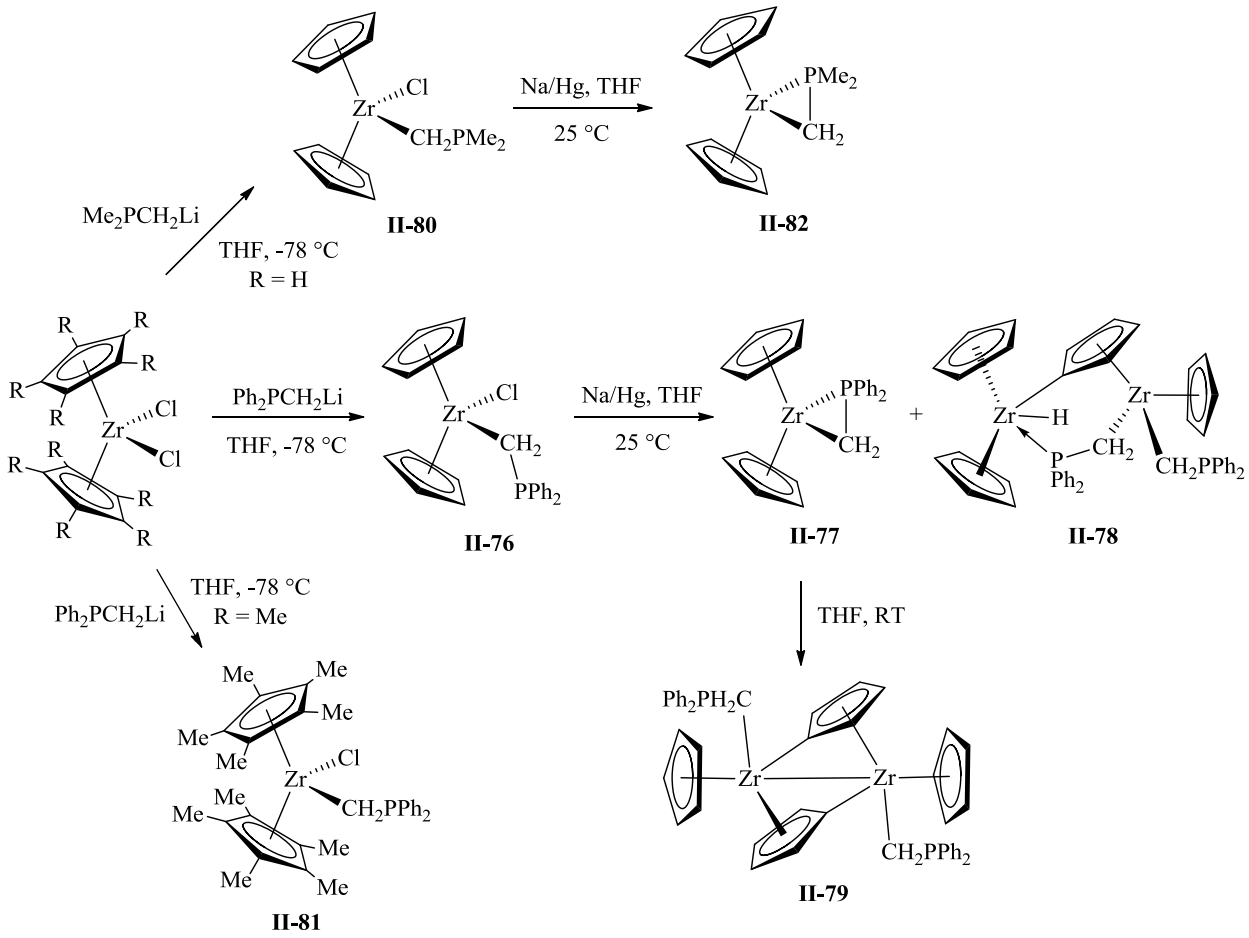

Scheme 21 – Synthesis of the cyclometallated complexes **II-77** and **II-82** with 20 % formation of complex **II-78**. Decomposition product **II-79** and phosphinomethyl derivatives **II-80** and **II-81** are shown.

Young and coworkers[92] examined the nature of phosphine binding in two distinct zirconocene phosphinomethyl complexes $Cp_2Zr(Cl)CH_2PMe_2$ (**II-80**) and $(Cp^*)_2Zr(Cl)CH_2PPh_2$ (**II-81**). Crystal structure analysis showed an unusually open Zr-C-P angle of 130° and a non-bonding Zr-P distance of 3.724 Å for complex **II-80**. Interestingly, the bulkier complex **II-81** displayed a shorter Zr-P contact (3.56 Å) and Zr-C-P angle (118°) placing the tertiary phosphine in a position suitable for partial overlap with the central lobe of the LUMO of the metal. Both

complexes were still found to be non-cyclometallated but reduction of **II-80** *via* sodium amalgam results in production of the paramagnetic cyclic species $Cp_2Zr(\eta^2\text{-}PMe_2CH_2)$ (**II-82**). Complex **II-81** does not display any observable (by ESR spectroscopy) hyperfine coupling between the Zr centre and phosphine ligand upon reduction due to the steric influence of the methyl groups on the Cp* rings.[92]

Complex **II-77** was found to be active catalyst in the hydrogenation of olefins and diolefins. In particular, specific reduction to the mono-ene species in the case of cyclo-octa-1,3-diene was observed. [93] Interestingly, stoichiometric reactions of alkenes with $Cp_2ZrH(CH_2PPh_2)$ lead to initial formation of the expected insertion product $Cp_2Zr(n\text{-alkyl})(CH_2PPh_2)$ followed by decomposition into **II-77** and release of the linear alkyl chain (i.e. hexane, cyclohexane, cyclobutane). No formation of the related $[Cp_2Zr(\mu\text{-}CH_2PPh_2)(\mu\text{-}CH{=}CHCH_2CH_3)ZrCp_2]$ by reacting $Cp_2ZrH(CH_2PPh_2)$ with butadiene was observed, which was attributed by the authors to the instability of the alkylzirconium species.[94]

The first of two tantalum complexes to exhibit a cyclometallated M-C-P group was found in 1983 by Gibson and coworkers[95] and was crystallographically characterized as $Ta(PMe_3)_3(\eta^2\text{-}CH_2PMe_2)(\eta^2\text{-}CHPMe_2)$ (**II-83**). This is a rare example of a cyclometallated M-C-P complex containing a carbene linkage to the metal centre. The position of the carbene hydrogen was found within the plane of the Ta-C-P ring and the Ta-C bond length of the carbene carbon was 0.31 Å shorter than that of the methylene carbon. ^{1}H-NMR data support this structure, with the C-H carbene proton displaying a resonance at 9.46 ppm as a dddt with the $^1J_{P\text{-}H}$ values of 21.5 Hz, 16.3 Hz and 3.2-3.24 Hz corresponding to coupling to the phosphine in the ring, the two phosphines sitting in the same plane as the P-C-Ta ring, and the *cis* phosphines in the apical positions of the P-C-Ta ring, respectively. The methylene C-H protons show a resonance at -0.87

ppm, with a splitting pattern displaying a ddt with the $^{1}J_{P\text{-}H}$ values of 13.8 Hz, 4.9 Hz, and 2.3 Hz. No further investigations into the mechanism of activation were undertaken.[95]

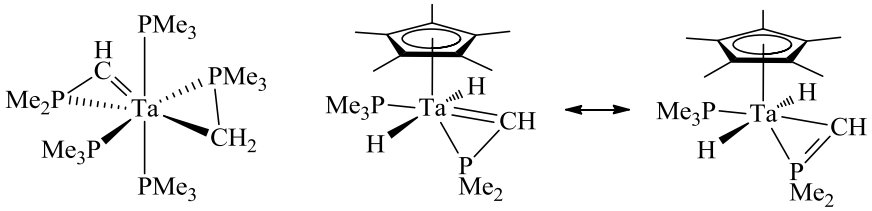

II-83 **II-84**

Another example of carbene coordination by the oxidative addition of two C-H protons of a PMe_3 ligand was shown by Kee and co-workers who synthesized the cyclometallated tantalum complex $Cp^*Ta(PMe_3)(H)_2(\eta^2\text{-}CHPMe_2)$ (**II-84**) by reducing Cp^*TaCl_4 with sodium in trimethylphosphine. **II-84** was crystallograhically characterized but the methylidyne proton and hydrides were not located in the crystal structure determination. The Ta-C bond length (2.005(10) Å) falls in the range of typical Ta=C double bonds, but the Ta-P bond length (1.714(9) Å) is shortened compared to other Ta-P single bonds, which was attributed by the authors to a delocalization between the two structures shown above. IR and NMR analyses suggest the presence of two hydride groups as well as the carbene linkage through the cyclometallated ring. The stretching frequency at 1635 cm^{-1} in the IR spectrum and the doublet of doublet at 3.87 ppm in the ^{1}H-NMR spectrum were attributed to two hydride ligands. The methylidyne proton was located at 9.19 ppm in ^{1}H-NMR and the low field ^{13}C resonance at 191.2 ppm ($^{1}J_{C\text{-}H}$ = 169.8 Hz) is typical for methylidyne carbons. Reactivity studies with complex **II-84** were conducted with simple small molecules, such as carbon monoxide and hydrogen gas, to afford the bisphosphine complexes $Cp^*Ta(PMe_3)_2(CO)_2$ and $Cp^*Ta(PMe_3)_2H_4$. Interestingly, insertion into the Ta-H bond was observed when electrophiles, such as MeX (X = I, Br) or chloroform, were added to **II-14** to give the monohydride $Cp^*Ta(PMe_3)(H)(X)(\eta^2\text{-}$

$CHPMe_2$) (X = I, Br, Cl) complexes or bis(halide) complexes upon addition of a second equivalent, with the ring structure remaining completely intact.

II.3.2 Phosphine Cyclometallation: M-C-P Ring of Group 6 Metals

The majority of reactivity studies performed on cyclometallated three-membered rings containing the M-C-P vertices has been done with group 6 metals. In particular, the tungsten complex $W(PMe_3)_4(\eta^2\text{-}CH_2PMe_2)H$ (**II-85**) was prepared and fully characterized by Gibson and co-workers in 1983. Since this time Parkin and coworkers have utilized this compound for a number of different transformations. Due to the fluxional behaviour of the molybdenum analogue, it is difficult to synthesize but the $Mo(PMe_3)_6$ (**II-86**) derivative is much more stable and typically used instead. This section will provide an overview of all studies done in this field pertaining to both Mo and W complexes. To date no cyclometallated three-membered metallacycles (M-C-P) have been found for chromium. Interestingly, Steinborn and co-workers synthesized the homoleptic chromium complex $[\{Li(thf)\}_2Cr_2(CH_2PMe_2)_6]$ (shown below) which contains a strong Cr^{II}-Cr^{II} quadruple bond (195.0(2) pm). This is a rare example of a bridging (dimethylphosphino)methyl ligand in a μ-η^2 fashion.[96]

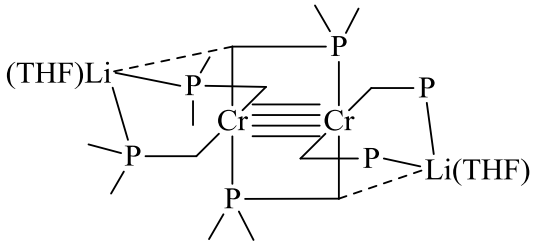

Complexes **II-85** and **II-86** were synthesized with the purpose of generating an electron rich centre which could be used for the activation of inert compounds, especially those containing C-H bonds or dinitrogen. Cloke and co-workers provided the first synthetic route to these species by metal vapour synthesis,[97] wherein metal beads are placed in a furnace and co-

condensed with excess PMe_3 followed by recrystallization to give the respective product. Using this method complex, **II-86** was obtained in 55 % yield (Scheme 22). In solution, an equilibrium mixture of two complexes exists, which were determined to be $Mo(PMe_3)_4(\eta^2\text{-}CH_2PMe_2)H$ (**II-87**) and $Mo(PMe_3)_5H_2$ (**II-88**). ^{1}H-NMR data contain hydride resonances at -4.00 ppm (quint, $^2J_{P\text{-}H}$ = 45.2 Hz) for **II-87** and -5.33 ppm (sext, $^2J_{P\text{-}H}$ = 40.5 Hz) for **II-88**. Complex **II-86** was characterized by X-Ray crystallography and found to contain an octahedral structure with elongated Mo-P bonds in all positions compared to other similar Mo(0) phosphine complexes, which is most likely due to the steric pressure caused by the relatively bulky six PMe_3 ligands.

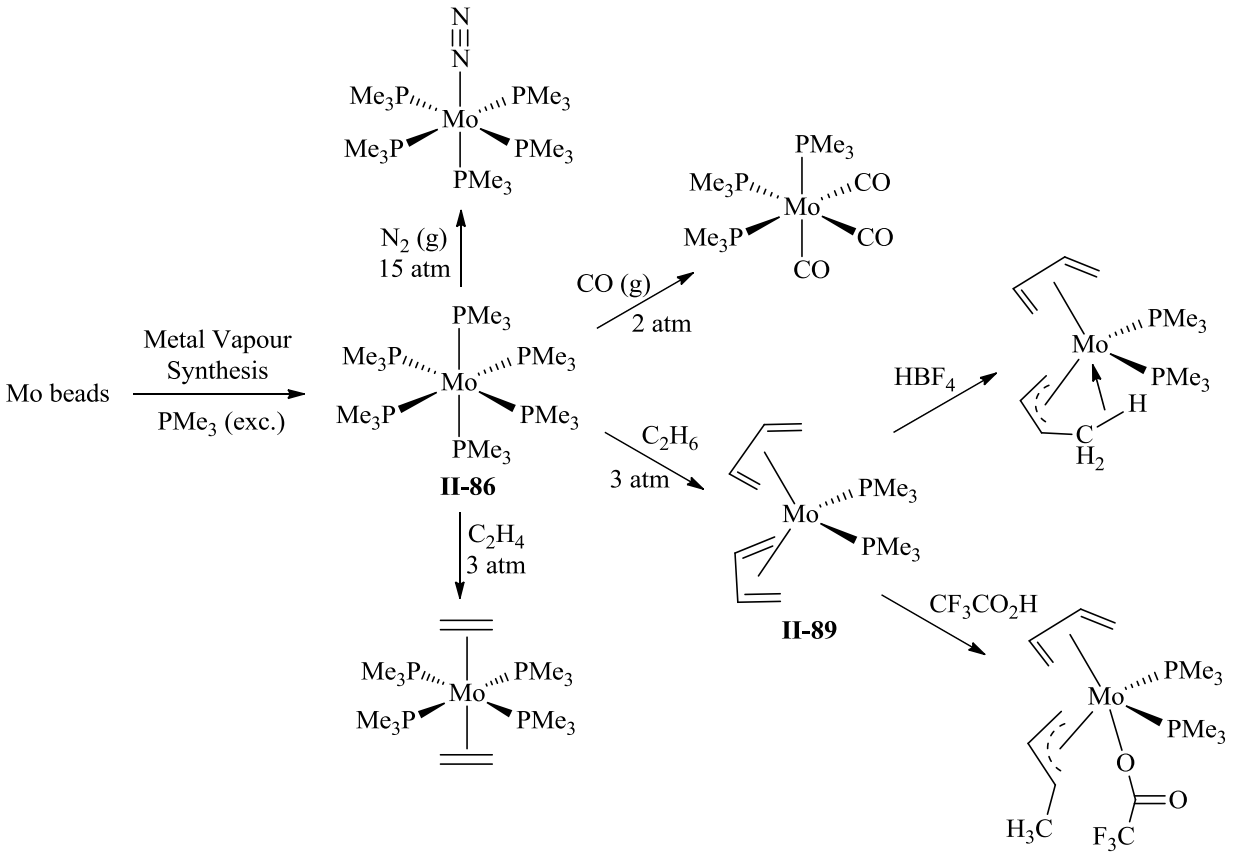

Scheme 22 – Synthesis and reactivity of complex **II-86** through metal vapour synthesis.

Treating solutions of **II-86** with dinitrogen results in loss of a phosphine ligands and coordination of N_2 to give $Mo(PMe_3)_5N_2$. Similar substitution reactions were seen using carbon

monoxide, ethylene, butadiene or cyclopentadiene (η^5-coordination), with substitution of one or two phosphine ligands.[98] Further studies with the butadiene complex *cis*-[$Mo(PMe_3)_2(\eta^4\text{-}C_4H_6)_2$] (**II-89**) were performed through the addition of tetrafluoroboric acid to give the interesting alyllic C-H agostic complex *cis*-[$Mo(PMe_3)_2(\eta^5\text{-}CH_2CHCHCH_2\text{-}H)_2(\eta^4\text{-}C_4H_6)$]$BF_4$ and trifluoroacetic acid to give the methylallyl complex $Mo(\eta^3\text{-}C_3H_4Me)(\eta^4\text{-}C_4H_6)(PMe_3)_2(O_2CCF_3)$ (Scheme 22).[99]

Complex **II-85** can be prepared in a similar manner through metal vapour co-condensation with excess PMe_3[86] or by reacting WCl_6 in PMe_3 with sodium sand[95] with average yields of 40%. Formation of $W(PMe_3)_6$ was not observed for each method used. However, this compound can be prepared by a quick workup of the reaction mixture for the reduction with Na(K) alloy. In solution, after 2 hours at room temperature slow conversion from $W(PMe_3)_6$ into **II-85** goes to full completion. Elucidation of activation parameters for this process suggests an entropically driven dissociation of PMe_3 in the rate determining step to give the 16-electron intermediate [$W(PMe_3)_5$], followed by a rapid oxidative addition of the PMe_3 C-H bond. The alternate mechanism involving PMe_3 dissociation accompanied by a concerted C-H bond activation is disfavoured due to the absence of significant kinetic isotope effect when $P(CD_3)_3$ was added to the mixture. Also, the addition of PMe_3 to the mixture results in a slower rate for conversion from $W(PMe_3)_6$ to **II-85**.[100]

Spectroscopic analysis revealed temperature dependence for **II-85** in the ^{1}H-NMR and ^{31}P-NMR. At -60 °C, the high-field W-H resonance at -3.75 ppm was observed as a doublet of doublet of triplets due to coupling with two equivalent and two inequivalent phosphines with the $^1J_{P\text{-}H}$ values of 9.5 Hz, 54 Hz and 78 Hz. At 25 °C, the hydride signal splits into a binomial quintet due to the fluxional behaviour of the four PMe_3 ligands which become equivalent at this temperature. Similar spectral data were seen in the ^{31}P-NMR, with four mulitplets observed at -

60 °C and broadening into two multiplets at room temperature, which is attributed to intramolecular exchange of the PMe_3 ligands.

Early reactivity studies using carbon monoxide, butadiene and dinitrogen gave simple substitution products resulting from loss of one or two PMe_3 ligands. Interestingly, reactions of **II-85** with 2 atm of either ethylene or propene result in dimerization of the ligand after a prolonged reaction time (4 days) to give $W(PMe_3)_2(\eta^4\text{-}C_4H_6)_2$ (**II-90**) and $W(PMe_3)_3\{\eta^4\text{-}CH_2C(Me)CHCH(syn\text{-}Me)H_2\}$ (**II-91**). Dihydrogen is heterolytically cleaved by complex **II-85** to give the dihydride species $W(PMe_3)_5H_2$ (**II-92**) upon addition of 2 atm $H_{2(g)}$ for 2 days at 70 °C. Further heating (120 °C) and prolonged reaction times (4 days) give the tetrahydride species $W(PMe_3)_4H_4$ (**II-93**). The addition of 1-2 atm of SiH_4 at 45 °C to **II-85** results in oxidative addition to give $W(PMe_3)_5(SiH_3)H$ (**II-94**) followed by the addition of one more equivalent of SiH_4 to give $W(PMe_3)_4(SiH_3)_2H_2$ (**II-95**). The IR spectra of **II-95** shows two stretches at 2040 and 1860 cm^{-1} which can be assigned to the Si-H and W-H bonds respectively. After 12 hours at 50 °C, ^{1}H-NMR analysis reveals a hydride resonance at -5.50 ppm (doublet of quintets) which converts slowly (2 days) into a hydride signal at -4.46 (quintet), which was suggested to be the conversion of **II-94** into **II-95**.[86] Reacting **II-85** with an arylhalide results in cleavage of a second methylene C-H proton of the cyclometallated ring to give the alkylidene species $[W(PMe_3)_4(\eta^2\text{-}CHPMe_2)H]X$ (X = Br (**II-96**), I (**II-97**)). Complexes **II-96** and **II-97** were crystallographically characterized and NMR data show downfield shifts for the ^{1}H-NMR (11.85 ppm, dquint) and ^{13}C-NMR (224.4 ppm, dd) of the alkylidene moiety. Fenske-Hall molecular orbital calculations allowed the description of this complex as an alkylidene-phosphine derivative due to the strong π-interaction of the W-C bond.[101]

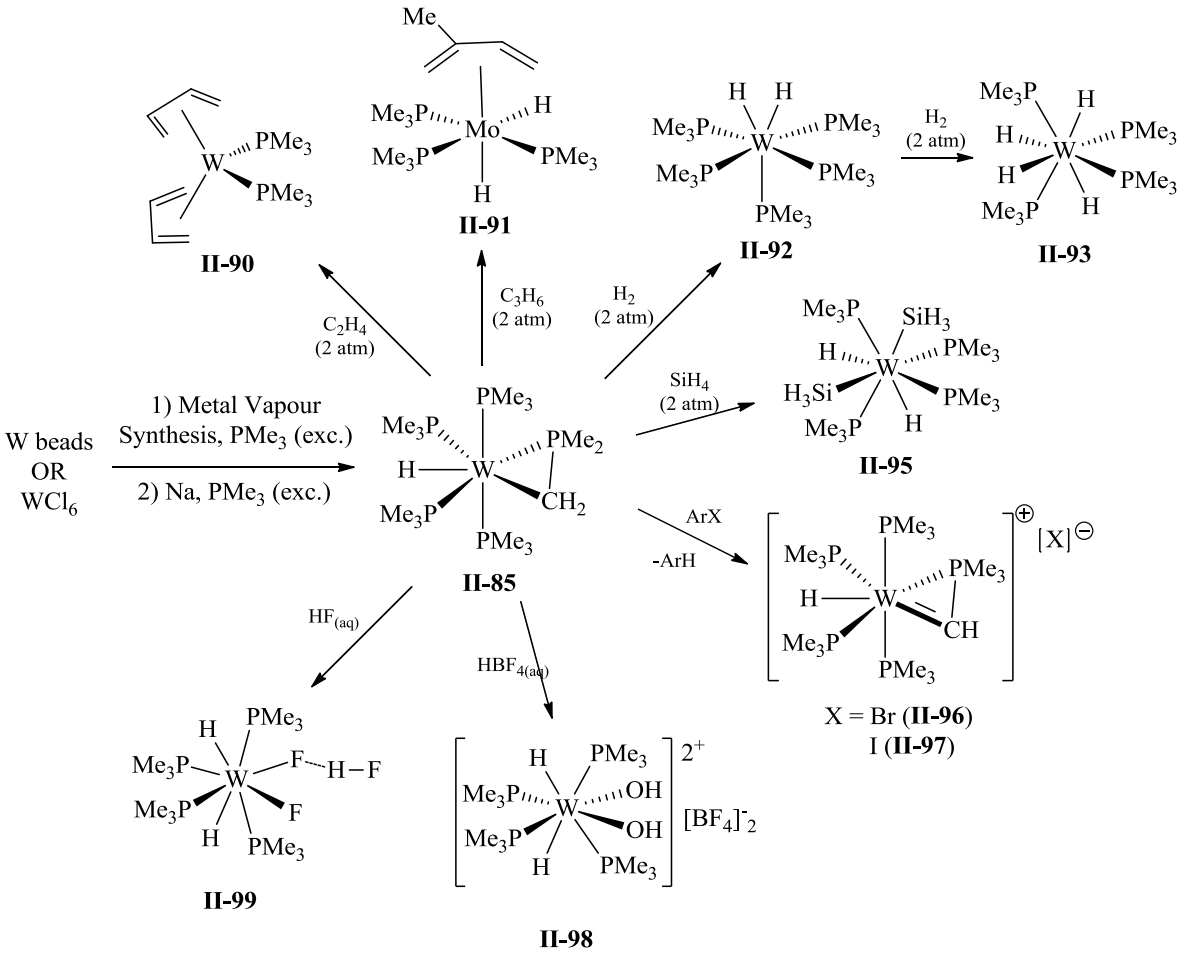

Scheme 23 – Synthesis and reactivity of complex **II-85** with various simple substrates.

Green and co-workers[102] studied the reactivity of protic acids, such as HBF_4, HF, HPF_6 and CF_3COOH. with complex **II-85**. Treatment with aqueous HBF_4 results in the bis(hydroxyl) product $[W(PMe_3)_4H_2(OH)_2][BF_4]_2$ (**II-98**) which can be transferred into **II-93** upon addition of a Na/K alloy in THF. IR confirms the presence of a hydroxyl group instead of aquo coordination of the water molecules, with a very strong band at 3470 cm^{-1}. Addition of aqueous HF to **II-85** results in the interesting cationic complex initially characterized by X-ray crystallography as $[W(PMe_3)_4H_2(OH_2)F]F$. However, it was found years later, through a neutron diffraction study, to contain a fluorine atom in place of the oxygen and was reformulated as $W(PMe_3)_4H_2F(FHF)$ (**II-99**), wherein one of the coordinated fluoride ligands is bound to an HF molecule via

hydrogen bonding.[103] The addition of potassium hydride to **II-99** results in formation of $W(PMe_3)_4(H)_2F_2$ (**II-100**). Protonation of **II-85** with aqueous HPF_6 and CF_3CO_2H gave the novel dihydride analogues $[W(PMe_3)_4H_2(OH_2)F][PF_6]$ (**II-101**) and $[W(PMe_3)_4H_2(O_2CCF_3)][CF_3CO_2]$ (**II-102**), respectively.

Extensive studies have been performed on the addition of alcohols to complex **II-85** . In particular, phenols provided unique structures. In the mid 1980's Green and co-workers[104] reacted **II-85** with methanol and were able to obtain the rare η^2-formaldehyde product $W(PMe_3)_4(\eta^2\text{-}CH_2O)H_2$ (**II-103**), which was the first of its kind to be prepared through methanol dehydrogenation. The proposed mechanism of activation involved initial oxidative addition of the MeO-H to the tungsten centre, followed by loss of PMe_3 ligand and subsequent oxidative addition of the C-H bond. Treating complex **II-103** with H_2 regenerates methanol and produces $W(PMe_3)_4H_4$ which goes through the intermediate trihydride complex $W(PMe_3)_4H_3(OMe)$.[104]

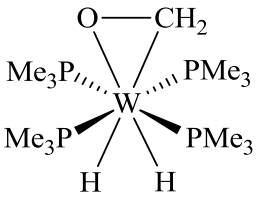

II-103

Reacting **II-85** and **II-86** with phenols results in the expected alkoxy insertion products which are quickly converted into metallacylces through C-H activation (**Scheme 24**). In 1990, Rabinovich and coworkers[105] formed four- and five-membered metallacycles by reacting **II-85** with substituted and unsubstituted phenols. Adding phenol directly to **II-85** results in complete conversion to the crystallographically characterized four-membered metallacycle $W(PMe_3)_4H_2(\eta^2\text{-}OC_6H_4)$ (**II-104**), in which the *ortho* carbon is bound to the tungsten centre. Reacting 2,6-dimethyl phenol with complex **II-85** gave a similar structure of five-membered

metallacycle $W(PMe_3)_4H_2\{\eta^2\text{-}OC_6H_3Me(CH_2)\}$ (**II-105**), in which the aliphatic methyl groups' C-H bond is cleaved. Preference for the 5-membered metallacyclic formation was observed when 2-methyl phenol was used but the addition of larger alkyl goups (i.e. Et, ^{i}Pr, ^{t}Bu) in the 2-position of the phenol ring results in a four-membered ring formation *via* activation of the aromatic *ortho*-C-H bond. In depth kinetic and labelling experiments showed an unusal activation mechanism of the phenol ring in which oxidative addition of the O-H bond across the metal centre does not occur. Rather, a direct interaction between the O-H bond and the W-C bond through either a protonation or metathesis reaction was observed to give the kinetic four-

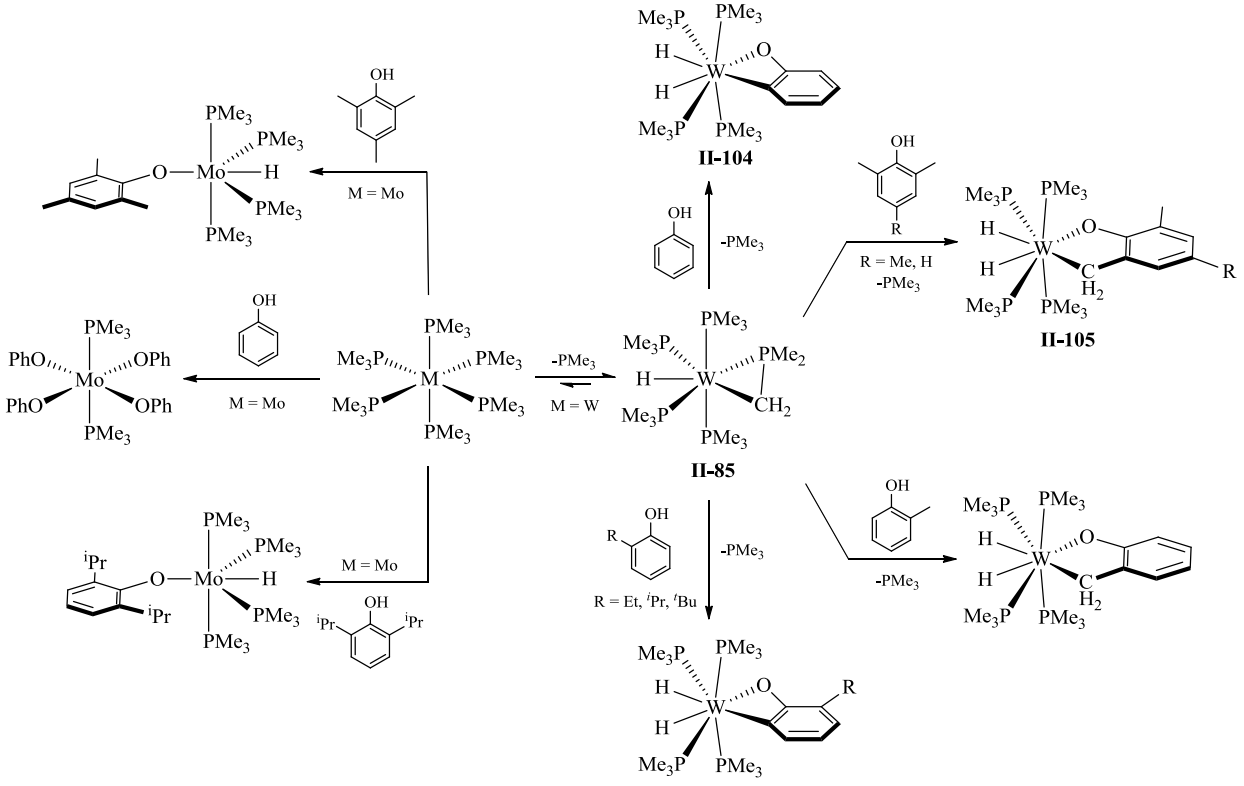

Scheme 24 – Synthesis of phenoxy complexes displaying 4- and 5-membered oxo-metallacycles based on reactivity of phenols with complex **II-85** and **II-86**.

membered metallacycle product or the thermodynamic five-membered metallacycle product.[100,105]

Complex **II-86,** on the other hand, reacts with substituted and non-substituted phenols to give the product of oxidative addition of the O-H bond across the metal centre with no cyclometallation to give 4-, 5-, or 6- membered rings. Addition of phenol gives the paramagnetic tetrakis(phenoxy) complex $Mo(PMe_3)_2(OPh)_4$ but with larger aromatic derivatives, such as 2,6-diisopropyl or mesityl, the monosubstituted hydride product $Mo(PMe_3)_4(OAr)H$ (Ar = 2,6-diisopropyl, mesityl) is produced. Based on deuterium labelling studies, the authors found scrambling into the *ortho*-methyl groups of the mesityl derivative, thus providing evidence of a reversible sp^3 C-H activation in a five-membered metallacyclic intermediate.[106]

In a search of oxo ligands that would act as linkers for multiple metal centres, Parkin's group studied the addition of two similar diphenols: bis(2-hydroxyphenyl)phenylamine and 2,2′-methylenebis(4,6-dimethylphenol) to complexes **II-85** and **II-86**. The products formed for the addition of bis(2-hydroxyphenyl)phenylamine to **II-85** are based on the ratio of ligand to complex and contain different binding modes that feature bidentate κ^2-O_2 or κ^2-OC, tridentate κ^3-O_2N and tetradentate κ^4-O_2CN coordinations. The addition of two equivalents gives the octahedral bis(diphenolate) complex $[\kappa^2\text{-}PhN(C_6H_4O)_2]_2W(PMe_3)_2$ (**II-106**), one equivalent gives the O-H and *ortho* C-H activated product $[\kappa^2\text{-}PhN(C_6H_4OH)(C_6H_3O)]W(PMe_3)_4H_2$ (**II-107**), and half an equivalent gives the dinuclear $[\mu\text{-}\kappa^2,\kappa^2\text{-}PhN(C_6H_4OH)(C_6H_3O)]\{W(PMe_3)_4H_2\}_2$ (**II-108**). Complex **II-107** participates in an O-H···O hydrogen bonding interaction which shows the preferred C-H activation as opposed to the expected O-H activation. This complex can react with one equivalent of $W(PMe_3)_4(\eta^2\text{-}PMe_2CH_2)H$ to generate complex **II-107** and can also convert to $[\kappa^3\text{-}PhN(C_6H_4O)_2]W(PMe_3)_4H_2$ (**II-109**) upon heating to 60 °C.[107]

Reacting the closely related 2,2′-methylenebis(4,6-dimethylphenol) with **II-85** in a 1:1

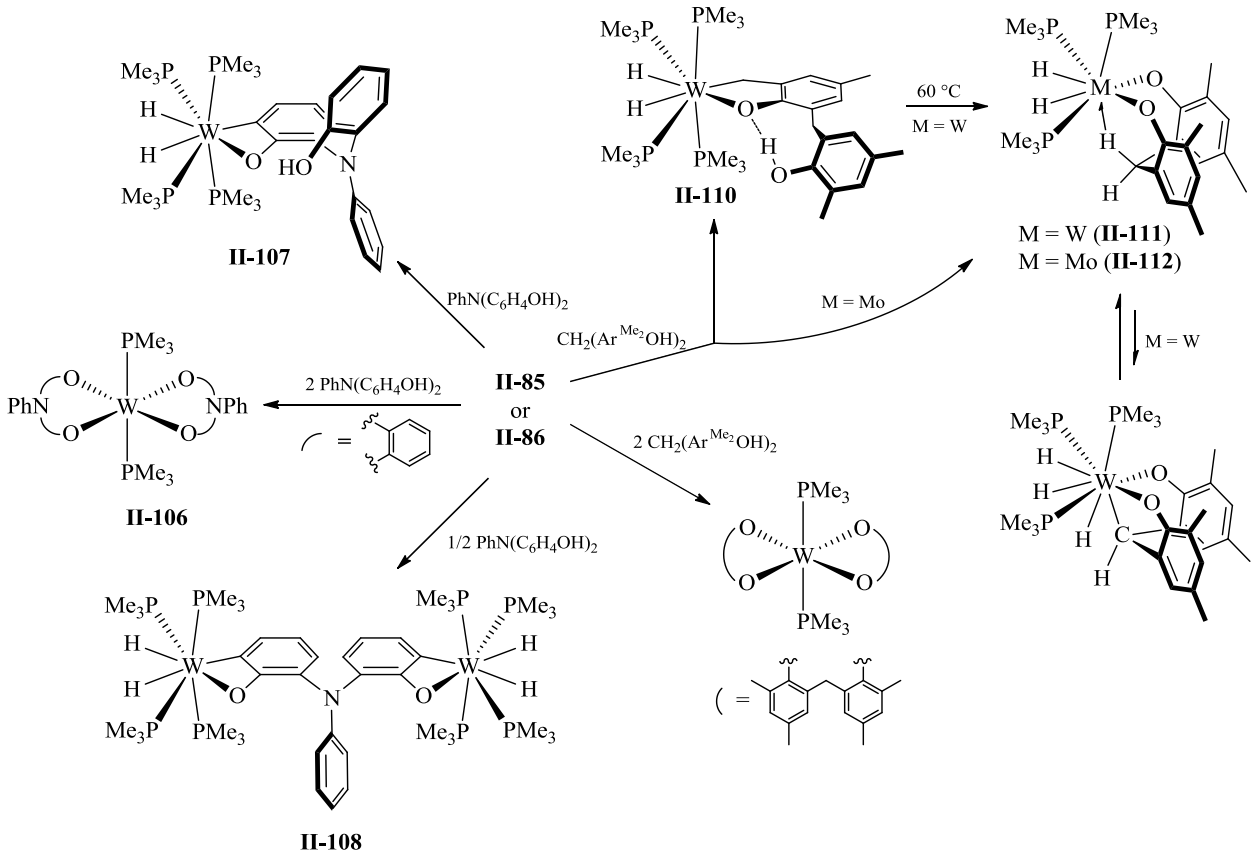

Scheme 25 – Addition of of $PhN(C_6H_4OH)_2$ and $CH_2(ArMe_2OH)_2$ to complexes **II-85** and **II-86** based on their stoichiometric equivalents.

stoichiometric ratio results in formation of the metallated monoxo-metallacyclic [κ^2-*O*,*C*-$CH_2(Ar^{Me}{}_2OH)\{C_6H_2Me)(CH_2)O\}]W(PMe_3)_4H_2$ (**II-110**) followed by conversion to the doubly O-H activated C-H agostic product [κ^2,η^2-$CH_2(Ar^{Me}{}_2O)_2]W(PMe_3)_3H_2$ (**II-111**), upon heating to 60 °C. **II-111** was found to be in equilibrium with the tridentate trihydride [κ^3-$CH(Ar^{Me}{}_2O)_2]W(PMe_3)_3H_3$ complex. Similarly, reacting this ligand with **II-86** results in initial formation of the C-H agostic product [κ^2,η^2-$CH_2(Ar^{Me}{}_2O)_2]M(PMe_3)_3H_2$ (**II-112**) which does not convert into the tridentate κ^3-O_2C complex even upon heating. However, adding a second equivalent of this ligand to **II-112** results in the bis(bidentate) complex [κ^2-$CH_2(Ar^{Me}{}_2O)_2]W(PMe_3)_2$.

The addition of *tert*-butyl carboxylic acid to **II-85** and **II-86** in water gives aqua-dihydride complexes of the type $M(PMe_3)_3(\kappa^1\text{-}O_2CBu^t)_2(OH_2)H_2$ (M = Mo (**II-113**), W (**II-114**)). Formation involves initial oxidative addition of one equivalent of carboxylic acid to give the carboxylate hydride complex $M(PMe_3)_4(\kappa^2\text{-}O_2CR)_2(OH_2)H_2$ followed by oxidative addition of another equivalent of acid to give the Mo(IV) or W(IV) complexes $M(PMe_3)_3(\kappa^2\text{-}O_2CBu^t)(\kappa^1\text{-}O_2CBu^t)H_2$ (M=Mo,W). Incorporation of one water molecule binds to the metal centre and stabilizes the η^1-coordination mode of the carboxylate groups through an intramolecular hydrogen bond.[108]

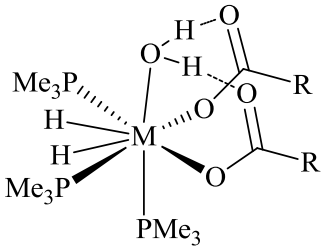

M = Mo (**II-113**), W (**II-114**)

Parkin's group synthesized a series of macrocyclic complexes featuring calixaranes and mercaptocalixaranes through the additions to both **II-85** and **II-86**. Adding one equivalent *p-tert*-$[Calix^{But}(OH)_4]$, or the tetrathiamercatocalixaranes $[S_4Calix^{But}(SH)_4]$ to both **II-85** and **II-86** results in complexes of similar composition, $\{[R]M(PMe_3)_3(H)_x\}$ (when R = $Calix^{But}(OH)_2(O)_2$, X=3, M = W (**II-115**), Mo (**II-116**) and when R = $S_4Calix^{But}(SH)_2(S)_2$, X=2, M = W (**II-117**), Mo (**II-118**), Figure 7).[109,110] Complexes **II-115** and **II-116** exist as an equilibrium in solution between the trihydride complex shown in Figure 7, as well as C-H agostic complex (not shown). The addition of two equivalents of $[S_4Calix^{But}(SH)_4]$ results in the dinuclear complex $[S_4Calix^{But}(S)_4][W(PMe_3)_3H_2]_2$ (**II-119**), which adopts both a *syn*- and *anti*-conformation in solution.

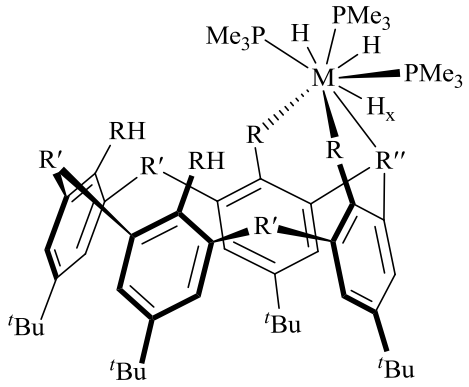

M = W, R = O, R′ = CH_2 , R″ = CH, X = 1 (**II-115**)
M = Mo, R = O, R′ = CH_2 , R″ = CH, X = 1 (**II-116**)

M = W, R = R′ = R″ = S, X = 0 (**II-117**)
M = Mo, R = R′ = R″ = S, X = 0 (**II-118**)

Figure 7 - *p-tert*-[Calix$^{Bu^t}$$(OH)_4$] and tetrathiamercatocalixaranes [S_4Calix$^{Bu^t}$$(SH)_4$] complexes of W and Mo, derived from **II-85** and **II-86**.

An in-depth look at hydrodesulfurization of thiophenes using complexes **II-85** and **II-86** was performed to ultimately remove sulfur impurities found in gasoline. Reacting one equivalent of thiophene with **II-86** produces the thiopene adduct (η^5-C_4H_4S)Mo$(PMe_3)_3$ (**II-120**) and the butadiene-thiolate complex (η^5-C_4H_5S)M(η^2-CH_2PMe_2)$(PMe_3)_2$ (M = W (**II-121**)[111], Mo (**II-122**)[112]) (Scheme 26). Complexes **II-121** and **II-122** exhibit a cyclometallated PMe_3 group which transfers the resultant hydride to the α-carbon of the thiophene ligand through a series of migrations and oxidative additions, as well as the generation of an important alkylidene species.[112] The addition of H_2 to **II-121** followed by thermolysis at 100 °C results in selective generation of but-1-ene and basic removal of any sulfur components. Interestingly, benzothiophene reacts with **II-85** and **II-86** to give alternate complexes in which the methylene carbon-sulfur bond is initially cleaved and isomerizes to give either an olefin-thiophenolate complex (κ^1,η^2-$CH_2CHC_6H_4S$)M$(PMe_3)_3$(η^2-CH_2PMe_2) (M = W (**II-123**), Mo (**II-124**)) or a 1-metallacyclopropene-thiophenolate complex (κ^1,η^2-$CH_2CC_6H_4S$)M$(PMe_3)_4$ (M = W (**II-125**), Mo (**II-126**)) depending on the temperatures used. The addition of H_2 to **II-125** and **II-126** results in formation of the trihydride thiolate complexes M$(PMe_3)_4$$(SC_6H_4Et)H_3$ (M = W (**II-127**), Mo (**II-128**)). Thermolysis of **II-127** at 100 °C results in selective generation of ethylbenzene through

HDS. Along the same lines, the addition of dithiobenzene to **II-85** gives an unusual dimeric tungsten species which upon addition of H_2 selectively gives biphenyl.

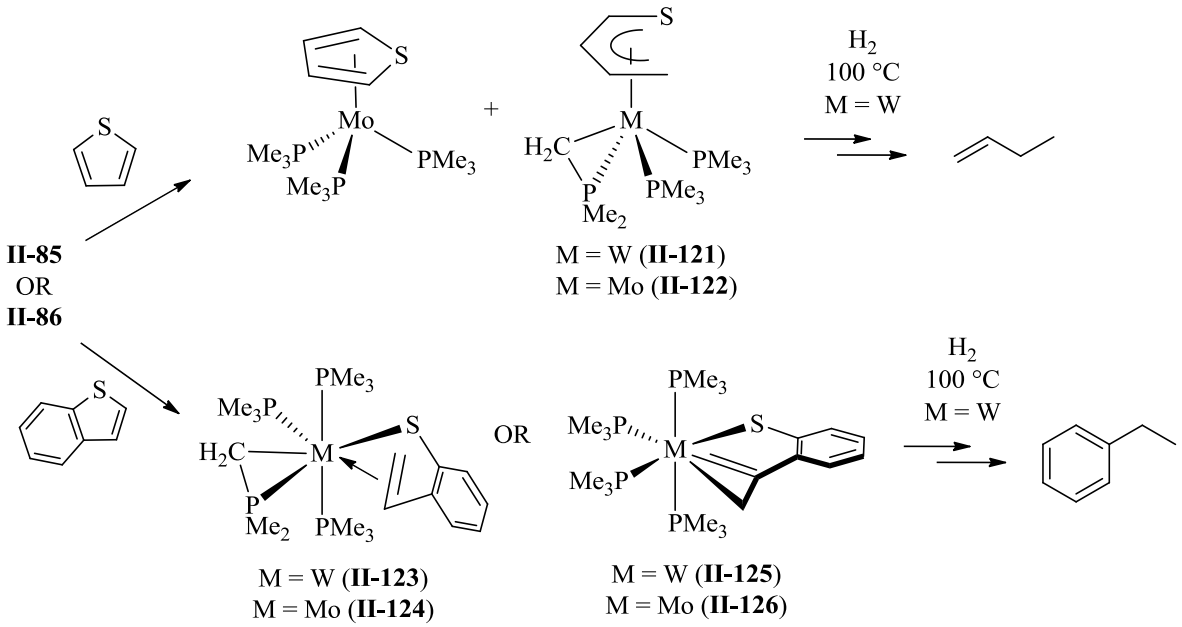

Scheme 26 – Hydrodesulfurization of thiophenes using complexes **II-85** or **II-86**.

A rare case of oxidative addition of a C-C bond to a transition metal centre was studied by Sattler and Parkin in 2010, where the addition of a quinoxaline to **II-85** results in the bidentate coordination brought about by C-C bond cleavage and dehydrogenation to give [κ^2-C_2-$C_6H_4(NC)_2$]W(PMe_3)$_4$ (**II-129**). Alternatively, the addition of the same substrate to **II-86** gives the expected (η^6-C_6-QoxH)Mo(PMe_3)$_3$ (Figure 8).[113] Crystal structure analysis for **II-129** shows that a C=C double bond of the quinoxaline ring is split by the metal as opposed to the expected splitting of the more reactive C=N bond. The suggested mechanism for formation of **II-129** involves the initial coordination *via* the N donor of the quinoxaline ring followed by oxidative addition of the *ortho*-hydrogen which induces a second oxidative addition of the adjacent ring C-H bond to give a dihydride species. Dehydrogenation followed by C-C bond cleavage gives the respective product. Theoretical calculations by three different research groups led to a better

understanding of the reaction pathway.[114-116] The basic mechanism was confirmed, although slight variations were obtained in the order of certain steps within the detailed mechanism at the theoretical level.

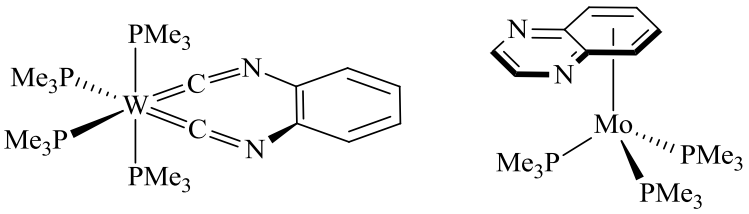

II-129

Figure 8 – C-C bond cleavage product **II-129** from the addition of quinoxaline to **II-85**.

Base-induced PMe_3 cyclometallation has been shown by van der Eide and co-workers upon addition of LDA of KCH_2Ph to the tungsten methylidyne species $(PMe_3)_4(Cl)W{\equiv}CH$. The resulting product $(PMe_3)_3(\eta^2\text{-}CH_2PMe_2)W{\equiv}CH$ (**II-130**) gives a cyclometallated PMe_3 group through initial nucleophilic substitution of the chloride ligand followed by deprotonation of the C-H proton (Figure 9). Based on X-ray crystallographic analysis, the methylene group of the cyclometallated ring was found *trans* to the methylidyne group. This results in significant lengthening of the methylidyne W≡C and methylene W-C bonds, possibly due to the strong competitive σ-donation from each ligand. The ^{1}H-NMR displays the methylene protons at -1.33 ppm (dddt) and the methylidyne signal at 8.61 ppm (ddtt), showing small observable coupling ($^4J_{H\text{-}H}$ = 0.9 ppm) to each other at room temperature. The $^{31}P\{^1H\}$ signal of the cyclometallated PMe_2 group shows a doublet of triplets with coupling to a mutually trans PMe_3 ligand and two inequivalent PMe_3 groups, confirming the C_s symmetry determined from the solid state structure.[117]

Another example of base induced cyclometallation came from Wolczanski`s group who were interested in generating low-coordinate, low-valent Group 6 M(II) compounds using the

bulky silox ligand (silox = $^{t}Bu_3SiO$) and subsequent trapping these species with PMe_3. In the case of the tungsten derivative, the reaction between $(silox)_3WCl$ and 2 equivalents of Na/Hg in the presence of 10 equivalents of PMe_3 selectively gave the cyclometallated species $(silox)_2HW(\eta^2\text{-}CH_2PMe_2)PMe_3$ (**II-131**, Figure 9). Alternatively, the same complex could be generated through the addition of four equivalents of Na/Hg in the presence of 3 equivalents of PMe_3 with $(silox)_2WCl_4$. The hydride signal was observed at 4.83 ppm in the ^{1}H-NMR and is located *trans* to the M-C-P metallacycle as determined by X-ray crystallography.[118]

Similar treatment of the cyclopentadienide tetrachloride complex $CpWCl_4(PMe_3)$ with excess Na/Hg (three equiv.) in the presence of PMe_3 gives the cyclometallated complex $Cp(H)(Cl)W(PMe_3)(\eta^2\text{-}CH_2PMe_2)$ (**II-132**, Figure 9). The ^{1}H-NMR shows a hydride signal at -5.99 ppm with a 16-line doublet of doublet of doublet of doublets splitting pattern due to the presence of diastereotopic methylene protons, two inequivalent phosphine ligands and ^{183}W satellites. The diastereotopic CH_2 signals are shifted to the high field region at δ 1.08 and 0.86 ppm. The four-legged piano stool structure of **III-132** was determined by X-ray crystallography

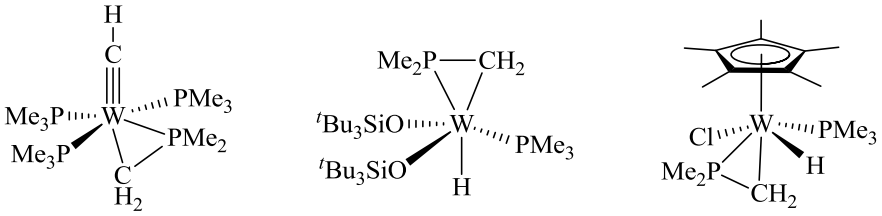

II-130 **II-131** **II-132**

Figure 9 – Examples of base-induced cyclometallations giving three-membered M-C-P rings.

and showed significant shortening of the cyclometallated W-P bond (2.35 Å) compared to the PMe_3 W-P bond (2.48 Å).[119]

In 2006 and later in 2008, Fillipou and coworkers showed interesting use of **II-85** to generate triple bonded species of both germanium and lead. The addition of one equivalent of the

bulky Ge^{II} compound RGeCl (R = C_6H_3-2,6-$Trip_2$, Trip = C_6H_2-2,4,6-^iPr) to **II-85** shows heterolytic cleavage of the Ge-Cl bond to give the $(PMe_3)_4ClW{\equiv}GeR$ (**II-133**) complex (Scheme 27). Low temperature NMR analysis showed initial formation of the hydrido-germylidene complex $(PMe_3)_3HClW\{\kappa^2$-P,Ge-$PMe_2(CH_2)Ge(R)\}$ confirmed by X-ray crystallographic analysis.[120] Similarly, reacting **II-85** with the dimeric aryl lead(II) amide $\{Pb(R)NMe_2\}_2$ (R = 2,6-$Trip_2C_6H_3$) or aryl lead bromide $\{Pb(R)Br\}_2$ gives the hydrido plumbylidyne complex *trans*-[H-$(PMe_3)_4W{\equiv}Pb$(2,6-$Trip_2C_6H_3$)] (**II-134**) or the bromo plumbylidyne complex *trans*-[Br-$(PMe_3)_4W{\equiv}Pb$(2,6-$Trip_2C_6H_3$)] (**II-135**), each confirmed by X-ray diffraction study (Scheme 27). Compound **II-134** displays a hydride quintet signal at -6.52 ppm and is located *trans* to the W≡Pb bond.[121]

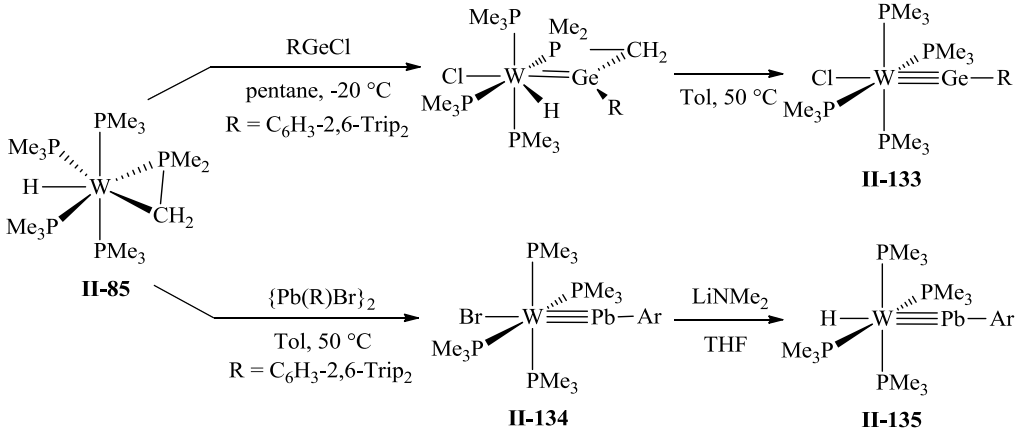

Scheme 27 – Generation of tungsten-lead and tungsten-germanium triple bonds from **II-85**.

II.3.3 Phosphine Cyclometallation: M-C-P Ring of Group 8 Metals

Compared to the large amount of work done on the corresponding tungsten cyclometallated compounds, much less attention has been focused on groups 8 through 10. The iron complex $(PMe_3)_3Fe(\eta^2$-$CH_2PMe_2)H$ (**II-136**) was independently synthesized in the mid 1970's by the groups of Muetterties[122] and Schmidbauer.[123] Each group was interested in

synthesizing electron rich metal centres using phosphine ligands. Muetterties and co-workers previously described the synthesis of the iron phosphite complex $Fe[P(OCH_3)_3]_5$ whereas their attempt to generate similar compounds through reduction of $FeCl_2(PMe_3)_2$ by Na/Hg resulted in formation of **II-136**. The IR spectrum showed a Fe-H band at 1820 cm^{-1} and a hydride resonance at δ – 14.7 ppm was observed by ^{1}H-NMR. The four phosphorous centres were found to be inequivalent through ^{31}P-NMR analysis. The high field resonance at δ 17.4 ppm in the ^{31}P-NMR was assigned to the cyclometallated phosphine. This was the first example of an intramolecular cyclometallation of a PMe_3 group on any transition metal centre.[122]

Karsch and co-workers determined the existence of an equilibrium between two alternative forms of **II-136**, $Fe^0(PMe_3)_4$ and $[(PMe_3)_3HFe(\mu\text{-}CH_2PMe_2)]_2$, with the cyclometallated being the most favoured. The addition of various ligands favouring low oxidation states of metals give the five-coordinate complexes $L_3L'_2Fe$ or $L_2L'_3Fe$ (L = PMe_3, L′ = CO, $P(OMe)_3$). The addition of protic acids largely result in $(PMe_3)_4FeH_2$ and iron (II) polymers.[124] The reaction of carbon dioxide with **II-136** led to an interesting discovery. When the reaction is performed at high temperatures in pentane, two products are formed, $(PMe_3)_4Fe(\eta^2\text{-}OC{=}O)$ and $(PMe_3)_4FeCO_3$, while using more polar solvents, such a THF, result in the insertion of CO_2 in the Fe-C bond to give $FeH(\kappa^2\text{-}O,P\text{-}OC(=O)CH_2PMe_2)(PMe_3)_3$ (**II-137**) followed insertion of another equivalent into the Fe-H bond to give $Fe[\kappa^2\text{-}O,O\text{-}OCH(=O)](\kappa^2\text{-}O,P\text{-}OC(=O)CH_2PMe_2)(PMe_3)_3$ (**II-138**).[125] Jones and coworkers[126] also found that reacting **II-136** with 3.5 equivalents of various isocyanides (CNR, R = 2,6-xylyl, Ph, CH_2CMe_3, ^{t}Bu, Me, ^{i}Pr) results in the generation of the isocyanide complex $(PMe_3)_2Fe(CNR)_3$.

An example of base-induced cyclometallation was shown by Antberg and co-workers in 1987 by reduction of the complex $FeCl_2[P(CH_2CH_2CH_2PMe_2)_3]$ containing a tetradentate

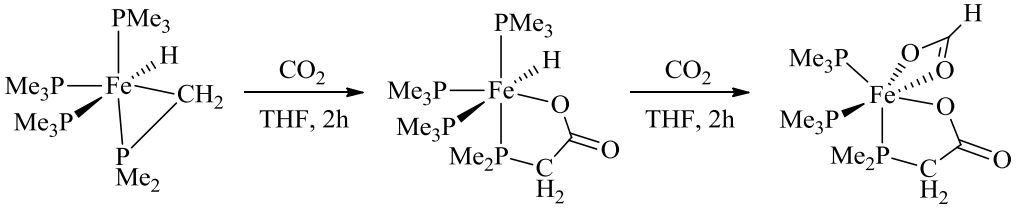

II-136 **II-137** **II-138**

Scheme 28 – Addition of CO_2(g) to the cyclometallated iron complex **II-136**.

phosphine ligand with Li in THF to activate one of the C-H bonds of the methyl groups to give FeH[P($CH_2CH_2CH_2PMe_2$)$_2$(κ^2-*P*,*C*-$CH_2CH_2CH_2$*P*(Me)-*C*H_2)] (**II-139**). Alternatively, the same procedure in the presence of $P(OMe)_3$ results in complete reduction to the Fe^0 complex Fe($P(OMe)_3$)[P($CH_2CH_2CH_2PMe_2$)$_3$]. The authors found that reacting complex **II-139** with CO_2 resulted in addition across the M-C bond and insertion into the Fe-H bond to give the FeH[P($CH_2CH_2CH_2PMe_2$)$_2$(κ^2-*P*,*O*-$CH_2CH_2CH_2$*P*(Me)CH_2C(=O)*O*)] complex.[127]

The Ru and Os derivatives of **II-136** could also be obtained through reduction using Na/Hg or $NaC_{10}H_8$ with *trans*-$MCl_2(PMe_3)_4$ to give the respective MH(η^2-CH_2PMe_2)$(PMe_3)_4$ [M = Ru (**II-140**)[128], Os (**II-141**)[129]] complexes. The reduction of the Os dichloride using Na/Hg does not provide any reactivity but the use of sodium napthalide gives the expected cyclometallated complex **II-141**. Complex **II-141** was also observed in the thermolysis of the tetraphoshine alkyl hydride complex $(PMe_3)_4OsH(CH_2{}^tBu)$ at 80 °C in cyclopentane.[130] Recently, complex **II-141** was prepared by the reduction using the easier-to-handle potassium graphite in THF.[131] The ^{1}H-NMR spectra of **II-140** and **II-141** exhibit the high field signals of their hydrides at δ -10.20 and -10.60 ppm, respectively, as well as the diastereotopic methylenes at δ -0.6/-0.59 and 0.45/-0.15 ppm. The inequivalency of each of the phosphine ligand was seen by ^{31}P-NMR displaying resonances of each phosphine group in each complex.

Compound **II-140** and **II-141** each react with electrophiles, such as CH_2X_2 (X = Cl, Br, I)

or MeI, to give the corresponding X/H exchange product derived from the initial M-H insertion compound $MX(\eta^2\text{-}CH_2PMe_2)(PMe_3)_3$ and the dihalo complexes *cis*-$MX_2(PMe_3)_4$. The diiodo complexes were postulated to form through attack of **II-140** or **II-141** at the methyl group of MeI to form the S_N2 substitution product $[HOs(CH_2PMe_2)(PMe_3)_3CH_3]^+I^-$ followed by elimination of methane and coordination of iodide. Reacting **II-140** or **II-141** with protic acids, such as HCl, CF_3CO_2H or PhC≡CH, results in generation of the tetraphosphine complexes $(PMe_3)_4MX_2$ (M = Ru; X = Cl, CF_3CO_2; M = Os; X = Cl, CF_3CO_2 or C≡CPh).[129] The addition of methanol to complexes **II-140** or **II-141** gives the initial O-H cleavage product *cis*-$MH(OMe)(PMe_3)_4$

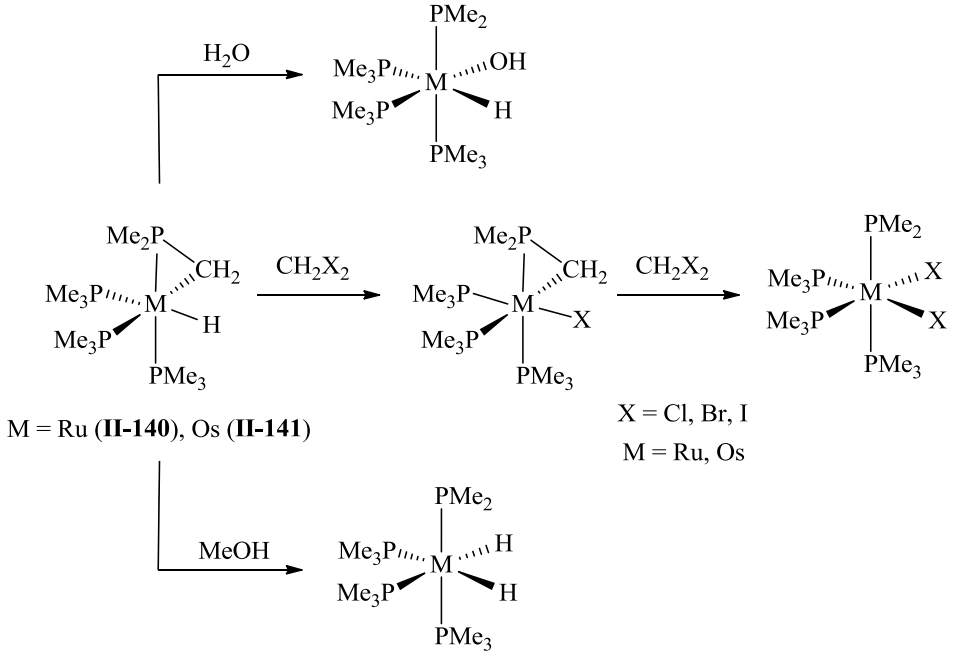

Scheme 29 – Addition of electrophiles, methanol and water to **II-140** and **II-141**.

followed by rearrangement into the dihydride complexes $MH_2(PMe_3)_4$ via β-CH activation in the methoxy ligand. The addition of H_2O to **II-141** results in generation of the hydroxyl hydride complex $(PMe_3)_4M(OH)(H)$ showing a hydride resonance at -8.0 ppm (ddt) and OH singlet at 2.73 ppm in the ^{1}H-NMR.[132]

In 2013, Bhadbhad and co-workers[131] studied the addition of CS_2 and CO_2 to complex **II-140** in the context of CO_2 utilization by means of transition metal catalysis. Similar to the results of Antberg discussed above, Bhadbhad's group found that carbon dioxide adds to the M-C bond to give [RuH(κ^2-*O*,*P*-OC(=O)CH_2PMe_2)(PMe_3)$_3$] (**II-142**) leaving the Ru-H bond intact. The Ru-H signal in the ^{1}H-NMR resonates at δ -8.29 ppm with a doublet of quartet splitting pattern ($^2J_{P\text{-}H}$ = 96.6 and 27.1 Hz), while the diasterotopic CH_2 group resonates at δ 2.54 and 2.32 ppm. Compound **II-142** was also characterized by X-ray crystallography showing the formation of the insertion product. Alternatively, the reaction with CS_2 at temperatures below 250 K initially generates the ([Ru(η^1-SC(=S)H)(η^2-CH_2PMe_2)(PMe_3)$_3$] (**II-143**) complex through attack at the Ru-H bond. Rearrangement, upon heating above 250 K, results in Ru-P bond cleavage to give

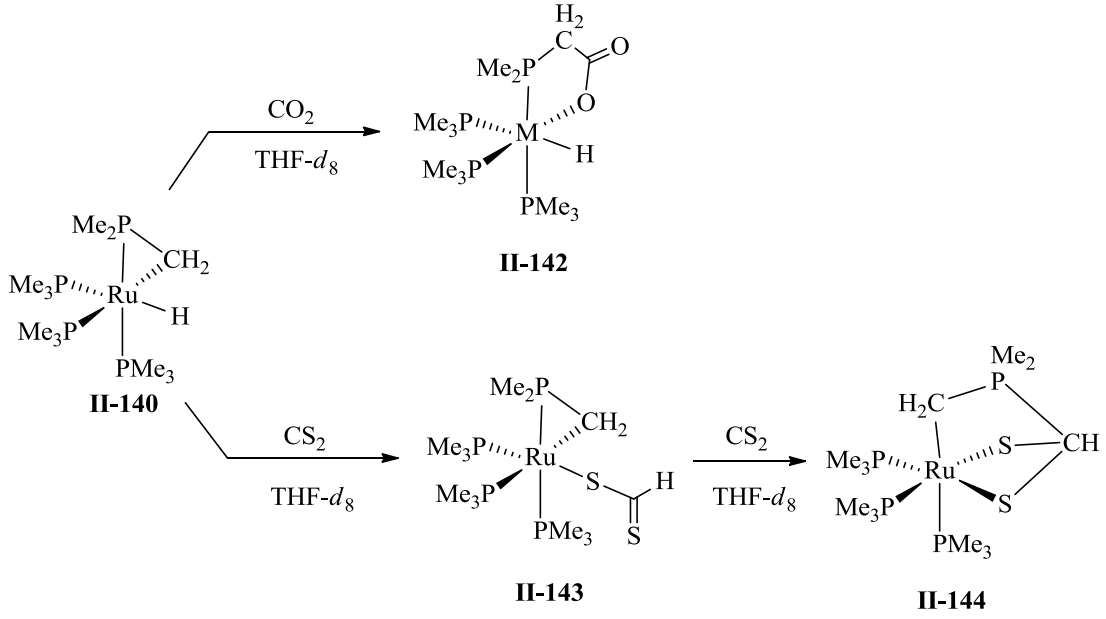

Scheme 30 – Differences in reactivity between CO_2 and CS_2 addition to **II-140**.

the tridentate complex [Ru(κ^3-*S*,*S*,*C*-S_2C(H)PMe_2CH_2-)(PMe_3)$_3$] (**II-144**). Adding excess CS_2 to this complex results in further addition across the Ru-S bond to give the [Ru(κ^3-*S*,*S*,*C*-*S*C(=S)SCH(−*S*)PMe_2*C*H_2-)(PMe_3)$_3$] (**II-145**).[131]

In their efforts to prepare Ru alkoxide complexes containing various phosphine ligands, Bergman's group found that addition of one equivalent of $LiBEt_3H$ to the dichloride tridentate phosphine complex $[MeSi(CH_2PMe_2)_3](PMe_3)RuCl_2$ results in selective salt elimination of one Ru-Cl bond to give the Ru-H complex $[MeSi(CH_2PMe_2)_3](PMe_3)Ru(H)(Cl)$. The addition of a strong base such as $KN(SiMe_3)_2$ or KO^tBu gives the cyclometallated product [κ^4-*P,P,P,C*-$MeSi(CH_2\mathit{P}Me_2)_2\mathit{CHP}Me_2](PMe_3)RuH$ (**II-146**), where one of the bridging CH_2 arms is deprotonated. Interestingly, heating the $[MeSi(CH_2PMe_2)_3](PMe_3)Ru(Me)(H)$ complex, generated from MeMgCl and hydride chloride precursor, gives a different type of cyclometallated product characterized as $[MeSi(CH_2PMe_2)_3]HRu(\eta^2\text{-}CH_2PMe_2)$ (**II-147**).[133]

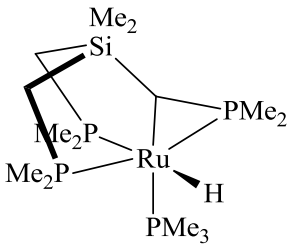

II-146

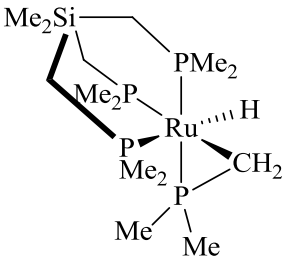

II-147

II.3.4 Phosphine Cyclometallation: M-C-P Ring of Group 9 Metals

Examples of group 9 cyclometallation through a phosphine ligand have been performed for the first time in 1981 by Al-Jibori and co-workers[134] who attempted to generate iridacycles through alkyl lithium addition. Surprisingly, they found that the dialkyl lithium species $Li(CH_2)_5Li$ or mono alkyl *n*-BuLi reacts with *mer*-$[IrCl_3(PMe_2Ph)_3]$ to give the cyclometallated compound $IrCl_2(PMe_2Ph)_2(\eta^2\text{-}CH_2PMePh)$ (**II-148**) where one of the C-H bonds of the phosphorous methyl group becomes deprotonated and attached to the metal centre. Optimization of conditions led them to use the bulky amide LiN^iPr_2 which gave **II-148** in 88 % yield. The ^{1}H-NMR shows the diastereotopic nature of the CH_2 group in the ring, showing resonances at δ 1.31

and 1.72 ppm ($^2J_{H-H}$ = 8.1 ppm). As well, a very high field shift of the ^{13}C signal is observed in the ^{13}C-NMR to δ -8.6 ppm (ddd).[134]

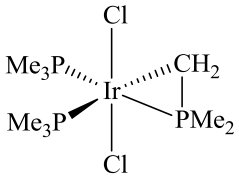

II-148

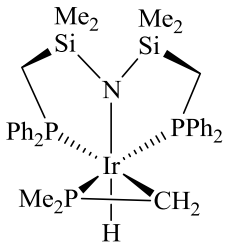

II-149

Later in 1987, Fryzuk and co-workers[135] found that heating $Ir(CH_3)PPh_2[N(SiMe_2CH_2PPh_2)_2]$to 50 °C in the dark results in the conversion to the cyclometallated complex *fac*-$Ir(\eta^2\text{-}CH_2PPh_2)H[N(SiMe_2CH_2PPh_2)_2]$ (**II-149**) where the tridentate ligand converts to the facial coordination mode and the resulting hydride sits *trans* to the amido donor. Interestingly, photolysis of the starting material or heating complex **II-149** results in the conversion to the Ir(I) phosphine complex $Ir(PMePh_2)[N(SiMe_2CH_2PPh_2)_2]$. The mechanistic pathway was studied in great detail, using kinetic analysis and stoichiometric reactivity studies. The conversion into **II-149** was suggested to go through initial C-H bond transfer from the methyl group to the phosphide centre bond generating a methylidene intermediate $(Ir(=CH_2)(PHPh_2)[N(SiMe_2CH_2PPh_2)_2]$. Then the P-H bond cleavage on the metal centre takes place to give the octahedral methylidene complex $(Ir(=CH_2)(PPh_2)(H)[N(SiMe_2CH_2PPh_2)_2]$ followed by transfer of phosphide to the carbon centre to give $(Ir(CH_2PPh_2)(H)[N(SiMe_2CH_2PPh_2)_2]$. Rearrangement and coordination of the lone pair on the phosphine centre gives complex **II-149**.[135]

Based on the ground-breaking work done by Bergman's group in the early 1990's on cationic iridium complexes in the context of mild C-H activation[136], Chen and co-workers became interested in understanding the mechanism behind this phenomenon using similar

complexes of the type $[CpIr(PMe_3)CH_3]^+$. Based on their initial work done in the gas phase using electrospray ionization and mass spectrometry, the C-H activation of a methyl group in the PMe_3 ligand results in methane loss and production of the cyclometallated Ir(III) complex $[CpIr(\eta^2\text{-}CH_2PMe_2)]^+$ (**II-150,** Scheme 31). Mass-spectroscopic studies of the addition of various R-D bonds (where R = alkyl or aryl, D = deuterium) to **II-150** showed deuterium incorporation into the PMe_3 group, which revealed the propensity of **II-150** to activate R-H bonds. Most

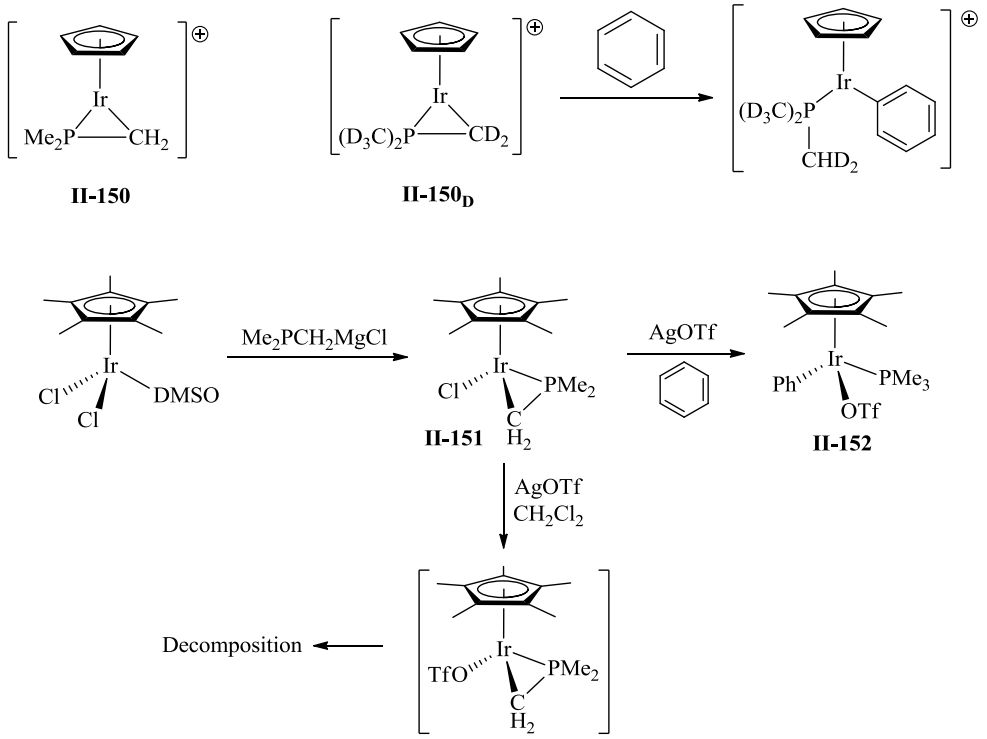

Scheme 31 – Chen (above) and Bergman's (below) work done to better understand the mechanism of C-H activation using complexes **II-150** and **II-151**.

importantly, the reaction of the *in situ* generated $[CpIr(\eta^2\text{-}CD_2P(CD_3)_2)]^+$ with C_6H_6 selectively generates $[CpIr\{P(CD_3)_2(CHD_2)\}(C_6H_5)]^+$.[137,138] Soon after Bergman and co-workers synthesized a derivative of Chen's complex through addition of $(Me_2PCH_2)MgCl$ to the Ir precursor $Cp^*(DMSO)IrCl_2$ to generate the cyclometallated $Cp^*Ir(\eta^2\text{-}CH_2PMe_2)Cl$ (**II-151**) complex (Scheme 31). Reacting **II-151** with AgOTf in benzene gives the C-H activated complex

Cp*Ir(PMe_3)Ph(OTf) (**II-152**). However, using CH_2Cl_2 as a solvent with AgOTf and excess benzene does not result in any C-H activated product, but only in decomposition. Based on these observations and the absence of deuterium incorporation into the PMe_3 ligand upon addition of C_6D_6, Bergman suggested that the solution based mechanism most likely involves the typical oxidative addition of the R-H bond across the Ir centre followed by methane elimination.[139] To better understand the mechanism, Hall and co-workers looked at two theoretical pathways using DFT calculations. The two mechanisms, termed intermolecular (no cyclometallation of PMe_3) and intramolecular (i.e via η^2-CH_2PMe_2 complex) C-H activation, were studied. Based on their calculations, the lower energy process was found to be the intermolecular activation pathway suggested by Bergman. This involves oxidative addition of the R-H group directly across the Ir centre with no activation of a methyl group on the PMe_3 ligand.[140]

II.3.5 Phosphine Cyclometallation: M-C-P Ring of Group 10 Metals

Early examples of phosphine α-C-H activation were performed using complexes of the group 10 metals, specifically those of platinum and palladium. One of the first examples was shown by Bresciani and co-workers in their search for understanding bonding in σ-carboranyl complexes. The reaction between *trans*-Pt(P^nPr_3)$_2Cl_2$ with 1-Li-2-phenyl-1,2-dicarbaclosododecaborane or 1-Li-2-methyl-1,2-dicarbaclosododecaborane results in substitution of one of the chloride ligands with σ-carboranyl ligation (Pt-C bond length of 2.13 and 2.09 Å) and metallation of the α-methylene group of the phosphine to give ($^nPr_3P$)Pt(κ^2-*P*,*C*-($^nPr_2$)*P*-*C*HCH_2CH_3){2-R-1,2-(σ-$B_{10}C_2H_{10}$)} (R = Ph (**II-153**)[141], Me (**II-154**)[142]). Based on their crystal structures and, in particular, given the observation of short P-C distances (1.76 and 1.73 Å respectively), each complex was described as containing a P=C double bond ligated to the Pt

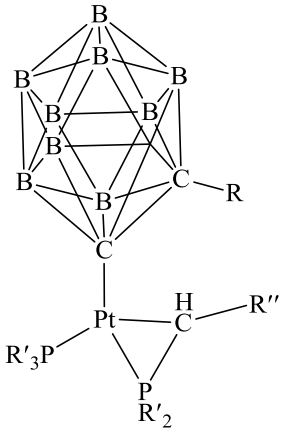

R = Ph, R′ = ^{n}Pr, R″ = Et (**II-153**)
R = Me, R′ = ^{n}Pr, R″ = Et (**II-154**)
R = Ph, R′ = Ph_2Me, R″ = H (**II-155**)
R = Ph, R′ = Bn, R″ = Ph (**II-156**)

centre. Alternatively, the reaction of the same Li carboranides with a Pt derivative containing different phosphine groups *cis*-$Pt(PR_3)_2Cl_2$ (R = Ph_2Me, CH_2Ph) results in a similar ligation of the carborane and more importantly shows selective cyclometallation of one Me group of the phosphine ligand to give $(Ph_2MeP)Pt(\kappa^2$-*P*,*C*-(Ph_2)*P*-*C*$H_2)\{2$-Ph-1,2-$(\sigma$-$B_{10}C_2H_{10})\}$ (**II-155**)[143] and $((PhCH_2)_3P)Pt(\kappa^2$-*P*,*C*-$(PhCH_2)_2$*P*-*C*HPh$)\{2$-Ph-1,2-$(\sigma$-$B_{10}C_2H_{10})\}$ (**II-156**).[144]

The synthesis of phosphaalkene complexes of Pt and Pd was performed by Jouaiti and co-workers in hopes of achieving different reactivities compared to their imine analogues. Addition of the di-phosphaalkene 1,3-bis[2-(2,4,6-$^{t}Bu_3$Ph)phosphanediylmethyl]benzene, to the nitrile complexes $M(N{\equiv}CR)_2Cl_2$ (when M = Pd, R = Ph; M = Pt, R = Me) results in formation of the bidentate $[MLCl_2]$ complexes. Reacting the Pd derivative with an equivalent of methanol or ethanol results in addition across one of the P=C bond, elimination of HCl and generation of a

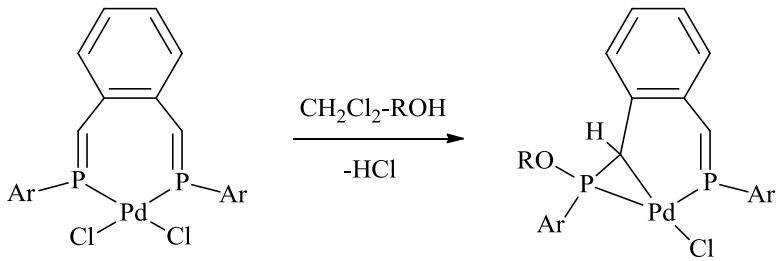

II-157

Scheme 32 – Synthesis of the ROH-induced cyclometallation to complex **II-157**.

metallated species {1-[2-(2,4,6-^{t}Bu$_3$Ph)-2-ethoxyphosphanemethyl-κ^2-*C,P*]-2-[2-(2,4,6-^{t}Bu$_3$Ph)phosphanediylmethyl-κ^1-*P*]benzene}chloropalladium (**II-157**) containing a new Pd-C bond (Scheme 32). The structure of complex **II-157** was confirmed by X-ray crystallography and the attack of the alcohol on the phosphaalkene is regio- and stereo-selective making **II-157** chiral.

Similar phosphaalkene ligands 3-(2-pyridyl)-phosphastyrene and 3-(*N*-phenylcarbaldimino)phosphastyrene were added to MePdCl(COD) to initialy give a dimeric palladium species involving the η^2-coordination of the P-C phosphaalkene to one Pd and ligation of the second Pd centre to the nitrogen of the same ligand. Dimeric complexes **II-158** and **II-159** are shown in Scheme 33 and can be converted to the monomeric form upon addition of one equivalent of PPh_3 to generate complexes **II-160** and **II-161**. Evidence for the lack of coordination of the pyridyl ring to **II-161** was provided by ^{1}H-NMR spectrum, in which a low field shift of the ortho proton in the ring was observed from δ 8.66 to 9.05 ppm.[145]

The generation of cationic palladium phosphine acetate complexes was attempted by Thirupathi and co-workers in 2005 due to their importance in such transformations as co-polymerization of carbon monoxide and olefins. Interested in better understanding the polymerization of norborene, using mixtures of cationic Pd complexes of the type *trans*-$[(R_3P)_2Pd(OAc)]$ with $[Li(OEt_2)_{2.5}][B(C_6F_5)_4]$,these authors studied reactions of various diphosphine diacetate Pd complexes with amido borates. In particular, the reaction between $(^iPr_3P)_2Pd(OAc)_2$ and $HOTs\cdot H_2O$ generates the diphosphine complex $[(R_3P)_2Pd(\kappa^2$-*O,O*-OAc)][OTs] which converts to $[(R_3P)_2Pd(\kappa^2$-*O,O*-OAc)][$B(C_6F_5)_4$] upon addition of $[Li(OEt_2)_{2.5}][B(C_6F_5)_4]$. Reacting the borate complex with two equivalents of pyridine generates the three-membered palladacylce $[(^iPr_3P)Pd(\eta^2$-P(^{i}Pr)$_2$C(Me)$_2$)(py)][$B(C_6F_5)_4$] (**II-162**) where the

isopropyl methine C-H bond is cleaved to give the pyridinium salt $[HNC_5H_5][OAc]$ (Scheme 34). Similarly, the addition of excess CD_3CN generates the cyclometallated complex

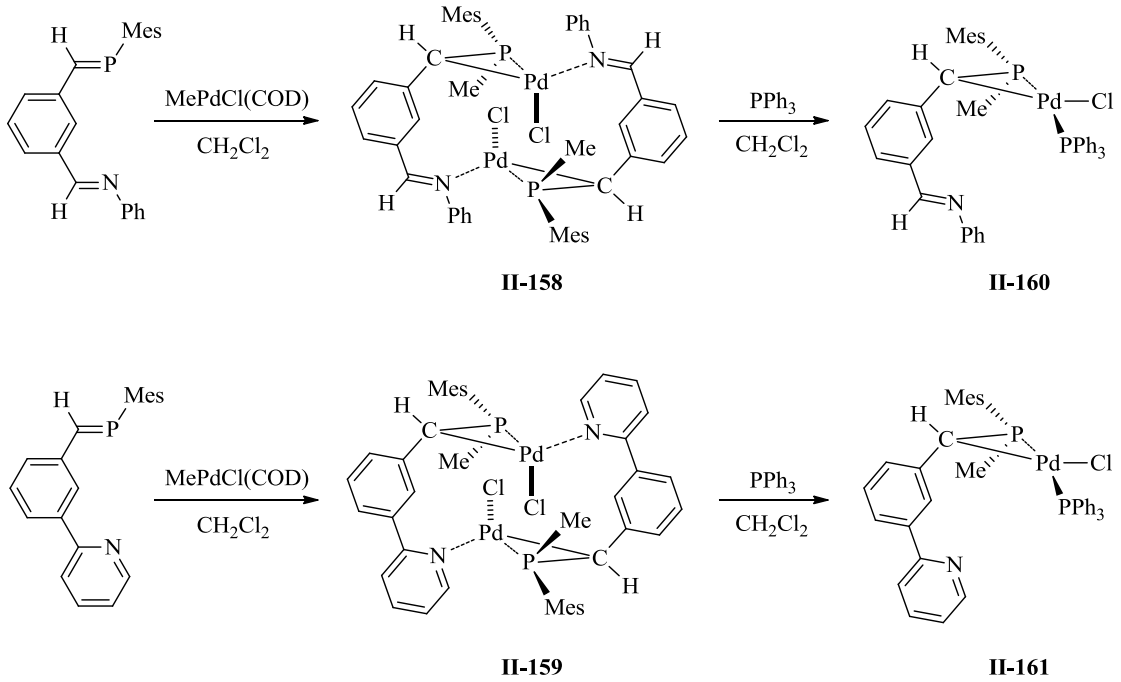

II-158 **II-160**

II-159 **II-161**

Scheme 33 – Addition of the imino and pyridyl phosphaalkenes to MePdCl(COD) to generate the dimeric species **II-158** and **II-159**, and monomeric forms **II-160** and **II-161**.

$[(^iPr_3P)Pd(\eta^2\text{-}P(^iPr)_2C(Me)_2)(N{\equiv}CCD_3)][B(C_6F_5)_4]$ (**II-163**) and acetic acid. Equilibrium was established based on the addition of excess HOAc to the mixture to regenerate more of the starting cationic Pd complex.

Recently in 2011, Sharp and co-workers serendipitously discovered an interesting cyclometallation of an ethyl group from a phosphine ligand.[146] The synthesis of the Pt(II) complex *cis*-$Pt(PEt_3)_2(Cl)(C_6Cl_5)$ is usually performed through the reaction of *cis*-$Pt(PEt_3)_2Cl_2$ with either LiC_6Cl_5 or C_6Cl_5MgCl followed by addition of HCl to quench any excess Grignard or alkyl lithium reagent present. However, before the addition of acid the initial complex formed was found to be the cyclometallated species $Pt(PEt_3)(\kappa^2\text{-}P,C\text{-}PEt_2CHMe)(C_6Cl_5)$ (**II-164**). The

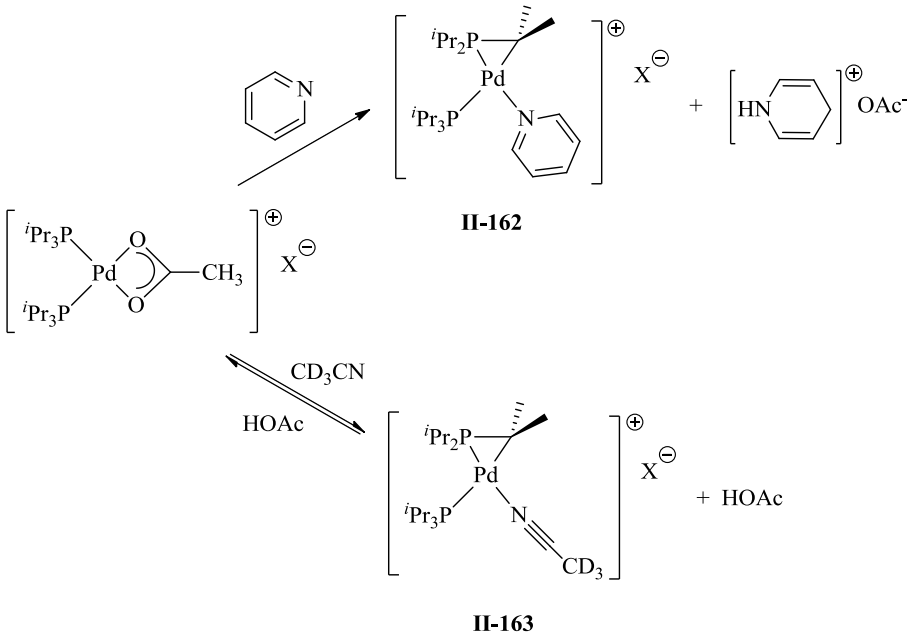

Scheme 34 – Synthesis of complexes **II-163** and **II-164** through addition of pyridine and deuterated acetonitrile.

structure was confirmed by X-ray crystallography and the α-C-H proton to one of the ethyl groups on the phosphine ligand becomes split by the Pt centre to generate the three-membered ring. The ^{13}C NMR shows a distinct downfield shifted carbon signal at δ 4.3 ppm attributed to the methine carbon in the ring. Interestingly, the addition of HCl to **II-164** results in generation of the expected *cis*-$Pt(PEt_3)_2(Cl)(C_6Cl_5)$ complex. However, addition of LiC_6Cl_5 to this complex

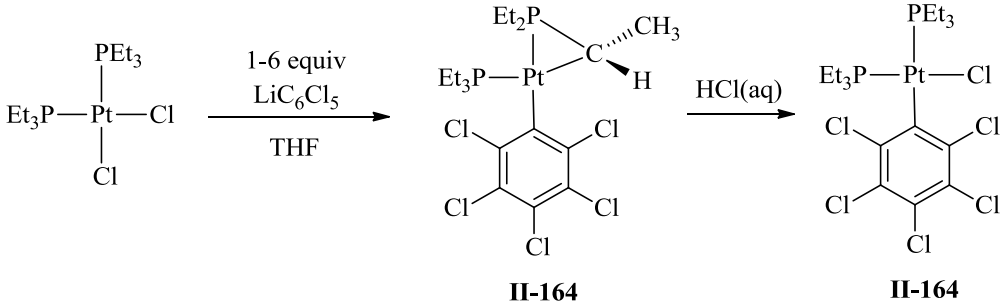

Scheme 35 – Unexpected formation of complex **II-164** upon addition of LiC_6Cl_6 followed by HCl(aq) to $(PEt_3)_2PtCl_2$.

does not convert it back to the cyclometallated species. Based on this fact and given that excess PEt_3 does not inhibit the reaction, the mechanism of activation was suggested to go through initial deprotonation of the methylene proton on a phosphine group to generate a phosphaalkene. This is followed by chlorine dissociation and η^2-coordination generating the M-C-P ring which results in attack of the anionic aryl group to give **II-164**.

II.4 Preparation of Molybdenum Bis(imido) and Mono(imido) Complexes

Within the last few decades transition metal imido chemistry has experienced a large growth within the chemical community. The introduction of an imido moiety into the coordination sphere of metal has certain advantages over the isolobal cyclopentadienyl, arene and tris(pyrazolyl)borate ligands. The ability of an imido linkage to exhibit both σ and either one or two π interactions with a metal can centre create both stability and/or interesting reactivity. The apendage of different R groups adjacent to the nitrogen atom allows various steric and electronic alterations to be made, resulting sometimes in drastic differences in chemical reactivity. This reactivity is dependent on a variety of factors, including the alternate ligand sets, the type of metal and its oxidation state. Many imido Mo complexes are known, most notably Schrock's alkylidene complexes used for the metathesis of olefins.[147,148] Importantly, these complexes can be used on industrial scale due to the cheap cost of starting materials and ease of synthesis.

There exists a wide variety of methods for introducing an imido moiety in transition metal complexes.[149] Some of the more common methods involve a [2+2] metathesis using isocyanates, phosphinimines, carbodiimides, organoimines or sulfinylamines with a respective metal-ligand double bond (ie. M=R; R = O, $CR`_2$, NR`). Similarly, bimolecular exchange between metal oxo, alkylidene or other imido ligands has been observed. This method allows the oxidation state to remain constant upon formation of the metal imido bond. Loss of an α-substituent on the nitrogen ligand such as N-H (amine or amido) or N-Si (silylamine or silylamido) bonds through deprotonation or migration to the metal itself are common. Typically this is followed by loss of either H_2O or siloxane. This work starts with the direct transformation

of the air stable and commercially available Na_2MoO_4 into the dichloride complexes $(RN)_2MoCl_2(DME)$ (R = Ar (**II-165**), ^{t}Bu (**II-166**)) prepared by Gibson and coworkers[150] by adaptation of a procedure originally developed by Schrock *et al.*[147] by using $(NH_4)_2Mo_2O_7$ as the starting material. The reaction proceeds *via* the addition of excess NEt_3 and Me_3SiCl in dimethoxyethane directly to Na_2MoO_4, followed by the addition of two equivalents of RNH_2 (R = Ar, ^{t}Bu). In contrast, the synthesis of **II-166** uses excess ^{t}BuNH$_2$ because some of the primary amine is consumed as a base instead of NEt_3. This procedure allows the isolation of the desired compounds in high yields and with high purity which avoids the task of recrystallization.

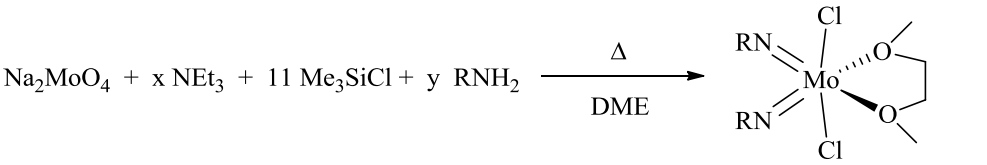

R = Ar (**II-165**); x = 4; y = 2
R = ^{t}Bu (**II-166**); x = 0; y = 6

Scheme 36 – Preparation of the starting dichloride Mo(VI) complexes $(RN)_2MoCl_2(DME)$ (**II-165** and **II-166**).

Complexes **II-165** and **II-166** are typically employed as starting materials for many transformations. The initial reduction of dichloride precursors to Mo(IV) phosphine complexes is a well-studied process and many complexes are known. The related tungsten derivatives have also been synthesized but their detailed discussion falls outside the scope of this review. Reduction of **II-165** can be performed using magnesium with excess trimethylphosphine (PMe_3) to produce the fluxional complex $(ArN)_2Mo(PMe_3)_3$ (**II-167**). Initially, complex **II-167** was characterized as a bis(phosphine) $(ArN)_2Mo(PMe_3)_2$[151], on the basis of X-ray study performed by Gibson *et al.* but was recently reformulated as a tris(phosphine) complex.[11] Namely, NMR studies suggest an equilibrium between the **II-167** and the bis(phosphine) derivative along with

free PMe_3. This equilibrium stems from an interplay between stabilization of an 18 electron tris(phosphine) complex due to partial lone pair donation from the imido groups to metal and the increased steric repulsion of the bulky imido and phosphine groups. Other aryl imido complexes have shown similar reactivity. Thus the compound $(MesN)_2Mo(PMe_3)_3$ with a smaller imido group was characterised by X-ray as a tris(phosphine) complex, although an equilibrium exists between the tris and bis(phosphine) derivatives.[152] Bulkier phosphine donors such as PMe_2Ph or PMe^iPr_2 stabilize the bis(phosphine) complexes validating the argument for steric restrictions.

Interestingly, performing the reduction from the starting alkyl imido derivative $(^tBuN)_2MoCl_2(DME)$ results in different reactivity. The two products observed under Mg reduction are the mononuclear bis(phosphine) derivative $(^tBuN)_2Mo(PMe_3)_2$ (**II-168**) and the imido bridged dinuclear complex $[(^tBuN)(PMe_3)Mo(\mu\text{-}N^tBu)]_2$. The complexes are difficult to separate via crystallization but prolonged heating of the mixture for three weeks at 75 °C under an excess of PMe_3 allows isolation of **II-168** and other insoluble byproducts. This process was suggested to proceed via decomposition of the dimer to higher oligomers of $[(^tBuN)_2(PMe_3)Mo]$ based on the lack of increase or decrease of free PMe_3 in the sample during heating. Although this presumed polymerization process does not change the overall stoichiometry, carrying out the reaction in the absence of free phosphine leads to significant decomposition of bis(phosphine) **II-168**, suggesting that this decomposition occurs via dissociation of PMe_3. On the other hand, the stability of the imido bridged dimer was seen from its inactivity towards addition of ethylene or propene to generate the known $(^tBuN)_2Mo(PMe_3)(C_2H_3R)$ (R = H, CH_3) complexes. Decreasing the steric bulk on the imido groups (i.e. when R = 4-MePh or Ph) typically leads to decomposition of the resulting reduced product in the magnesium reduction approach. An ideal starting material should be that one which easy to prepare and isolate. In this

regard, the above method suffers from a lengthy reaction time, the use of expensive PMe_3 and significant waste of Mo in the form of an imido polymer.

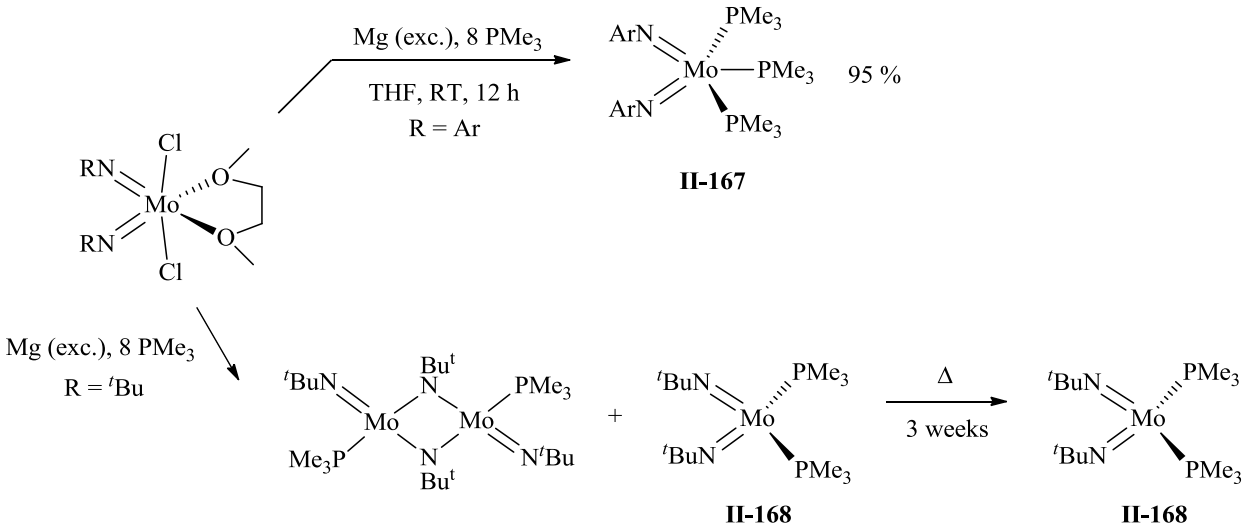

Scheme 37 – Reduction of complex **II-165** and **II-166** *via* Mg and excess PMe_3 generating **II-167** and **II-168**.

For this reason the choice of the starting Mo(IV) material should be based on the relative simplicity of its preparation. One of the major drawbacks of preparing complex **II-167** is the separation from the resulting magnesium salts. Due to the low solubility of complex in aliphatic solvents and significant solubility of by-products in ethereal solvents, the isolation of **II-167** requires the use of large amounts of hexanes for the purpose of extraction. This process is unreasonably slow and highly time consuming, which is unfavorable when large quantities are needed. Also, the use of excess PMe_3 is needed to drive the reaction to completion which in turn increases the cost of the reaction. Above all, complex **II-167** is extremely air and moisture sensitive, so an utmost care must be taken when performing the synthetic workup.

In order to circumvent some of these issues, bis(imido) Mo(IV) derivatives incorporating alternative two-electron donors, could be used. In particular, Gibson *et al.* has reported a method of preparing bis(imido) complexes with ethylene and propylene ligands, starting from the

dichloride precursors $(RN)_2MoCl_2(DME)$. The syntheses can be performed through the use of relatively inexpensive Grignard reagents (EtMgBr or PrMgBr) and only stoichiometric amounts of phosphine. For example, addition of two equivalents of EtMgBr to $(^tBuN)_2MoCl_2(DME)$ in the presence of only one equivalent of PMe_3 gives the ethylene phosphine complex $(^tBuN)_2Mo(PMe_3)(\eta^2\text{-}C_2H_4)$ (**II-169**) in up to 75 % yield after recrystallization from hexanes. The advantage of this method compared to the previously reported synthesis of **II-168** is the reduced preparation time, decreased amounts of solvent by an order magnitude and the use of stoichiometric amount of PMe_3. Similarly, adding two equivalents of EtMgBr to complex **II-165** in the presence of two equivalents of PMe_3 gives $(ArN)_2Mo(PMe_3)_2(\eta^2\text{-}C_2H_4)$ (**II-170**), which can easily be isolated as a dark purple powder in 70 % yield. The addition of phosphine is necessary as bis(ethylene) complexes are difficult to isolate and typically provide mixtures of products which are highly fluxional at room temperature as observed by NMR.[150,151] These mixtures are likely to contain various multinuclear complexes which were not sufficiently characterized and are insignificant for this project. Complex **II-170** coordinates two PMe_3 groups most likely due to the weaker donating ability of the NAr than N^{t}Bu groups in **II-169** because of partial delocalization of nitrogen lone pair on the aromatic ring of Ar group. In contrast, the alkyl imido groups are at the limit of π-saturation and can form triple bonds between the metal and nitrogen atom.[152]

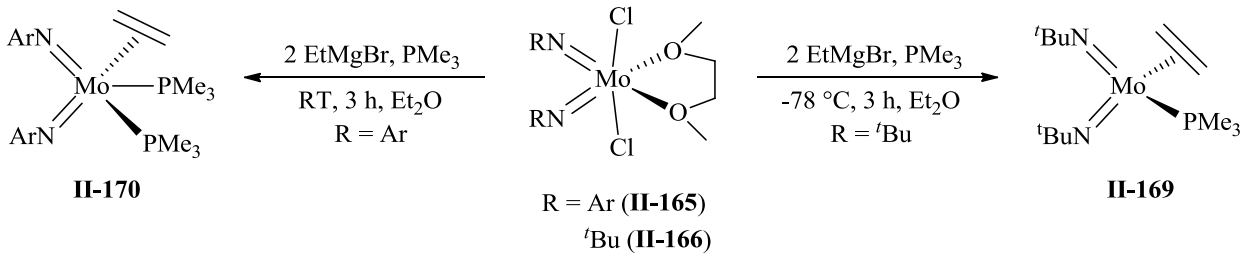

Scheme 38 – Synthesis of **II-169** and **II-170** using the Grignard reagent EtMgBr with PMe_3.

Interest in the reactivity of complexes **II-167** to **II-170** towards silane addition became an interest in our group as β-agostic silylamido complexes are thought to be intermediates in mechanisms of hydrosilylation.[3] Reacting Ar imido complexes **II-167** and **II-169** or ^{t}Bu complexes **III-168** or **II-170** with di- and monochloro silanes results in the unexpected addition across the imido bond to give the β-agostic silylamido complexes of the type (RN)Mo(PMe_3)$_2$(η^3-N^{t}Bu-SiR′$_2$-H)Cl (R = Ar, ^{t}Bu; R′ = Me_2, MePh, Ph_2, MeCl), with no silyl hydride derivatives being observed (See Section II.1.1)[11]. The addition of three equivalents of $HSiCl_3$ results in production of a silanimine dimer and the resulting dichloride complex (RN)Mo(PMe_3)$_3Cl_2$ (R = Ar (**II-171**), ^{t}Bu (**II-172**)). Complex **II-172** can also be prepared through a different method proposed by Green and co-workers in 1992, where the reduction of Cp(ArN)$MoCl_2$ using a sodium amalgam in the presence of excess trimethylphosphine results in production of complex **II-172** presumably through the displacement of the cyclopentadienyl ring.[153] As has already been mentioned in Section II.2.2, the addition of hydrosilanes, in particular, $PhSiH_3$ to **II-167** or **II-169** results in formation of agostic bis(silyl) complex (ArN)Mo(SiH_2Ph)(η^3-NAr-SiHPh-H)(PMe_3). This proved to be an efficient catalyst towards the

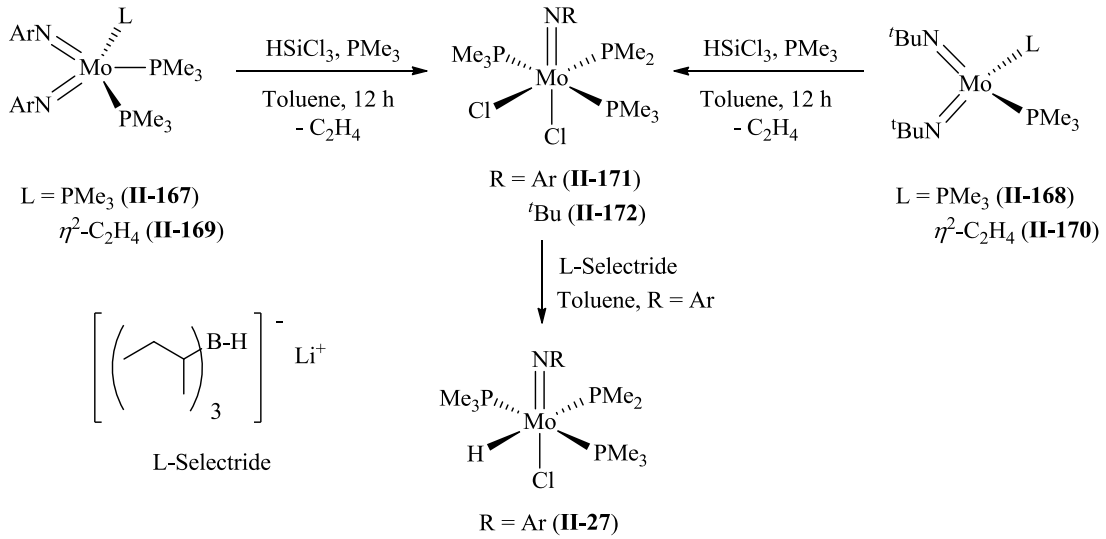

Scheme 39 – Preparation of mono(imido) tris(phosphine) complexes **II-171** and **II-172**.

hydrosilylation of alkenes, carbonyls and benzonitrile. Mechanistic investigations towards ethylene hydrosilylation led to an unexpected conclusion that involves insertion of ethylene into a rare silanimine intermediate.[12,154]

Complex **II-171** is relatively inert to common reduction methods including excess $NaBH_4$, $MeLi/H_2$, $Na(Hg)/H_2$ and KC_8/H_2. Alternatively, lithium borohydrides of the type $Li[R_3BH]$ (R = H, ^{sec}Bu, Et) can activate the complex in different ways. Thus, the addition of $LiBH_4$ results in displacement of both chloride ligands to give the bis borohydride complex $(ArN)Mo(PMe_3)_2(\eta^2\text{-}BH_4)_2$.[11] Alternatively , the addition of an equivalent of either L-Selectride ([(*sec*-Bu)$_3$BH]Li) or L-Superhydride ([(Et)$_3$BH]Li) generates the hydrido chloride complex $(ArN)Mo(H)(Cl)(PMe_3)_3$ which has been extensively utilized as catalysts for the reduction of carbonyls, alkenes, alkynes and nitriles.[13,14] Interestingly, despite hydride resonances being typically found in the high field region of ^{1}H-NMR, this complex shows a distinct low-field hydride signal at 5.31 ppm (dt, $^2J_{H\text{-}P}$ = 28.5 Hz, 51.9 Hz) coupled to two equivalent and one nonequivalent PMe_3 groups. Many of the hydride complexes discussed in the subsequent sections will exhibit this type of behaviour for many of the hydride signals. Also, it is noteworthy that the PMe_3 group trans to the hydride ligand is significantly elongated which plays a crucial role in understanding the mechanisms of reduction. The addition of an extra equivalent of L-Selectride results in production of the dihydride complex $(ArN)Mo(PMe_3)H_2$ which is highly fluxional in solution and slowly decomposes into a variety of different products over time.[14]

III Results and Discussion

III.1 Introduction

The focus of the research project to be discussed in the following sections is based on expanding the scope of Mo imido complexes which display non-classical Si-H interactions in hopes of ultimately utilizing them as hydrosilylation catalysts. We hypothesized that unsymmetrical complexes of the type (RN)(R′N)Mo$(PMe_3)_x$ (R ≠ R′) would be good candidates as starting materials for this type of investigation, where the addition of silanes would induce imido/silane coupling and provide new and interesting routes to various mixed systems containing two electronically and sterically different R groups.

The first part of the discussion will be a look into the synthetic methodologies of preparing both symmetrical and unsymmetrical imido complexes. Our investigation into the mechanism of hydrosilylation of carbonyls mediated by the symmetrical *β*-agostic complex $(ArN)_2Mo(\eta^3\text{-}N^tBu\text{-}SiMe_2\text{-}H)(H)$ will then be discussed. We will then show our attempted synthesis at unsymmetrical Mo imido complexes using the known tris(phosphine) complexes (RN)Mo$(PMe_3)_3Cl_2$, which led to an unexpected scenario involving cyclometallation of the PMe_3 group through base-induced C-H activation. Finally, intermediates formed during the synthesis of the novel tris(silyl) complex $(^tBuN)Mo(SiH_2Ph)(H)\{(\mu\text{-}N^tBu)(SiHPh)_2\}(PMe_3)$ will be shown, along with reactivity studies involving organic substrates such as carbonyls, alkenes, alkynes and nitriles.

III.2 Synthesis of Symmetrical Mo(VI) Silylamido Complexes

Preparation of transition metal silylamido complexes are typically performed via salt elimination of an alkali metal silylamide (i.e. Li[NRSiR′$_3$]) with a metal halide. Interest and functionalization of silylamido complexes first came from work done by Berry *et al.* in 1991, where the addition of Li[N(^{t}Bu)SiHMe$_2$] to the zirconocene hydride chloride complex Cp$_2$ZrH(Cl) gave the β-agostic silylamido complex Cp$_2$Zr(η^3-N^{t}Bu-SiMe$_2$-H)(H).[36] In this family of compounds the Si-H bond has an addition linkage to the metal via a nitrogen bridge. Halogenated derivatives Cp$_2$ZrX(η^3-NBu^t-SiMe$_2$-H) (X = F, Cl, Br; Figure 10) were prepared by halogen/hydride exchange and were also found to possess similar agostic interactions. The bonding situation in these compounds was studied by X-ray diffraction and by NMR analysis. Particularly, the coupling constant values ($^1J_{\text{Si-H}}$) provide evidence for strong agostic interactions showing the expected reduced values between 113 Hz and 132 Hz compared to the free silylamines and lithiated silylamides, both having $^1J_{\text{Si-H}}$ values above 180 Hz.

Recently our group has had success in preparing similar isolobal complexes of both Group 5 and Group 6 complexes. Using the isolabal relationship between the cyclopentadienide and imido groups, the preparations of CpTa(ArN)(N(R)SiHMe$_2$)X and (ArN)$_2$Mo(N(R)SiHMe$_2$)X (X = H, Cl, I; R = ^{t}Bu, Ar′) derivatives were done and the extent of agostic interaction was studied (Figure 10). The chloride derivatives were prepared from the dichloride starting material Cp(ArN)TaCl$_2$ or (ArN)$_2$MoCl$_2$(DME) (**III-1**). The addition of one equivalent of Li[N(^{t}Bu)SiHMe$_2$](THF) to either of the two complexes results in elimination of LiCl to give the respective silylamido species CpTa(ArN)(N(^{t}Bu)SiHMe$_2$)Cl (**III-2**) or (ArN)$_2$Mo(N(^{t}Bu)SiHMe$_2$)Cl (**III-3,** Scheme 40). Each reaction could be carried out in one hour

and in moderate yields. ^{1}H-NMR analysis shows the Si-H resonances at 4.76 and 5.65 ppm for **III-2** and **III-3**, respectively. As mentioned in the historical section, chemical shifts of Si-H protons in β-agostic complexes are typically largely shifted upfield. However, in both **III-2** and **III-3** the Si-H resonances showed up close to the parent silylamide Li[N(^{t}Bu)SiHMe$_2$](THF) (4.91 ppm). This behaviour is indicative of the presence of a classical silylamido ligand with no Si-H interaction with the metal centre. Supporting this notion are the large $^{1}J_{\text{Si-H}}$ values of 183.6 Hz and 172.9 Hz for **III-2** and **III-3**, respectively, which is higher than in typical agostic complexes of this type.

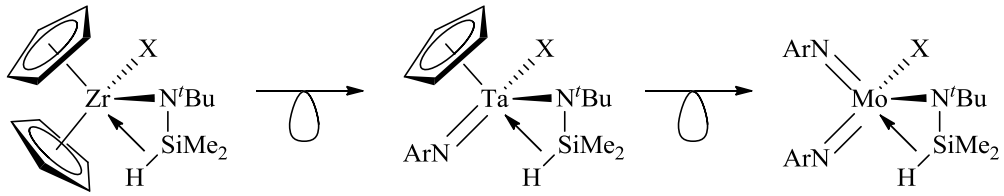

X = H, Cl, I; Ar = 2,6-diisopropylphenyl

Figure 10 – Isolobal relationship between the *β*-agostic silylamido complexes from Groups 4-6.

Satisfyingly, crystals suitable for X-ray diffraction analysis were grown for the Mo derivative **III-3** and, based on the acute Mo-N-Si bond angle (103.59°) and the N-Si-H bond angle (97.0°), the possibility of interaction between the Si-H bond and the metal centre in the solid state was concluded. For comparison, in the known bis(imido) derivative (ArN)$_2$Mo{N(SiMe$_3$)$_2$}Cl prepared by Chen and co-workers in 2003, more open Mo-N-Si bond angles of 124.2(2)° and 115.8(2)° for each silyl substituent of the silylamido ligand were observed. Comparing these values with **III-3** gives a difference of 12.2°, suggesting an interaction between the Si-H bond and the metal centre. The elongated Si-H bond (1.36 Å) and relatively short Mo-Si (2.9264 Å) distance fall within the regions for structurally characterized agostic Mo complexes but due to the uncertainty involved in locating hydrogen atoms by X-ray

diffraction analysis in heavy element environment, the Si-H distance cannot be determined with certainty.

Interestingly, complex **III-3** is relatively inert towards substitution of the chloride ligand. Attempts at abstraction using $(Me_3SiCH_2)MgCl$, L-Selectride, Superhydride, $Me_3Si(CF_3SO_3)$, LiBAF/PMe_3 or $AgBF_4$/PMe_3 all provided no reactivity. This phenomenon was rationalized based on the electron deficient nature of the Ta(V) centre which is formally 16 e^- complex, assuming that the imido group is a 6e donor. However, the chloride is a recognized π donor too. Keeping in mind that the extent of agostic interaction is dictated by the donation from the σ-bonding orbital of the Si-H bond to the same "vacant" orbital on metal which is involved in π interaction with chloride, the strong Ta-Cl bond can be attribute to the competition between the chloride ligand and the Si-H bond. In this regard, the Cl ligand can donate extra electron density into the electron deficient metal centre from its lone pairs, occupying empty orbitals situated on the metal that could otherwise be used for σ-donation from the Si-H bond. This contradicts Berry`s result which demonstrated strongly agostic zirocnocene chloride derivatives. The steric effect of the imido group may be the determining effect in this case as the bulky Ar ligand is situated further from the metal centre (compared to the Cp ligand) allowing the Cl ligand to penetrate closer to the metal centre.

Based on this, an alternative route to the hydrido derivatives was performed. Our group has recently found a convenient route to the production of the Ta(V) dihydride complex $Cp(ArN)TaH_2(PMe_3)$ through the addition of excess $NaBH_4$ and PMe_3 to $Cp(ArN)TaCl_2$. This complex can be reacted with an equivalent of $SiHMeCl_2$ or $PhPCl_2$ to generate the hydrido chloride derivative $Cp(ArN)Ta(H)(Cl)(PMe_3)$ (**III-4**). More conveniently, treating $Cp(ArN)TaCl_2$ with an equivalent of L-Selectride and PMe_3 generates **III-4** in moderate yield

(70 %). The subsequent addition of the Li[N(^{t}Bu)SiHMe$_2$](THF) to **III-4** results in a difficult to separate mixture of various Cp containing complexes but the adding one equivalent of BPh_3 at the beginning of the reaction produces one major product characterized as Cp(ArN)Ta(η^3-N^{t}Bu-SiMe$_2$-H)(H) (**III-5**) and eliminates the $Me_3P{\cdot}BPh_3$ adduct. The reduced $^1J_{Si\text{-}H}$ value of 155.0 Hz, upfield shifting of the ^{1}H and ^{29}Si resonances and the observed coupling between the hydride and Si-H signals in the ^{1}H-^{1}H COSY spectrum are all indicative of a nonclassical interaction of the Si-H bond and the Mo centre. However, large scale preparation and isolation of this derivative proved to be difficult due to decomposition and high solubility in aliphatic solvents.

Alternatively, the group 6 analogue **III-3** can be easily converted into the hydride derivative through a simple addition one equivalent of L-Selectride (Scheme 40). The hydride derivative (ArN)$_2$Mo(η^3-N^{t}Bu-SiMe$_2$-H)(H) (**III-6**) displays upfield shifted ^{1}H NMR ($\delta_{Si\text{-}H}$ = 4.24 ppm) and ^{29}Si INEPT+ NMR ($\delta_{Si\text{-}H}$ = -52.9 ppm) signals indicating greater shielding due to the proximity to the metal centre. The ^{1}H-NMR at δ 0.47 ppm corresponding to the Si methyl groups displays an interesting doublet of quartets suggesting coupling to the Mo-H. This was confirmed in the ^{1}H-^{1}H COSY spectrum which shows coupling between the Mo-H and Si-H signals. In the case of non-agostic behaviour, significant $^4J_{Si\text{-}H}$ coupling between these two signals is highly unlikely.

Although **III-6** can be cleanly generated in solution, its isolation proved difficult as reducing the volume of solution under pressure even for a short period of time results in decomposition to a mixture of uncharacterized products. Typical crystallization techniques, both at room temperature and low temperatures (-30 and -80 °C), using aliphatic and ethereal solvents were unsuccessful due to the high solubility of the complex. Chlorinated solvents, such as dichloromethane, chloroform or chlorobenzene all led to decomposition to a variety of products,

none of which seem to include complex **III-6**.

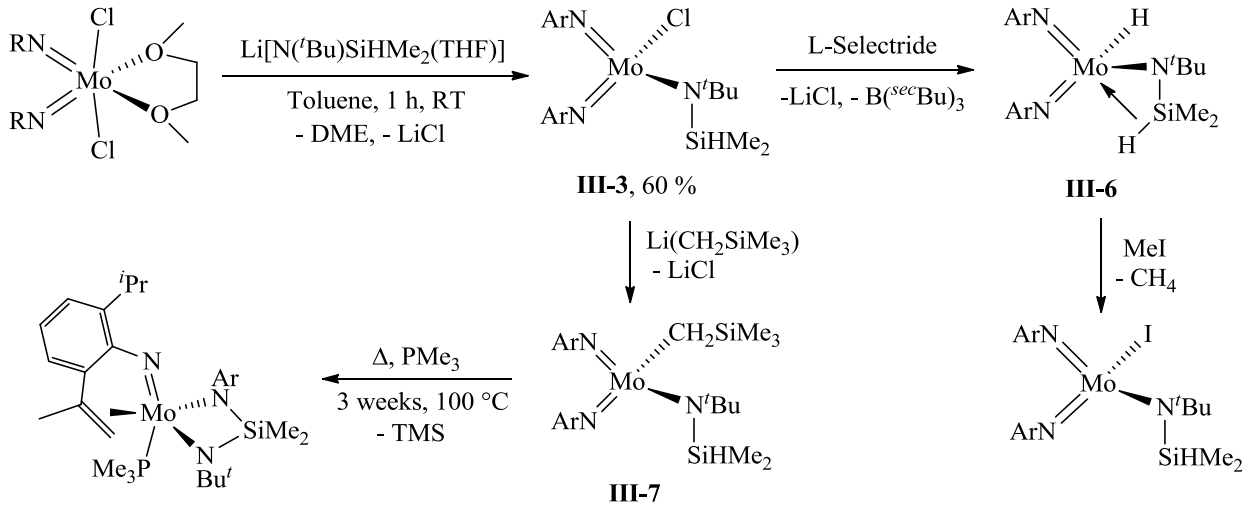

Scheme 40 – Synthesis and derivatization of the *β*-agostic silylamido complex **III-6**.

The iodide derivative could also be synthesized by adding one equivalent of MeI *in situ* to a freshly prepared sample of **III-6**. Similar to **III-3**, the NMR data seem to indicate a non-agostic bonding scenario as seen from the $^{1}J_{\text{Si-H}}$ value of 165.7 Hz and the downfield shifted ^{1}H and ^{29}Si signals of 5.45 ppm and -31.6 ppm respectively. Interestingly, a correlation can be made between these three complexes. As Berry at al.[8] suggested, the π-donor effect of the halogenated ligands to the electron deficient metal centre act to stabilize these complexes. In this case the same effect is observed, which determines the extent of σ-donation from the Si-H bond. For a purely σ-donor, such as the hydride ligand, greater agostic interaction is seen, whereas with π-donors (chloride and iodide), weaker agostic interaction results. The amount of π-donation can be rationalized by the size of the ligands themselves. The larger iodine ligand shows weaker donation compared to chloride possibly due to the increased radial size. The $^{1}J_{\text{Si-H}}$ coupling constant values are indicative of this, where reduced values correlate with larger size.

Agostic Si-H bonds are considered intermediates *en route* to silyl hydrides, the products of complete bond cleavage on a metal centre. In the presence of a metal with the d^0

configuration, back-donation to a Si-H antibonding orbital is not possible, which prevents full oxidative addition. Efforts at further Si-H bond activation in **III-6** were attempted in hopes of producing a silanimine complex by reasoning that the loss of the Si-H proton could be facilitated through appropriate ligand coordination. Silanimine complexation is rare and limited to only a few examples, however interesting reactivity has been shown with possible utility in catalysis. For example, small molecules such as ethylene, formaldehyde, carbon dioxide or carbon disulfide can insert directly into the silanimine bond to produce 5-membered metallacycles.[155] Also, activation of hydrogen gas was observed under ambient conditions. Berry *et al.* showed that upon addition of PMe_3 to the trimethylsilylmethyl derivative $Cp_2Zr(N^tBu\text{-}SiMe_2H)(CH_2SiMe_3)$, the bulky alkyl ligand abstracts the silicon-bound proton resulting in elimination of tetramethylsilane and formation of the d^0 Zr(IV) silanimine complex $Cp_2Zr(\eta^2\text{-}N^tBu\text{-}SiMe_2)(PMe_3)$.[8] In a similar vein, substitution of the chloride ligand in $(ArN)_2Mo(\eta^3\text{-}N^tBu\text{-}SiMe_2\text{-}H)(Cl)$ by using trimethylsilylmethyl lilthium was easily done to produce the alkyl derivative $(ArN)_2Mo(N(^tBu)SiHMe_2)(CH_2SiMe_3)$ (**III-7**, Scheme 40). However, attempts at mixing PMe_3 and **III-7** gave no reactivity even at elevated temperatures (100 °C). Only after a period of three weeks was decomposition observed showing no presence of the desired silanimne complex. Interestingly, through 2D-correlation techniques, activation of one of the isopropyl groups was seen involving the loss of hydrogen gas and tetramethylsilane to give olefin coordination of the dehydrogenated isopropyl group and cyclization involving an unusual Mo-κ^2-N,N-$(N^tBu\text{-}SiMe_2\text{-}NAr^*)$[†] coordination mode (Scheme 40).

Silanimine coordination may not be possible for the isolobal Mo system based on the electronics and steric restrictions of the system. The imido ligands provide extra electron density

[†] Ar* is the newly formed 2,6-diisopropylphenyl containing the dehydrogenated isopropyl group.

to the metal centre through lone pair donation from the nitrogen atoms. This may induce a stabilizing effect allowing the agostic interaction to weaken and essentially saturate the metal centre providing no back donation to the Si-H σ* antibonding orbital. Nevertheless, attempts at hydrosilylation were performed using **III-6** as a catalyst.

III.2.1 Catalytic Hydrosilylation of Carbonyls using $(ArN)_2Mo(\eta^3\text{-}N^tBu\text{-}SiMe_2\text{-}H)H$

The reduction of carbonyls is an important process as the products give protected forms of alcohols typically used in organic syntheses. Hydrolysis of these products gives the resulting alcohols which are extensively utilized in natural product synthesis and can be further derivatized to give esters, alkenes (dehydration), carboxylic acids or alkenyl chlorides. Typical reduction methods used in the laboratory preparation of alcohols use stoichiometric amounts of either sodium borohydride ($NaBH_4$) or lithium aluminum hydride ($LiAlH_4$) which are corrosive and toxic chemicals when used in large quantities.[156] Many efforts have been put forth utilizing transition metals as catalysts in this regard, including a great deal of work done using nonprecious metals. Recently, cheap and abundant first row transition metals such as iron[57] and nickel[157-161] have been used in hydrosilylation and shown excellent turnover numbers and chemoselectivity. As such Mo has received much less attention, despite its cheap and environmentally benign nature being the only second row transition metal to be met in biological systems (Mo cofactor; Moco).[59] Our group has had success in utilizing the Mo imido complexes $(ArN)Mo(SiH_2Ph)(\eta^3\text{-}NAr\text{-}SiHPh\text{-}H)(PMe_3)$, $(ArN)Mo(PMe_3)_3(H)(Cl)$ and $(ArN)Mo(PMe_3)_3(H)(SiH_2Ph)$ as hydrosilylation catalysts displaying unusual mechanistic pathways (see Section II.2.2). However, preparation of these complexes can be somewhat tedious and expensive due to the use of phosphine ligands. Alternatively, the synthesis of the

hydride **III-6** provides an interesting route towards hydrosilylation as preparation is simple, relatively cheap and avoids the use of PMe_3 as a ligand. As has been mentioned, hydride complexes are known to be excellent catalysts towards the reduction of unsaturated substrates. Also, based on the fact that *β*-agostic complexes are thought to be intermediates in reduction mechanisms, **III-6** seemed to be an excellent candidate for reduction *via* hydrosilylation.

Although complex **III-6** cannot be easily isolated, preparation using one equivalent of L-Selectride was shown to go to 100% completion within 5 minutes. Hence, all catalytic runs demonstrated below (Table 1) generate **III-6** *in situ* followed by the addition of substrate and silane after a 5 minute reaction period (Scheme 41). Initially, the 1:1 reaction of benzaldehyde and $PhSiH_3$ using 5 mol. % compound **III-6** was found to be effective after only 10 minutes of reactivity to give two major products; $PhHSi(OBn)_2$ (95%) and $PhSiH_2(OBn)$ (5 %) (entry 1,

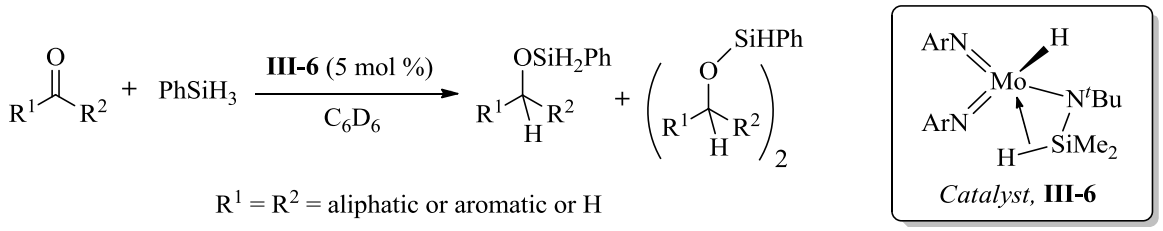

Scheme 41 – General procedure for the hydrosilylation of carbonyls using **III-6** as a catalyst.

Table 1).

Typically, distribution of products is observed due to the presence of three Si-H bonds on $PhSiH_3$. The process is reproducible and gave similar reaction times and conversions for each run (done three times using same procedure and concentrations). Increasing the ratio of benzaldehyde to $PhSiH_3$ to 3:1 results in distribution of the products as $PhSiH_2(OBn)$ (2 %) $PhHSi(OBn)_2$ (30 %),and $PhSi(OBn)_3$ (68 %) after 1 hour at room temperature. Alternative silanes significantly decreased reaction times and lowering catalyst loading below 1 % deactivates the catalyst. The use of a secondary silanes such as $PhMeSiH_2$ results in the

conversion to both the PhMeHSi(OBn) (80 %) and $PhMeSi(OBn)_2$ (20 %). The use of a 1:1 mixture of tetramethyldisiloxane (TMDS) and PhCHO results in the 100% conversion to the monosubstituted $(Me_2HSi)Me_2Si(OBn)$ product after 5 hours of reactivity. The selectivity for monosubstitution as opposed to both Si-H bonds becoming hydrosilylated is most likely due to the steric bulk after addition of the first equivalent of PhCHO. Tertiary alkyl silanes such as Me_2PhSiH and Et_3SiH show no reactivity and deactivate the catalyst after 1 hour at room temperature. The use of tertiary silanes such as $(EtO)_3SiH$ shows quick conversion to the silyl ether $(EtO)_3Si(OBn)$ but upon closer inspection, significant redistribution into $(EtO)_2Si(OBn)_2$ and $(EtO)_4Si$ was observed. Although, $(EtO)_2MeSiH$ is much less prone to redistribution even after days of reactivity and shows quick conversion to the resulting silylether $(EtO)_2MeSi(OCH_2Ph)$ (i.e. one hour using PhCHO).

Expansion of the substrate scope was probed and the catalyst was found to be tolerant to a variety of different functional groups as can be seen from Table 1 (entries 1 through 12). The use of electron withdrawing substrates, such as 4-bromobenzaldehyde, using $PhSiH_3$ at 5 mol % loading produced $PhH_2Si(OCH_2Ph^{Br})$ and $PhHSi(OCH_2Ph^{Br})_2$ in 52 % and 48 % yields, respectively (entry 2). Chemoselective reduction of cinnamaldehyde to the α,β-unsaturated silylethers $PhH_2Si(OCH_2CHCHPh)$ (67 %) and $PhHSi(OCH_2CHCHPh)_2$ (33 %) was observed in under 10 minutes using $PhSiH_3$ (entry 3). Aliphatic aldehydes were also tolerated with butyraldehyde showing 100% conversion in 10 minutes time under optimized conditions (entry 4). Typically, these types of substrates are much more difficult to reduce due to the weaker electrophilicity of the C=O double bond due to the inductively donting alkyl substituent. In the case of aromatic aldehydes, resonance with the phenyl group activates the C=O double bond making it more susceptible towards attack from the hydride ligand if indeed Mo-H insertion is an

Table 1 - Hydrosilylation of carbonyls mediated by **III-6** at 5 mol % loading.[a]

Entry	Substrate	Time (h)	Products	Yield (%)[b]	TON	TOF (h^{-1})
1	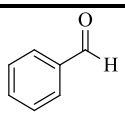	0.2	$PhSiH_2(OBn)$ $PhSiH(OBn)_2$	5 95	20	100
2	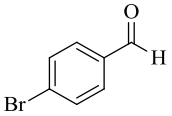	0.2	$PhH_2Si(OCH_2Ph^{Br})$ $PhHSi(OCH_2Ph^{Br})_2$	52 48	20	100
3	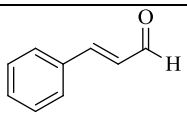	0.2	$PhH_2Si(OCH_2CHCHPh)$ $PhHSi(OCH_2CHCHPh)_2$	67 33	20	100
4	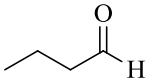	0.2	$PhH_2Si[O(CH_2)_3CH_3)]$ $PhHSi[O(CH_2)_3CH_3)]_2$	55 45	20	100
5	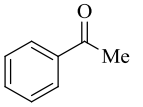	10	$PhH_2Si[OCH(Me)Ph]$ $PhHSi[OCH(Me)Ph]_2$	35 65	20	2
6	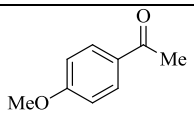	20	$PhH_2Si[OCH(Me)Ph^{OMe}]$ $PhHSi[OCH(Me)Ph^{OMe}]_2$	32 68	20	1
7	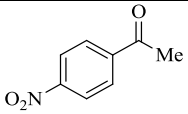	0	NR	NR	--	--
8	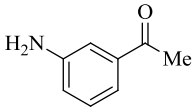	2	$PhH_2Si[OCH(Me)Ph^{NH_2}]$ $PhHSi[OCH(Me)Ph^{NH_2}]_2$	28 72	20	10
9	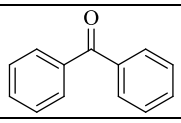	144	$PhH_2Si(OCH_2Ph_2)$ $PhHSi(OCH_2Ph_2)_2$	76 24	20	1.7
10		1	$PhSiH_2(O^iPr)$ $PhSiH(O^iPr)_2$	77 23	20	40
11	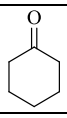	42	$PhSiH_2(OCy)$ $PhSiH(OCy)_2$	73 27	20	0.48
12	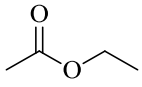	23	$PhSiH_2(OEt)$ $PhSiH(OEt)_2$	20 80	20	0.90

[a] Catalyst and KO^tBu loading at 5 mol %, with 1:1 ratio between silane and substrate. All reactions carried out at room temperature. [b] Determined by ^{1}H-NMR using residual solvent as internal standard.

initial step in the mechanism (see Scheme 8, Section II.2.1).

Longer reaction times are needed when acetophenone and $PhSiH_3$ are added to 5 mol % catalyst to give $PhSiH[OCH(Me)Ph]_2$ (65%) and $PhSiH_2[OCH(Me)Ph]$ (32%) after 10 hours at room temperature (entry 5). Increased reaction rates are typically observed for ketones attributed to the bulkier nature of the substrate compared to aldehydes. The use of donating groups in the 4-position of the phenyl ring (i.e. 4-methoxyacetophenone) results in the increased reaction time (entry 6) whereas electron withdrawing groups, such as 4-nitroacetophenone, shows no reactivity after many days with deactivation of the catalyst observed (entry 7). This is known to occur for other molybdenum based catalysts (i.e. MoO_2Cl_2[64]). Substitution of the 3-position of the phenyl ring with an amino group (NH_2) gives good conversion in only 2 hours (Entry 8). Increasing the steric bulk of the ketone to benzophenone gives 100 % conversion to the respective hydrosilylation products ($PhSiH_2[OCH(Ph)_2]$ 76 %, $PhSiH_2[OCH(Ph)_2]_2$ 24%) after a lengthy 6 days at room temperature (entry 9). Aliphatic ketones are tolerated such as acetone or cyclohexanone with full conversion seen after one and 42 hours, respectively (entries 10 and 11). Interestingly, hydrosilylation of ethyl acetate was attempted and cleavage of the C-O bond was observed to give full conversion to the respective silyl ethers, $PhSiH_2(OEt)$ (20 %) and $PhSiH(OEt)_2$ (80 %), in 23 hours (entry 12). Attempts at hydrosilylation with other substrates containing unsaturated double or triple bonds results in complete inactivity.

Catalytic reduction of amides is an important process as the products generated are typically primary, secondary or tertiary amines. These have extensive uses in laboratory and industrial chemistry with a major focus on drug production. Typically, reductions are done similar to those for carbonyls which utilize hazardous hydride agents such as $LiAlH_4$ or $NaBH_4$. However, the last decade has seen a large amount of research dedicated to optimization of this

process, driven by the need of leading pharmaceutical companies to have a "green" amide reduction process.[162] Attempts at reduction of the secondary amide *N*-phenylpropionamide with catalyst **III-6** led to no reactivity after days at room temperature. Only decomposition of the catalyst was seen without any change in the added amide or silane.

As previously mentioned, our group has identified interesting mechanisms for the reduction of carbonyls using Mo catalysts. To better understand the catalytic process occurring with compound **III-6**, stoichiometric reactions were carried out with various unsaturated substrates as well as silanes. This methodology allows the determination of important intermediates or deactivation pathways of catalytic cycles and is an excellent first step in gathering information of the catalytic processes. Initially, a 1:1 reaction of $PhSiH_3$ with **III-6** showed no reactivity according to NMR analysis even after many days. No exchange with the hydride group was seen at room temperature, as confirmed by 1D-EXSY experiments. However, this does not rule out an exchange as the process may be much slower than the timescale of EXSY experiment at this temperature. In order to confirm this, $PhSiD_3$ was added to **III-6** and indeed partial deuteration of the hydride group was seen by ^{2}H-NMR after only 10 minutes at room temperature. Interestingly, no exchange between the agostic silane and free silane is seen, even at increased amounts of silane. Leaving the reaction overnight at room temperature maintains the same ratio of deuteration. Longer reaction times result in decomposition of complex **III-6**. It is unlikely that the exchange process goes through oxidative addition of silane to the metal centre as Mo(VI) is already saturated. One possibility is the activation through a σ bond metathesis proceeding through $(ArN)_2Mo\{N(^tBu)SiMe_2H\}(H^{\cdots}SiD_2Ph^{\cdots}D^{\cdots})$ transition state. A second thinkable pathway could be coupling of the silane to one of the imido groups on the Mo centre to give a bis(silylamido) dihydride complex

$(ArN)Mo(ArNSiH_2Ph)(^tBuNSiMe_2H)(H)_2$ which can then decompose by recombination of the incoming silyl group with the alternative hydride to produce $PhSiH_3$ (Scheme 42). This would maintain the oxidation state of the metal and has been shown to occur for other Mo systems.[10,11,163] Also, similar couplings have been shown to occur for both Mo=O[64] and Re=O[164] systems, which involve addition of the Si-H bond across the metal oxo bond to generate a siloxy hydride complex (H-M-OSi). An argument against this mechanism is the lack of elimination of

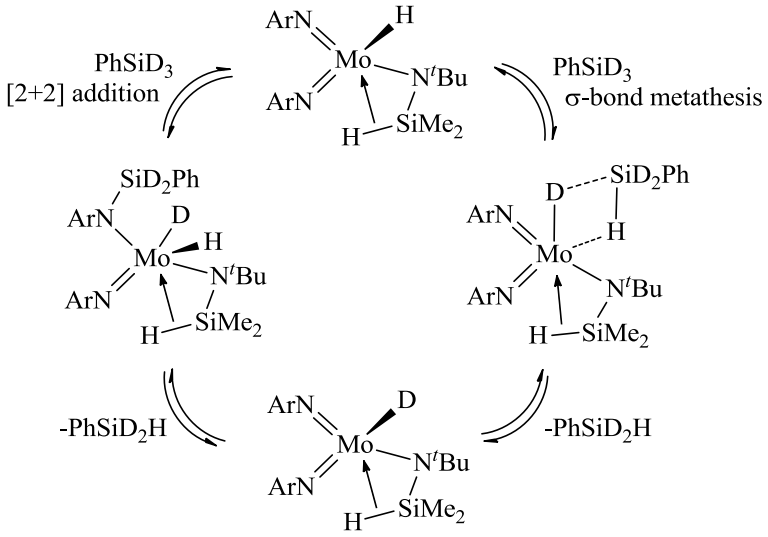

Scheme 42 – Two pathways depicting H/D exchange of the hydride ligand of **III-6** with $PhSiD_3$.

H_2SiMe_2, which is deemed possible from the bis(silylamide) intermediate.

On the other hand, the 1:1 addition of benzaldehyde to compound **III-6** showed the expected insertion product into the Mo-H bond to generate complex the benzoxy complex $(ArN)_2Mo(N^tBuSiHMe_2)(OBn)$ (**III-8**) characterized by NMR techniques. The ^{1}H-NMR shows a downfield shift of the Si-H resonance to 5.15 ppm with a $^1J_{Si\text{-}H}$ value of 198 Hz indicative of a classical silylamido coordination. The methylene unit of the benzoxy ligand appears as a singlet at 5.35 ppm. The formation of the singlet indicates C_s symmetry within the molecule. Compound **III-8** can be produced on large scale in good yields (65 %) through *in situ* generation of complex **III-6** followed by addition of one equivalent of benzaldehyde then by recrystallization at low

temperature in hexanes. The reaction with acetophenone or acetone leads to a similar insertion products albeit with longer reaction times. The alkoxy complexes are much more stable than the hydride analogues with no degradation seen after 8 hours at 50 °C. However, extensive heating (80 °C) for a few days leads to decomposition to a mixture of unidentifiable products. Alternatively, an attempt at **III-8** synthesis through the addition of LiOBn to the chloride derivative (**III-3**) does not generate **III-8** even after prolonged heating to 50 °C.

The addition of one equivalent of $PhSiH_3$ to **III-8** regenerates the hydride complex after many days at room temperature but, the addition of 10 equivalents of $PhSiH_3$ does not affect the rate of hydride formation. Typically, mechanisms of carbonyl hydrosilylation for d^0 systems using early transition metals proceed through insertion of the carbonyl into the hydride bond followed by σ-bond metathesis with $PhSiH_3$ regenerating the initial hydride complex and producing the respective silylether. However, similar rates are observed when either compound **III-8** or **III-6** are used as catalysts. These important observations suggest that hydrosilylation may not proceed *via* an expected hydride mechanism.

The possibility of non-hydride mechanisms have been proposed by our group for the hydrosilylation of carbonyls.[72] Reacting one equivalent of tris(pyrazolyl) borate (Tp) with $(ArN)Mo(PMe_3)_3(H)(Cl)$ generates the isolobal system $Tp(ArN=)Mo(H)(PMe_3)$ (**III-9**) through loss of LiCl and two equivalents of PMe_3. Complex **III-9** proved to be a potent catalyst for the hydrosilylation of carbonyls and mechanistic studies produced interesting results. Initial studies showed the rate determining step to be the dissociation of one arm of the pyrazolyl ligand and not dependent on the PMe_3 ligand (see Section II.2.2). The reaction of $PhSiH_3$ with **III-9** showed no reactivity but insertion of benzaldehyde was observed. Alternatively, the reactivity with ketones is incredibly sluggish and not compatible with the hydride mechanism. This led to the

discovery of a 1:1:1 reaction between **III-9**, PhCHO and $PhSiD_3$ which showed the unexpected retention of the hydride ligand in the protio form and complete deuterium transfer to the resulting silyl ether product $PhCHDOSiD_2Ph$. Similar results were obtained using cyclohexanone and $PhSiD_3$. This led to a conclusion of Lewis acid catalyzed hydrosilylation, which have been shown for other transition metals such as $Ti(O^iPr)_4$, $ZrCl_4$ and $HfCl_4$.[156]

Reacting complex **III-8** in a 1:1:1 ratio with $PhSiD_3$ and benzaldehyde results in generation of the expected hydrosilylation product $PhH_xD_ySiOCH_xD_yPh$ (x+y=2) with deuteration scrambling into the methylene unit of the product. As well, the partial protonation of the Si-H signals are observed. Most interesting is the preservation of complex **III-8** showing no deuterium scrambling into any position. The expected hydride pathway, shown in Scheme 43, would generate a deuteride complex from the metathesis with $PhSiD_3$ followed by insertion of the added benzaldehyde into the Mo-D bond to regenerate a benzoxy complex with deuterium incorporated into the methylene position. These unusual results suggest the conventional hydride

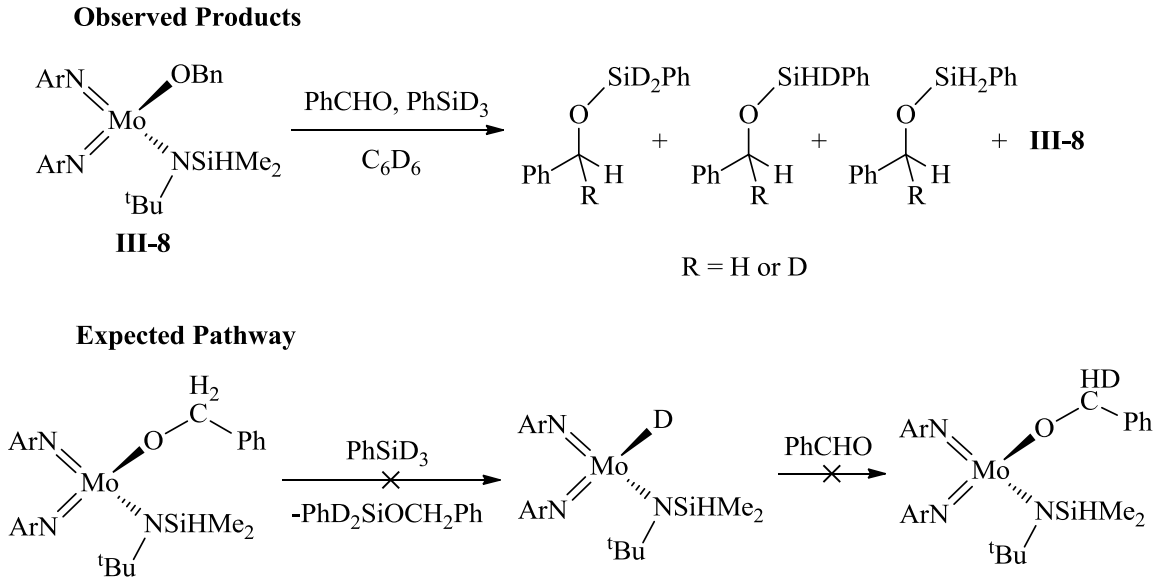

Scheme 43 – 1:1:1 reaction between complex **III-8**, benzaldehyde and $PhSiD_3$ (top) as well as the expected pathway shown below.

mechanism does not operate in this system.

To shed more light on this mechanistic puzzle, kinetic studies were performed to obtain quantitative information on reaction rates and to understand the rate limiting step for the system. Working under pseudo first order conditions in aldehyde, i.e. by using a large excess of silane, the rate law with respect to catalyst and aldehyde concentration can be deduced. To eliminate the impact of competing of mono-, di- and trisubstitution involved when $PhSiH_3$ is used, the choice of silane was switched to $(EtO)_2MeSiH$. A series of experiments with different silane concentrations were performed under the pseudo first order regime (see Appendix Figure 17). Plotting the effective reaction rate constant k_{obs} vs. silane concentration, allowed us then to find a linear correlation between the reaction rate and silane concentration, thus establishing that the reaction law is rate=k[catalyst][aldehyde][silane], i.e. an overall second order in reagents (Figure 11). Unfortunately, such a kinetic law does not tell us much about the mechanism, as it shows no preference for any of reagent to react with the catalyst in the first step. No saturation behaviour was observed even at high concentrations of silane addition (12 equivalents), that would be

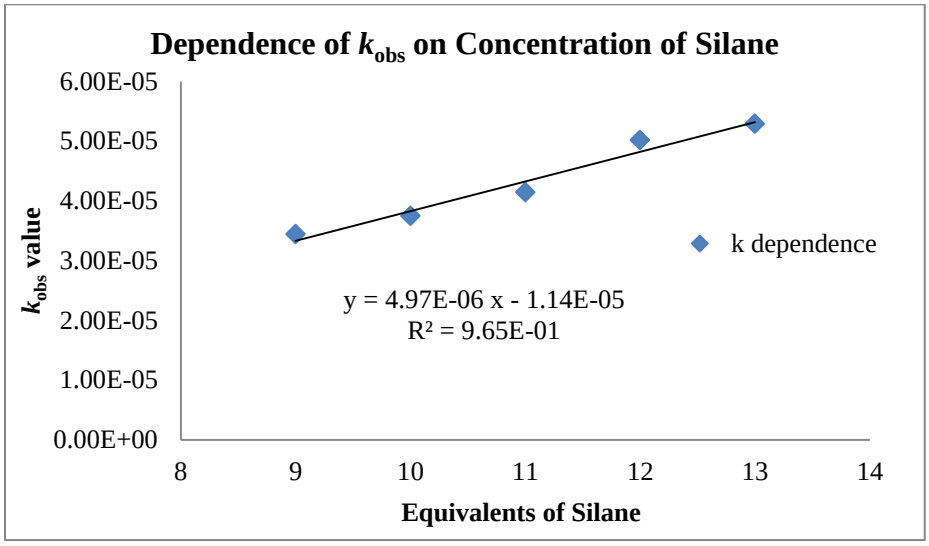

Figure 11 – k_{obs} vs. equivalents of silane added for the hydrosilylation of PhCHO using 5 mol % **III-8** under pseudo first-order conditions in aldehyde.

indicative of a pre-equilibrium step.

Next, the pseudo first order kinetic experiment was attempted under kinetic conditions (at 5 mol % loading of catalyst **III-8**) by using excess aldehyde. However, upon addition of 10 equivalents of benzaldehyde with respect to one equivalent of $(EtO)_2MeSiH$ deactivation of the catalyst took place and no hydrosilylation products observed. Importantly, signals pertaining to imine formation in the ^{1}H-NMR allowed the speculation about an oxo/imido deactivation pathway. Such an exchange is a known phenomenon.[165-167] Indeed, in 1992 Gibson and co-workers found that addition of $ArNH_2$ to the $(^tBuN)_2Mo(O^tBu)_2$ complex produced an equilibrium mixture of the mixed imido system $(ArN)(^tBuN)Mo(O^tBu)_2$ and $^tBuNH_2$. They also found that adding excess benzaldehyde to $(^tBuN)_2Mo(O^tBu)_2$ results in the complete conversion into the oxo molybdenum complex $(^tBuN)(^tBuO)_2Mo{=}O$ and the loss of one equivalent of the imine $^tBuN{=}CHPh$.[168] In the case of complex **III-8**, the addition of excess benzaldehyde seems to produce similar structures deduced by NMR, with the C-H imine proton (i.e. ArN=C*H*Ph) resonating at δ 8.25 ppm (s) in the ^{1}H-NMR. Similar kinetic studies with tertiary alkyl silanes, such as Me_2PhSiH and Et_3SiH, also showed signals for the respective imine products. This observation shows that the rate of hydrosilylation using these tertiary alkyl silanes is much slower than that of deactivation *via* imine production.

Currently, no conclusive evidence points towards one mechanism in particular; non-hydride or otherwise. However, based on the reactivity we can postulate that indeed a non-hydride mechanism is likely. A simplified explanation for the hydrosilylation of carbonyls mediated by **III-6** could be Lewis acid catalysis. In this case, the Mo(VI) complex **III-6** could be considered a 16 e^- complex assuming minimal lone pair donation from the imido nitrogen. This allows coordination and subsequent activation of the C=O double bond. Attack of Si-H hydride

could give the respective silylether in a concerted fashion and regenerate complex **III-6**. To test this theory, we reacted $(ArN)_2Mo(N(^tBu)SiHMe_2)(Cl)$ (**III-3**) at 5 mol % with $PhSiH_3$ and PhCHO. Reduction to the respective silylether was observed after 8 hours, as opposed to 10 minutes with **III-3**. Saturation of the Mo(VI) centre by the lone pair donation from the chloride ligand would thereby prohibit coordination of the carbonyl in line with a Lewis acid catalyzed process.

Recently, reports on nickel based alkoxy complexes acting as suitable catalysts for the hydrosilylation of carbonyls have been shown.[158,161] The mechanisms seem to generate a reactive hydride complex followed by insertion of carbonyl then subsequent addition of silane to give silylether and regeneration of hydride.[158] Based on this fact and that the alkoxy complex **III-8** proved to be a potent catalyst for the hydrosilylation of carbonyls, other simple Mo(VI) alkoxy complexes were tested. The reaction between $(ArN)_2MoCl_2(DME)$ and 2 equivalents of KO^tBu gives the known alkoxy complex $(ArN)_2Mo(O^tBu)_2$ (**III-10**).[168] This complex was tested towards hydrosilylation at 5 mol % catalyst loading and was found to give excellent conversions in a short period of time. The decrease in reaction time for ketones was most surprising with acetophenone showing 100 % conversion in one hour at room temperature (entry 2, Table 2). The related ^{t}Bu derivative $(^tBuN)_2Mo(O^tBu)_2$ (**III-11**) showed even higher activity with the full conversion of acetophenone finishing in only 15 minutes (entry 2, Table 3). Other substrates were tested using each system and higher activity was shown across the board compared to the Mo(VI) complex **III-6**. Donating groups on the phenyl ring were tolerated and showed full conversion after one hour for **III-10** and 15 minutes for **III-11**. In both cases, the electron withdrawing nitro substituent (4-NO_2-acetophenone) deactivates the catalyst and no reduction to the corresponding silylether was observed (entry 4). The reduction of bulkier substrates like

benzophenone were converted in just 12 hours for **III-10** and 6 hours for **III-11** (entry 5). Aliphatic carbonyls such as acetone were convereted to $PhSiH_2(O^iPr)$ and $PhSiH(O^iPr)_2$ in under an hour. Interestingly, the reduction of cyclohexanone was sluggish for **III-10**, furnishing the silylether products $PhSiH_2(OCy)$ (37 %) and $PhSiH(OCy)_2$ (63 %) in 24 hours (entry 7, Table 2). Complex **III-11** was much more efficient showing conversion in 30 minutes to a similar yield of mono- and di-substituted silylether products at room temperature. The reduction of esters was also probed, and ethyl acetate could be easily reduced in 1 hour using **III-10** or 15 minutes using **III-11**.

Table 2 – Hydrosilylation of carbonyls mediated by **III-10** with KO^{t}Bu.[a]

Entry	Substrate	Time (h)	Products (%)	Yield (%)[b]	TON	TOF (h^{-1})
1	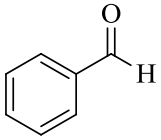	0.2	$PhSiH_2(OBn)$ $PhSiH(OBn)_2$	35 65	20	100
2	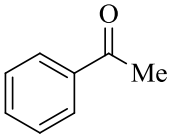	1	$PhH_2Si[OCH(Me)Ph]$ $PhHSi[OCH(Me)Ph]_2$	33 67	20	20
3	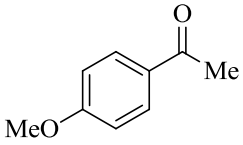	1	$PhH_2Si[OCH(Me)Ph^{OMe}]$ $PhHSi[OCH(Me)Ph^{OMe}]_2$	32 68	20	20
4	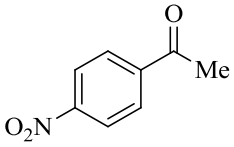	NR	NR	NR	--	--
5	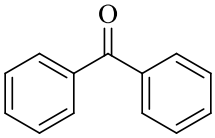	12	$PhH_2Si(OCH_2Ph_2)$ $PhHSi(OCH_2Ph_2)_2$	25 75	20	1.7
6		0.5	$PhSiH_2(O^iPr)$ $PhSiH(O^iPr)_2$	28 72	20	40
7	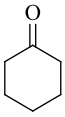	24	$PhSiH_2(OCy)$ $PhSiH(OCy)_2$	37 63	20	0.83
8	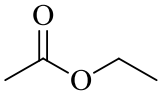	1	$PhSiH(OEt)_2$ $PhSi(OEt)_3$	90 10	20	20

[a] Catalyst and KO^{t}Bu loading at 5 mol %, with 1:1 ratio between silane and substrate. All reactions carried out at room temperature. [b] Determined by ^{1}H-NMR using residual solvent as internal standard.

Table 3 – Hydrosilylation of carbonyls mediated by **III-11** with KO^{t}Bu.[a]

Entry	Substrate	Time (h)	Products (%)	Yield (%)[b]	TON	TOF (h^{-1})
1	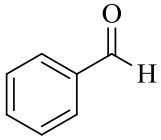	0.2	$PhSiH_2(OBn)$ $PhSiH(OBn)_2$	35 65	20	100
2	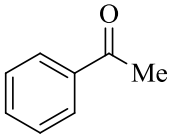	0.25	$PhH_2Si[OCH(Me)Ph]$ $PhHSi[OCH(Me)Ph]_2$	33 67	20	80
3	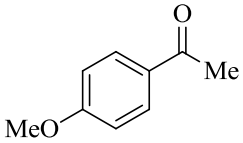	0.25	$PhH_2Si[OCH(Me)Ph^{OMe}]$ $PhHSi[OCH(Me)Ph^{OMe}]_2$	32 68	20	80
4	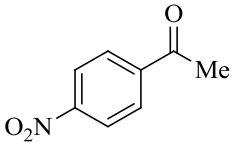	NR	NR	NR	--	--
5	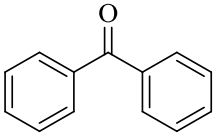	6	$PhH_2Si(OCH_2Ph_2)$ $PhHSi(OCH_2Ph_2)_2$	22 78	20	1.7
6		0.5	$PhSiH_2(O^iPr)$ $PhSiH(O^iPr)_2$	30 70	20	40
7	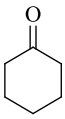	0.5	$PhSiH_2(OCy)$ $PhSiH(OCy)_2$	47 53	20	40
8	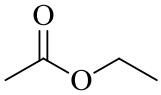	0.25	$PhSiH(OEt)_2$ $PhSi(OEt)_3$	80 20	20	80

[a] Catalyst and KO^{t}Bu loading at 5 mol %, with 1:1 ratio between silane and substrate. All reactions carried out at room temperature. [b] Determined by ^{1}H-NMR using residual solvent as internal standard.

III.3 Base Induced Cyclometallation of PMe_3 Ligand

Our interest in hydrosilylation by using group 6 catalysts stemmed from the observation of interesting and diverse reactivity of silane addition to various bis(imido) complexes. As previously mentioned, many derivatives of these complexes have proven to be efficient catalysts for hydrosilylation and shown to go through new interesting mechanisms. One of the major aspects of this thesis is to investigate the reactivity of similar complexes containing different imido functionalities of the type $(RN)(R'N)Mo(PMe_3)_n$ (n = 2, 3) and study their reactivity towards silane addition. Based on previous work, these complexes may provide interesting uses as hydrosilylation catalysts and allow us to study the non-classical β-agostic silylamido complexes that are often formed upon addition of silanes to the M=NR moiety.

From a retrosynthetic point of view, we reckoned that either the monoimido hydride chloride or dichloride complexes $(RN)Mo(PMe_3)_3(Cl)(X)$ (X = Cl, H) could be used as a viable starting material, being relatively robust and easily synthesized on large scale with high purity. The addition of one equivalent of the appropriate silylamide to these starting compounds could

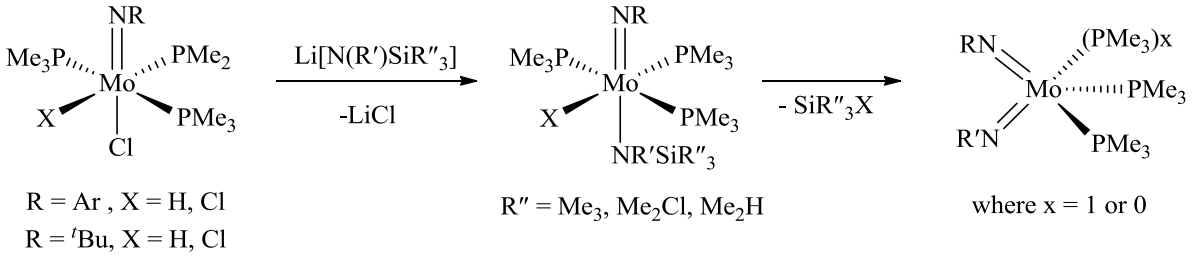

Scheme 44 – Postulated pathway for the formation of unsymmetrical bis(imido) phosphine complexes.

generate the corresponding silylamido complex as shown in Scheme 44. The choice of silylamide reagent is important as we envisioned the loss of the silyl group in the form of silane $HSiR_3$ or chlorosilane $ClSiR_3$ to generate the corresponding mixed bis(imido) system. Loss of

silane through addition of a silylamide ligand is a known process for generating imido groups, as has been shown for example, in the addition of Li[RNSiMe$_3$] to CpMCl$_4$ (M = Nb, Ta) to give Cp(RN=)MoCl$_2$ and ClSiMe$_3$ as the resulting products.[9]

To our surprise, the addition of one equivalent of Li[N(^{t}Bu)SiHMe$_2$](THF) to the hydride chloride complex (ArN)Mo(PMe$_3$)$_3$(H)(Cl) (**III-12**) did not generate a silylamido derivative, but in fact showed an unexpected C-H activation of a methyl groups on a pendant PMe$_3$ ligand to generate a cyclometallated three-membered ring complex (ArN)Mo(PMe$_3$)$_2$(η^2-CH$_2$PMe$_2$)H (**III-13**), Scheme 45). Alternative attempts at generating the mixed imido systems by using such silylamides as Li[N(Ar′)SiMe$_3$] or Li[N(^{t}Bu)SiMe$_3$] also resulted in conversion to complex **III-13**. We then found that addition of simpler amides, such as Li[NHAr], Li[NH^{t}Bu], LiHMDS (HMDS = hexamethylsilylamide) or lithium piperdide, all give complex **III-13**, albeit at different rates depending on the size of the base. In contrast, alkoxides showed no reactivity and no production **III-13** over a period of a few days at room temperature. Complex **III-13** can be synthesized on gram scale in up to 70 % yield. Characterization was done by multinuclear and correlation NMR with the stereochemical assignments established by 1D-NOESY experiments.

Complex **III-13** exists as a mixture of two isomers in a ratio of 10:1 in solution. The major isomer displays the methylene resonance of the cyclometallated ring at -0.98 ppm as a doublet of doublet of doublets ($^2J_{H-P}$ = 12.2 Hz, $^3J_{H-P}$ = 3.7 Hz, $^3J_{H-H}$ = 0.9 Hz) in the ^{1}H-NMR. The Mo-CH_2 signal couples to the two equivalent PMe$_3$ groups, the cyclometallated phosphine and the hydride ligand. This downfield shift of the methylene position is typically observed for complexes of the type M(η^2-CH$_2$PMe$_2$).[86] The Mo-hydride signal is seen at 4.08 ppm (t, $^3J_{H-H}$ = 38.2 Hz), which is downfield shifted compared to other metal hydride complexes. This phenomenon is typically observed for mono imido complexes of Mo with the hydride ligand *cis*

to the imido group, and can be attributed to the anisotropy of the latter. For example, the Mo hydride complex **III-12** contains a *cis* hydride ligand displaying a hydride at 5.31 ppm[11], whereas the silyl hydride complex (ArN)Mo(PMe_3)$_3$(SiH_2Ph)(H) containing a *trans* hydride ligand displays its resonance at -3.92 ppm.[15] The ^{31}P-NMR shows two signals at δ 5.36 ppm (d, $^2J_{P\text{-}P}$ = 18.7 Hz) and triplet -37.20 (t, $^2J_{P\text{-}P}$ = 19.0 Hz) with relative intensities in a 2:1 ratio respectively. This is typically seen for Mo tris(phosphine) complexes where each of the three phosphine groups lie in the same plane in a meridonal fashion. The ^{13}C{^{1}H}-NMR spectrum also displays a significant downfield shifted methylene resonance at δ -5.14 ppm (dt, $^2J_{C\text{-}P}$ = 26.3 Hz, $^2J_{C\text{-}P}$ = 7.7 Hz) coupling to all three phosphines.

Interestingly, the minor isomer shows two different resonances for each diastereotopic methylene proton at δ -1.62 and -0.71 ppm. This is indicative of the loss of symmetry as a result of different relative orientation of the ligands on the metal. Based on 1D-NOESY experiments and the relative downfield shifted methylene signals suggest the imido group and methylene unit of the cyclometallated ring remain trans to each other. Each of the three phosphine ligands of the minor isomer are inequivalent according to ^{31}P-NMR, displaying three distinct doublets at δ 7.79, -2.92 and -16.69 ppm. The hydride multiplet at δ 3.25 ppm in the ^{1}H-NMR couples to all phosphine signals determined by ^{1}H-^{31}P HSQC as well as each methylene proton of the cyclometallated ring. Based on these observations two orientations were suggested and are shown in Scheme 45. The major isomer exhibits a plane of symmetry running through the Mo-C-P ring, allowing the two *trans* PMe_3 groups to become equivalent. Alternatively, the minor isomer contains a hydride *trans* to one of PMe_3 groups resulting in the decrease of symmetry to C_1 which accounts for the inequivalency of phosphine ligands.

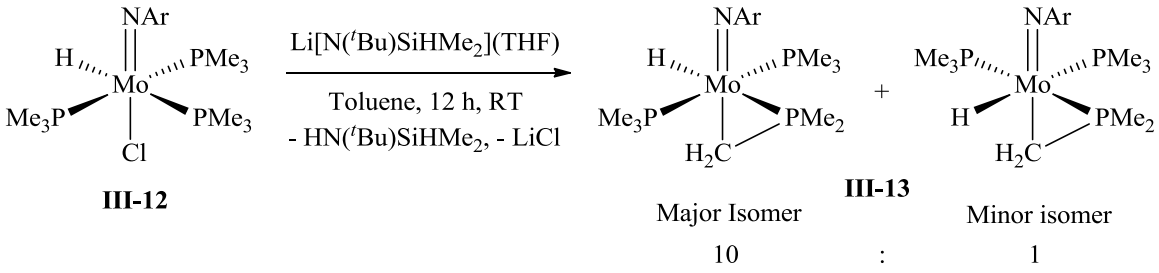

Scheme 45 – Base induced cyclometallation of **III-12** through the addition of Li[N(^{t}Bu)SiHMe$_2$](THF), generating complex **III-13**.

Unexpectedly, similar reactions of the precursor dichloride complex (ArN)Mo(PMe$_3$)$_3$(Cl)$_2$ with various silylamides, primary amides or secondary amides gave no reactivity even after prolonged heating at 50 °C. In contrast, the related ^{t}Bu imido derivative (^{t}BuN)Mo(PMe$_3$)$_3$(Cl)$_2$ (**III-14**) can be indeed easily activated through the addition of any of the above mentioned amide bases. Reacting one equivalent of Li[N(^{t}Bu)SiHMe$_2$](THF) with **III-14** results in 70 % conversion into the cyclometallated complex (^{t}BuN)Mo(PMe$_3$)$_2$(η^2-CH$_2$PMe$_2$)Cl (**III-15**) over a period of eight hours at room temperature, with 30 % starting material remaining. Through optimization studies we found that adding 1.6 equivalents of Li[NH(^{t}Bu)] results in complete conversion to complex **III-15**. The need for excess amide is unclear but seems to push the reaction to completion. Unlike the Ar derivative, isolation of complex **III-15** is difficult due to decomposition into a variety of different products overnight and high solubility in aliphatic solvents, such as hexanes or pentanes, even at low temperatures. According to NMR data, **III-15** exists as a mixture of isomers (10:1) similar to the Ar derivative.

NMR characterization suggests a similar structure to **III-13** showing a methylene proton resonance at -0.47 ppm (td, $^3J_{H\text{-}P}$ = 12.5 Hz, $^2J_{H\text{-}P}$ = 3.8 Hz) in the ^{1}H-NMR coupling to two PMe$_3$ groups and the PMe$_2$ group of the cyclometallated ring. The ^{31}P-NMR displays a doublet at -2.18 ppm and triplet at -6.23 ppm cosisitant with all three phosphine lying in the same plane.

The ligand environment most likely resembles that of **III-13** with the chloride ligand occupying a position *trans* to the phosphine of the cyclometallated ring as well as *trans* imido and CH_2 groups. The hydride derivative (^{t}BuN)Mo(PMe_3)$_2$(η^2-CH_2PMe_2)(H) could also be synthesized by adding one equivalent L-Selectride to **III-14** followed by 1.5 equivalents Li[N(tbu)$SiHMe_2$(THF)]. All NMR spectra are in agreement with a similar structure to that of the Ar derivative **III-13**, with a methylene CH_2 resonance at δ -1.11 ppm (tdd, $^3J_{H\text{-}P}$ = 11.5 Hz, $^2J_{H\text{-}P}$ = 4.4 Hz, $^3J_{H\text{-}H}$ = 1.8 Hz) coupled to the hydride resonance at δ 4.06 ppm (t, $^3J_{H\text{-}P}$ = 38.7 Hz) in the ^{1}H-NMR.

III.3.1 E-H Bond Activation using (ArN)Mo(PMe_3)$_2$(η^2-CH_2PMe_2)H

Facile activation of E-H σ-bonds is an interesting challenge for synthetic chemists and finds use in many areas of research including renewable energy applications and petrochemical industries.[169] Late transition metal complexes bearing electron rich metal centres can be used for this purpose especially in the field of catalysis where hydrogenations or hydrosilylations typically require the oxidative addition of the H-H or Si-H bond.[2,49] Alternatively, Parkin's work using the cyclometallated tungsten complex W(PMe_3)$_4$(η^2-CH_2PMe_2)H shows that a wide range of reactivity is possible for early transition metal E-H bond activation. As has been previously described in Section II.3, addition of E-H bonds (E = O, C, Si, S) to electron rich cyclometallated complexes containing a M-P-C three-membered ring proceeds through addition across the M-C bond. We envisioned complexes **III-13** and **III-15** to be prone to similar bond activations due to the presence of a relatively electron rich metal centre. The presence of different R groups on the imido ligand provides different electronic and steric situations, allowing comparisons to be drawn in each case.

The activation of Si-H bonds is an important process as it is believed to be the key step in

catalytic hydrosilylation. Reactions of **III-13** with the primary and secondary silanes $PhSiH_3$ and $PhMeSiH_2$, respectively, were attempted but gave a variety of intractable products in each case. In the case of tertiary silane $PhMe_2SiH$, no reactivity was observed even upon heating to 50 °C overnight. The silyl hydride complex $(ArN)Mo(PMe_3)_3(SiH_2Ph)(H)$ has been previously prepared in a similar manner through the treatment of **III-12** with $LiBH_4$ in the presence of PMe_3 and $PhSiH_3$.[170] Mechanistic NMR studies suggested the intermediacy of the mono(borohydride) derivative $(ArN)Mo(PMe_3)_2(\eta^2\text{-}BH_4)(H)$ followed by addition of $PhSiH_3$ to give BH_3 and H_2. In the case of **III-13,** a variety of hydritic products (high field signals between δ -5 to -8 ppm in ^{1}H-NMR) are observed suggesting redistribution of silane or oligomer formation followed by decomposition of the complex.

Along the same lines, the activation of B-H bonds to generate new boryl complexes represents an important aspect of hydroboration, production of hydrogen from such hydrogen storage materials as aminoboranes, and in synthetic organic chemistry (i.e. in preparation of Suzuki reagents by direct borylation of arenes).[171] The Nikonov group has recently utilized complex **III-12** in catalytic hydroboration which was shown to go through an interesting agostic Mo···H-B amino-borane intermediate. However, direct addition of HBR_2 (R = cat, pin) to complex **III-12** does not show any reactivity with the to give boryl complexes of the type $(ArN)Mo(PMe_3)_3(BR_2)(Cl)$. We envisioned addition of HBcat or HBpin would furnish boryl complexes of this type when added to complex **III-13**. Unfortunately, the reactions are sluggish and mixtures of products are typically observed. The Lewis acid/base adduct $R_2HB{\cdot}PMe_3$ (R = cat, pin) is seen for both reactions.

The reaction between Ph_2PH and **III-13** results in the addition across the Mo-C bond to give the phosphido hydride complex $(ArN)Mo(PMe_3)_2(PPh_2)(H)$ (**III-16**). The loss of PMe_3 can

be attributed to both the incorporation of a large PPh_2 phosphido ligand sterically and to the extra π-donation of the phosphide lone pair to the metal. This is typical for electron deficient metals containing vacant orbitals, which is the case of the d^2 Mo(IV) complex **III-13**. ^{1}H NMR study of **III-16** revealed a hydride resonance at 3.22 ppm appearing as a triplet with the large $^2J_{H\text{-}P}$ value of 44.0 Hz coupling to each phosphine ligand determined by ^{1}H-^{31}P HSQC. The ^{31}P-NMR displays a low field triplet at 168.21 ppm ($^2J_{P\text{-}P}$ = 35.1 Hz) corresponding to the phosphido ligand. The high field doublet at 13.48 ppm ($^2J_{P\text{-}P}$ = 35.7 Hz) corresponds to the two equivalent PMe_3 ligands. The addition of a second equivalent of Ph_2PH to **III-16** results, after 2 days at room temperature, in phosphine/hydride σ-metathesis generating the bis(phosphido) complex $(ArN)Mo(PMe_3)_2(PPh_2)_2$ (**III-17**). Like for the parent compound **III-16**, the ^{31}P-NMR exhibits a similar low field singlet at 115.31 ppm corresponding to two equivalent PPh_2 ligands, as well as the corresponding high field triplet at -9.84 ppm. The downfield shift of the phosphide signal in the ^{31}P-NMR is typical for Mo(IV) phosphide complexes, such as $Mo(NMe_2)_2(PPh_2)_2$ (δ = 190 ppm), or $Mo(NMe_2)_3(PPh_2)$ (δ = 154 ppm).[172] However, these shifts are dependent on the types metal used, ligands in the coordination sphere and oxidation state of the metal.[171] Interestingly,

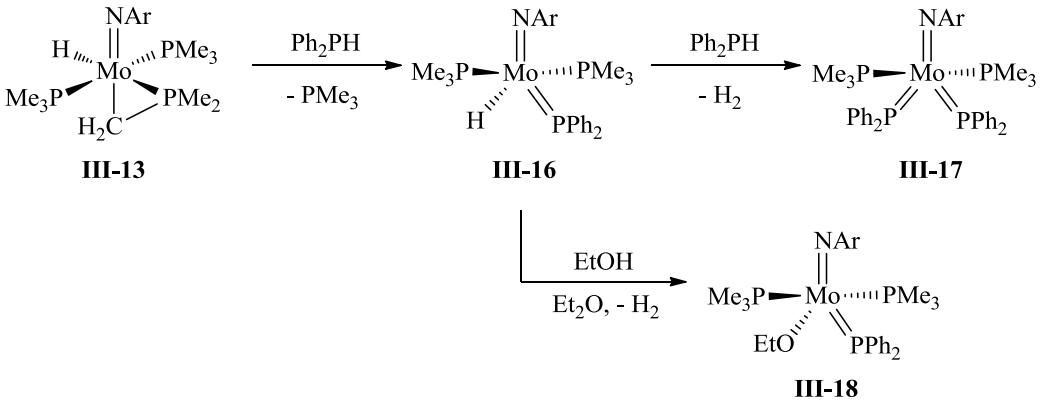

Scheme 46 – Synthesis of the phosphide hydride complex **III-16**, bis(phosphide) complex **III-17**, and ethoxy phosphide complex **III-18**.

the addition of EtOH to **III-13** results in a similar σ-metathesis generating hydrogen gas and producing the ethoxy phosphide complex (ArN)Mo(PMe_3)$_2$(PPh_2)(OEt) (**III-18**). The downfield shift of the phosphide ligand at 108.65 ppm, coupled to a doublet at -5.46 ppm in the $^{31}P\{^1H\}$-NMR, indicates a similar structure as in **III-17**. The CH_2 signal of the ethoxy moiety couples to both the CH_3 group and to each of the phosphine and phosphide ligands ($^4J_{H\text{-}P}$ = 1.1 Hz) as determined by ^1H-^{31}P HSQC and $^1H\{^{31}P\}$ NMR.

The molecular structure of **III-17** was determined by X-ray crystallography (Figure 12) and adopts a trigonal bipyramidal geometry with two trans PMe_3 groups (P3-Mo1-P4 172.45(8)°; Table 4) and a basal plane consisting of the imido and phosphido groups (sum-of-the-angles = 359.4°). The Mo-P bond distances of the PPh_2 ligands (2.303(2) and 2.446(2) Å) are shorter than the M-P bond distances of the PMe_3 ligands (2.531(2) and 2.505(2) Å). This is indicative of possible multiple bond character (Mo=P) between Mo and phosphorous of the PPh_2 groups. Further evidence comes from summation of the angles around the phosphide ligands (summation-of-angles; P1 = 357.1°, P2 = 349.8°). The significant trigonal planar geometry associated with P1 and P2 is indicative of lone pair donation from each phosphide to the d^2 Mo(IV) centre. For example, the structure of Mo(NMe_2)$_2$(PPh_2)$_2$, reported by Chisholm and coworkers, also displays this type of behaviour (summation-of-angles; 358.5° and 357.9°)[172].

Acidic C-H bonds such as alkynes can be added across the M-C bond of the cyclometallated complex **III-13**. The addition of phenylacetylene to **III-13** produces 70% of the bis(phenylacetylene) complex (ArN)Mo(PMe_3)(η^2-C(H)≡CPh)$_2$ (**III-19**) in a 2:1 ratio with a minor isomer and 30 % the Mo-H insertion product (ArN)Mo(PMe_3)$_2$(η^2-CH_2PMe_2)(CH=CHPh) (**III-20**) (Scheme 47). All complexes were characterized by 1D and 2D NMR techniques. The major isomer of complex **III-19** displays a single resonance for the terminal C-H protons at 8.77

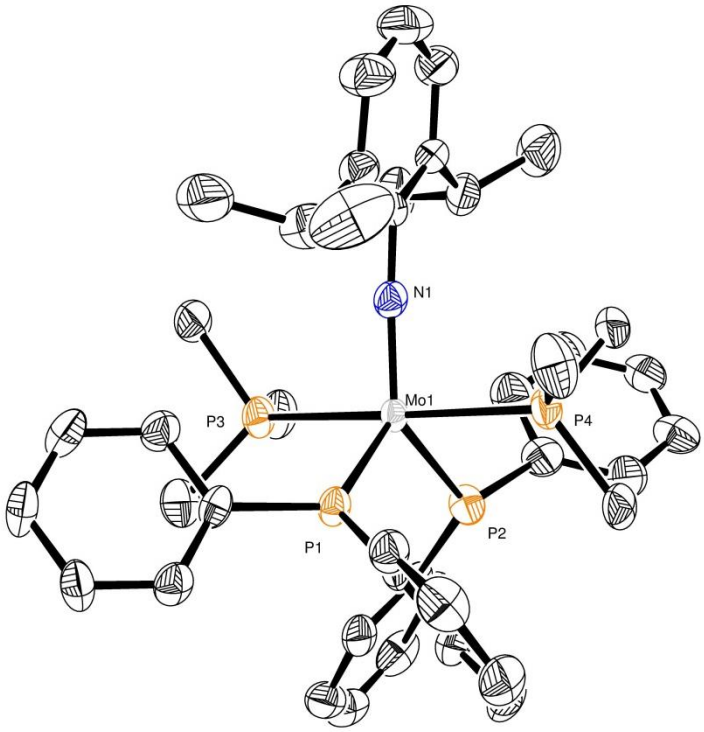

Figure 12 - ORTEP plot of the molecular structure of **III-17** (hydrogen atoms are omitted for clarity). Anisotropic displacement parameters are plotted at 50 % probability.

Table 4 – Selected bond distances (Å) and angles (°) for complex **III-17**.

Distances (Å)		Angles (°)			
Mo1-N1	1.771(6)	Mo1-N1-C31	172.7(6)	C1-P1-C7	101.9(4)
Mo1-P1	2.303(2)	N1-Mo1-P1	119.3(2)	Mo1-P1-C7	127.5(3)
Mo1-P2	2.446(2)	N1-Mo1-P2	131.5(2)	Mo1-P1-C1	127.7(3)
Mo1-P3	2.531(2)	P1-Mo-P2	108.5(8)	C19-P2-C13	105.5(12)
Mo1-P4	2.505(2)	N1-Mo1-P3	86.8(2)	Mo1-P2-C13	120.0(10)
		N1-Mo1-P4	92.6(2)	Mo1-P2-C19	124.2(3)
		P3-Mo1-P4	172.45(8)		

ppm (d, $^{3}J_{H\text{-}P}$ = 17.8 Hz). The fact that only one signal is seen indicates C_s symmetry within the tetrahedral molecule in which each phenyacetylene moiety lie in the same plane, with the terminal C-H protons facing each other. A second plane running through the N-Mo-P fragment

causes each phenylacetylene moiety to be equivalent. On the other hand, the minor isomer is C_1 symmetric due to each terminal C-H bond facing in opposite direction (Scheme 47). The ^{1}H-NMR confirms this with two distinct signals seen at 8.66 ppm (d, $^3J_{H\text{-}P}$ = 16.5 Hz) and 10.41 ppm (d, $^3J_{H\text{-}P}$ = 5.5 Hz) for each terminal C-H proton. The related complex (^{t}BuN)$_2$Mo(PMe$_3$)(η^2-C(H)≡CPh) displays similar behaviour, with the terminal C-H proton resonating at 8.58 ppm (d, $^3J_{H\text{-}P}$ = 14.8 Hz).[173] The acetylenic carbons resonate in the range 145–175 ppm, which is intermediate between the ranges observed for two-electron (110-120 ppm) and four-electron (190-210 ppm) alkyne ligands, suggested by Templeton *et al.*[174] This indicates that, to some extent, partial donation of electron density from the $\pi_\perp$-orbital of the alkyne ligands may be present.

Complex **III-20** was characterized as a Mo vinyl complex where one equivalent of phenylacetylene inserts into the Mo-H bond. The vinylic protons resonate at 6.98 and 10.09 ppm in the ^{1}H-NMR and couple to both ^{31}P signals at -2.61 and -29.19 ppm. Likewise, downfield shifted ^{13}C signals were observed at 134.45 and 185.64 ppm. The cyclometallated CH_2 methylene group displays a resonance at -0.77 ppm (dt, $^3J_{H\text{-}P}$ = 9.9 Hz, $^3J_{H\text{-}P}$ = 3.8 Hz) and couples to each ^{31}P group. Related vinyl complexes

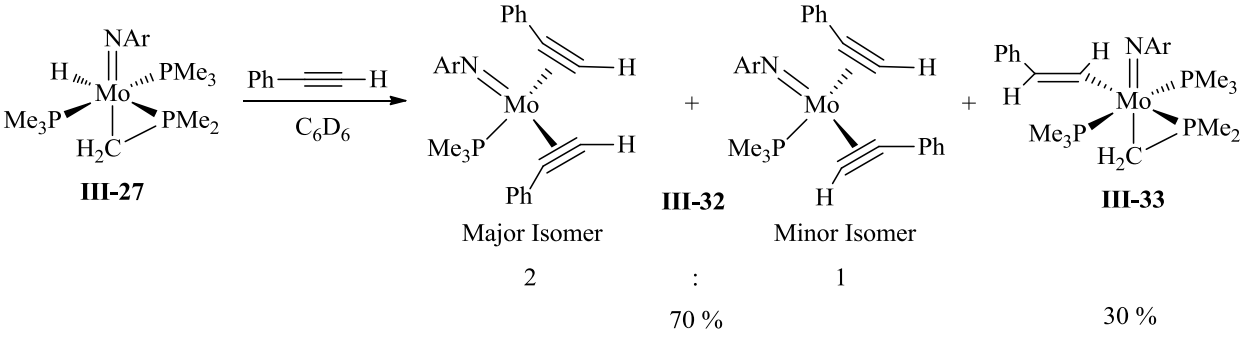

Scheme 47 – Addition of phenylacetylene to **III-13** producing two isomers of complex **III-19** along with the insertion product **III-20**.

The addition of 1 atm of ethylene gas to **III-13** results in regeneration of the PMe_3 ligand and formation of a 5-membered metallacyclopentane derivative $(ArN)Mo(PMe_3)_2(\eta^2\text{-}C_2H_4)(\eta^2\text{-}CH_2CH_2\text{-})_2$ (**III-21**). Metallacyclopentane complexes are important intermediates in the cyclotrimerization and polymerization of ethylene.[175] A possible pathway leading to the molybdacyclopentane **III-21** is shown in Scheme 48. Apparently, complex **III-21** forms upon hydride migration to the metalated phosphine unit and coupling of two ethylene units on the metal centre. Initial formation of the trisphosphine complex $(ArN)Mo(PMe_3)_3$ may be the first step followed by coordination of ethylene to give the Mo(II) complex $(ArN)Mo(PMe_3)_3(\eta^2\text{-}CH_2{=}CH_2)$. Loss of phosphine frees a coordination site for another equivalent of ethylene to give a Mo(II) species $(ArN)Mo(PMe_3)_2(\eta^2\text{-}CH_2{=}CH_2)_2$. Coupling of ethylenes generates the molybdacyclopentane complex $(ArN)Mo(PMe_3)_2(CH_2)_4$ which can add an extra equivalent of ethylene to furnish the complex **III-21**. The four methylene groups of the ring of **III-21** give distinct signals in the ^{1}H-NMR, which resonate from -1 to 2.5 ppm. The α-methylene protons (δ = -1.04 and 2.64 ppm) ligated to the molybdenum centre are split by both PMe_3 ligands and the adjacent β-methylene protons to give a triplet of triplet splitting pattern with larger $^3J_{H\text{-}P}$ values (14.6 and 20.8 Hz) and the expected $^3J_{H\text{-}H}$ value of 6.6 and 6.9 Hz. The diastereotopic β-methylene signals are found at 1.92 and 2.28 ppm and couple to each α-methylene proton. The relative geometry was determined 1D-NOESY studies. The upfield chemical shift value at -1.04 ppm is similar to the methylene signal of **III-13**, which was found to be trans to the imido group. One α-methylene of the ring is in the proximity to the isopropyl methine proton of the imido Ar group and both methylene protons are adjacent to the PMe_3 groups. One methylene group of the ethylene fragment "sees" the Mo-CH_2 group trans to the imido ligand while the other "sees" the isopropyl methyl protons of the Ar group. Taking all these observations into account, the

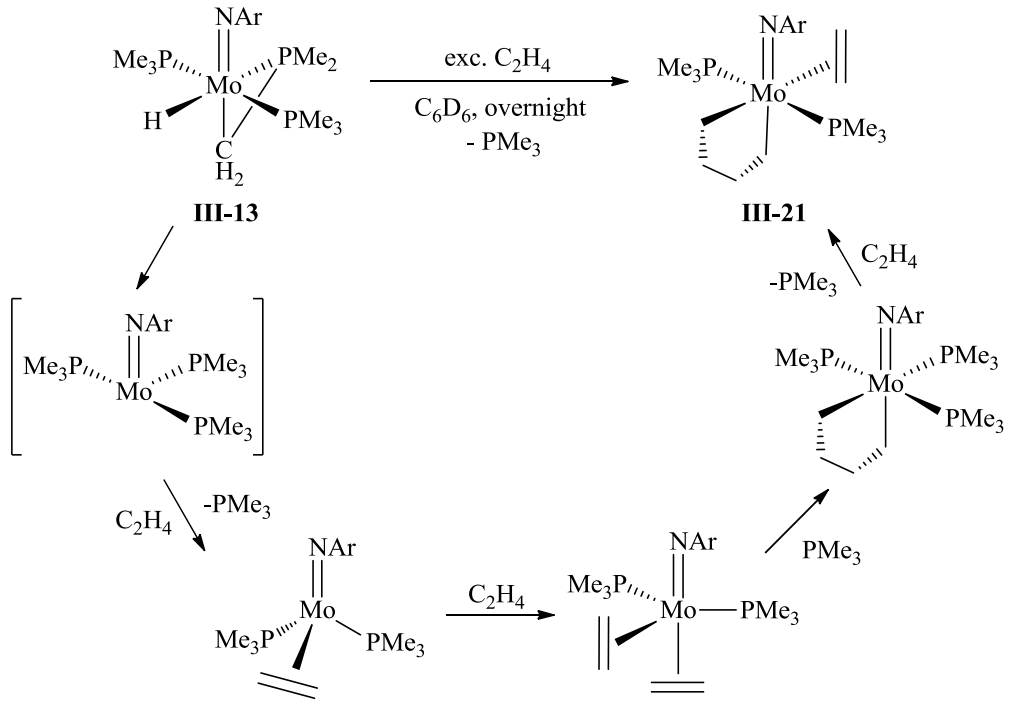

Scheme 48 – Synthesis and possible synthetic pathway for the formation of **III-21**.

connectivity of complex **III-21** can be deduced as shown in Scheme 48. The pseudo octahedral structure contains two equivalent *trans*-PMe_3 ligands and a molybdacyclopentane with one Mo-CH_2 group in the basal plane and the other in the apical position trans to the imido group. The ethylene ligand is along the N-Mo-C vector, with one CH_2 unit pointing in the direction of the imido Ar group and other in the direction of the apical CH_2 group.

The addition of electrophiles such as MeI, *p*-bromotoluene or CH_2Cl_2 results in substitution of the hydride ligand to give the respective halo-derivative $(ArN)Mo(PMe_3)_2(\eta^2\text{-}CH_2PMe_2)(X)$ (X = I (**III-22**), Br (**III-23**), Cl (**III-24**), Scheme 49). The ^{1}H-NMR shows downfield shifts for each methylene signals (dt, δ_I = -0.48 ppm, δ_{Br} = -0.36 ppm, , δ_{Cl} = -0.27 ppm,) of the cyclometallated rings compared to the parent complex **III-13** ($\delta_{hydride}$ = -0.98 ppm). All other signals in the ^{1}H, ^{31}P{^{1}H} and ^{13}C{^{1}H}-NMR are consistent with the structures shown in Scheme 49. This type of substitution pattern has been shown for analogous cyclometallated

hydride complexes of the type HM(η^2-CH_2PMe_2) (M = W, Fe, Ru; See Section II.3). Interestingly, 30 % formation of the hydrido bromide complex (ArN)Mo(PMe_3)$_3$(Br)(H) was seen in the reaction between **III-13** and *p*-bromotoluene. The tell-tale downfield hydride signal at 4.88 (dt, $^2J_{H\text{-}P}$ = 44.5 Hz, $^2J_{H\text{-}P}$ = 28.6 Hz) couples to one *trans* and two *cis* PMe_3 groups.

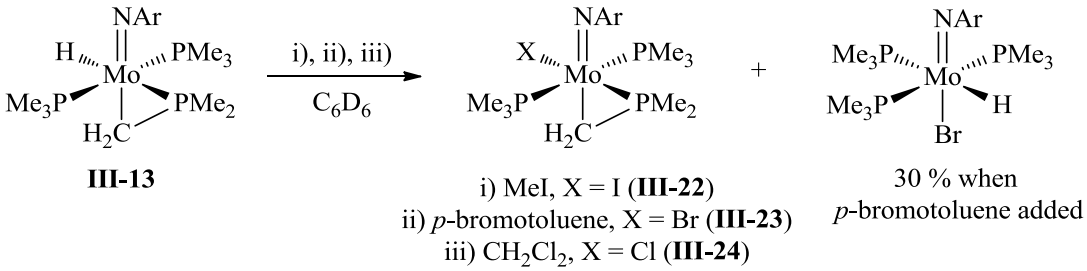

Scheme 49 – Synthesis of halo-derivatives for complex **III-13**.

Reacting complex **III-13** with alcohols results in addition of the O-H bond across the M-C bond to give the alkoxy complexes of the type (ArN)Mo(PMe_3)$_3$(OR)(H). The addition of the alkyl alcohols ^{i}PrOH and EtOH gives the alkoxy complexes **III-25** (R = ^{i}Pr) and **III-26** (R = Et, respectively. The ^{1}H-NMR of **III-25** is fluxional at room temperature but lowering to 7 °C allows clear distinction of all signals. At this temperature the hydride signal appears at 4.22 ppm (dt, $^2J_{H\text{-}P}$ = 77.1 Hz, $^2J_{H\text{-}P}$ = 24.9 Hz) indicative of the *cis* positioning relative to the imido group. In ^{1}H{^{31}P}-NMR the hydride signal becomes a singlet indicating that all coupling in ^{1}H-NMR is due to the phosphine ligands. Interestingly, at room temperature the Ar isopropyl methine signals are incredibly fluxional but lowering the temperature results in their decoalescence to two septets at 3.76 and 5.28 ppm. This fluxionality is most likely associated with flipping between isopropyl groups possibly through initial dissociation of a PMe_3 group. Complex **III-26** exhibits similar signals with two Ar signals becoming broadened into the baseline at room temperature. The hydride signal was located at 4.25 ppm indicating cis positioning of the hydride relative to the imido group. The presence of a hydride ligand is also evident from the IR stretch at 1720 cm^{-1}

which corresponds to the Mo-H stretch.[14]

The molecular structure of **III-26** confirms that the Mo centre adopts an octahedral geometry (Figure 13) with the ethoxy ligand laying *trans*- to the NAr imido group (N1-Mo1-O1 angle is 176.48 °; Table 5), consistent with the *trans*- effect of a strongly donating ArN^{2-} ligand.[176,177] The Mo1-O1 (2.019 Å) distance correlates well with other known Mo(IV) alkoxy complexes such as the cyclohexoxy chloride complex (ArN)Mo(PMe_3)$_3$(OCy)(Cl) (1.984(2) Å)[14], the imido alkoxy complex Mo(NAr)($CHCMe_2Ph$)(2,5-$Ph_2NC_4H_2$)[$OC(CF_3)_2Me$](PMe_3) (2.0846(14) Å)[178] or the Cp/imido complex (Cp)(ArN)Mo(OCH_2Ph)(PMe_3) (2.0485(11) Å).[73] The Mo-H distance 1.70(8) Å compares well with the known hydride chloride precursor (ArN)Mo(PMe_3)$_3$(H)(Cl) (1.76(4) Å). The PMe_3 *trans*- to hydride forms a longer Mo-P bond than the *cis*-phosphines (2.5643(7) Å for Mo1-P1 vs. 2.4708(7) Å for the two equivalent Mo1-P2 bonds), which has also previously been observed.[14] The linear Mo1-N1-C1 linkage (173.40(13) °) suggests lone pair donation from the imido nitrogen to molybdenum stabilizing the 18 electron valence shell.[149]

Parkin and co-workers showed that addition of phenol and 2,6-dimethylphenol to the tungsten complex W(PMe_3)$_4$(η^2-CH_2PMe_2)(H) at room temperature results in quick reaction to give the *ortho*- or methyl C-H activated complexes W(PMe_3)$_4H_2$(η^2-OC_6H_4) and W(PMe_3)$_4H_2${η^2-$OC_6H_3Me(CH_2)$}, respectively.[105] However, reacting the electron rich Mo(PMe_3)$_6$ complex with excess phenol gives the tetra(aryloxy) complex Mo(PMe_3)$_2$(OPh)$_4$. We found that reacting **III-13** with phenol results in production of the phenoxy hydride complex (ArN)Mo(PMe_3)$_3$(OPh)(H) (**III-27**). Similar to complex **III-25** and **III-26**, the Ar isopropyl methine signals are in exchange at room temperature but lowering down to -50 °C

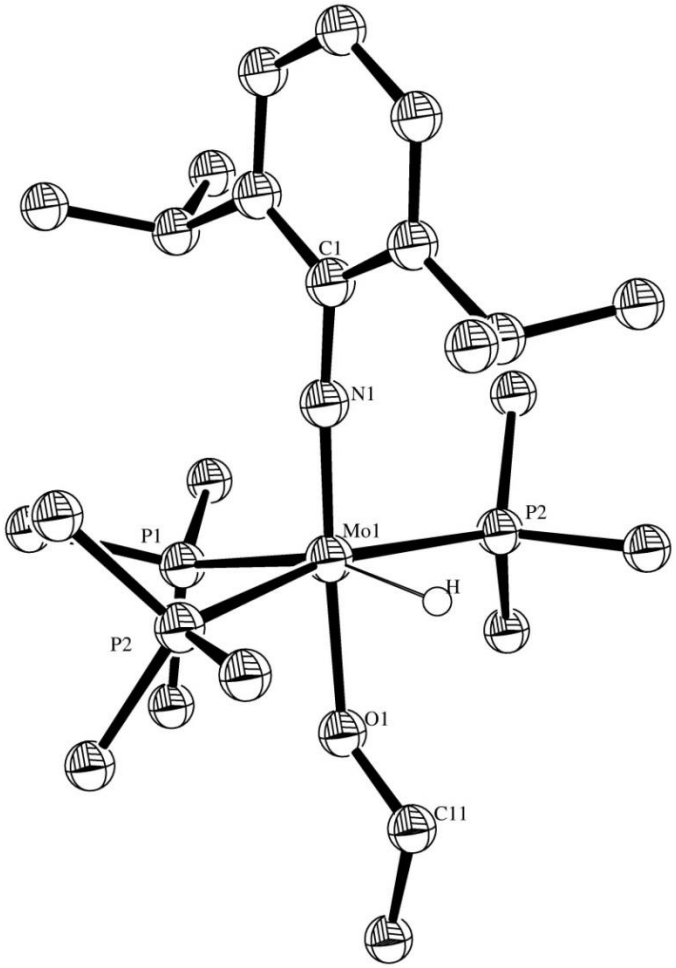

Figure 13 - ORTEP plot of the molecular structure of **III-26** (hydrogen atoms are omitted for clarity). Anisotropic displacement parameters are plotted at 50 % probability.

Table 5 – Selected bond distances (Å) and angles (°) for complex **III-26**.

Distances (Å)		Angles (°)	
Mo1-N1	1.780(15)	Mo1-N1-C1	173.40(13)
Mo1-O1	2.019(14)	N1-Mo1-O1	176.47(6)
Mo1-H	1.70(8)	P1-Mo1-H	162.0(7)
Mo1-P1	2.5643(7)	P2-Mo1-P2	165.62(2)
Mo1-P2	2.4708(7)	N1-Mo1-H	95.5(3)
Mo1-P2	2.4708(7)	P2-Mo1-H	83.7(2)
N1-C1	1.389(2)	N1-Mo1-P1	102.49(5)

results in separation of the signals at 3.85 and 5.26 ppm. Exchange between the isopropyl groups was observed at this temperature by EXSY NMR and the activation parameters were obtained ($\Delta H^{\ddagger}$ = 15.2 ± 0.2 kcal/mol, $\Delta S^{\ddagger}$ = 7.4 ± 0.8 cal/mol) from an Eyring plot based on kinetic studies over the temperature range from -55 °C to -25 °C (Appendix; Figure 19). The positive value of $\Delta S^{\ddagger}$ suggests a dissociatively activated exchange between the isopropyl groups. The mechanism may proceed via complete dissociation of PMe_3 followed by rotation of the Ar group and recombination with phopshine, or alternatively may involve significant elongation of of the Mo-P to an extent that enough room is freed for the rotation. The relatively low value of the entropy of activation is more consistent with the second possibility. No C-H activation in the *ortho* position of the phenol ring was observed even after prolonged heating for 2 days at 50 °C, showing the stability of the phenoxy complex.

Interestingly, Parkin *et al*. previously suggested that the mechanism of formation of C-H activated complex of tungsten involves the initial formation of a monohydride phenoxy complex $W(PMe_3)_4(OPh)(H)$ which, however, was not observed even at low temperatures (Scheme 50). However, the initial product of O-H oxidative addition can be intercepted by hydrogen gas to give the trihydride complex $W(PMe_3)_4(OPh)(H)_3$. In this regard, phenol addition to the cyclometallated complex **III-13** to give complex **III-27** is interesting in that it selectively results in a phenoxy hydride product unobtainable by Parkin *et al*. The main reason for this discrepancy is most likely the difference in electronic structure of these complexes. It is known that oxidative addition to more electron rich and less hindered metal centres tends to be more favorable than oxidative addition to more hindered and electron deficient metal centres, which originates from a thermodynamic effect.[169] Therefore, the proposed electron rich and relatively non-bulky tetra(phosphine) complex $W(PMe_3)_4(OPh)(H)$ is able to quickly activate the C-H methyl group

of the phenoxy ligand generating the cyclometallated product $W(PMe_3)_4H_2\{\eta^2\text{-}OC_6H_3Me(CH_2)\}$. In this case, steric hinderance from the bulky imido group and a less electron rich d^2 Mo(IV) centre halts at the alkoxy hydride complex **III-27**. As such, activation of the *ortho* position is not observed even at elevated temperatures. Interestingly, the addition of a second equivalent of

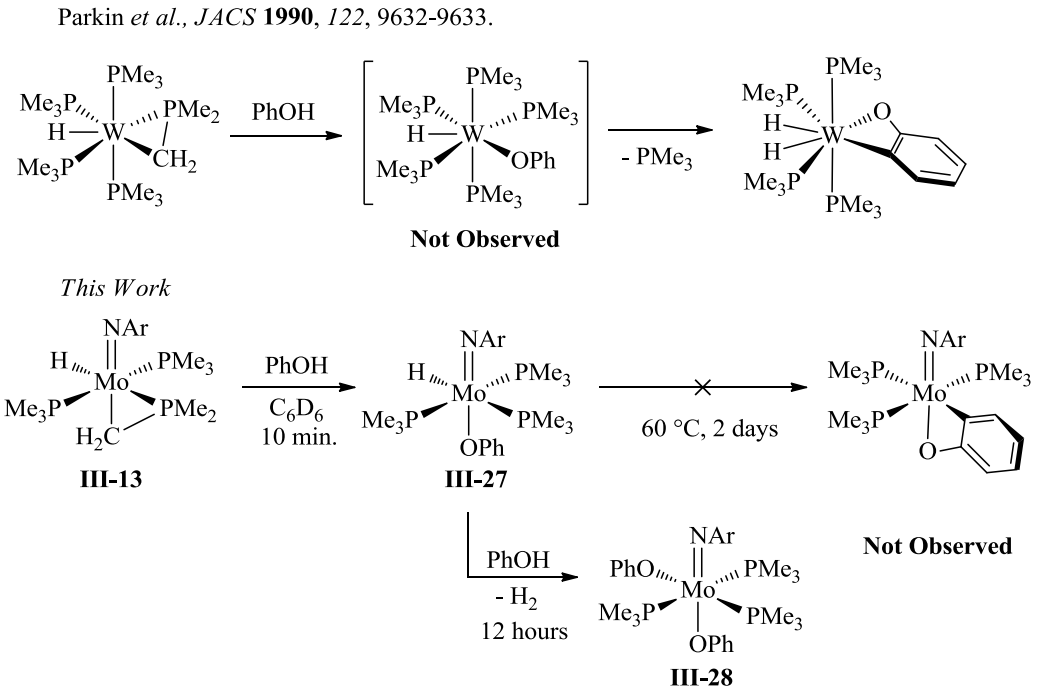

Scheme 50 – Synthesis of the **III-27** and **III-28** and comparison to the tungsten analogue $W(PMe)_4(\eta^2CH_2PMe_2)(H)$.

phenol generates the diphenoxy complex $(ArN)Mo(PMe_3)_3(OPh)_2$ (**III-28**) after 12 hours at room temperature.

Although the phenoxy complex showed no activation of the *ortho* C-H bond, the reaction of the 2,6-dimethyl derivative shows activation of one methyl group upon heating to 50 °C overnight. The initial product obtained upon addition of 2,6-dimethylphenol to **III-13** is the $(ArN)Mo(PMe_3)_3(OPh(CH_3)_2)(H)$ (**III-29**) complex which is fluxional at room temperature (Scheme 51). Lowering the temperature to -20 °C results in resolution of all signals with the

expected downfield shifted hydride signal at 5.05 ppm (dt, $^{2}J_{H\text{-}P}$ = 79.6 Hz, $^{2}J_{H\text{-}P}$ = 27.1 Hz) coupling to the two *cis*- and one *trans*-phosphine. Subsequent heating over a 12 hour period at 50 °C in C_6D_6 results in selective formation of the cyclometallated product (ArN)Mo(PMe_3)$_3$(κ^2-*O*,*C*-OPh(Me)CH_2) (**III-30**, Scheme 51). The ^{1}H-NMR displays the methylene resonance of the ring at 3.57 ppm, which couples to the *trans*-phosphine and two *cis*-phosphines ($^{3}J_{H\text{-}P_{trans}}$ = 13.9 Hz, $^{3}J_{H\text{-}P_{cis}}$ = 4.2 Hz). The downfield shifted methylene signal, compared to the cyclometallated phosphine precursor **III-13** (δ_{CH_2} = -0.99 ppm), suggests *cis* orientation of the imido group and CH_2 moiety. Loss of dihydrogen (δ_{H_2} = 4.47 ppm) was also observed during the reaction. Oxidative addition of the C-H bond on the molybdenum centre to form the Mo(VI) intermediate (ArN)Mo(PMe_3)$_3$(H)$_2$(κ^2-*O*,*C*-OPh(Me)CH_2) may be a possible first step in the formation of complex **III-30**. Alternatively, loss of PMe_3 may precede this type of addition, opening a vacant site on the metal centre.

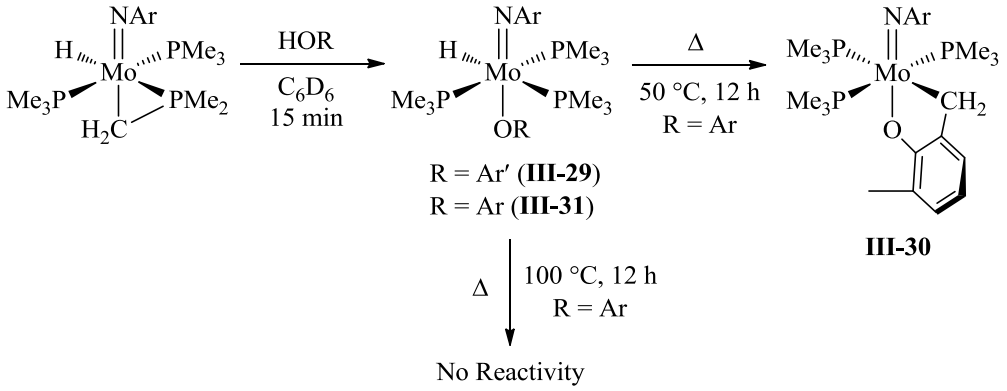

Scheme 51 – Synthesis of the aryl hydrido complexes **III-29** and **III-31**, with formation of the C-H activated product **III-30**.

Similar reactivity with 2,6-diisopropylphneol (ArOH), initially generates the fluxional hydride complex (ArN)Mo(PMe_3)$_3$(OAr)(H) (**III-31**) characterized by low temperature 1D and 2D NMR techniques (Scheme 51). However, heating **III-31** up to 100 °C overnight shows no

activation of either the methylene or methyl groups on the isopropyl moieties of the OAr ligand. This surprising result is similar to that observed by Parkin and coworkers[105]. A possible rationale for this may be due to the formation of an 18-electron oxametallacycle. Typically, intramolecular formation of six-membered oxametallacyclces, derived from substituted phenols, occur on electron *deficient* metal centres. Structural studies have shown large Mo-O-C bond angles corresponding to favourable lone-pair donation from oxygen to the metal centre.[179] In this case, for the possible 18-electron complex, lone-pair donation would not be expected to contribute significantly to oxametallacycle stability, thus preference for six-membered ring formation is unlikely.[105]

III.3.2 E-H Bond Activation using (^{t}BuN)Mo(PMe$_3$)$_2$(η^2-CH$_2$PMe$_2$)Cl

Reactions of the ^{t}Bu derivative (^{t}BuN)Mo(PMe$_3$)$_2$(η^2-CH$_2$PMe$_2$)Cl (**III-15**) with various E-H bonds show vastly different reactivity especially towards silane addition. The addition of one equivalent of PhSiH$_3$ to **III-15** results in the addition across the M-C bond to give the silyl chloride complex (^{t}BuN)Mo(PMe$_3$)$_3$(SiH$_2$Ph)Cl (**III-32**). The SiH$_2$Ph signal shows up in the ^{1}H-NMR at 5.35 ppm as a doublet of triplets, which can be attributed to coupling to two equivalent and one inequivalent PMe$_3$ group. The ^{29}Si INEPT+ signal appears at -21.32 ppm which is in accord with other Mo-Si complexes with similar octahedral structures.[15] NOESY NMR experiments allow us to elucidate the relative spatial arrangements of ligands. The resulting structure is shown in Scheme 52 and shows the SiH$_2$Ph ligand *trans* to the ^{t}BuN group and all PMe$_3$ ligands are located on the same equatorial plane, *cis* to the imido ligand. Although NMR experiments could not determine the position of the chloride ligand directly, based on similar structures and the positions of observable NMR ligands, it is likely located in the equatorial plane *cis* to the imido group. The main reason for such an unusual geometry appears to be the

minimization of steric repulsion between the bulky phosphine ligands. The addition of one equivalent of L-Selectride to the chloride complex **III-32** generates the hydride derivative (^{t}BuN)Mo(PMe_3)$_3$(SiH_2Ph)(H) (**III-33**). The distinctive upfield chemical shift of the hydride signal appears at -4.49 ppm in the ^{1}H-NMR and is indicative of its positioning *trans* to the imido group, as was previously observed for the related compound (ArN)Mo(PMe_3)$_3$(SiH_2Ph)(H). The silicon hydride signals appear at 5.38 ppm with a $^1J_{Si\text{-}H}$ value of 146.7 Hz, typical for Mo(IV) silyl complexes.[15]

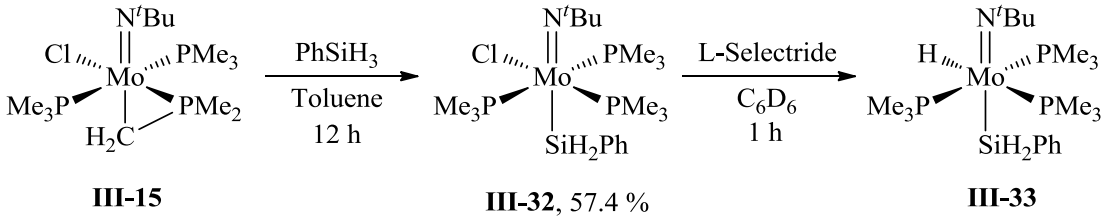

III-15 **III-32**, 57.4 % **III-33**

Scheme 52 – Preparation of the silyl complexes **III-32** and **III-33**.

Complex **III-32** was also synthesized on preparative scale through direct silane addition to **III-15**. Due to the difficulty in isolation of **III-15** as a solid, its generation *in situ* could be performed through addition of LiNH(^{t}Bu) to (^{t}BuN)Mo(PMe_3)$_3$$Cl_2$ followed by filtration and removal of volatiles. Addition of hexanes and $PhSiH_3$ directly to the oil obtained results in complete conversion to **III-32** after 2 hours at room temperature. Dissolution in small amount of benzene followed by benzene sublimation at -70 °C under reduced pressure gives pure **III-32** as a red gummy solid.

III.4 Synthesis and Reactivity of Unsymmetrical Mixed Imido Complexes

As stated above, our initial efforts in producing unsymmetrical bis(imido) complexes by chloride/amide metathesis led instead to the observation of a serendipitous deprotonation of a PMe_3 methyl group in the hydrido chloride complex $(ArN)Mo(PMe_3)_3(H)(Cl)$ (**III-12**). This discovery provided access to reactive metalated phosphine complexes which suggested investigation of their reactivity in activation of E-H bonds. Nevertheless, we sought alternate routes for the synthesis of mixed imido systems with the general formula $(RN)(R'N)Mo(PMe_3)_3$ (where $R \neq R'$). Literature search for alternative starting materials showed that Gibson and co-workers had been able to synthesize the mixed imido dichloride complexes $(ArN)(^tBuN)MoCl_2(DME)$[180-182] (**III-34**) and $(AdN)(F_5C_6N)MoCl_2(DME)$[180] (**III-35**; Ad = adamantane) using an approach similar to the preparation of symmetrical analogues.[150] Attempts at synthesizing **III-34** by using a 1:1 ratio of $ArNH_2$ and $^tBuNH_2$ with excess Me_3SiCl and NEt_3 in dimethoxyethane (DME) were successful and gave pure **III-34** in 40 % yield after three sequential recrystallizations in Et_2O at -30 °C (Scheme 53). The low yield is attributed to the unavoidable production of a hard to separate mixture of both $(ArN)_2MoCl_2(DME)$ (**III-1**) and $(^tBuN)_2MoCl_2(DME)$ (**III-36**) in the mother liquor over a period of three days even at low temperature. Alternatively, complex **III-34** can be synthesized through the addition of one equivalent $ArNH_2$ to $(^tBuN)_2MoCl_2(DME)$ at 60 °C for 1 hour.[180] Similar yields (42 %) are obtained in gram scale quantities after recrystallization.

We envisioned reduction of complex **III-34** to the Mo(IV) phosphine derivatives by either Mg reduction in the presence of excess PMe_3 or through addition of the Grignard reagent

EtMgBr to generate an ethylene phosphine complex, as it had been established for symmetrical analogues **III-1** and **III-36**. In the latter case, a strong dependence on the type imido R substituent (i.e. aryl or alkyl imide) was noticed. For the aryl derivative **III-1**, magnesium reduction selectively gives the tris(phosphine) complex $(ArN)_2Mo(PMe_3)_3$ (**III-37**) whereas harsher conditions are required to generate the alkyl imido derivative $(^tBuN)_2Mo(PMe_3)_2$ (**III-38**; 75 °C for 3 weeks), which has only two phosphine ligands. Magnesium reduction of **III-34** in the presence of excess PMe_3 (5 equivalents) in THF, results in the formation of a difficult to separate mixture of products. According to ^1H and ^{31}P NMR, formation of both $(ArN)Mo(PMe_3)Cl_2$ and $(^tBuN)Mo(PMe_3)Cl_2$ was seen in a 2:1 ratio in 20 % overall yield, along with the novel dimer $[(ArN)Mo(PMe_3)(\mu\text{-}N^tBu)]_2$ (**III-39**; 80 % overall) containing bridging ^{t}BuN imido groups (Scheme 53). A related dimer $[(^tBuN)Mo(PMe_3)(\mu\text{-}N^tBu)]_2$ has also been reported by Gibson and co-workers.[183] We assign the ^{t}BuN group to the bridging position due to its greater Lewis basicity compared to the terminal ArN moiety.

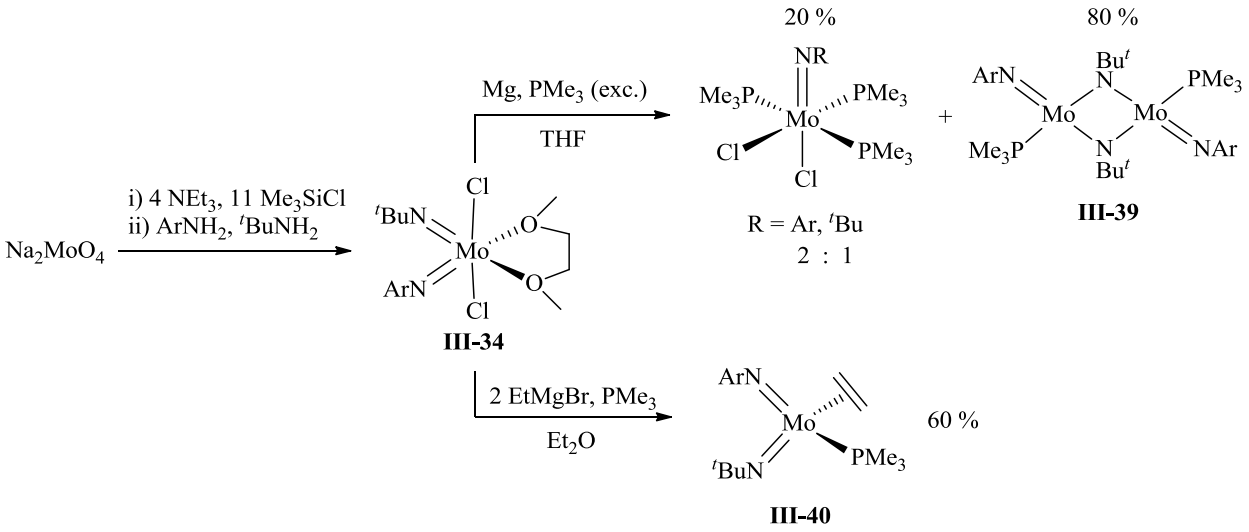

Scheme 53 – Synthesis of $(ArN)(^tBuN)MoCl_2(DME)$ (**III-34**) and subsequent reduction using Mg (top) and EtMgBr (bottom).

Alternatively, addition of two equivalents of EtMgBr to **III-34** in the presence of one equivalent of PMe_3 results in selective generation of the Mo(IV) complex (ArN)(^{t}BuN)Mo(PMe_3)(η^2-CH_2=CH_2) (**III-40**). ^{1}H-NMR analysis at room temperature shows broad signals for both the ethylene and PMe_3 resonances. The addition of 10 mol % BPh_3 produced the Lewis acid/base adduct $Ph_3B{\cdot}PMe_3$ as well as a clear spectral pattern for both ethylene and phosphine fragments. This may indicate an exchange between free and coordinated PMe_3 which could occur dissociatively or associatively. Associative exchange is possible as the bis(phosphine) ethylene analogue $(ArN)_2Mo(PMe_3)_2(\eta^2\text{-}CH_2{=}CH_2)$ is known, however conclusive evidence for this remains elusive. Each proton of the ethylene ligand is represented in the ^{1}H-NMR by its own unique resonance at δ 1.38, 1.48, 2.22 and 2.54 ppm indicating chirality of the tetrahedral molybdenum centre and the lack of rotation of the ethylene ligand. The $^{31}P\{^1H\}$-NMR shows a sharp singlet at δ 22.2 ppm, but the addition of one equivalent of PMe_3 coalescences all phosphorus signals into a broad resonance at δ 35 ppm. The spatial arrangement of ligands was determined by 1D NOESY experiments and the resulting structure is shown in Scheme 53. No decomposition of complex **III-40** was seen upon heating to 80 °C for 12 hours, displaying the robustness of the complex.

The development of an efficient method to synthesize the Mo(IV) ethylene phosphine complex **III-40** allowed us to investigate its reactivity with both chloro- and hydrosilanes. Ultimately, the formation of β-agostic silylamido and silanimine complexes was anticipated based on previous studies with complexes **III-37** and **III-38** (see Section II.1.3). However, steric and electronic differences of the imido groups greatly affect the outcome of silane addition. For example, $PhSiH_3$ addition to complex **III-37** produces the bis(silyl) complex (ArN)Mo(η^3-NAr-SiH_2Ph-H)(SiH_2Ph)(PMe_3)[12] whereas addition to **III-38** selectively gives the tris(silyl) complex

(^{t}BuN)Mo(H)(SiH_2Ph){($SiHPh)_2$(μ-N^{t}Bu)}($PMe_3)_2$. The following sections will present our attempts at preparing novel mixed imido β-agostic silylamido and silanimine complexes through an imido silane coupling approach.

III.4.1 Reactivity of III-46 with chloro- and hydrosilanes

Within the last decade our group has actively been studying the addition of chloro- and hydrosilanes to early transition metal complexes. In particular, complexes with the general formula $L_nM(=NR)$ give either silyl hydride $L_n(RN=)M(H)(SiHR'_2)$ or *β*-agostic silylamido products $L_n(Cl)M(\eta^3$-NR-SiR'_2-H). For example, the addition of $HSiMe_2Cl$ to $Cp(ArN)Nb(PMe_3)_2$ results in the formation of the non-classical complex $CpNb(\eta^3$-NAr-$SiMe_2$-$H)(PMe_3)_2$[9], whereas addition of the same silane to $Cp(ArN)Ta(PMe_3)_2$ gives $Cp(ArN)Ta(H)(SiMe_2Cl)(PMe_3)_2$ showing no interaction of the silane and imido group.[9,184] The addition of Lewis acidic silanes, such as MePhSiHCl, Ph_2SiHCl, $PhSiH_2Cl$, to the Nb derivative results in initial formation of silyl hydride and eventually rearrangement into the silyl chloride species with no agostic interactions observed. Alternatively, silane addition to the isolobal bis(imido) complexes of molybdenum shows selective formation of the *β*-agostic complexes of the type (RN)Mo(η^3-NR-SiR'_2-H)($PMe_3)_3$(Cl) (R = Ar, Ar′, ^{t}Bu; R′ = Me_2, MePh, MeCl, Ph_2, PhH). Bonding in Mo(IV) *β*-agostic complexes can be represented by two different forms one of which contains a silanimine character and the other a simple classical silylamido ligation, as shown in Figure 14. Silanimine complexes are rare and have been shown to be important intermediates in catalytic hydrosilylation mechanisms (see Scheme 15).[154] Recently, the *β*-agostic complex (ArN)Mo(SiH_2Ph)(η^3-NAr-$SiPhH_2$-H)($PMe_3)_2$ was found to react stoichiometrically with bezaldehyde and bulky nitriles to induce the loss of $PhSiH_3$ and produce fluxional silanimine products of the type (ArN)Mo(η^2-NAr-SiHPh)(PMe_3)(L) (L = η^2-N≡CR

(**III-41**), η^2-O=CHPh (**III-42**)).[154] The reactive nature of the silanimine fragment is evident for complex **III-41** which rearranges into the 5-membered metalloheterocyclic complex (ArN)Mo(κ^2-*N*,*N*-NAr-SiHPh-C(R)=N)(PMe_3) by insertion of the coordinated nitrile into the Mo-Si bond. We envisioned the mixed imido Mo(IV) complex **III-40** to be an appropriate precursor for stabilizing both agostic and silanimine complexes. In particular, we expected that the donating ^{t}BuN imido group will provide greater stabilization for a possible 16-electron silanimine complexes of the type (^{t}BuN)Mo(η^2-ArN-SiR_2)(PMe_3)$_2$.

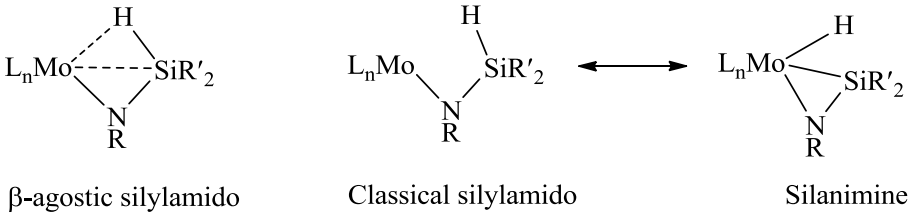

Figure 14 – Different representations of bonding in Mo(IV) *β*-agostic silylamido complexes showing the two extremes from classical to silanimine coordination.

Reacting complex **III-40** with one equivalent of Me_2SiHCl at room temperature shows an approximate 1:1 mixture of the Mo(IV) complexes (^{t}BuN)Mo(η^2-ArN-$SiMe_2$)(η^2-C_2H_4)(Et) (**III-43**) and (^{t}BuN)Mo(η^3-NAr-$SiMe_2$-H)(PMe_3)$_2$ (**III-44**) (Scheme 54). Both complexes have been characterized by 1D NMR and 2D correlation studies. In particular, the general spatial orientations of ligands in the coordination sphere of Mo have been elucidated by 1D NOESY experiments. Interestingly, complex **III-44** is fluxional at room temperature but cooling to -20 °C resolves all ^{1}H and ^{31}P NMR signals. This fluctionality is most likely due to either an inter- or intramolecular PMe_3 exchange. At -20 °C the ^{1}H-NMR displays two septets for the methine protons of the Ar moiety, at δ 3.75 and 4.46 ppm, displaying the expected loss of symmetry due to the unsymmetrical nature of the imido ligands. The *β*-agostic Si-H proton is obscured by the ^{t}Bu and PMe_3 resonances but was located by ^{1}H-^{29}Si-HSQC JC at δ 0.89 ppm, showing a

reduced $^{1}J_{Si\text{-}H}$ value of 91.2 Hz, indicative of a non-classical interaction at the Mo centre. The ^{1}H-^{29}Si HSQC shows an upfield shifted ^{29}Si projection at δ -64.5 ppm also indicating the agostic nature of the Si-H bond shielded by the d^2 Mo(IV) centre. Two doublets at δ -7.38 and 3.25 ppm ($^{2}J_{P\text{-}P}$ = 9.2 Hz) indicate two PMe_3 ligands in a *cis* orientation.

Alternatively, complex **III-43** is stable at room temperature and decomposes only after three days at room temperature. The ^{1}H NMR also displays two distinct septets for the methine protons and four distinct CH_3 doublets from the ArN moiety. The ethyl groups displays a CH_3 triplet at δ 2.04 ppm ($^{3}J_{H\text{-}H}$ = 7.4 Hz) and two diastereotopic methylene resonances at δ 2.31 (dq, $^{2}J_{H\text{-}H}$ = 9.9 Hz, $^{3}J_{H\text{-}H}$ = 7.4 Hz,) and 3.36 ppm (dq, $^{2}J_{H\text{-}H}$ = 9.7 Hz, $^{3}J_{H\text{-}H}$ = 7.0 Hz). Four distinct CH resonances of the ethylene fragment with a doublet of doublet of doublet splitting are observed at δ 1.74, 2.20, 2.41, 2.68 ppm. The methyl groups of the $SiMe_2$ fragment resonate at δ 0.10 and 0.32 ppm and show no coupling to a Si-H hydride. Furthermore, a ^{1}H-^{29}Si-HSQC JC experiment showed absence of correlation with the protons of the ethylene ligand, suggesting the lack of Si-C coupling and therefore the formation of a silanimine ligand.

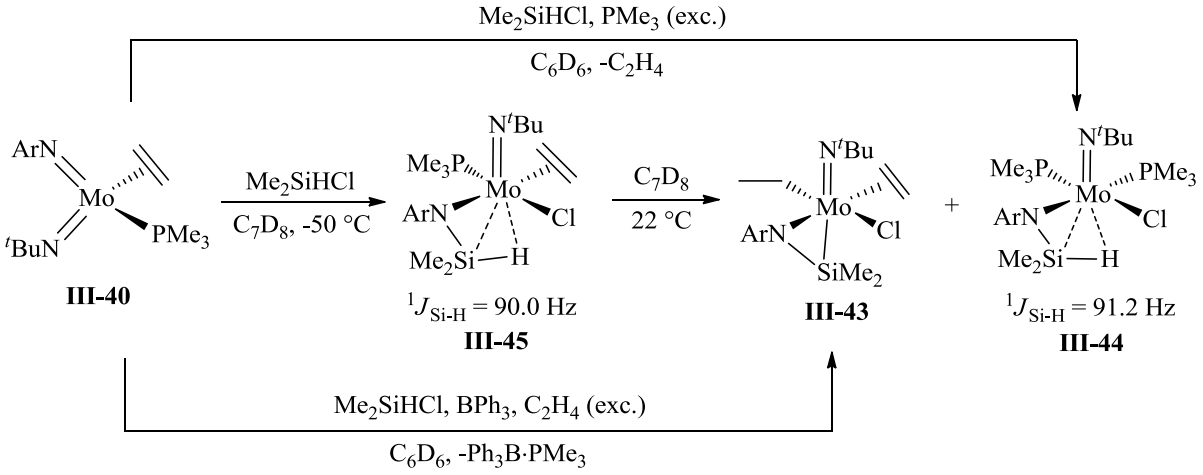

Scheme 54 – Synthesis of the silanimine and *β*-agostic complexes **III-43** and **III-44** along with the intermediate complex **III-45** observed by low temperature NMR.

In order to better understand the formation of **III-43** and **III-44**, low temperature NMR studies were conducted to observe possible intermediates. The addition of Me_2SiHCl to a frozen (liquid N_2) sample of **III-40** in toluene-d_8 and subsequent warming to -50 °C on a pre-cooled 600 MHz NMR spectrometer showed initial formation of the β-agostic silylamido derivative (^{t}BuN)Mo(η^3-NAr-$SiMe_2$-H)(η^2-C_2H_4)(PMe_3)(Cl) (**III-45**, Scheme 54). The Si-H resonance was found by ^{1}H-^{29}Si-HSQC JC at δ 1.37 ppm in the ^{1}H NMR with a reduced $^1J_{Si\text{-}H}$ value of 90.0 Hz. This, and the upfield shifted ^{29}Si signal at δ -69.7 ppm, indicates interaction of the Si-H bond with the metal centre. Resonances for the Ar and ethylene fragments were seen in the ^{1}H-NMR with distinct methine and methyl resonances of the Ar moiety and four distinct ethylene resonances. The ^{31}P-NMR also shows a singlet at -4.22 and 1D NOESY studies suggest the ligand orientation shown in Scheme 54. Warming this complex to room temperature generates both complex **III-43** and **III-44**. The formation of **III-43** most likely goes through Si-H bond cleavage to give the Mo(IV) hydride species (^{t}BuN)Mo(H)(PMe_3)(η^2-NAr-$SiMe_2$)(PMe_3)(η^2-C_2H_4) followed by hydride migration to coordinated ethylene to give ethyl ligand and ligand substitution (ethylene for PMe_3) to give **III-43.**

Selective generation of complexes **III-43** and **III-44** could be done through addition of either phosphine or borane, respectively. The addition of excess PMe_3 (two or three equivalents) to the 1:1 mixture results in selective formation of complex **III-44** and loss of ethylene gas (δ 5.25 ppm). Adding BPh_3 to the mixture generates a greater amount of complex **III-43** along with other decomposition products. Alternatively, the addition of BPh_3 with excess ethylene gas gives solely complex **III-43** and formation of the borane phosphine adduct $Ph_3B{\cdot}PMe_3$. Preparative scale synthesis for each was attempted but isolation of either complex **III-43** or **III-44** proved difficult due to the high solubility in both aliphatic (i.e. hexanes, pentanes or diethyl ether) and

aromatic solvents (i.e. C_6H_6 or C_7H_8) even at low temperatures. Unfortunately, the addition of other chlorohydrosilanes, such as MePhSiHCl, PhH_2SiCl or $MeSiHCl_2$, results in the formation of a complicated mixture of products indistinguishable by NMR.

The addition of secondary and tertiary hydrosilanes, such as $MePhSiH_2$ or Me_2PhSiH_2, also proved to be sluggish, with no reactivity seen in the latter case. However, $PhSiH_3$ addition (2 equivalents) to **III-40** shows full reactivity of the starting material in ten minutes at room temperature to furnish the β-agostic species (^{t}BuN)Mo(η^3-NAr-SiHPh-H)(PMe_3)(SiH_2Ph) (**III-46**). The ^{1}H-NMR of **III-46** displays two broad resonances at δ 5.04 and 3.94 ppm corresponding to the classical and non-classical SiH protons of the silylamido moiety, respectively. Each signal correlates to the downfield ^{29}Si signal at -77.9 ppm found by ^{1}H-^{29}Si HSQC. These data correspond well to the related complex (ArN)Mo(η^3-NAr-SiHPh-H)(PMe_3)(SiH_2Ph) where the agostic Si-H proton resonates at 4.35 ppm and the ^{29}Si signal at -72.9 ppm.[12] The asymmetry of **III-46** is evident from both the four distinct CH_3 resonances and two distinct CH signals of the ArN group. The classical SiH protons of the silyl ligand are diastereotopic signals at 5.55 and 5.72 ppm and correlate to the upfield ^{29}Si signal at -7.2 ppm.

The formation of **III-46** could proceed via a similar mechanism suggested for (ArN)Mo(η^3-NAr-SiHPh-H)(PMe_3)(SiH_2Ph).[154] One equivalent of $PhSiH_3$ could add across the Mo=NAr bond of **III-46** forming the agostic hydride species (^{t}BuN)Mo(H)(η^3-NAr-SiHPh-H)(PMe_3)(η^2-C_2H_4) (**III-47**, Scheme 55). In the case of **III-46**, dihydrogen elimination was observed due to metathesis of a second equivalent of $PhSiH_3$ with the Mo-H bond. In this case, production of one equivalent of ethane was seen (δ_{ethane} 0.89 ppm) in the ^{1}H-NMR, so formation of the ethyl agostic species (^{t}BuN)Mo(H)(η^3-NAr-SiHPh-H)(PMe_3)(η^2-C_2H_4) (**III-48**) followed by PhH_2Si-H metathesis with the Mo-C bond may be a viable pathway. An alternative route

could be oxidative addition of a second equivalent of $PhSiH_3$ to give a Mo(VI) species followed by ethane elimination (Scheme 55). Complex **III-46** is unstable at room temperature and decomposes into a mixture of products after a few hours. The appearance of a quartet at -4.83 ppm and triplet at -5.03 ppm in the ^{1}H-NMR is similar to that of the tetrahydride species $(ArN)MoH_4(PMe_3)_3$ ($\delta_{hydride}$ -5.27 ppm) and γ-agostic species $(PMe_3)_3MoH_3(\eta^3$-SiHPh-N(Ar)-SiHPh-H) ($\delta_{hydride}$ -6.58 ppm) seen for the addition of excess $PhSiH_3$ to $(ArN)_2Mo(PMe_3)_3$.[154] The upfield shift of each hydride signal, in the case of $PhSiH_3$ to **III-40**, signal suggests the substitution of the ArN imido group for the ^{t}BuN substituent to give both $(^t$BuN$)MoH_4(PMe_3)$ and $(PMe_3)_3MoH_3(\eta^3$-SiHPh-N(^{t}Bu)-SiHPh-H). Also, the hydrosilylation product $PhEtSiH_2$ and rearrangement into Ph_2SiH_2 was also observed.

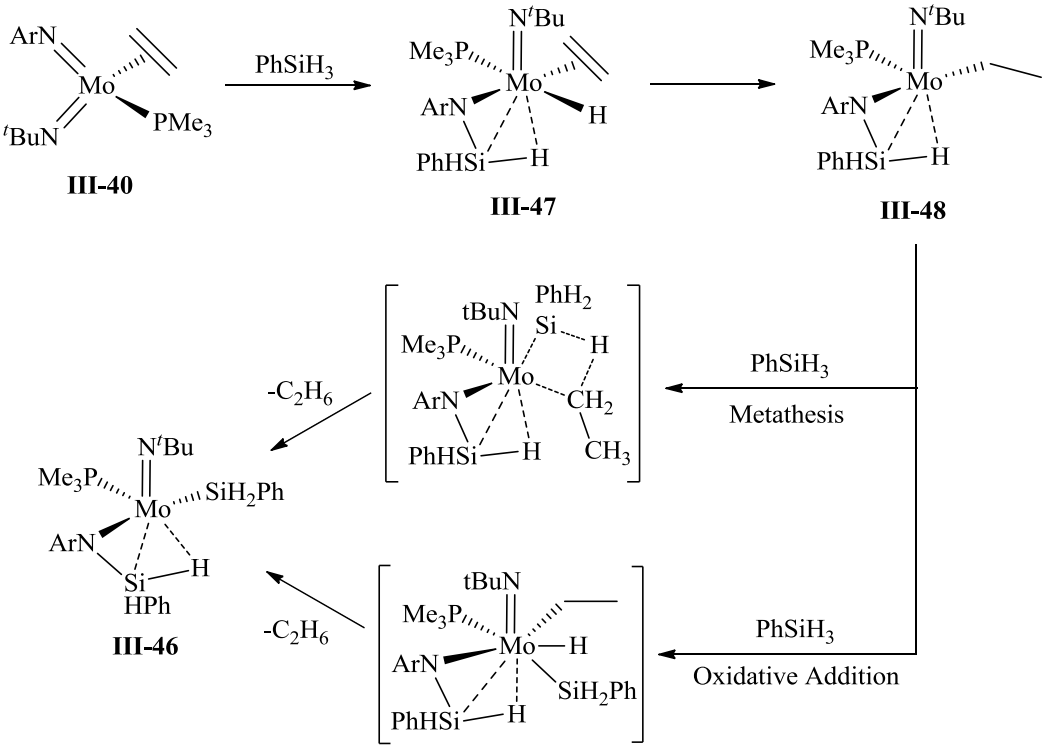

Scheme 55 – Possible synthetic pathway for the formation of complex **III-46** by addition of $PhSiH_3$ to **III-40**.

Although mono- and dichlorohydrosilanes give a variety of different products when reacted with **III-40**, treatment with $HSiCl_3$ produces the unexpected complex (^{t}BuN)Mo(PMe_3)$_2$(η^2-C_2H_4)Cl_2 (**III-49**) with loss of the silanimine dimer (ArNSiHCl)$_2$. This is in contrast to the alternative symmetrical imido complexes with the general formula (RN)Mo(PMe_3)$_{x-1}$(L) (R = Ar′, x = 3, L = PMe_3; R = Ar, x = 3, L = PMe_3 or η^2-C_2H_4; R = ^{t}Bu, x = 2, L = η^2-C_2H_4) which give the mono(imido) complexes (RN)Mo(PMe_3)$_3Cl_2$ in all cases. Interestingly, adding excess PMe_3 does not result in formation of (^{t}BuN)$MoCl_2$(PMe_3)$_3$. The ^{1}H-NMR exhibits a singlet at δ 0.66 ppm representing the ^{t}Bu methyl group and a virtual triplet at δ 1.44 ppm ($^2J_{H-P}$ = 8.1 Hz) for the two equivalent trans PMe_3 methyl groups correlating to a singlet at δ -6.11 ppm in the $^{31}P\{^1H\}$ NMR. The ethylene fragment shows two multiplets at δ 2.27 and 2.62 ppm, each displaying unique splitting patterns associated with $^2J_{H-H}$ geminal and $^3J_{H-H}$ vicinal proton coupling as well as $^3J_{H-P}$ phosphine coupling. 1D NOESY experiments confirmed the orientation shown in Scheme 56 (distorted octahedral), where the CH_2 groups of η^2-C_2H_4 sit above and below the equatorial plane and the ^{t}BuN and Cl groups occupy the axial sites.

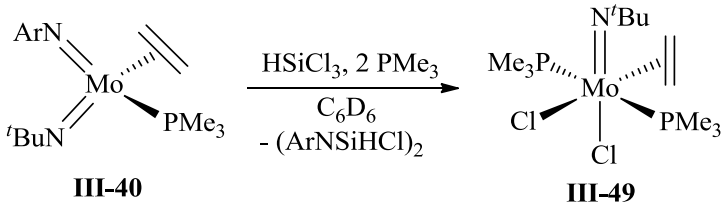

Scheme 56 – Selective synthesis of (^{t}BuN)Mo(PMe_3)$_2$(η^2-C_2H_4)Cl_2 (**III-49**) from the addition of $HSiCl_3$ and PMe_3 to **III-40**.

III.5 Mechanistic and Reactivity Study of $(^t\text{BuN})\text{Mo(H)}(\text{SiH}_2\text{Ph})\{(\text{SiHPh})_2(\mu\text{-N}^t\text{Bu})\}(\text{PMe}_3)_2$*

The coupling of silane with imido groups has been extensively studied within our group and provided interesting complexes displaying agostic interactions with various metal centres which have been exploited in the area of catalytic hydrosilylation[12,13,15,73,154,185]. Much of this work has been based on the use the Ar and Ar′ moieties bound to the imido nitrogen which contain isopropyl and methyl groups respectively. In particular, a series of agostic silylamide complexes of group 5 and 6 metals were obtained by a novel synthetic approach: the direct coupling of imido ligands with hydrosilanes. However, the use of alkyl substituents in the imido group has not been looked into, until recently. Given the different steric and electronic properties of the alkyl and aryl substituents, we expected to observe different reactivity's. For this reason, we elected to study the *tert*-butyl imido group as a coupling partner in reactions with silanes by using either the bis(phosphine) complex $(^t\text{BuN})_2\text{Mo}(\text{PMe}_3)_2$ (**III-38**) or the ethylene phosphine complex $(^t\text{BuN})_2\text{Mo}(\text{PMe}_3)(\eta^2\text{-C}_2\text{H}_4)$ (**III-50**) as starting materials.

The addition of the secondary silane PhMeSiH_2 to **III-38** or **III-50** results in 55 % conversion by Si-H oxidative addition to the Mo(VI) complex $(^t\text{BuN})_2\text{Mo}(\text{PMe}_3)(\text{SiHMePh})(\text{H})$ and the mono(imido) Mo(IV) complex $(^t\text{BuN})\text{Mo}(\text{PMe}_3)_3(\text{SiHMePh})(\text{H})$. These complexes are unstable and were found to decompose during large scale preparation. Similarly, reacting more Lewis acidic silane $(\text{EtO})_3\text{SiH}$ with **III-38** or **III-50** results in decomposition and only trace amounts of the tris(phosphine) complex $(^t\text{BuN})\text{Mo}(\text{PMe}_3)_3(\text{OEt})_2$ could be observed.[186]

However, it was recently found[186] by our group that reacting complex **III-38** or **III-50**

* A version of this chapter has been accepted for publication. Khalimon, A. Y.; McLeod, N. A.; Ignatov, S. K.; Okhapkin, A. I.; Kuzmina, L. G, Howard, J. A. K.; Nikonov, G. I. *Dalton Trans.* **2014**, DOI 10.1039/C4DT00154K.

with one equivalent of $PhSiH_3$ results in the formation of a 1:1 mixture of the tris(silyl) complex (^{t}BuN=){μ-^{t}BuN(SiHPh)$_2$}Mo(H)(SiH$_2$Ph)(PMe$_3$)$_2$ (**III-51**) and the tetrahydride silanimine complex (η^2-^{t}BuN=SiHPh)MoH$_4$(PMe$_3$)$_3$ (Scheme 57). Increasing the amount of silane to three equivalents results in the selective formation of **III-51**, which represents a rare example of triple silane addition to a single metal centre. Complex **III-51** can be prepared on gram scale through the direct addition of excess $PhSiH_3$ to **III-38** or **III-50** (extra equivalent PMe_3 is required for **III-50**) at -30 °C followed by removal of volatiles at 0 °C. The crystal structure of **III-51** was obtained and allowed the determination of multicomponent coupling of two SiHPh moieties to a single

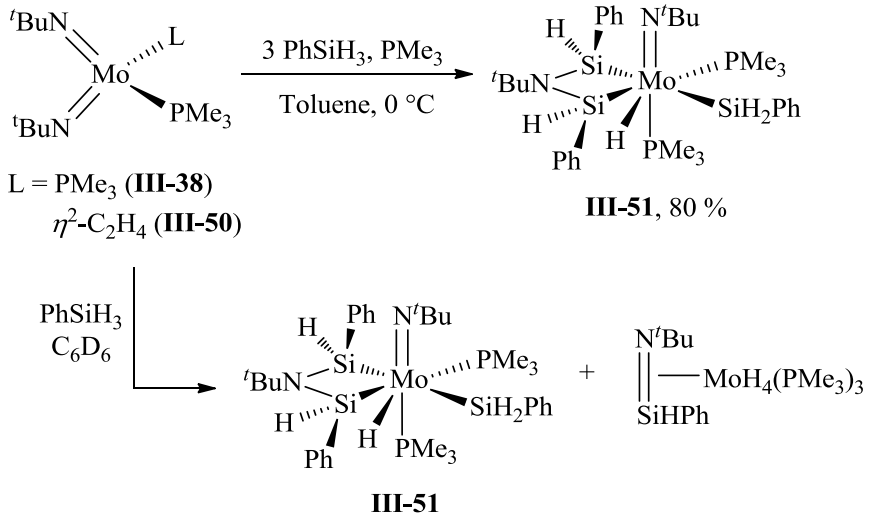

Scheme 57 – Synthesis of the tris(silyl) complex **III-51** from the addition of $PhSiH_3$ and PMe_3 to **III-38** or **III-50**.

N^{t}Bu group. This involves the complete detachment of one imido group from the metal centre itself which is unprecedented in the literature. Complexes similar to **III-51** have been synthesized but go through addition of amines to bis(silyl) or disilene complexes to produce bridging products.[187] In the early 1990's Berry and co-workers synthesized the molybdocene complex $Cp_2Mo\{(SiMe_2)_2(\mu\text{-}NSiMe_3)\}$ through addition of trimethylsilylazide to $Cp_2Mo(\eta^2$-

$SiMe_2SiMe_2$) with concomitant loss of N_2.[187] Nikonov *et al.* have shown the formation of $[Cp_2Nb(H)\{(SiMe_2)_2NR\}]$ (R = ^{t}Bu, Et) through addition of excess amine RNH_2 to $[Cp_2Nb(SiMe_2I)_2H]$.[188] In the case of complex **III-51**, the silane addition dictates the formation of bridging species as opposed to amine addition.

Structurally, **II-51** exhibits an interesting Si-Si bond distance (Si-Si 2.594(3) Å) and can be considered at the high end of Si-Si single bonds known in the literature. The ^{1}H-NMR spectra conform to the structure as two different Si-H signals are seen at δ 5.05 and 5.50 ppm (d, $^3J_{P\text{-}H}$ = 19.4 Hz; bddd, $^3J_{P\text{-}H}$ = 15.9 Hz, $^2J_{H\text{-}H}$ = 7.4 Hz, SiH_2Ph) for the diastereotopic Si-*H*'s on the silyl ligand. Two distinct signals are also observed at δ 6.04 (dd, $^3J_{P\text{-}H}$ = 3.7 Hz, $^3J_{P\text{-}H}$ = 9.2 Hz, {(Si*H*Ph)$_2$(*u*-N^{t}Bu)}) and 6.59 ppm (ddd, $^2J_{H\text{-}H}$ = 5.8 Hz, $^3J_{P\text{-}H}$ = 11.6 Hz, $^3J_{P\text{-}H}$ = 17.5 Hz, {(Si*H*Ph)$_2$(*u*-N^{t}Bu)}) which are attributed to two nonequivalent Si*H*'s within the ring. The

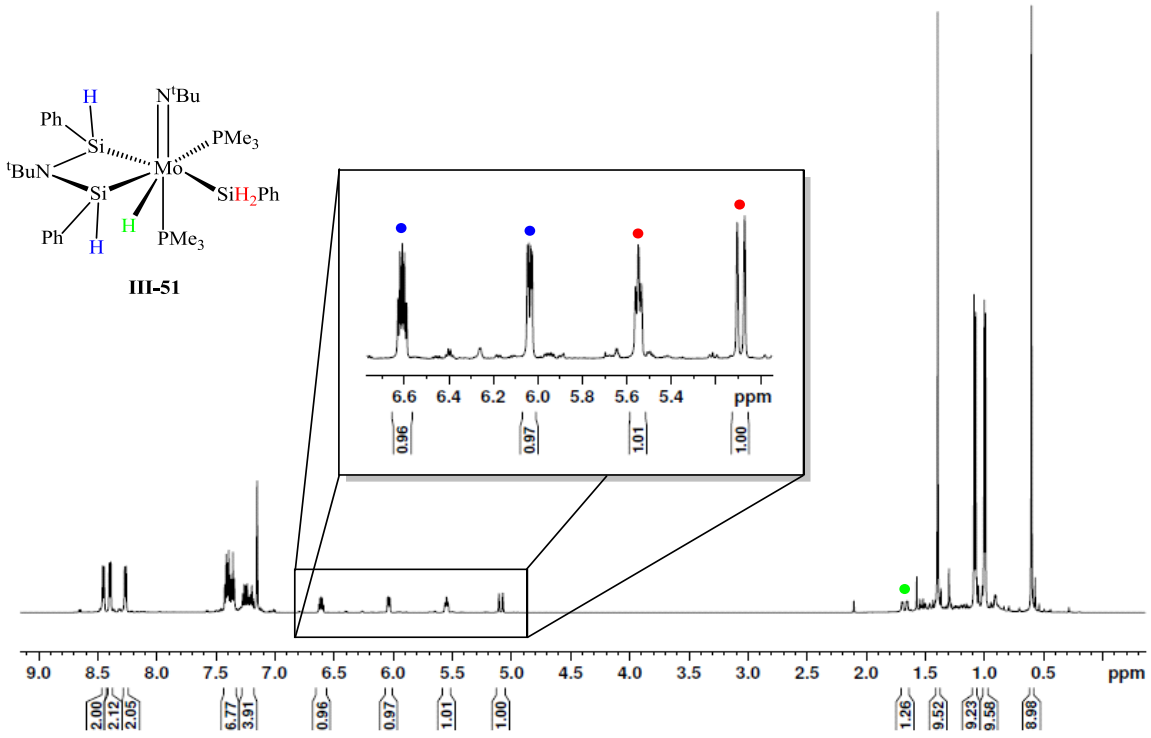

Figure 15 – ^{1}H-NMR of the tris(silyl) complex **III-51** with each Si-H and Mo-H shown with respective colour coordination. Inset is ^{1}H-NMR region from 5.5 to 6.7 ppm.

hydride signal can be observed at room temperature at δ 1.50 (bd, $^{2}J_{P\text{-}H}$ = 21.0 Hz) which shows coupling to the *trans*-PMe_3 group (Figure 15). The relatively large $^{1}J_{Si\text{-}H}$ values (154.5, 186.0, and 166.9 Hz) are consistent with the classical structure as opposed to any unclassical Si-H interactions with the metal centre. The fact that all silicon signals were non-equivalent in the ^{1}H-NMR also agrees with the ^{29}Si INEPT spectrum where three distinct signals were observed at δ -14.3, -5.0 and 1.4 ppm.

In light of this interesting reactivity, mechanistic investigation of formation of **III-51** was studied by low temperature NMR, using the bis(phosphine) complex **III-38** and one equivalent of $PhSiH_3$. Only one intermediate was observed at -30 °C and this was characterized as a rare γ-SiH agostic complex (^{t}BuN)Mo(H)(η^3-PhHSi-N(^{t}Bu)-SiHPh-H)(PMe_3)$_2$ (**III-52**), which differs from the disialazametalabutane derivative **III-51** in that one of the arms of the 4-membered ring contains a Si-H bond coordinated to the Mo centre. Heating this complex to room temperature results in the formation of the silanimine complex (η^2-^{t}BuN=SiHPh)$MoH_4(PMe_3)_3$ (previously mentioned) and **III-51** after only 30 min. All attempts to isolate **III-52** on large scale resulted in isolation of **III-51** even at low temperatures. Complex **III-52** was fully characterized by multinuclear NMR experiments.

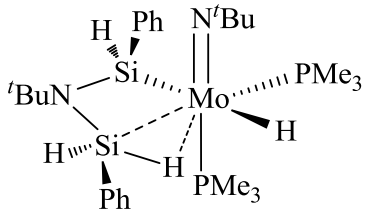

III-52

The ^{1}H-NMR of **III-52** at room temperature displays a broad resonance at 6.81 ppm corresponding to the classical Si-H protons of the γ-agostic ring. The agostic Si-H and the Mo-bound hydride signals cannot be observed at this temperature due to the high degree of

fluxionality. However, cooling to -30 °C results in observance of both Si-$H_{agostic}$ and Mo-H at δ 0.37 (dt, $^{2}J_{H-P}$ = 45.5 Hz, $^{2}J_{H-H}$ = 4.4 Hz) and -4.43 (ddd, $^{2}J_{H-P}$ = 46.1 Hz, $^{2}J_{H-P}$ = 16.7 Hz, $^{2}J_{H-H}$ = 4.4 Hz) ppm, respectively. The Si-$H_{classical}$ is also separated into a small doublet at δ 6.84 (bd, $^{2}J_{H-H}$ = 5.3 Hz) and a singlet at 6.92 (bs) ppm. The doublet at 6.84 ppm was assigned to the classical Si-H proton on the agostic silicon centre by ^{1}H-^{1}H COSY and ^{1}H-^{29}Si HSQC experiments. The small doublet stems from germinal coupling between Si-$H_{classical}$ and Si-$H_{agostic}$ (Figure 16).

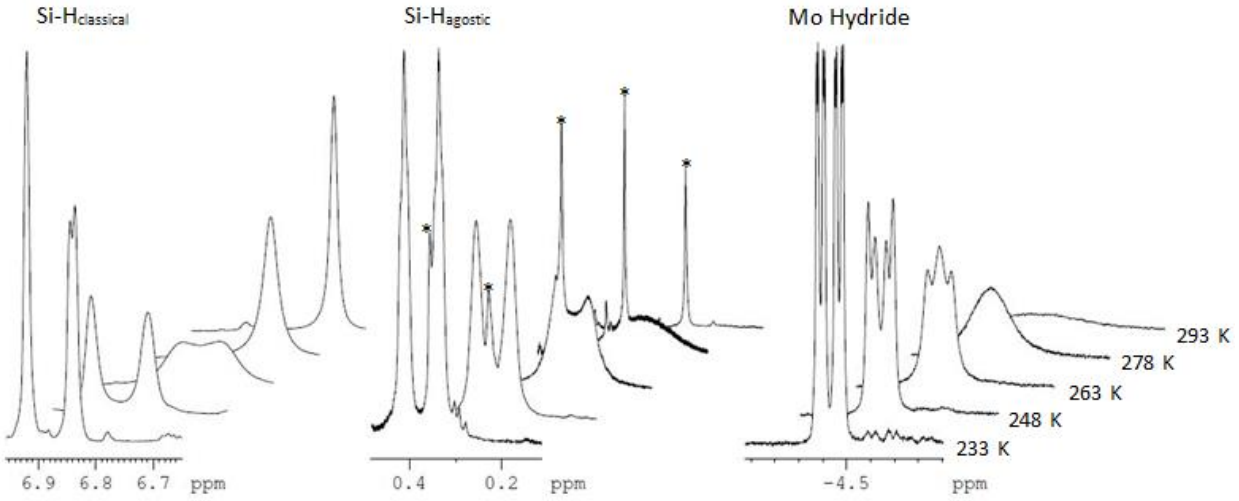

Figure 16 - Variable temperature ^{1}H-NMR for complex **III-52** beginning at 233 K and warming to 293 K. The respective peaks are labelled accordingly. (* - residual silicon grease peak).

Compound **III-52** could be generated as the major product by reacting **III-50** with 2 equivalents of $PhSiH_3$ and one equivalent of PMe_3 for 3 hours at -20 °C. Addition of one equivalent $PhSiD_3$ to a freshly prepared sample of **III-52** led to the observation that all Si-H and Mo-H positions become deuterated in the final product. Similarly, reacting complex **III-51** with an equivalent of $PhSiD_3$ results in deuterium scrambling into all the same positions. This exchange process can be accounted for by reversible Si-H bond oxidative addition/reductive elimination on both sides of the PhHSi-N(^{t}Bu)-SiHPh unit. D-scrambling in **III-51** can be also

explained by reversible Si-H bond formation and cleavage between the silicon atom of the disilacyclobutane ring and the Mo-bound hydride.

Although only one intermediate could be observed using complex **III-38** as a starting material, we attempted the same reaction using complex **III-50** containing an ethylene moiety. Interestingly, lowering the initial temperature to -80 °C drastically affects the observance of intermediate products. The results of this low temperature NMR study are discussed in the following section.

III.5.1 VT NMR Study for complex III-51

The reaction of (^{t}BuN)$_2$Mo(PMe$_3$)(η^2-C$_2$H$_4$) with PhSiH$_3$ in the presence of PMe$_3$ was studied by low temperature NMR (-80 to +20 °C) over a period of a few days (

Scheme 58). Adding one equivalent of PhSiH$_3$ to (^{t}BuN)$_2$Mo(PMe$_3$)(η^2-C$_2$H$_4$) at -40 °C results in 13% consumption of the starting material into a 1:1 mixture of (^{t}BuN)Mo(η^3-N^{t}Bu-SiHPh-H)(PMe$_3$)$_2$(Et) (**III-53**) and (^{t}BuN)Mo(η^3-N^{t}Bu-SiHPh-H)(PMe$_3$)$_2$(SiH$_2$Ph) (**III-54**) after 15 minutes. After 2 hours at -40 °C, approximately 80% of the starting complex is consumed and an increase in both complex **III-53** and **III-54** is seen, maintaining the same 1:1 ratio. A small amount of the γ-agostic silylamido (^{t}BuN)Mo(η^3-SiHPh-N^{t}Bu-SiHPh-H)(PMe$_3$)$_2$(H) (**III-52**) was also produced at this temperature most likely formed from initial mixing at somewhat higher temperature during the addition silane (some deviation from thermal equilibrium may happen locally during addition of silane and during placing the sample into the NMR machine). At -40 °C, complex **III-53** exhibits broad Si-H resonances at 5.62 ppm and -0.85 ppm for both the classical and agostic Si-H protons respectively. Reducing the temperature to -53 °C, results in significant sharpening of both the Si-H and PMe$_3$ signals in the ^{1}H-NMR. The reduced $^1J_{\text{Si-H}}$ value of 125.1 Hz (found by ^{1}H-^{29}Si HSQC 1D JC) for Si-H$_{\text{agostic}}$ is indicative of a non-classical

interaction with the Mo centre, whereas the $^{1}J_{Si\text{-}H}$ value of 212.0 Hz for the Si-$H_{classical}$ proton suggests a non-agostic interaction. Direct coupling of Si-$H_{agostic}$ and Si-$H_{classical}$ protons to the PMe_3 groups through the Mo centre was observed in the ^{1}H-^{31}P HSQC. The large coupling constant value, $^{2}J_{P\text{-}P}$ = 291.8 Hz, of the two PMe_3 doublets in the ^{31}P-NMR strongly suggests a *trans* arrangement of the phosphine ligands. The ethyl fragment displays two broad multiplets in ^{1}H- NMR for the methylene protons at 2.61 and 2.49 ppm, which couple to a triplet at 1.96 ppm ($^{3}J_{H\text{-}H}$ = 7.53 Hz) for the metrhyl group, as well as with the PMe_3 groups according to ^{1}H-^{31}P HSQC. The^{1}H-^{29}Si HSQC Si projections show that both Si-$H_{classical}$ and Si-$H_{agostic}$ couple to the same Si signal at -74.5 ppm. This high field ^{29}Si resonance is also indicative of an agostic interaction.[3] 1D EXSY experiments indicate an exchange between non-equivalent Si-H protons

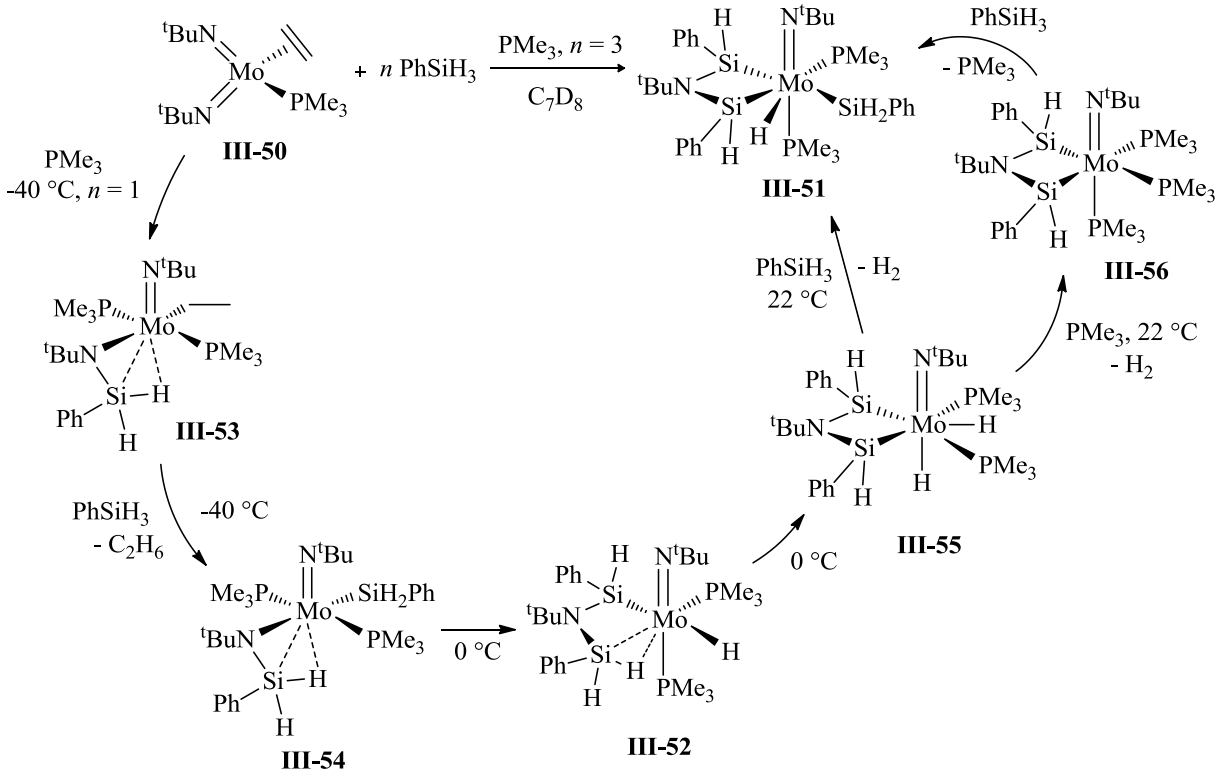

Scheme 58 –Intermediates observed by using low temperature NMR techniques en route to complex **III-51**.

but no exchange with free $PhSiH_3$. NOESY experiments are consistent with the geometry shown. The complex can be described as having pseudo-octahedral geometry, with the agostic Si-H bond (which is a weak σ-donor) situated *trans* to the strong *trans* influencing imido group. The *trans* PMe_3 groups are situated on the equatorial plane *cis* to both the Mo-N^{t}Bu bond and the Mo-CH_2CH_3 group.

At -40 °C, complex **III-54** shows a broad triplet at 5.69 ppm corresponding to the Si-H protons of silyl group with a $^3J_{H\text{-}P}$ value of 4.3 Hz. The Si-$H_{classical}$ and Si-$H_{agostic}$ resonance are unresolved in the ^{1}H-NMR at this temperature. However, lowering the temperature to -57 °C results in two extremely broad singlets at 5.43 ppm and 0.18 ppm for the Si-$H_{classical}$ and Si-$H_{agostic}$ protons, respectively. Further lowering to -80°C results in significant sharpening of these peaks and interestingly, the Si-H protons of the silyl group decoalesce into two singlets at 5.78 and 5.83 ppm. The ^{31}P-NMR displays two doublets showing a significant roofing effect, with large coupling constant value of $^2J_{P\text{-}P}$ = 267.7 Hz, indicative of *trans* disposition of non-equivalent phosphine ligand similar to complex **III-53**. It is worth noting the reduced $^2J_{P\text{-}P}$ values compared to complex **III-53**, which is possibly due to the steric effect of the larger silyl ligand as opposed to the smaller ethyl moiety, which may cause a deviation from the ideal *trans* geometry. From the Si projections in the ^{1}H-^{29}Si HSQC 2D spectra, the silyl group shows a resonance at -8.4 ppm and the agostic silylamido fragment shows a Si resonance at -81.1 ppm. Similar to comlex **III-53**, a reduced $^1J_{Si\text{-}H}$ value of 110.3 Hz (found by ^{1}H-^{29}Si HSQC 1D JC) was observed for the Si-$H_{agostic}$ along with a larger $^1J_{Si\text{-}H}$ value of 226.1 Hz (found by ^{1}H-^{29}Si HSQC 1D JC) for the Si-$H_{classical}$. The 1D EXSY experiment revealed an exchange at -80 °C between the Si-H groups of the silylamido ligand, but no exchange was observed with the terminal silyl group or free $PhSiH_3$ at this temperature. Such an exchange of diasterotopic SiH protons can occur via

opening of the agostic Si-H···Mo bond and its reformimg on the opposite site after rotation around the N-Mo bond. Interestingly, free ethane is seen in the ^{1}H-NMR (δ_{ethane} = 0.92 ppm), suggesting that complex **III-54** may be formed *via* a metathesis between the ethyl group on complex **III-53** and free $PhSiH_3$, to generate the subsequent silyl ligand.

Warming the 1:1 mixture of **III-53**:**III-54** from -80 °C to 0 °C showed formation of the γ-agostic silylamido complex (^{t}BuN)Mo(η^3-SiHPh-N^{t}Bu-SiHPh-H)(PMe_3)$_2$(H) (**III-52**). Careful monitoring at 10 °C intervals revealed the expected broadening of the Si-$H_{agostic}$ and Si-$H_{classical}$ signals of the *β*-agostic silylamido fragment for **III-52** and **III-53**, from -80 °C to -20 °C, while the silyl group resonance still remained sharp but transformed back into a triplet. From -20 °C to -10 °C, however, a significant amount of free H_2 (δ = 4.57 ppm) was seen along with nearly full conversion of **III-52** and **III-53** directly into **III-54**. No other intermediates were observed at these temperatures. Heating to room temperature resulted in formation of the tris(silyl) complex (^{t}BuN)Mo(SiH_2Ph)(H){(SiHPh)$_2$(μ-N^{t}Bu)}(PMe_3)$_2$ (**III-51**).

In a separate experiment, reacting (^{t}BuN)$_2$Mo(PMe_3)(η^2-C_2H_4) with 2 equivalents of $PhSiH_3$ in the presence of PMe_3 for 3 hours at -20 °C results in 80% conversion to (^{t}BuN)Mo(H)(η^3-PhHSi-N(^{t}Bu)-SiHPh-H)(PMe_3)$_2$ (**III-52**), 2% conversion to the final complex (^{t}BuN)Mo(SiH_2Ph)(H){(μ-N^{t}Bu)(SiHPh)$_2$}(PMe_3)$_2$ (**III-51**) and 18 % conversion to (^{t}BuN)Mo{(SiHPh)$_2$(μ-N^{t}Bu)}(PMe_3)$_2H_2$ (**III-55**). At 0 °C, complex **III-55** exhibits two Si-H resonances in the ^{1}H-NMR at 5.92 and 6.51 ppm, correlating to two different silicon centres, as seen by the ^{1}H-^{29}Si HSQC. The splitting pattern for each Si-H signal differs slightly but both couple to each PMe_3 ligand and to a Mo-H hydride. In the ^{1}H{^{31}P}-NMR, each Si-H signal is split into a doublet with different $^3J_{H\text{-}H}$ values indicating coupling to two distinct Mo-H hydride signals. Although the hydride resonances could not be directly observed in the ^{1}H-NMR, 2D

correlation experiments (^{1}H-^{1}H COSY, ^{1}H-^{29}Si HSQC (*J* value of 7 Hz), and ^{1}H-^{31}P HSQC) provide the necessary evidence to confirm their existence. When ^{1}H-^{29}Si HSQC was run with a low coupling constant value of 7 Hz, the spectrum showed coupling of each Si resonances to the hydride signal in the ^{1}H-NMR at 1.48 ppm but only the Si resonance at 4.05 ppm couples to the hydride at 1.25 ppm. The ^{1}H-^{31}P HSQC shows coupling of the ^{31}P signal at -34.6 to each hydride signal, whereas the -9.7 ppm signal shows coupling to the hydride at 1.48 ppm in the ^{1}H-NMR. In the ^{31}P{^{1}H}-NMR spectrum selectively decoupled from the methyl group at 1.10 ppm, the signal at -31.3 ppm comes up as a broad multiplet in which coupling to one Si-H ($^{3}J_{\text{Si-H}}$ = 13.0 Hz), the alternate phosphine ($^{2}J_{\text{P-P}}$ = 27.6 Hz) and one hydride ligand ($^{2}J_{\text{P-H}}$ = 51.7 Hz) can be observed. Decoupling from the methyl group at 1.05 ppm in the ^{1}H-NMR results in the ^{31}P resonance at -9.6 ppm to become a broad triplet with the $^{2}J_{\text{P-P}}$ value of 33.4 Hz. However, when decoupled from the hydride at 1.25 ppm this same ^{31}P signal converts back into a doublet indicating that one hydride has the $^{2}J_{\text{H-P}}$ coupling constant close to that of the $^{2}J_{\text{P-P}}$ value of 33.4 Hz.

Interestingly, keeping complex **III-52** at -30 °C for three days, formation of the tetrahydride silanimine complex (^{t}BuN)(η^{2}-^{t}BuN=SiHPh)MoH$_4$(PMe$_3$)$_2$ and the novel tris-phosphine complex (^{t}BuN)Mo{(SiHPh)$_2$(μ-N^{t}Bu)}(PMe$_3$)$_3$ (**III-56**). At 0 °C, complex **III-56** exhibits two Si-H resonances in the ^{1}H-NMR, at 5.36 ppm (ddd) and 7.05 ppm (bd). The splitting pattern for the Si-H resonance at 5.36 ppm is indicative of $^{3}J_{\text{H-P}}$ coupling to three inequivalent PMe$_3$ groups. Although the second Si-H resonance is partially obscured by solvent peaks, a broad doublet can be seen displaying a $^{3}J_{\text{H-P}}$ coupling value of approximately 9.2 Hz. The PMe$_3$ peaks in the ^{1}H-NMR spectrum show 3 distinct doublets between 1-2 ppm validating the large splitting of the Si-H signal. The ^{31}P-NMR displays a triplet at 5.67 ppm and two doublet of

doublets, displaying large and small $^{2}J_{P\text{-}P}$ values of approximately 91 Hz and 20 Hz each. This is indicative of two *trans* PMe_3 groups both coupled to a *cis* PMe_3 group. The ^{29}Si INEPT+ spectra revealed two ^{29}Si resonances corresponding to two distinct Si atoms on one Mo centre. The broad doublet at 41.7 ppm showed a $^{1}J_{Si\text{-}H}$ value of 169.3 Hz, whereas the alternate signal showed visible splitting into a dddd pattern with a $^{1}J_{Si\text{-}H}$ value of 152.0 Hz and different $^{2}J_{Si\text{-}P}$ values ranging from 19.3 Hz to 38.3 Hz.

III.5.2 Stoichiometric Reactivity with Carbonyls, Alkenes and Alkynes

Interested in utilizing this multicomponent coupling of silane for the overall detachment of functionalised silanes from the metal centre, we investigated the reaction of **III-51** with various carbonyls, alkenes, and alkynes. Insertion of various substrates into the ring structure of **II-51** could result in making new Si-C and Si-N bonds and ultimately lead to development of new multicomponent catalytic processes.

Reacting **III-51** with two equivalents of benzaldehyde or acetophenone generates the hydrosilylation products PhH_2SiOBn and $PhH_2SiOCH(Me)Ph$ as well as a variety of different Mo-H species which were observed in the ^{1}H-NMR between -3 to -6 ppm. This mixture did not seem to contain any coordinated carbonyls or show insertion into the 4-membered ring system. NMR analysis proves difficult to determine the exact structures of the decomposition products due to the large amount of by-product produced. This reaction goes rather quickly, with complete decomposition seen after 10 minutes at room temperature. Hydrosilylation products were observed, which are most likely formed by fast insertion of the carbonyl into the Mo-H bond bond followed by quick reductive elimination of the Si-OR bond and subsequent decomposition into various products. Interestingly, catalytic reactivity is observed when 5 mol % loading of **III-51** is used with a 1:1 ratio between benzaldehdye and $PhSiH_3$. Full conversion of benzaldehyde

is observed in 20 minutes at room temperature to give a mixture of PhH_2SiOBn, $PhHSi(OBn)_2$ and $PhSi(OBn)_3$. This mixture contains some residual $PhSiH_3$ and addition of an extra equivalent of benzaldehyde results in further reactivity to produce similar silylether products within two hours.

A similar observation was made when phenylacetylene or styrene were used as substrates, however the rates of reaction at room temperature were significantly longer. The addition of styrene to **III-51** results in the generation of a small amount of the Markovnikov product $PhCH_2(SiH_2Ph)CH_3$. The reaction goes to completion after three days at room temperature and no alternative products of incorporation of styrene into the ring are observed. However, the ^{1}H-NMR revealed the formation of an intractable mixture of various decomposition products many of which show hydride signals in the high field region. Interestingly, **III-51** was still seen in the solution after 2 days at room temperature, which is in contrast with the observation of complete decomposition of pure **III-51** in a C_6D_6 solution overnight at room temperature. This implies that styrene somehow slows the decomposition of the starting material, either by reversible insertion into the metal hydride bond or through η^2-coordination and subsequent dissociation of one of the PMe_3 groups. Similarly, the use of phenylacetylene seems to generate a small amount of the hydrosilylation product HC_2=CH(SiH_2Ph)Ph along with a spectrum of decomposition products.

Along the same lines, a reaction between **III-51** and ethylene gave a variety of different products, however, the ^{1}H-NMR spectrum was intriguing as a number of well-defined doublets and triplets were observed in the high field region between δ 0 to -2 ppm. This was in addition to broad signals in the hydride region between δ -5 to -7 ppm, although fewer signals were observed compared to that of styrene or phenylacetylene. 2D-correlation studies indicated the

formation of a product of insertion directly into the ring, the complex (^{t}BuN)Mo(κ^2-*Si*,*C*-*Si*HPh-N^{t}Bu-SiHPh-*C*H(Me))(PMe$_3$)(η^2-C$_2$H$_4$) (**III-57**, Scheme 59).

The ^{1}H-NMR of **III-57** displays a resonance at 1.02 ppm found to correlate with a methine carbon signal found by ^{1}H-^{13}C HSQC and DEPT-135, as well as coupling to both an upfield methyl signal at -2.12 ppm ($^3J_{H\text{-}H}$ = 6.9 Hz). This former signal is overlapped by a variety of different peaks from various products but is most consistent with a methine group coupled to the methyl CH_3. The high field chemical shift value of the C-H proton is comparable to that of the cyclometallated complexes **III-13** and **III-15** containing a methylene group lying *trans* to the imido group. Based on this analogy, we propose a structure containing a 5-membered ring with a methine group *trans* to the imido group. Both Si-H signals appear close to each other in the ^{1}H-NMR at 6.64 ppm and 6.65 ppm, and couple to 29Si signals at -8.9 and 39.6 ppm, respectively, as determined by ^{1}H-^{29}Si HSQC (J = 200 Hz). The ^{1}H signal at 6.64 displays a doublet splitting pattern ($^2J_{H\text{-}P}$ = 7.8 Hz) , which becomes a singlet in the ^{1}H{^{31}P}-NMR. Based on this data and 1D NOESY studies, the structure shown in Scheme 59 with one silicon centre bound to molybdenum and one silicon centre with no interaction with Mo, seems to be a reasonable.

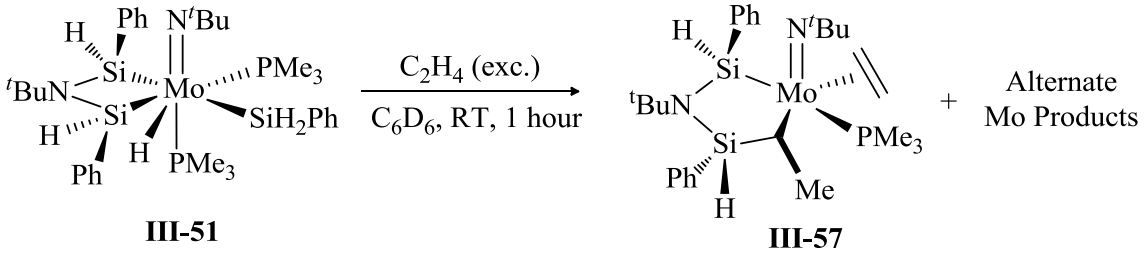

III-51 **III-57**

Scheme 59 – Addition of ethylene to **III-51** showing formation of the insertion product **III-57**.

In an attempt to trap intermediates formed during the synthesis of **III-51** (Section III.6.1), or possibly selectively produce **III-57**, we added two equivalents of PhSiH$_3$ to a mixture of (^{t}BuN)$_2$Mo(PMe$_3$)(η^2-C$_2$H$_4$) and excess ethylene gas. Surprisingly, one major product was

observed in the NMR, which was characterized as the β-agostic silylamido complex (^{t}BuN)Mo(η^3-N^{t}Bu-Si(Et)Ph-H)(Et)(η^2-C_2H_4) (**III-58**, Scheme 60). The agostic Si-H signal could not be directly observed in the ^{1}H-NMR but using ^{1}H-^{29}Si HSQC (J = 125 Hz) and 1D ^{1}H-^{29}Si HSQC JC NMR the signal was located at δ 1.36 ppm with a reduced $^1J_{Si\text{-}H}$ coupling constant value of 149.3 Hz. The ethyl fragment contains two signals at δ 2.17 ppm (t, $^3J_{H\text{-}H}$ = 7.7 Hz) and 2.7 ppm (m) corresponding to the methylene and methyl groups, respectively. The ethyl moiety on the agostic silane was unobservable due to overlap of signals in the aliphatic region but could be located by ^{1}H-^{29}Si HSQC(J = 15 Hz) in the ^{1}H-NMR at 1.02 ppm and 1.13 ppm. A similar structure was suggested for the Ar imido complex (ArN)Mo(SiH_2Ph)(η^3-NAr-Si(Et)Ph-H)(η^2-C_2H_4) found during the mechanistic investigation of hydrosilylation using complex (ArN)Mo(SiH_2Ph)(η^3-NAr-SiHPh-H)(PMe_3).[154]

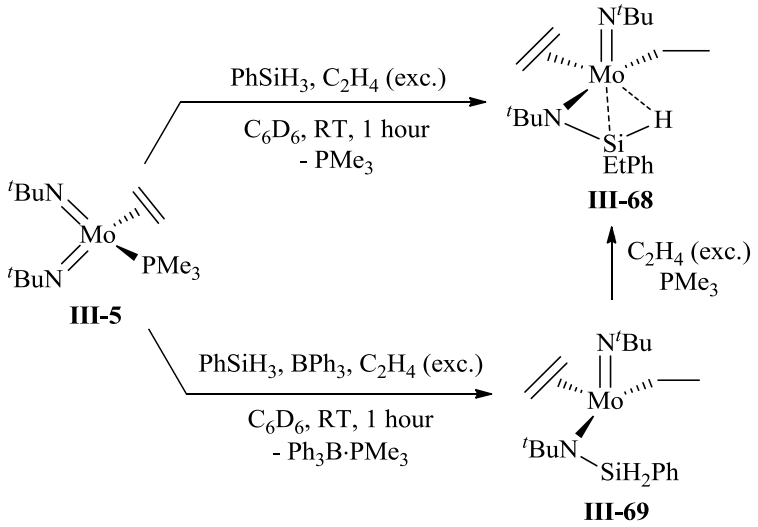

Scheme 60 – Attempted trapping of intermediates en route to complex **III-51** using ethylene gas. Formation and interconversion between **III-59** and **III-58** is also shown.

Adding one equivalent of BPh_3 to the starting mixture of (^{t}BuN)$_2$Mo(PMe_3)(η^2-C_2H_4) and ethylene gas, results in release of the phosphinyl borane $Ph_3B{\cdot}PMe_3$ and generation of the silylamido complex (^{t}BuN)Mo(N^{t}BuSiH_2Ph)(Et)(η^2-C_2H_4) (**III-59**, Scheme 60). Two distinct

diastereotopic Si-H signals appear at 3.08 and 3.44 ppm and show increased $^{1}J_{Si\text{-}H}$ coupling constant values of 197.8 and 188.1 Hz. Resonances at 2.85 and 2.17 ppm were attributed to the methylene and methyl fragment, overlapping with four distinct resonance between 1.79 to 2.76 ppm and correlating with the η^2-C_2H_4 moiety. Interestingly, the addition of PMe_3 to a freshly prepared sample of **III-59** converts to **III-58** after one night at room temperature. Both complexes are unstable in solution and slowly decompose after 3 days to a mixture of compounds. The isolation of each complex proved to be difficult even though NMR samples showed fairly clean conversions. This hurdle is due to the high solubility of **III-58** in aliphatic solvents, such as hexanes or pentanes and its subsequent decomposition after a day.

Interestingly, performing the same reaction with $PhSiD_3$, BPh_3 and excess ethylene gives the expected complex **III-58** but shows selective deuteration into certain positions in the complex. After one hour at room temperature deuterium scrambling was observed only in the methyl position of the ethyl moiety in the complex. No deuterium incorporation was seen in the methylene position according to ^{2}H-NMR. Also, there is deuterium scrambling into the silyl group bound to the nitrogen atom, so that a mixture of SiH_2Ph, SiDHPh and SiD_2Ph derivatives is formed. The mechanism of formation of **III-59** could possibly include initial silane/imido coupling followed ethylene coordination and insertion into the Mo-hydride bond. Deuterium exchange can then take place by Si-H bond activation to give the Mo(VI) deuteride hydride silanimine complex (^{t}BuN)Mo(η^2-N^{t}Bu-SiDPh)(η^2-C_2H_4)(η^2-H_2C=CHD)(H)(D) and, finally, recombination of silicon atom with alternate hydride and deuteride. The process could be repeated to give full deuteration of the methyl groups and protonation of the silane (Scheme 61).

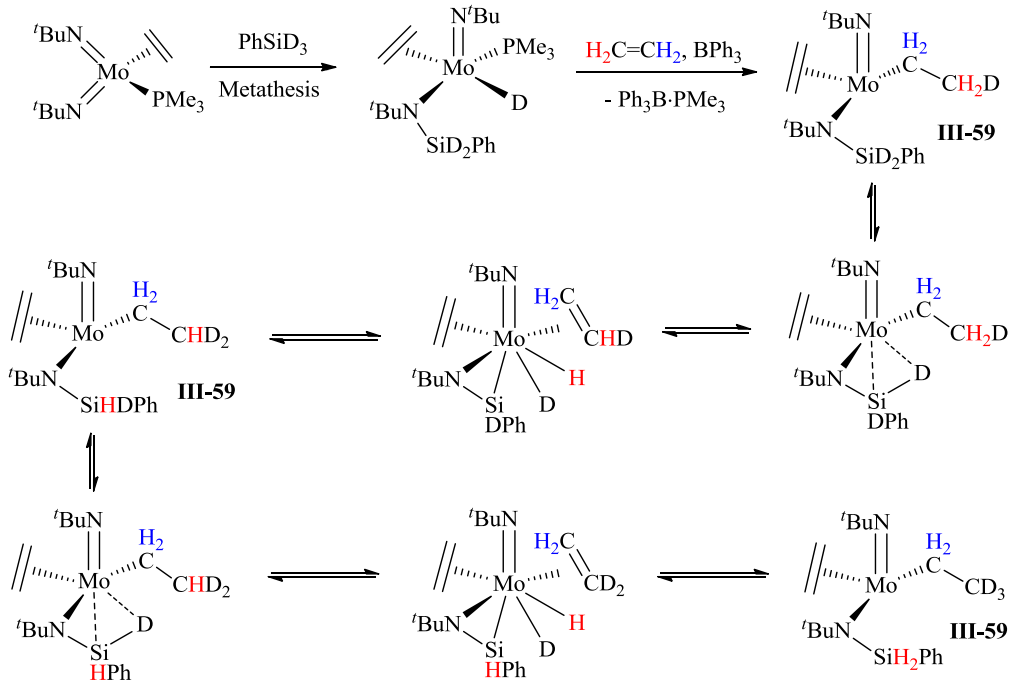

Scheme 61 – Possible mechanism of formation of complex **III-59**, along with exchange process using $PhSiD_3$.

III.5.3 Stoichiometric Reactivity with Nitriles

Reacting complex **III-51** with an equivalent of either alkyl or aryl nitriles results in loss of $PhSiH_3$ and generation of the nitrile insertion complexes of the type (^{t}BuN=)Mo(η^2-SiHPh-N^{t}Bu-SiHPh-N=C(R))$(PMe_3)_2$ (R = Me (**III-60**), Ph (**III-61**), Ph-4-OMe (**III-62**). Each complex was characterized by multinuclear NMR and IR spectroscopy, and the relative ligand orientation was determined by 1D NOESY experiments. Complexes **III-60** to **III-62** exist as a mixture of two isomers in solution, whose ratios vary according to the nature of R. For each complex, distinct signals for the Si-H protons of the major isomer appear at approximately δ 6.4 and 7.1 ppm, similar to that of the parent complex **III-51** (δ_{SiH} = 6.03 and 6.67 ppm). However, the ^{29}Si resonances, which appear at 37 and -25 ppm determined by Si INEPT + NMR, suggest a different type of structure to that of **III-51**. The upfield shifting of the latter peak, along with a

high $^{1}J_{Si\text{-}H}$ value of 216.5 Hz (for R = Ph (**III-61**)), suggests one Mo bound silicon, while the other exhibits no bonding interaction with the Mo centre.[2] The following spectroscopic data suggest insertion of the nitrile into the ring, as opposed to a side-on or end-on nitrile coordination to the Mo centre. Namely, the observation of low C=N stretching frequency at 1432 cm^{-1} (for R = 4-OMe-Ph (**III-62**)) in the IR speaks against a side-on (η^2-coordination) nitrile complex, which typically exhibit C≡N stretches around 1700 cm^{-1}, and against an end-on (κ^1-coordination) nitrile complex, which usually show stretches above 2100 cm^{-1}. For comparison, literature search shows that transition metal complexes with the [M-C=N] fragments display IR stretching frequencies between 1450-1610 cm^{-1},[189-192] suggesting a similar motif for complexes **III-60** to **III-62**. Furthermore, the downfield shift of the ^{13}C signal at 258.32 ppm (for R = Ph (**III-61**)) coupled to both phosphine ligands ($^{2}J_{H\text{-}P}$ = 12.0 Hz) indicates direct coordination of the nitrile carbon to the Mo centre and agrees well with similar complexes.[189-192] For comparison, in the related iminoyl complex of Mo, $(ArN)_2Mo\{C[Si(SiMe_3)_3]=NAr'\}(Cl)$, the ^{13}C signal comes at 232.8 ppm and the related IR stretch is observed at 1608 cm^{-1}. Further supporting binding of nitrile to silicon via the nitrogen atom in complex **III-61** is the absence of coupling between the Si-H resonances and the nitrile carbon in the $^{1}H\text{-}^{13}C$ HMBC. Based on the large $^{2}J_{P\text{-}P}$ value of 230 Hz the *trans* configuration of the two PMe_3 ligands was suggested, as large $^{2}J_{P\text{-}P}$ values are typically associated with *trans* phosphine coordination.[169,193,194] 1D-NOESY experiments showed that the methyl groups of the imido ^{t}Bu moiety "see" only two PMe_3 groups and in the case when R = Ph or 4-OMe-Ph, the *ortho* protons of the phenyl rings. The ^{t}Bu group attached to the ring "sees" both Si-H signals, the *ortho* protons of the silyl phenyl rings and only one PMe_3 group. Each Si-H signal "sees" its own *ortho* protons of the respective silyl phenyl rings as well as the ring ^{t}Bu group. Taking into account all the data, the structure shown in Scheme 62 seems

to be appropriate.

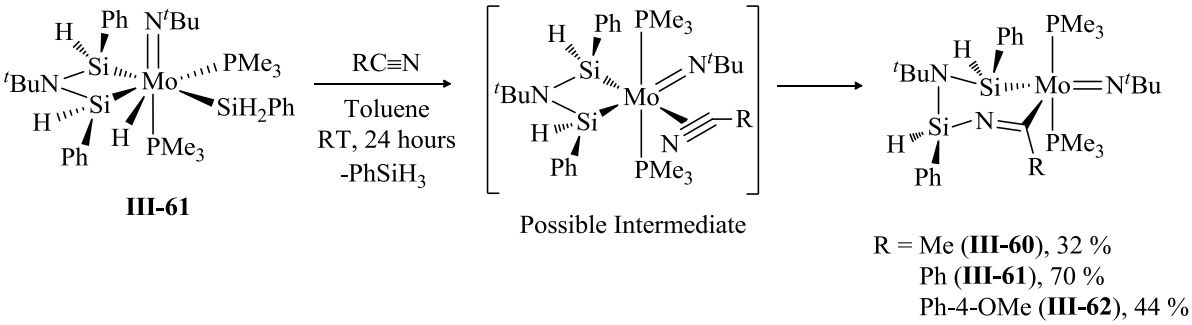

Scheme 62 – Synthesis of the nitrile insertion complexes **III-60** to **III-62**.

In an attempt to generate complex **III-61** directly from the starting bis(imido) precursor **III-50**, we added one equivalent of benzonitrile in the presence of two equivalents of $PhSiH_3$ and an extra equivalent of PMe_3 and observed formation of the classical silylamido complex (^{t}BuN)Mo(PMe_3){N^{t}Bu(SiH_2Ph)}(Et)(η^2-N≡CPh) (**III-63**, Scheme 63). The ^{1}H-NMR for complex **III-63** exhibits a multiplet at 2.52 and triplet at 2.20 ppm corresponding to the ethyl fragment. **III-63** most likely forms upon addition of $PhSiH_3$ across the ^{t}BuN=Mo double bond to generate the silylamido hydride complex (^{t}BuN)Mo(PMe_3){N^{t}Bu(SiH_2Ph)}(η^2-C_2H_4)(H) **III-63** which then undergoes hydrogen shift to ethylene to give ethyl ligand followed by coordination of nitrile. No β-agostic Si-H interaction with the Mo was evident, as indicated by the rather high $^1J_{Si\text{-}H}$ value of 199.6 Hz. The side-on coordination of the benzonitrile ligand was suggested based on the downfield shift of the nitrile carbon at 198.5 ppm. Exchange between both ^{t}BuN imido groups was observed by EXSY NMR in the temperature range 10 °C to 34 °C and the activation parameters were obtained ($\Delta H^{\ddagger}$ = 32.9 ± 0.8 kcal/mol, $\Delta S^{\ddagger}$ = 43.7 ± 1.2 cal/mol) from the Eyring plot (Appendix; Figure 20 and Figure 21). Similarly, a second exchange process was found between the free and coordinated phosphines. Likewise, the activation parameters were obtained in the same temperature ranges listed above ($\Delta H^{\ddagger}$ = 26.5 ± 0.7 kcal/mol, $\Delta S^{\ddagger}$ = 24.7 ± 1.0 cal/mol). The positive value of $\Delta S^{\ddagger}$ suggests a dissociatively activated exchange process in each

case. We believe that in both cases dissociation of phosphine takes place. Such dissociation PMe_3 opens a vacant coordination site allowing for migration of the silyl group from the silylamido ligand to the Mo centre. This would generate the bis(imido) complex (^{t}BuN)$_2$Mo(SiH$_2$Ph)(Et)(η^2-N≡CPh), which has both ^{t}Bu groups equivalent. The exchange will be complete be re-addition of the silyl fragment to either of two ^{t}BuN=Mo imido moieties. All attempts at isolation of **III-63** were unsuccessful due to its fast decomposition in approximately 12 hours at room temperature. Interestingly, production of 20 % of complex **III-61** was observed, however, this was accompanied by a variety of decomposition products.

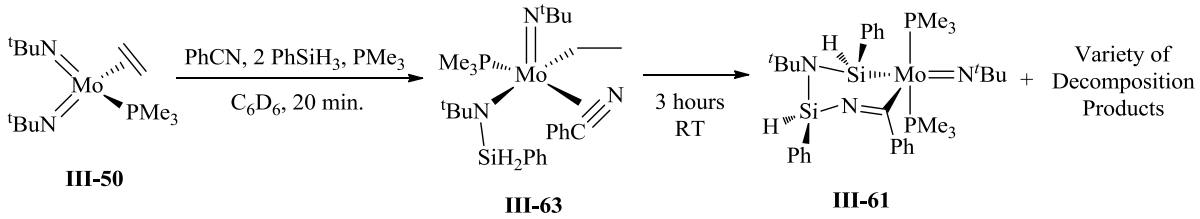

Scheme 63 – Synthesis of intermediate **III-63** along with 20 % production of **III-61** after 3 hours.

IV. Conclusions and Future Work

In an effort to extend the scope of Mo imido systems for their use as hydrosilylation catalysts we undertook a research programme devoted to the investigation of various novel mixed(imido) systems in hopes of producing unclassical *β*-agostic silylamido complexes. We attempted preparation of unsymmetrical bis(imido) complexes of the type (RN)(R′N)Mo(PMe_3)$_2$ from the mono(imido) precursors (RN)Mo(PMe_3)$_3$(X)$_2$ (X = Cl_2 or HCl). To our surprise, the addition of various silylamide salts induces formation of the cyclometallated complex (RN)Mo(PMe_3)$_2$(η^2-CH_2PMe_2)(X) (R = Ar, X = H (**VI-1**); R = ^{t}Bu, X = Cl (**VI-2**)). These complexes were found to activate a variety of E-H bonds (E = Si, P, and O) through addition across the Mo-C bond. Aryl alcohol addition to **VI-1** led to the activation of the O-H bond in all cases and for 2,6-dimethylphenol, heating the resultant hydride complex (ArN)Mo(PMe_3)$_3$(OPh^{Me_2})(H) to 50 °C led to C-H activation of one methyl group to give the 5-membered oxametallacycle (ArN)Mo(PMe_3)$_3$(κ^2-OPh(Me)CH_2). The addition of alkenes and terminal alkynes produced interesting products including the molybdacylopentane complex (ArN)Mo(PMe_3)$_2$(CH_2)$_4$(η^2-C_2H_4) and bis(alkynyl) complex (ArN)$_2$Mo(PMe_3)(η^2-CPh≡CH)$_2$. The analogous tungsten cyclometallated complex (PMe_3)$_4$WH(η^2-CH_2PMe_2), developed by Parkin and coworkers, has been abundantly used for various transformations including hydrodesulfurization of thiophenes[112] and aromatic C-C bond activation[195]. In this regard, complexes **VI-1** and **VI-2** could be used for similar transformations.

Despite the successful reactivity of complexes **VI-1** and **VI-2**, an new alternative pathway was developed for the synthesis of mixed imido systems where the addition of EtMgBr to (ArN)(^{t}BuN)$MoCl_2$(DME) generates (ArN)(^{t}BuN)Mo(PMe_3)(η^2-C_2H_4) (**VI-3**). Based on our groups previous success reacting symmetrical bis(imido) phosphine Mo(IV) precursors (i.e.

$(ArN)_2Mo(PMe_3)_3$ and $(^tBuN)_2Mo(PMe_3)_2$) with hydro- and chlorosilanes led us to test complex **VI-3** with similar substrates. The addition of $PhSiH_3$ resulted in the production of the β-agostic silylamido complex $(^tBuN)Mo(\eta^3\text{-}NAr\text{-}SiHPh\text{-}H)(SiH_2Ph)(PMe_3)$. Of greater interest was the addition of Me_2SiHCl, which generates both the bis(phosphine) complex $(^tBuN)Mo(\eta^3\text{-}NAr\text{-}SiMe_2\text{-}H)(Cl)(PMe_3)_2$ (**VI-4**) and the rare silanimine complex $(^tBuN)Mo(\eta^2\text{-}NAr\text{-}SiMe)(Cl)(Et)(\eta^3\text{-}C_2H_4)$ (**VI-5**). Selective generation of complex **VI-5** through the addition of BPh_3 under an atmosphere of ethylene gas shows promise as a new pathway for silanimine synthesis.

As part of our investigation into the generation of new hydrosilylation catalysts, we examined the catalytic ability of the β-agostic silylamido complex $(ArN)_2Mo(\eta^3\text{-}N^tBu\text{-}SiMe_2\text{-}H)(H)$ (**VI-6**), which importantly does not feature any phosphine ligation, saving on cost and inherent toxicity of waste. The complex was found to be active for the hydrosilylation of various aldehydes and ketones. Reacting complex **VI-6** with benzaldehyde generated the benzoxy complex $(ArN)_2Mo(\eta^3\text{-}N^tBu\text{-}SiMe_2\text{-}H)(OBn)$ (**VI-7**), which showed similar reaction rates compared to **VI-6**. Regeneration of **VI-6** upon addition of excess silane over a period of many days suggests **VI-6** may not be part of the catalytic cycle. Based on our observations a Lewis acid catalyzed process was suggested.

Lastly, the mechanism of formation for the disilamolybdacyclic complex $(^tBuN)Mo(SiH_2Ph)(H)\{(\mu\text{-}N_tBu)(SiHPh)\}(PMe_3)_2$ was followed by NMR spectroscopy at various temperatures. 5-intermediates were observed during and a proposed pathway was suggested. Also, the reactivity with organic substrates, in particular nitriles, showed insertion into the heterocyclic ring to give the expanded ring complexes $(^tBuN=)Mo(\eta^2\text{-}SiHPh\text{-}N^tBu\text{-}SiHPh\text{-}N=C(R))(PMe_3)_2$ (R = Me, Ph, 4-OMePh).

V. Experimental

General Methods and Instrumentation

All manipulations were carried out using conventional inert atmosphere glove-box and Schlenk techniques. Dry diethyl ether, toluene, hexanes, and acetonitrile were obtained, using Grubbs-type purification columns, other solvents were dried by distillation from appropriate drying agents. C_6D_6, PhMe-d_8 were dried by distillation from K/Na alloy, and $CDCl_3$ was dried by distillation from CaH_2. NMR spectra were obtained with a Bruker DPX-300 and Bruker DPX-600 instruments (^{l}H: 300 and 600 MHz; ^{2}H: 92.1 MHz; ^{13}C: 75.5 and 151 MHz; ^{29}Si: 59.6 and 119.2 MHz; ^{31}P: 121.5 and 243 MHz; ^{11}B: 96.3 and 192.6 MHz). NMR analysis was done at room temperature unless specified. IR spectra were measured on a Perkin-Elmer 1600 FT-lR spectrometer. Elemental analyses were performed in "ANALEST" laboratories (University of Toronto). Correct elemental analyses for $(ArN)_2Mo(\eta^2\text{-}CH_2{=}CH_2)(PMe_3)_2$ and new (RN)2Mo(PR')n were not obtained because these compounds are highly sensitive to air and for n = 3 easily loose the phosphine. $PhSiCl_3$, $(EtO)_3SiH$, $SiMe_4$, $SiCl_4$, Me_2SiHCl, MePhSiHCl, $PhMeSiCl_2$, PMe_3, PPh_3, PMe_2Ph, $BH_3(THF)$, BPh_3, CatBH, EtMgBr, (*m*-Tol)MgCl, $NaBH_4$, and $LiBH_4$ (solution in THF, 1M) were purchased from Aldrich. PEt_3 was generously donated by Cytec Canada Inc. Organic substrates (benzaldehyde, acetophenone, acetone, 1-hexene, cyc1ohexene, ethylene, styrene, benzonitrile, acetonitrile, ^{i}PrCN, ^{t}BuCN, l-octyne, phenyl acetylene, 3-hexyne, ethanol, and propanol) were purchased from Sigma-Aldrich and used without further purification. Amines ($PhNH_2$, $ArNH_2$, $Ar'NH_2$, $^{t}BuNH_2$, NEt_3, and 2,6-lutidine) were purchased from Sigma-Aldrich and distilled prior utilization. All catalytic, NMR scale reactions and kinetic experiments were done under nitrogen atmosphere using NMR tubes equipped with Teflon valves. The structures and yields of all hydrosilylated products were

determined by NMR analysis using residual solvent peak as an internal standard. In specified cases Cp_2Fe was also used as a standard.

Preparation of starting materials and reagents

Preparation of $(ArN)_2MoCl_2(DME)$ (III-1)

Na_2MoO_4 (5.0 g, 0.024 mol) was suspended in 200 mL of DME. NEt_3 (13.5 ml, 0.097 mol), Me_3SiCl (26.4 ml, 0.206 mol) and $ArNH_2$ (9.16 ml, 0.049 mol) were added sequentially to the suspension at room temperature, each over a period of about 5 min. The reaction mixture was heated at 65°C overnight. During the heating the colour of the mixture became dark-red. Then the reaction mixture was cooled to room temperature and filtered to remove ammonium salts. The salts were washed with Et_2O until the solvent ran through colorless. The volatile components were removed from the filtrate in vacuum to give a dark-red solid, which was washed three times with 20 ml of cold (-30°C) hexane. Yield: 14.56 g, 99 %. The NMR spectra and the physical properties of the compound are identical to those previously reported in the literature.[153]

Preparation of $(^tBuN)_2MoCl_2(DME)$ (III-36)

Me_3SiCl (44 ml, 0.34 mol) was added dropwise to a solution of $^tBuNH_2$ (20.4 mL, 0.19 mol) in 130 ml of DME. A white precipitate formed. To this slurry was added $NaMoO_4$ (5.004 g, 0.024 mol) all at once as a solid. The reaction mixture was heated at 65°C for 24 h. Then the solution was filtered and the solvent was removed in vacuum. The residue was extracted with hexanes (200 ml). Hexanes were removed in vacuum to give a yellow solid, which was dried in vacuum. Yield: 9.38 g, 97 %. The NMR spectra and the physical properties of the compound are identical to those previously reported in the literature.[153]

Preparation of $(ArN)(^tBuN)MoCl_2(DME)$ (III-34)

A. Na_2MoO_4 (2.046 g, 9.93 mmol) was placed in a flask fitted with a screw cap for heating along with DME (100 mL). The flask was evacuated under vacuum and filled with N_2 gas. To this mixture solutions of NEt_3 (39.7 mL, 39.7 mmol) and Me_3SiCl (13.86 mL, 109.2 mmol) in 20 mL of DME were sequentially added. After 10 minutes, solutions of $ArNH_2$ (mL, mol) and $^tBuNH_2$ (mL, mol) were added quickly, one after the other. This was heated to 70 °C and heated overnight (12 h). The mixture turned red in colour and product was extracted using Et_2O (100 mL) until the colour of red filtrate ran clear. Solvent volume was reduced to 20 mL in vacuum and placed in the -30 °C overnight where red square crystals of the desired product were grown. After three sequential crystallizations and washing with cold hexanes, pure (ArN)(^{t}BuN)$MoCl_2$(DME) is obtained Yield: 2.40 g, 48 %.

B. (^{t}BuN)$_2MoCl_2$(DME) (1.2900 g, 3.23 mmol) was placed in a capped flask along with DME (50 mL) and $ArNH_2$ (0.61 mL, 3.23 mmol). The mixture was then heated for one hour at 70 °C, where a colour change was seen from yellow to red. All volatiles were removed in vacuum to give a chunky red solid. Recrystallization from Et_2O at -30 °C followed by washing in cold hexanes gives a red solid product characterized as (ArN)(^{t}BuN)$MoCl_2$(DME). Yield: 0.700 g, 40 %.

^{1}H-NMR (300 MHz; benzene-d_6; δ, ppm): 7.13 (d, 2H, $^3J_{H\text{-}H}$ = 6.8 Hz, *m*-Ph), 6.95 (t, 1H, $^3J_{H\text{-}H}$ = 7.8 Hz, *p*-Ph), 4.32 (sept., 2H, $^3J_{H\text{-}H}$ = 7.8 Hz, C*H*Me$_2$), 3.41 (s, 6H, *Me*OCH$_2$CH$_2$O*Me*), 3.18 (s, 4H, MeOC*H*$_2$C*H*$_2$OMe), 1.42 (d, 12H, $^3J_{H\text{-}H}$ = 6.8 Hz, CH*Me*$_2$), 1.30 (s, 9H, ^{t}Bu). **^{13}C{^{1}H}-NMR (**75.4 MHz, benzene-d_6; δ, ppm): 154.4 (s, *i*-Ph), 143.1 (s, *o*-Ph), 125.9 (s, *p*-Ph), 123.3 (s, *m*-Ph), 75.4 (s, *C*Me$_3$), 70.6 (s, MeO*C*H$_2$*C*H$_2$OMe), 62.4 (s, *Me*OCH$_2$CH$_2$O*Me*), 29.4 (s, C*Me*$_3$), 28.1 (s, *C*HMe$_2$), 24.8 (s, CH*Me*$_2$).

Preparation of (ArN)$_2$Mo(PMe$_3$)$_3$ (III-37)

A solution of $(ArN)_2MoCl_2(DME)$ (2.95 g, 4.86 mmol) in 50 ml of THF was added at room temperature to a suspension of Mg (1.77g, 72.8 mmol) and PMe_3 (4.0 ml, 38.8 mmol) in 50 ml of THF. After 30 min of stirring the colour of the reaction mixture turned dark-green. The mixture was stirred overnight at room temperature. Then the solvent was removed in vacuum and the residue was extracted with hexane until the filtrate was colourless. All volatiles were pumped off to leave a dark-green solid, which was dried in vacuum. Yield: 3.16 g, 97 %.

^{1}H-NMR (300 MHz; benzene-d_6; δ, ppm): 1.05 (bs, 27H, PMe_3); 1.32 (d, 24H, $^3J_{H-H}$ = 6.9 Hz, 8 C*H*$_3$, ArN); 3.77 (sept, 4H, $^3J_{H-H}$ = 6.9 Hz, 4 C*H*, ArN); 6.91 (t, 2H, $^3J_{H-H}$ = 7.5 Hz, ArN); 7.16 (d, 4H, $^3J_{H-H}$ = 7.5 Hz, ArN). **^{31}P-NMR** (121.5 MHz; benzene-d_6; δ, ppm): -12.7 (bs, 2P, 2 PMe_3); 23.2 (bs, 1 P, PMe_3). **^{1}H-NMR** (300 MHz, Toluene-d_8, -40 °C; δ, ppm): 7.18 (d, 2H, $^3J_{H-H}$ = 7.5 Hz, *m*-H, ArN); 7.09 (d, 2H, $^3J_{H-H}$ = 7.5 Hz, *m*-H, ArN); 6.90 (t, 2H, $^3J_{H-H}$ = 7.5 Hz, *p*-H, ArN); 3.81 (sept, 2H, $^3J_{H-H}$ = 6.9 Hz, 2 C*H*, ArN); 3.66 (sept, 2H, $^3J_{H-H}$ = 6.9 Hz, 2 C*H*Me_2, ArN); 1.42 (d, 12H, $^3J_{H-H}$ = 6.9 Hz, 4 C*H*$_3$, ArN); 1.29 (d, 12H, $^3J_{H-H}$ = 6.9 Hz, 4 C*H*$_3$, ArN); 1.21 (d, 9H, $^2J_{H-P}$ = 7.5 Hz, P*Me*$_3$), 0.89 (vt, 18H, $^2J_{H-P}$ = 2.3 Hz, 2 P*Me*$_3$). **^{13}C{^{1}H}-NMR** (75.4 MHz, Toluene-d_8,- 40 °C; δ, ppm): 128.9; 127.9; 31.7 (CH); 31.2 (CH); 31.4 (CH_3, ArN); 29.6 (CH_3, ArN); 28.8 (PMe_3); 23.3 (PMe_3). **^{31}P{^{1}H}-NMR** (121.4 MHz, Toluene-d_8, - 20 °C; δ, ppm): -29.9 (s, 1P, PMe_3); -5.0 (s, 2P, 2 PMe_3).

Preparation of (^{t}BuN)$_2$Mo(PMe$_3$)(η^2-C$_2$H$_4$) (III-50)

A solution of EtMgBr in Et_2O (7.79 mL, 23.4 mmol, C = 3.0 M) was added at -90 °C mixture of (^{t}BuN)$_2$MoCl$_2$(DME) (4.667 g, 11.7 mmol) and PMe_3 (1.21 mL, 11.7 mmol) in 50 mL of Et_2O. Immediately after addition the colour of the reaction mixture turned to yellow-green and the formation of yellow gummy precipitate was observed. The mixture was stirred at room temperature for additional 3 hours at room temperature. All volatiles were pumped off and the

residue was extracted with hexanes (50 mL). The solvent was removed in vacuum to leave a brown solid, which was recrystallized from concentrated hexane solution at - 30°C to give yellow crystals. Yield: 2.7433 g, 69 %. The NMR spectra and physical properties of the compound are identical to those previously reported in literature.[150]

Preparation of $(ArN)_2Mo(\eta^2\text{-}C_2H_4)(PMe_3)_2$ (II-169)

A solution of EtMgBr in Et_2O (2.2 mL, 6.58 mmol, C = 3.0 M) was added at -78°C to a solution of $(ArN)_2MoCl_2(DME)$ (2.0 g, 3.29 mmol) and PMe_3 (0.69 mL, 6.58 mmol) in 100 ml of Et_2O. The reaction mixture was allowed to warm up to room temperature and then was stirred for 3 h. During this time the colour of the mixture changed from red to purple. All volatiles were pumped off; the residue was dried and extracted with hexanes (150 mL). The solvent was removed in vacuum to leave a purple solid. Yield: 1.45 g, 70 %.

^{1}H-NMR (300 MHz, Benzene-d_6, 22 °C, δ, ppm): 0.97 (bs, 18H, 2 P*Me*$_3$), 1.24 (d, $^3J_{H\text{-}H}$ = 6.9 Hz, 24H, 8 C*H*$_3$, 2 NAr), 1.84 (bs, 4H, η^2-C_2H_4), 3.52 (bs, 4H, 4 C*H*, 2 NAr), 6.86 (t, $^3J_{H\text{-}H}$ = 7.5 Hz, 2H, *p*-Ph, 2 NAr), 7.04 (d, $^3J_{H\text{-}H}$ = 7.5 Hz, 4H, *m*-H, 2 NAr). **^{31}P{^{1}H}-NMR** (121.5 MHz; Benzene-d_6, 22 °C, δ, ppm): -6.9 (bs, 2 *P*Me$_3$). **^{13}C{^{1}H}-NMR** (75.5 MHz; Benzene-d_6, 22 °C, δ, ppm): 15.3 (bs, 2 PMe_3), 24.5 (s, 8 C*H*$_3$, ArN), 27.5 (s, 4 CH, ArN), 120.4, 122.7, 138.4, 154.1 (aromatic carbons of 2 ArN).

Preparation of $(ArN)MoCl_2(PMe_3)_3$ (II-171)

To a solution of $(ArN)_2Mo(PMe_3)_3$ (1.64 g, 2.43 mmol) in Et_2O, PMe_3 (0.25 mL, 2.45 mmol) and $HSiCl_3$ (0.74 mI, 7.29 mmol) were added at room temperature. The reaction mixture was stirred overnight at room temperature. Then the mixture was concentrated and filtered. The residue was washed with hexanes and dried in vacuum to give greenish blue solid of $(ArN)MoCl_2(PMe_3)_3$. Yield: 1.08 g, 78 %. The combined fractions of mother liquor were

evaporated slowly in vacuum at -30°C to leave a yellow-brown oil, which according to NMR analysis mostly contained of $(ArN\text{-}SiClH)_2$.

^{1}H-NMR (300 MHz, Benzene-d_6, 22 °C, δ, ppm): 7.01 (t, $^3J_{H\text{-}H}$ = 7.7 Hz, 1H, *p*-H, ArN), 6.87 (d, $^3J_{H\text{-}H}$ = 7.7 Hz, 2H, *m*-H, ArN), 4.12 (sept, $^3J_{H\text{-}H}$ = 6.8 Hz, 2H, 2 C*H*, ArN), 1.40 (vt, $^2J_{H\text{-}P}$ = 2.4 Hz, l8H, 2 P*Me*$_3$), 1.27 (d, $^2J_{H\text{-}P}$ = 8.4 Hz, 9H, PMe_3), 1.17 (d, $^3J_{H\text{-}H}$ = 6.6 Hz, 12H, 4 C*H*$_3$, ArN). **^{31}P{^{1}H}-NMR** (121.5 MHz; Benzene-d_6, 22 °C, δ, ppm): 3.6 (t, $^2J_{P\text{-}P}$ = 16.7 Hz, 1 *P*Me_3), -7.8 (d, $^2J_{P\text{-}P}$ = 16.7 Hz, 1 *P*Me_3). **^{13}C{^{1}H}-NMR** (75.5 MHz; Benzene-d_6, 22 °C, δ, ppm): 146.8, 126.7 (p-C, ArN), 123.9 (*m*-C, ArN), 27.1 (s, *C*H, ArN), 25.4 (s, *C*H_3, ArN), 23.1 (d, $^1J_{C\text{-}P}$ = 23.0 Hz, P*Me*$_3$), 17.1 (vt, $^1J_{C\text{-}P}$ = 11.5 Hz, P*Me*$_3$).

Preparation of (^{t}BuN)$MoCl_2(PMe_3)_3$ (II-172/III-14)

(^{t}BuN)$_2$Mo(PMe_3)(η^2-C_2H_4) (2.7576 g, 8.058 mmol) was dissolved in 50 mL of Et_2O in a Schlenk flask. Two equivalents of PMe_3 (1.67 mL, 16.12 mmol) followed by $HSiCl_3$ (1.30 mL, 12.88 mmol). Instantaneous reaction occurs, resulting in the formation of a brown precipitate and a large amount of a white aerosol. The flask was vented several times before allowed to stir overnight. After one night the mixture was filtered off to leave a solid purple pwder. The residue was washed with 10 mL of Et_2O and dried to give 2.0950 g of the (^{t}BuN)$MoCl_2(PMe_3)_3$ complex. Crystallization from the mother liquor kept in the -30 °C freezer overnight, gives another 0.5550 g of the complex. Yield: 2.650 g, 71 %.

^{1}H-NMR (300 MHz, Benzene-d_6, 22 °C, δ, ppm): 1.43 (vt, $^2J_{H\text{-}P}$ = 3.6 Hz, 18H, *trans*-PMe_3), 1.25 (d, $^2J_{H\text{-}P}$ = 7.6 Hz, 9H, *cis*-PMe_3), 1.01 (s, 9H, ^{t}BuN). **^{31}P{^{1}H}-NMR** (121.5 MHz; Benzene-d_6, 22 °C, δ, ppm): 7.3 (bs, 1P, *cis*-PMe_3), -5.9 (bs, *trans*-PMe_3).

Preparation of (ArN)Mo(H)(Cl)$(PMe_3)_3$ (III-12)

A solution of L-Selectride in THF (1.9 ml, 1.9 mmol, 1.0 M) was added at -30°C to a solution of $(ArN)MoCl_2(PMe_3)_3$ (1.05 g, 1.9 mmol) in 50 mL of toluene. The mixture was stirred at -30°C for 15 min., then allowed to reach ambient temperature and stirred for additional two hours. Once the reaction reached room temperature the colour of the mixture changed from pale green to brown and formation of precipitate was observed. The mixture was filtered and the residue was extracted with 50 mL of toluene. All volatiles were removed in vacuum to give a fine brown solid of $(ArN)Mo(H)(Cl)(PMe_3)_3$. Yield: 0.55 g, 65 %.

^{1}H-NMR (300 MHz, Benzene-d_6, 22 °C, δ, ppm): 1.19 (d, $^3J_{H-H}$ = 6.6 Hz, 4 CH_3, NAr), 1.35 (d, $^2J_{H-P}$ = 5.7 Hz, 9H, PMe_3), 1.45 (vt, $^2J_{H-P}$ = 3.4 Hz, 18H, 2 PMe_3), 4.37 (sept, $^3J_{H-H}$ = 6.9 Hz, 2H, 2 C*H*, NAr), 5.31 (dt, $^2J_{H-P}$ = 28.5 Hz, $^2J_{H-P}$ = 51.9 Hz, l H, Mo-H), 6.86 (m, 3H, NAr). **^{31}P{^{1}H}-NMR** (121.5 MHz; Benzene-d_6, 22 °C, δ, ppm): -17.75 (t, $^2J_{P-P}$ = 13.4 Hz, 1 P, *P*Me_3), -1.10 (d, $^2J_{P-P}$ = 13.4 Hz, 2P, 2 *P*Me_3). **^{13}C{^{1}H}-NMR** (75.5 MHz; Benzene-d_6, 22 °C, δ, ppm): 21.1 (vt, $^1J_{C-P}$ = 11.3 Hz, P*Me*$_3$), 21.2 (d, $^1J_{C-P}$ = 15.9 Hz, P*Me*$_3$), 24.2 (s, *C*H_3, NAr), 26.6 (s, *C*H, NAr), 123.2, 124.9, 144.3 (all singlets, N*Ar* aromatic carbons).

Preparation of Mo(VI) Silylamido Complexes

Preparation of $(ArN)_2Mo(N(^tBu)SiHMe_2)Cl$ (III-3)

$(ArN)_2MoCl_2(DME)$ (0.8769 g, 1.56 mmol) was added to a flask and dissolved in 50 mL of toluene. This solution was added to $Li(N(^tBu)SiHMe_2$ (0.3168g, 1.51 mmol) in 10 mL of toluene, to produce a dark red mixture with formation of a white precipitate. After stirring for one day at room temperature the mixture was filtered and product extracted with 10 mL of toluene. The solution was placed in the -80°C freezer for six days where large dark red crystals were seen. These were washed with cold (-30°C) hexane and dried in vacuum. Yield: 0.8142g, 88%.

^{1}H-NMR (300 MHz, Benzene-d_6, 22 °C, δ, ppm): 6.97 (m, 6 H, *m*-Ph, *p*-Ph), 5.65 (sept, $^{3}J_{H\text{-}H}$ = 3.3 Hz, 1 H, Si*H*Me$_2$), 3.92 (sept, $^{3}J_{H\text{-}H}$ = 6.9 Hz, 4 H, C*H*Me$_2$, Ar), 1.41 (s, 9 H, ^{t}Bu), 1.20 (d, $^{3}J_{H\text{-}H}$ = 6.9 Hz, 12 H, CH*Me*$_2$, Ar), 1.13 (d, $^{3}J_{H\text{-}H}$ = 6.9 Hz, 12 H, CH*Me*$_2$, Ar), 0.36 (d, $^{3}J_{H\text{-}H}$ = 3.3 Hz, 6 H, SiH*Me*$_2$). **^{13}C{^{1}H}-NMR** (75.5 MHz; Benzene-d_6, 22 °C, δ, ppm): 153.9 (*i*-Ph), 143.2 (*o*-Ph), 127.0 (*m*-Ph), 123.0 (*p*-Ph), 62.1 (N*C*(CH$_3$)$_3$), 34.2 (NC(*C*H$_3$)$_3$), 28.2 ([Ar-*C*HMe$_2$]$_2$), 24.4 (Ar-CH*Me*$_2$), 23.6 (Ar-CH*Me*$_2$), 0.6 (Si(*C*H$_3$)$_2$). **^{29}Si INEPT+** (119 MHz, Benzene-d_6, 22 °C, *J* = 180 Hz, δ, ppm): -25.18 (d-quin, $^{1}J_{Si\text{-}H}$ = 172.9 Hz).

Preparation of (ArN)$_2$Mo(η^3-N^{t}Bu-SiMe$_2$-H)(H) (III-6)

(ArN)$_2$Mo(N(^{t}Bu)SiHMe$_2$)Cl (21.8 mg, 0.0400 mmol) was dissolved in C_6D_6 and transferred to an NMR tube. L-Selectride (36.0 μL, 0.04 mmol, 1.6 M) in THF was added directly to the NMR tube via a 50 μL syringe. This solution was thoroughly mixed and after 15 minutes at room temperature, selective formation of the β-agostic silylamido complex (ArN)$_2$Mo(η^3- N^{t}Bu-SiMe$_2$-H)(H).

^{1}H-NMR (300 MHz, Benzene-d_6, 22 °C, δ, ppm): 7.02 (m, 6 H, *m*-Ph, *o*-Ph, *p*-Ph), 6.49 (d, $^{3}J_{H\text{-}H}$ = 3.0 Hz, 1 H, Mo-H), 4.13 (sept, $^{3}J_{H\text{-}H}$ = 3.0 Hz, 1 H, Si*H*Me$_2$), 4.06 (sept, $^{3}J_{H\text{-}H}$ = 6.9 Hz, 4 H, C*H*Me$_2$, Ar), 1.35 (s, 9 H, ^{t}Bu), 1.21 (d, $^{3}J_{H\text{-}H}$ = 7.2 Hz, 12 H, CH*Me*$_2$, Ar), 1.18 (d, $^{3}J_{H\text{-}H}$ = 6.6 Hz, 12 H, CH*Me*$_2$, Ar), 0.12 (d, $^{3}J_{H\text{-}H}$ = 3.0 Hz, 6H, SiH*Me*$_2$). **^{13}C{^{1}H}-NMR** (75.5 MHz; Benzene-d_6, 22 °C, δ, ppm): 153.1 (*i*-Ph), 141.9 (*o*-Ph), 125.5 (*m*-Ph), 122.5 (*p*-Ph), 59.0 (N*C*(CH$_3$)$_3$), 35.1 (NC(*C*H$_3$)$_3$), 27.9 ([Ar-*C*HMe$_2$]$_2$), 23.7 (Ar-CH*Me*$_2$), 23.1 (Ar-CH*Me*$_2$), 0.9 (Si(*C*H$_3$)$_2$). **^{29}Si INEPT+** (119 MHz, Benzene-d_6, 22 °C, *J* = 125 Hz, δ, ppm): -52.9 (d, $^{1}J_{Si\text{-}H}$ = 125.3 Hz).

Preparation of (ArN)$_2$Mo(N(^{t}Bu)SiMe$_2$H)(OBn) (III-8)

To a freshly prepared sample of $(ArN)_2Mo(\eta^3\text{-}N(^tBu)Si(Me_2)\text{-}H)(H)$ (0.764 mmol) in toluene (10 mL) using the procedure described above, benzaldehyde (77.9 μL, 0.400 mmol) was directly added *via* 100 μL syringe. The dark brown solution turned a light red colour and was removed of all volatiles in vacuum to give a red oil. A small amount of hexanes were added and the solution place in the -80 °C freezer overnight. A light orange solid was observed after one night in the -80 °C freezer, so the solution was decanted and washed with cold hexane (2 mL) to give 160.0 mg of pure $(ArN)_2Mo(N(^tBu)SiMe_2H)(OBn)$. Yield: 31 %.

^{1}H-NMR (300 MHz, Benzene-d_6, 22 °C, δ, ppm): 0.37 (d, 6H, Si*Me*$_2$, $^3J_{H\text{-}H}$ = 3.4 Hz), 1.09 (d, 12 H, C*H*$_3$, *Ar*N, $^3J_{H\text{-}H}$ = 6.8 Hz), 1.16 (d, 12 H, C*H*$_3$, *Ar*N, $^3J_{H\text{-}H}$ = 6.8 Hz), 1.44 (s, 9H, ^{t}*Bu*N), 3.88 (sept, 4H, C*H*, *Ar*N, $^3J_{H\text{-}H}$ = 6.8 Hz), 5.55 (sept, 1H, Si*H*, $^3J_{H\text{-}H}$ = 3.3 Hz), 5.74 (s, 2H, C*H*$_2$, OBn), 6.92 (m, 2H, *p*-Ph, *Ar*N), 6.99 (m, 4H, *m*-Ph, *Ar*N). **^{13}C{^{1}H}-NMR** (75.5 MHz; Benzene-d_6, 22 °C, δ, ppm): 1.85 (s, *C*H$_3$, Si*Me*$_2$), 23.47 (s, *C*H$_3$, *Ar*N), 24.33 (s, *C*H$_3$, *Ar*N), 28.09 (s, *C*H, *Ar*N), 34.51 (s, *C*H$_3$, ^{t}*Bu*N), 79.59 (s, *C*H$_2$, OBn), 122.83 (s, *p*-Ph, *Ar*N), 125.85 (s, *m*-Ph, *Ar*N). **^{29}Si INEPT+** (119 MHz, Benzene-d_6, 22 °C, J = 125 Hz, δ, ppm): -21.92 (dsept, H*Si*Me$_2$, $^1J_{Si\text{-}H}$ = 176.4 Hz, $^2J_{Si\text{-}H}$ = 6.9 Hz).

General Procedure for Hydrosilylation using $(ArN)_2Mo(N(^tBu)SiMe_2H)(OBn)$ (III-8) or $(ArN)_2Mo(\eta^3\text{-}N^tBu\text{-}SiMe_2\text{-}H)(H)$ (III-6)

To an NMR tube loaded with either $(ArN)_2Mo(N(^tBu)SiMe_2H)(OBn)$ (5 mol %) or $(ArN)_2Mo(\eta^3\text{-}N(^tBu)Si(Me_2)\text{-}H)(H)$ (5 mol %) in 0.6 mL of C_6D_6, silane and carbonyl were added in a 1:1 ratio sequentially using the appropriate μL syringe. The reactions were monitored by ^{1}H-NMR spectroscopy at room temperature over the appropriate length of time. All structures were determined using 2D-NMR techniques or compared to known spectra.

Reactions of (ArN)Mo(PMe$_3$)$_2$(η^2-CH$_2$PMe$_2$)H with E-H Bonds

Preparation of (ArN)Mo(PMe$_3$)$_2$(η^2-CH$_2$PMe$_2$)H (III-13)

(ArN)Mo(PMe$_3$)$_3$HCl (0.5306 g, 0.990 mmol) and Li[N(^{t}Bu)SiHMe$_2$](THF) (0.2101, 1.01 mmol) were placed in a Schlenk flask and dissolved in toluene (20 mL). The solution was allowed to stir overnight at which time a white precipitate formed. The solution was filtered and all volatiles removed in vacuum to give an oily brown solid. This was recrystallized from hexanes to give 0.3477 g of (ArN)Mo(PMe$_3$)$_2$(η^2-CH$_2$PMe$_2$)H as a 10:1 mixture of isomers. Yield: 72 %.

^{1}H-NMR (300 MHz, Benzene-d_6, 22 °C, δ, ppm): - 1.62 (dtd, 1 H, C*H*$_2$, η^2-C*H*$_2$PMe$_2$, $^2J_{H\text{-}P}$ = 20.3 Hz, $^3J_{H\text{-}H}$ = 7.4 Hz, $^2J_{H\text{-}Hgem}$ = 7.4 Hz, $^3J_{H\text{-}P}$ = 3.1 Hz, minor isomer), - 0.99 (tdd, 2 H, C*H*$_2$, η^2-C*H*$_2$PMe$_2$, $^3J_{H\text{-}P}$ = 12.2 Hz, $^2J_{H\text{-}P}$ = 3.7 Hz, $^3J_{H\text{-}H}$ = 0.9 Hz, major isomer), -0.71 (m, 1 H, C*H*$_2$, η^2-C*H*$_2$PMe$_2$, $^3J_{H\text{-}H}$ = 7.4 Hz, minor isomer), 1.07 (d, 9 H, C*H*$_3$, P*Me*$_3$, $^2J_{H\text{-}P}$ = 6.4 Hz, minor isomer), 1.26 (vt, 18 H, C*H*$_3$, 2 P*Me*$_3$, $^2J_{H\text{-}P}$ = 6.7 Hz, major isomer), 1.32 (d, 12 H, C*H*$_3$, *Ar*N, $^3J_{H\text{-}H}$ = 7.0 Hz, major isomer), 1.43 (d, 9 H, C*H*$_3$, P*Me*$_3$, $^2J_{H\text{-}P}$ = 6.9 Hz, minor isomer), 1.46 (d, 6 H, C*H*$_3$, P*Me*$_2$, η^2-CH$_2$P*Me*$_2$, $^2J_{H\text{-}P}$ = 8.9 Hz, major isomer), 1.48 (d, 3 H, C*H*$_3$, η^2-CH$_2$P*Me*$_2$, $^2J_{H\text{-}P}$ = 10.5 Hz, minor isomer), 1.97 (d, 3 H, C*H*$_3$, η^2-CH$_2$P*Me*$_2$, $^2J_{H\text{-}P}$ = 10.6 Hz, minor isomer), 3.25 (m, 1 H, Mo*H*, $^3J_{H\text{-}H}$ = 7.1 Hz, minor isomer), 4.08 (t, 1 H, Mo*H*, $^3J_{H\text{-}H}$ = 38.2 Hz, major isomer), 4.51 (sept, 2 H, C*H*, *Ar*N, $^3J_{H\text{-}H}$ = 6.9 Hz, minor isomer), 4.70 (sept, C*H*, *Ar*N, $^3J_{H\text{-}H}$ = 6.9 Hz, major isomer), 7.06 (bs, mixture of *m*-Ph & *p*-Ph of *Ar*N for both major and minor isomers). **^{1}H{^{31}P}-NMR** (300 MHz, Benzene-d_6, 22 °C, δ, ppm, selected signals): - 1.62 (t, 1 H, C*H*$_2$, η^2-C*H*$_2$PMe$_2$, $^3J_{H\text{-}H}$ = 7.4 Hz, minor isomer), - 0.99 (d, 2 H, C*H*$_2$, η^2-C*H*$_2$PMe$_2$, $^3J_{H\text{-}H}$ = 0.9 Hz, major isomer), -0.71 (t, 1 H, C*H*$_2$, η^2-C*H*$_2$PMe$_2$, $^3J_{H\text{-}H}$ = 7.4 Hz, minor isomer), 3.25 (t, 1 H, Mo*H*, $^3J_{H\text{-}H}$ = 7.1 Hz, minor isomer), 4.08 (bs, 1 H, Mo*H*, major isomer), **^{31}P{^{1}H}-NMR** (121.5 MHz, Benzene-d_6, 22 °C, δ, ppm): 7.79 (dd, 1 P, *P*Me$_3$, $^2J_{P\text{-}P}$ = 19.31 Hz, $^2J_{P\text{-}P}$ = 22.5 Hz, minor

isomer), 5.36 (d, 1 P, *PMe*$_3$, $^2J_{P\text{-}P}$ = 18.7 Hz, major isomer), - 2.92 (dd, 1 P, *P*Me$_3$, $^2J_{P\text{-}P}$ = 16.5 Hz, $^2J_{P\text{-}P}$ = 18.5 Hz, minor isomer), - 16.69 (dd, 1 P, η^2-CH$_2$*P*Me$_2$, $^2J_{P\text{-}P}$ = 16.7 Hz, $^2J_{P\text{-}P}$ = 18.5 Hz, minor isomer), - 37.20 (t, 2 P, P*Me*$_3$, η^2-CH$_2$*P*Me$_2$, $^2J_{P\text{-}P}$ = 19.0 Hz, major isomer). **^{13}C{^{1}H}-NMR** (75.5 MHz; Benzene-d_6, 22 °C, δ, ppm): - 5.14 (dt, η^2-*C*H$_2$PMe$_2$, $^2J_{C\text{-}P}$ = 26.3 Hz, $^2J_{C\text{-}P}$ = 7.7 Hz, major isomer), 17.66 (m, *C*H$_3$, η^2-CH$_2$P*Me*$_2$, minor isomer), 20.16 (d, *C*H$_3$, η^2-CH$_2$P*Me*$_2$, major isomer), 21.85 (t, *C*H$_3$, P*Me*$_3$, $^1J_{C\text{-}P}$ = 11.9 Hz, major isomer overlapped with minor P*Me*$_3$), 23.66 (d, *C*H$_3$, P*Me*$_3$, $^1J_{C\text{-}P}$ = 11.8 Hz, minor isomer), 23.74 (s, *C*H$_3$, *Ar*N), 25.62 (m, *C*H$_3$, η^2-CH$_2$P*Me*$_2$, minor isomer), 26.60 (s, *C*H, *Ar*N, major isomer), 26.75 (*C*H, *Ar*N, minor isomer), 122.30 (s, *p*-Ph, *Ar*N, minor isomer), 122.62 (s, *p*-Ph, *Ar*N, major isomer), 123.60 (s, *m*-Ph, *Ar*N, major isomer), 143.44 (s, *o*-Ph, *Ar*N, minor isomer), 143.76 (s, *o*-Ph, *Ar*N, major isomer), 152.11 (s, *i*-Ph, *Ar*N, major isomer).

NMR Reaction of (ArN)Mo(PMe$_3$)$_2$(η^2-CH$_2$PMe$_2$)H (III-13) with ^{i}PrOH

Isopropanol (2.2 mg, 0.0232 mmol) was directly added to a Et$_2$O solution of (ArN)Mo(PMe$_3$)$_2$(η^2-CH$_2$PMe$_2$)H (0.0116 g, 0.0232 mmol). Immediately, a colour change was seen from dark brown to dark green. NMR analysis showed generation of a fluxional compound characterized as (ArN)Mo(PMe$_3$)$_3$(O^{i}Pr)H (**III-25**) as the major product when the temperature is reduced to 7 °C.

^{1}H-NMR (600 MHz; Benzene-d_6; 7 °C, δ, ppm): 1.11 (d, 6H, (C*H*$_3$)$_2$CH, O^{i}Pr, $^3J_{H\text{-}H}$ = 5.9 Hz), 1.15 (d, 6H, (C*H*$_3$)$_2$CH, Ar, $^3J_{H\text{-}H}$ = 7.0 Hz), 1.25 (d, 9H, PMe$_3$, $^2J_{P\text{-}H}$ = 4.9 Hz), 1.34 (vt, 18 H, 2 PMe$_3$, $^2J_{P\text{-}H}$ = 4.1 Hz). 1.36 (d, 6H, (C*H*$_3$)$_2$CH, Ar, $^3J_{H\text{-}H}$ = 7.0 Hz), 3.76 (sept., 1H, (CH$_3$)$_2$C*H*, Ar, $^3J_{H\text{-}H}$ = 6.9 Hz), 3.93 (sept., 1H, (CH$_3$)$_2$C*H*, O^{i}Pr, $^3J_{H\text{-}H}$ = 5.9 Hz), 4.22 (dt, 1H, Mo-*H*, $^2J_{P(trans)\text{-}H}$ = 77.1 Hz, $^2J_{P(cis)\text{-}H}$ = 24.9 Hz), 5.28 (sept., 1H, (CH$_3$)$_2$C*H*, Ar, $^3J_{H\text{-}H}$ = 6.6 Hz), 6.88 (d, 1H, *m*-Ph, Ar, $^3J_{H\text{-}H}$ = 7.6 Hz), 6.94 (t, 1H, *p*-Ph, Ar, $^3J_{H\text{-}H}$ = 7.5 Hz), 7.00 (d, 1H, *m*-Ph, Ar, $^3J_{H\text{-}H}$

= 7.6 Hz). **^{1}H{^{31}P}-NMR** (600 MHz, Benzene-d_6; 7 °C, δ, ppm, selected signals): 1.25 (s, 9H, PMe_3), 1.34 (s, 18 H, 2 PMe_3), 4.22 (s, 1H, Mo-*H*). **^{31}P{^{1}H}-NMR** (243 MHz, Benzene-d_6; 7 °C, δ, ppm): -3.83 (d, 2 PMe_3, $^{2}J_{P\text{-}P}$ = 10.2 Hz), -18.05 (t, PMe_3, $^{2}J_{P\text{-}P}$ = 10.0 Hz). **^{13}C{^{1}H}-NMR** (151 MHz, Benzene-d_6; 7 °C, δ, ppm): 20.30 (d, P(*C*H_3)$_3$, $^{1}J_{C\text{-}P}$ = 11.6 Hz), 20.91 (t, 2 P(*C*H_3)$_3$, $^{1}J_{C\text{-}P}$ = 9.1 Hz), 24.46 (s, (*C*H_3)$_2$CH, Ar), 24.58 (s, (*C*H_3)$_2$CH, Ar), 25.22 (s, (CH_3)$_2$*C*H, Ar), 26.34 (s, (CH_3)$_2$*C*H, Ar), 28.16 (s, (*C*H_3)$_2$CH, O^{i}Pr), 70.88 (d, (CH_3)$_2$*C*H, O^{i}Pr, $^{3}J_{C\text{-}P}$ = 6.6 Hz), 122.10 (s, *m*-Ph, Ar), 122.27 (s, *p*-Ph, Ar), 123.36 (s, *m*-Ph, Ar), 140.86 (s, *o*-Ph, Ar), 146.34 (s, *o*-Ph, Ar), 150.34 (s, *i*-Ph, Ar).

NMR reaction of (ArN)Mo(PMe_3)$_2$(η^2-CH_2PMe_2)H (III-13) with phenol

Phenol (2.2 mg, 0.0232 mmol) was directly added to a C_6D_6 solution of (ArN)Mo(PMe_3)$_2$(η^2-CH_2PMe_2)H (0.0116 g, 0.0232 mmol). Immediately, a colour change was seen from dark brown to dark green. NMR analysis showed generation of a fluxional compound characterized as (ArN)Mo(PMe_3)$_3$(OPh)H (**III-27**) as the major product.

^{1}H-NMR (600 MHz; Toluene-d_8; -50 °C, δ, ppm): 1.18 (d, 6H, (C*H*$_3$)$_2$CH, Ar, $^{3}J_{H\text{-}H}$ = 6.5 Hz), 1.26 (bs, 18 H, 2 P*Me*$_3$), 1.30 (d, 9H, P*Me*$_3$, $^{2}J_{H\text{-}P}$ = 5.2 Hz), 1.46 (d, 6H, (C*H*$_3$)$_2$CH, Ar, $^{3}J_{H\text{-}H}$ = 5.1 Hz), 3.85 (sept., 1H, (CH_3)$_2$C*H*, Ar, $^{3}J_{H\text{-}H}$ = 6.5 Hz), 5.21 (dt, 1H, Mo-*H*, $^{2}J_{H\text{-}P}$ = 26.2 Hz, $^{2}J_{H\text{-}P}$ = 66.1 Hz), 5.26 (bs, 1H, (CH_3)$_2$C*H*, Ar), 6.80 (m, 2H, *p*-Ph/Ar, *p*-Ph/OPh), 6.95 (m, *m*-Ph, Ar), 7.24 (m, *m*-Ph, OPh), 7.31 (bt, *o*-Ph, OPh, $^{3}J_{H\text{-}H}$ = 7.2 Hz). **^{31}P{^{1}H}-NMR** (243 MHz, Toluene-d_8; -50 °C, δ, ppm): 2.01 (bs, 2P, 2 *P*Me_3), -13.44 (bs, 1 P, *P*Me_3). **^{1}H{^{31}P}-NMR** (600 MHz, Toluene-d_8; -50 °C, δ, ppm, selected signals): 1.30 (s, 9H, P*Me*$_3$), 5.20 (s, 1H, Mo-*H*). **^{13}C{^{1}H}-NMR** (151 MHz, Toluene-d_8; -50 °C, δ, ppm): 20.09 (P(*C*H_3)$_3$, found by ^{1}H-^{13}C HSQC, overlapped with solvent peak), 24.38 (s, 2 (*C*H_3)$_2$CH, Ar), 25.73 (s, (CH_3)$_2$*C*H, Ar), 26.47 (s, (CH_3)$_2$*C*H, Ar), 115.1 (s, *p*-Ph, OPh), 119.7 (s, *m*-Ph, OPh), 122.4 (s, *p*-Ph, Ar), 123.5 (s, *m*-Ph,

Ar), 123.8 (s, *m*-Ph, Ar), 129.1 (s, *o*-Ph, OPh, found by ^{1}H-^{13}C HSQC, overlapped by solvent peaks), 141.3 (s, *m*-Ph, Ar), 145.7 (s, *m*-Ph, Ar), 149.5 (s, *i*-Ph, Ar), 166.5 (d, *i*-Ph, OPh, $^{3}J_{C\text{-}P}$ = 3.9 Hz).

NMR reaction of (ArN)Mo(PMe$_3$)$_2$(η^2-CH$_2$PMe$_2$)H (III-13) with 2,6-dimethylphenol

2,6-dimethylphenol (5.0 mg, 0.0404 mmol) was directly added to a C_6D_6 solution of (ArN)Mo(PMe$_3$)$_2$(η^2-CH$_2$PMe$_2$)H (20.2 mg, 0.0404 mmol). Immediately, a colour change was seen from dark brown to dark green. NMR analysis showed full conversion of the starting material in 15 minutes at room temperature. Generation of a fluxional compound was characterized by low temperature NMR as (ArN)Mo(PMe$_3$)$_3$(O(2,6-Me$_2$-Ph))H (**III-29**). Heating this complex to 50 °C overnight resulted in complete conversion to the C-H activated complex (ArN)Mo(PMe$_3$)$_3$(κ^2-*O*,*C*-OPh(Me)CH$_2$) (**III-30**).

(ArN)Mo(PMe$_3$)$_3$[O(2,6-Me$_2$-Ph)]H: **^{1}H-NMR** (600 MHz, Toluene-d_8, -50 °C, δ, ppm): 1.18 (bd, 6 H, C*H*$_3$, *Ar*N, $^{3}J_{H\text{-}H}$ = 6.4 Hz), 1.27 (bs, 9 H, P*Me*$_3$), 1.31 (bs, 18 H, 2 P*Me*$_3$), 1.36 (bd, 6 H, C*H*$_3$, *Ar*N, $^{3}J_{H\text{-}H}$ = 6.2 Hz), 2.19 (s, 3 H, C*H*$_3$, O(2,6-*Me*$_2$-Ph), 2.76 (s, 3 H, C*H*$_3$, O(2,6-*Me*$_2$-Ph), 4.06 (sept, 1 H, C*H*, *Ar*N, $^{3}J_{H\text{-}H}$ = 6.5 Hz), 4.71 (sept, 1 H, C*H*, *Ar*N, $^{3}J_{H\text{-}H}$ = 6.5 Hz), 5.05 (dt, 1 H, Mo*H*, $^{2}J_{H\text{-}P}$ = 79.6 Hz, $^{2}J_{H\text{-}P}$ = 27.1 Hz), 6.78 (d, 1 H, *m*-Ph, *Ar*N, $^{3}J_{H\text{-}H}$ = 7.5 Hz), 6.85 (m, *p*-Ph, O(2,6-Me$_2$-*Ph*)), 6.87 (d, 2 H, overlapping doublet of *m*-Ph for O(2,6-Me$_2$-*Ph*) and *Ar*N, $^{3}J_{H\text{-}H}$ = 7.5 Hz), 6.95 (t,1 H, *p*-Ph, *Ar*N, $^{3}J_{H\text{-}H}$ = 7.6 Hz), 7.16 (d, 1 H, *m*-Ph, O(2,6-Me$_2$-*Ph*), $^{3}J_{H\text{-}H}$ = 6.9 Hz). **^{1}H{^{31}P}-NMR** (600 MHz, Toluene-d_8, -50 °C, δ, ppm, selected signals): 5.05 (s, 1 H, Mo*H*). **^{31}P{^{1}H}-NMR** (243.0 MHz, Toluene-d_8, -50 °C, δ, ppm): -3.90 (bs, 2 P, 2 *P*Me$_3$), -18.74 (bs, 1 P, *P*Me$_3$). **^{13}C{^{1}H}-NMR** (151 MHz; Toluene-d_8, -50 °C, δ, ppm): 18.27 (s, *C*H$_3$, *Ar*N), 20.63 (overlapping peaks of all P*Me*$_3$, and *C*H$_3$ of O(2,6-*Me*$_2$-Ph) with residual solvent), 24.39 (s, *C*H$_3$, *Ar*N), 25.21 (s, *C*H$_3$, *Ar*N), 25.88 (s, *C*H, *Ar*N), 26.02 (s, *C*H, *Ar*N), 115.29 (s, *p*-Ph, O(2,6-

Me_2-*Ph*)), 123.04 (s, *m*-Ph, *Ar*N), 123.73 (s, *m*-Ph, *Ar*N), 123.83 (s, *m*-Ph, O(2,6-Me_2-*Ph*)), 124.33 (s, *p*-Ph, *Ar*N), 127.37 (s, *o*-Ph, O(2,6-Me_2-*Ph*)), 128.29 (s, *o*-Ph, O(2,6-Me_2-*Ph*)), 128.49 (s, *m*-Ph, O(2,6-Me_2-*Ph*)), 142.14 (s, *m*-Ph, *Ar*N), 145.82 (s, *m*-Ph, *Ar*N), 149.22 (s, *i*-Ph, *Ar*N), 162.62 (s, *i*-Ph, O(2,6-Me_2-*Ph*)).

(ArN)Mo(PMe$_3$)$_3$(κ^2-O,C-OPh(Me)CH$_2$): **^{1}H-NMR** (600 MHz, Benzene-d_6, 22 °C, δ, ppm): 1.02 (vt, 18 H, 2 P*Me*$_3$, $^2J_{H-P}$ = 5.8 Hz), 1.19 (d, 12 H, C*H*$_3$, *Ar*N, $^3J_{H-H}$ = 6.6 Hz), 1.35 (d, 9 H, P*Me*$_3$, $^2J_{H-P}$ = 6.1 Hz), 2.16 (s, 3 H, C*H*$_3$, κ^2-O,C-OPh(*Me*)CH$_2$), 3.57 (td, 2 H, C*H*$_3$, κ^2-O,C-OPh(Me)C*H*$_2$, $^3J_{H-P}$ = 13.9 Hz, $^3J_{H-P}$ = 4.2 Hz), 3.97 (bs, 2 H, C*H*, *Ar*N), 6.81 (t, *p*-Ph, κ^2-O,C-O*Ph*(Me)CH$_2$, $^3J_{H-H}$ = 7.2 Hz), 6.95 (t, *p*-Ph, *Ar*N, $^3J_{H-H}$ = 7.4 Hz), 7.00 (d, *m*-Ph, κ^2-O,C-O*Ph*(Me)CH$_2$, $^3J_{H-H}$ = 7.4 Hz), 7.04 (t, *m*-Ph, *Ar*N, $^3J_{H-H}$ = 7.2 Hz), 7.61 (d, *m*-Ph, κ^2-O,C-O*Ph*(Me)CH$_2$, $^3J_{H-H}$ = 7.3 Hz). **^{1}H{^{31}P}-NMR** (600 MHz, Benzene-d_6, 22 °C, δ, ppm, selected signals): 3.57 (s, 2H, κ^2-O,C-OPh(Me)C*H*$_2$) **^{31}P{^{1}H}-NMR** (243.0 MHz, Benzene-d_6, 22 °C, δ, ppm): -1.81 (bs, 2P, *P*Me$_3$), -6.21 (bs, 2P, *P*Me$_3$). **^{13}C{^{1}H}-NMR** (151 MHz; Benzene-d_6, 22 °C, δ, ppm):16.11 (d, *C*H$_3$, P*Me*$_3$, $^1J_{C-P}$ = 18.7 Hz), 17.83 (s, *C*H$_3$, Ph*Me*), 21.45 (d, *C*H$_3$, P*Me*$_3$, $^1J_{C-P}$ = 15.6 Hz), 24.43 (s, *C*H$_3$, *Ar*N), 26.37 (s, *C*H, *Ar*N), 33.55 (dt, *C*H$_2$, κ^2-O,C-OPh(Me)*C*H$_2$, $^2J_{C-P}$ = 29.3 Hz, $^2J_{C-P}$ = 8.9 Hz), 114.8 (s, *p*-Ph, O*Ph*Me), 169.8 (d, *i*-Ph, $^2J_{C-P}$ = 14.2 Hz).

NMR reaction of (ArN)Mo(PMe$_3$)$_2$(η^2-CH$_2$PMe$_2$)H (III-13) with 2,6-diisopropylphenol

(ArN)Mo(PMe$_3$)$_2$(η^2-CH$_2$PMe$_2$)H (30.0 mg, 0.0601 mmol) was added to an NMR tube as a toluene-d$_8$ solution. 2,6-diisopropylphenylphenol (8.35 µL, 0.0601 mmol) was directly added to and immediately the colour turned darker brown. NMR analysis showed full conversion of the starting material in 15 minutes at room temperature. Generation of (ArN)Mo(H)(PMe$_3$)$_3${O(2,6-^{i}Pr$_2$-Ph)} (**III-31**) as well as 5 % (ArN)Mo(PMe$_3$)$_3${O(2,6-^{i}Pr$_2$-Ph)}$_2$ was seen by NMR. At room temperature this compound is highly fluxional but lowering to -50 °C resolves all signals.

^{1}H-NMR (600 MHz, Toluene-d_8, -50 °C, δ, ppm): 1.20 (bd, 6H, CH_3, O*Ar*, $^{3}J_{H\text{-}H}$ = 6.2 Hz), 1.32 (broad multiplet, 39 H, 3 PMe_3 & CH_3 of *Ar*N), 1.55 (d, 6H, $(CH_3)_2$CH, O*Ar*, $^{3}J_{H\text{-}H}$ = 6.1 Hz), 3.23 (bsept, 1H, $(CH_3)_2$C*H*, O*Ar*, $^{3}J_{H\text{-}H}$ = 6.4 Hz), 4.03 (bsept, 1H, (CH_3)C*H*, *Ar*N, $^{3}J_{H\text{-}H}$ = 6.4 Hz), 4.55 (bsept, 1H, (CH_3)C*H*, *Ar*N, $^{3}J_{H\text{-}H}$ = 6.6 Hz), 5.12 (dt, 1H, Mo*H*, $^{2}J_{H\text{-}P}$ = 27.3 Hz), 6.78 (d, 1H, *m*-Ph, O*Ar*, $^{3}J_{H\text{-}H}$ = 7.4 Hz), 6.90 (d, 1H, *m*-Ph, O*Ar*, $^{3}J_{H\text{-}H}$ = 7.4 Hz), 6.96 (m, 2H, *p*-Ph, *Ar*N & O*Ar*), 7.09 (d, 1H, *m*-Ph, *Ar*N, $^{3}J_{H\text{-}H}$ = 7.7 Hz), 7.23 (d, 1H, *m*-Ph, *Ar*N, $^{3}J_{H\text{-}H}$ = 7.1 Hz). **^{31}P{^{1}H}-NMR** (243.0 MHz, Toluene-d_8, -50 °C, δ, ppm): -3.52 (bs, 2 P, *P*Me_3), -20.54 (bs, 1 P, *P*Me_3). **^{13}C{^{1}H}-NMR** (75.5 MHz; Toluene-d_8, -50 °C, δ, ppm): 20.40 (m, PMe_3, (CH_3)$_2$CH, *Ar*N), 24.06 (bs, (CH_3)$_2$CH, O*Ar*), 25.44 (bs, (CH_3)$_2$CH, O*Ar*), 26.00 (d, PMe_3, $^{2}J_{C\text{-}P}$ = 14.2 Hz), 26.20 (s, (CH_3)$_2$CH, O*Ar*), 116.2 (s, *p*-Ph, O*Ar*), 123.1 (s, *m*-Ph, *Ar*N), 123.2 (s, *m*-Ph, O*Ar*), 123.6 (s, *m*-Ph, O*Ar*), 124.3 (s, *p*-Ph, *Ar*N), 124.5 (s, *m*-Ph, *Ar*N), 135.4 (s, *o*-Ph, O*Ar*), 137.1 (s, *o*-Ph, O*Ar*), 141.8 (s, *o*-Ph, *Ar*N), 146.0 (s, *o*-Ph, *Ar*N), 149.4 (s, *i*-Ph, O*Ar*), 159.5 (s, *i*-Ph, *Ar*N).

NMR reaction of (ArN)Mo(PMe$_3$)$_2$(η^2-CH$_2$PMe$_2$)H (III-13) with phenylacetylene

(ArN)Mo(PMe$_3$)$_2$(η^2-CH$_2$PMe$_2$)H (15.0 mg, 0.0237 mmol) was dissolved in C_6D_6. Phenylacetylene (2.61 μL, 0.0237 mmol) was directly added and mixed for an hour. After this time NMR analysis showed selective production (ArN)Mo(PMe$_3$)(η^2-C(H)≡CPh)$_2$ (**III-19**).

^{1}H-NMR (300 MHz, Benzene-d_6, 22 °C, δ, ppm): 1.09 (d, 12 H, CH_3, *Ar*N, $^{3}J_{H\text{-}H}$ = 6.9 Hz), 1.28 (d, 9H, CH_3, PMe_3, $^{2}J_{H\text{-}P}$ = 9.2 Hz), 3.57 (sept, 2 H, C*H*, *Ar*N, $^{3}J_{H\text{-}H}$ = 6.9 Hz), 6.94 (bs, 1 H, *m*-Ph, *Ar*N), 7.03 (bs, 2 H, *p*-Ph, *Ar*N), 7.07 (t, 2 H, *p*-Ph, 2 η^2-C(H)≡C*Ph*, $^{3}J_{H\text{-}H}$ = 7.6 Hz), 7.21 (t, 4 H, *m*-Ph, 2 η^2-C(H)≡C*Ph*, $^{3}J_{H\text{-}H}$ = 7.5 Hz), 7.87 (d, 4 H, *m*-Ph, 2 η^2-C(H)≡C*Ph*, $^{3}J_{H\text{-}H}$ = 8.4 Hz), 8.77 (d, 2 H, 2 η^2-C(*H*)≡CPh, $^{3}J_{H\text{-}P}$ = 17.8 Hz). **^{1}H{^{31}P}-NMR** (300 MHz, Benzene-d_6, 22 °C, δ, ppm, selected signals): 1.28 (s, 9 H, PMe_3), 8.77 (s, 2 H, 2 η^2-C(*H*)≡CPh). **^{31}P{^{1}H}-NMR** (243.0 MHz, Benzene-d_6, 22 °C, δ, ppm): 19.79 (s, *P*Me_3). **^{13}C{^{1}H}-NMR** (151 MHz; Benzene-d_6, 22

°C, δ, ppm): 16.82 (d, *C*H_3, P*Me*$_3$, $^1J_{C\text{-}P}$ = 28.9 Hz), 23.04 (s, *C*H_3, *Ar*N), 27.87 (s, *C*H, *Ar*N), 122.26 (s, *p*-Ph, *Ar*N), 122.92 (s, *m*-Ph, *Ar*N), 127.84 (overlapping *m*-Ph & *p*-Ph of η^2-C(H)≡C*Ph* with residual solvent peak), 130.49 (s, *o*-Ph, η^2-C(H)≡C*Ph*), 139.55 (d, *i*-Ph, η^2-C(H)≡C*Ph*, $^4J_{C\text{-}P}$ = 2.8 Hz), 144.27 (s, *o*-Ph, *Ar*N), 147.38 (s, *C*H, η^2-*C*(H)≡CPh),152.42 (s, *i*-Ph, *Ar*N), 176.91 (d, η^2-C(H)≡*C*Ph, $^2J_{C\text{-}P}$ = 2.7 Hz).

NMR reaction of (ArN)Mo(PMe$_3$)$_2$(η^2-CH$_2$PMe$_2$)H (III-13) with HPPh$_2$

(ArN)Mo(PMe$_3$)$_2$(η^2-CH$_2$PMe$_2$)H (9.5 mg, 0.0196 mmol) was dissolved in C_6D_6. Diphenylphosphine (3.41 μL, 0.0196 mmol) was directly added and mixed for a half hour. After this time NMR analysis showed production of P-H activated complex (ArN)Mo(PMe$_3$)$_2$(PPh$_2$)(H) (**III-16**). The addition of another equivalent of HPPh$_2$ generated the insertion product (ArN)Mo(PMe$_3$)$_2$(PPh$_2$)$_2$ (**III-17**) with H_2 seen in the NMR

(ArN)Mo(PMe$_3$)$_2$(PPh$_2$)(H): **^{1}H-NMR** (600 MHz, Benzene-d_6, 22 °C, δ, ppm): 1.29 (vt, 18 H, C*H*$_3$, 2 P*Me*$_3$, $^2J_{H\text{-}P}$ = 6.5 Hz), 1.32 (d, 12 H, C*H*$_3$, *Ar*N, $^3J_{H\text{-}H}$ = 7.0 Hz), 3.22 (t, 1 H, Mo*H*, $^2J_{H\text{-}P}$ = 44.0 Hz), 4.47 (sept, 2 H, C*H*, *Ar*N, $^3J_{H\text{-}H}$ = 7.0 Hz), 7.02 (d, 2 H, *p*-Ph, P*Ph*$_2$, $^3J_{H\text{-}H}$ = 8.1 Hz), 7.05– 7.11 (overlapping peaks of *m*-Ph & *p*-Ph for *Ar*N), 7.13 (t, 4 H, *m*-Ph, P*Ph*$_2$, $^3J_{H\text{-}H}$ = 8.1 Hz), 7.84 (dd, 4 H, *o*-Ph, P*Ph*$_2$, $^3J_{H\text{-}P}$ = 7.8 Hz, $^3J_{H\text{-}H}$ = 7.2 Hz). **^{1}H{^{31}P}-NMR** (600 MHz, Benzene-d_6, 22 °C, δ, ppm, selected signals): 1.29 (s, 18 H, C*H*$_3$, 2 P*Me*$_3$), 3.22 (s, 1H, Mo*H*), 7.84 (d, 4 H, *o*-Ph, P*Ph*$_2$, $^3J_{H\text{-}H}$ = 7.2 Hz) **^{31}P{^{1}H}-NMR** (243.0 MHz, Benzene-d_6, 22 °C, δ, ppm): 168.21 (t, 1 P, *P*Ph$_2$, $^2J_{P\text{-}P}$ = 35.1 Hz), 13.48 (d, 2 P, *P*Me$_3$, $^2J_{P\text{-}P}$ = 35.7 Hz). **^{13}C{^{1}H}-NMR** (151 MHz; Benzene-d_6, 22 °C, δ, ppm): 22.21 (vt, *C*H$_3$, 2 P*Me*$_2$, $^1J_{C\text{-}P}$ = 26.7 Hz), 23.96 (s, *C*H$_3$, *Ar*N), 27.49 (s, *C*H, *Ar*N), 122.63 (s, *p*-Ph, *Ar*N), 124.17 (s, *m*-Ph, *Ar*N), (s, *m*-Ph, *Ar*N), 126.57 (s, *p*-Ph, P*Ph*$_2$), 127.82 (overlapping *m*-Ph of P*Ph*$_2$ with residual C_6H_6), 134.03 (d, *o*-Ph, P*Ph*$_2$,

$^{2}J_{C\text{-}P}$ = 7.6 Hz), 143. 13 (s, *o*-Ph, *Ar*N), 153.46 (m, *i*-Ph, P*Ph*$_2$), 154.47 (d, *i*-Ph, *Ar*N, $^{3}J_{C\text{-}P}$ = 7.00 Hz).

(ArN)Mo(PMe$_3$)$_2$(PPh$_2$)$_2$: **^{1}H-NMR** (600 MHz, Benzene-d_6, 22 °C, δ, ppm): 1.01 (vt, 18 H, C*H*$_3$, 2 P*Me*$_3$, $^{2}J_{H\text{-}P}$ = 6.5 Hz), 1.34 (d, 12 H, C*H*$_3$, *Ar*N, $^{3}J_{H\text{-}H}$ = 6.9 Hz), 4.50 (sept, 2 H, C*H*, *Ar*N, $^{3}J_{H\text{-}H}$ = 7.0 Hz), 6.97 (t, d, 4 H, *p*-Ph, 2 P*Ph*$_2$, $^{3}J_{H\text{-}H}$ = 8.1 Hz), 7.00 – 7.07 (overlapping peaks of *m*-Ph & *p*-Ph for *Ar*N), 7.09 (t, 4 H, *m*-Ph, 2 P*Ph*$_2$, $^{3}J_{H\text{-}H}$ = 8.1 Hz), 7.87 (dd, 8 H, *o*-Ph, 2 P*Ph*$_2$, $^{3}J_{H\text{-}H}$ = 7.3 Hz, $^{3}J_{H\text{-}P}$ = 6.8 Hz). **^{1}H{^{31}P}-NMR** (600 MHz, Benzene-d_6, 22 °C, δ, ppm, selected signals): 1.01 (s, 18 H, C*H*$_3$, 2 P*Me*$_3$), 7.87 (d, 8 H, *o*-Ph, 2 P*Ph*$_2$, $^{3}J_{H\text{-}H}$ = 7.3 Hz) **^{31}P{^{1}H}-NMR** (243.0 MHz, Benzene-d_6, 22 °C, δ, ppm): 115.31 (s, 2 P, 2 *P*Ph$_2$), -9.84 (s, 2 P, 2 *P*Me$_3$). **^{13}C{^{1}H}-NMR** (151 MHz; Benzene-d_6, 22 °C, δ, ppm): 19.99 (t, *C*H$_3$, P*Me*$_3$, $^{1}J_{C\text{-}P}$ = 11.4 Hz), 24.79 (s, *C*H$_3$, *Ar*N), 26.99 (s, *C*H, *Ar*N), 123.68 (s, *p*-Ph, *Ar*N), 125.58 (s, *m*-Ph, *Ar*N), 126.29 (s, *p*-Ph, 2 P*Ph*$_2$), 127.73 (overlapping *m*-Ph of P*Ph*$_2$ with residual C_6H_6), 134.34 (d, *o*-Ph, P*Ph*$_2$, $^{3}J_{C\text{-}P}$ = 6.1 Hz), 143.92 (s, *o*-Ph, *Ar*N), 150.19 (s, *i*-Ph, P*Ph*$_2$), 155.12 (bs, *i*-Ph, *Ar*N).

NMR reaction between (ArN)Mo(PMe$_3$)$_2$(η^2-CH$_2$PMe$_2$)(H) (III-13) and Ethylene

(ArN)Mo(PMe$_3$)$_2$(η^2-CH$_2$PMe$_2$)(H) (13.3 mg, 0.0266 mmol) was added to a flask as a C_6D_6 solution to an NMR tube in a glove box. The NMR was then placed on a Schlenk line and freeze-pump-thawed three times using liquid nitrogen. At room temperature, 1 atm of ethylene gas was added and mixed overnight where a colour change from dark brown to dark green was observed. NMR analysis showed complete conversion of the starting material to the 5-membered metallacycle complex (ArN)Mo(PMe$_3$)$_2$(η^2-C$_2$H$_4$)(CH$_2$)$_4$ (**III-21**).

^{1}H-NMR (600 MHz; Benzene-d_6; δ, ppm): -1.04 (tt, 2H, *α*-C*H*, Mo(CH$_2$)$_4$, $^{3}J_{H\text{-}P}$ = 14.6 Hz, $^{3}J_{H\text{-}H}$ = 6.6 Hz), 1.04 (d, 6H, (C*H*$_3$)$_2$CH, Ar, $^{3}J_{H\text{-}H}$ = 6.8 Hz), 1.21 (vt, 18 H, 2 PMe$_3$, $^{2}J_{H\text{-}P}$ = 6.4 Hz), 1.25 (d, 6H, (C*H*$_3$)$_2$CH, Ar, $^{3}J_{H\text{-}H}$ = 6.7 Hz), 1.92 (tt, 2H, *β*-C*H*, Mo(CH$_2$)$_4$, $^{3}J_{H\text{-}H}$ = 6.2 Hz, $^{3}J_{H\text{-}H}$

= 6.2 Hz), 2.10 (m, 2H, CH_2, η^2-C_2H_4), 2.21 (m, 2H, CH_2, η^2-C_2H_4), 2.28 (tt, 2H, *β*-C*H*, Mo$(CH_2)_4$, $^3J_{H\text{-}H}$ = 6.3 Hz, $^3J_{H\text{-}H}$ = 6.3 Hz), 2.55 (sept., 1H, $(CH_3)_2$C*H*, Ar, $^3J_{H\text{-}H}$ = 6.9 Hz), 2.64 (tt, 2H, *α*-C*H*, Mo$(CH_2)_4$, $^3J_{H\text{-}P}$ = 20.8 Hz, $^3J_{H\text{-}H}$ = 6.9 Hz), 4.09 (sept., 1H, $(CH_3)_2$C*H*, Ar, $^3J_{H\text{-}H}$ = 6.8 Hz), 6.75 (d, 1H, *p*-Ph, Ar, $^3J_{H\text{-}H}$ = 6.8 Hz), 6.87 (d, 1H, *m*-Ph, Ar, $^3J_{H\text{-}H}$ = 7.5 Hz). **^{1}H{^{31}P}-NMR** (600 MHz, Benzene-d_6; δ, ppm, selected signals): -1.04 (t, 2H, α-C*H*, Mo$(CH_2)_4$, $^3J_{H\text{-}H}$ = 6.5 Hz), 1.21 (s, 18 H, 2 PMe_3), 2.10 (d, 2H, CH_2, η^2-C_2H_4, $^3J_{H\text{-}H}$ = 9.3 Hz), 2.21 (d, 2H, CH_2, η^2-C_2H_4, $^3J_{H\text{-}H}$ = 9.4 Hz), 2.65 (t, 2H, α-C*H*, Mo$(CH_2)_4$, $^3J_{H\text{-}H}$ = 6.7 Hz). **^{31}P{^{1}H}-NMR** (243 MHz, Benzene-d_6; δ, ppm): -0.32 (s, 2 PMe_3). **^{13}C{^{1}H}-NMR** (151 MHz, Benzene-d_6; δ, ppm): 122.9 (s, *m*-Ph, *p*-Ph, Ar, overlapping signals), 43.16 (t, α-*C*H_2, Mo$(CH_2)_4$, $^2J_{P\text{-}C}$ = 9.2 Hz), 42.23 (t, η^2-C_2H_4, $^2J_{P\text{-}C}$ = 4.4 Hz), 38.93 (s, β-*C*H, Mo$(CH_2)_4$), 36.84 (s, β-*C*H, Mo$(CH_2)_4$), 34.86 (t, α-*C*H_2, Mo$(CH_2)_4$, $^2J_{P\text{-}C}$ = 12.6 Hz), 26.47 (s, $(CH_3)_2$*C*H, Ar), 24.25 (s, (*C*$H_3)_2$CH, Ar), 15.55 (vt, 2 PMe_3, $^2J_{P\text{-}C}$ = 23.2 Hz).

NMR reaction between (ArN)Mo$(PMe_3)_2$(η^2-CH_2PMe_2)(H) (III-13) and 4-bromotoluene

(ArN)Mo$(PMe_3)_2$(η^2-CH_2PMe_2)(H) (14.2 mg, 0.0293 mmol) was added to an NMR tube as a dark brown C_6D_6 solution. To this 4-bromotoluene (3.61 µL, 0.0293 mmol) was added *via* 10 µL syringe. After a few days at room the insertion product (ArN)Mo$(PMe_3)_2$(η^2-CH_2PMe_2)(Br) (70 %, **III-23**) was observed as well as the hydrido bromide complex (ArN)Mo$(PMe_3)_3$(H)(Br) (30 %).

ArN)Mo$(PMe_3)_2$(η^2-CH_2PMe_2)(Br) **^{1}H-NMR** (600 MHz; Benzene-d_6; δ, ppm): -0.32 (ddd, 1H, η^2-PMe_2CH_2, $^2J_{H\text{-}P}$ = 8.4 Hz, $^3J_{H\text{-}P}$ = 2.7 Hz, $^3J_{H\text{-}P}$ = 2.7 Hz), 1.20 (vt, 18 H, 2 P(C$H_3)_3$, $^3J_{H\text{-}P}$ = 6.5 Hz), 1.24 (d, 12 H, 2 CH(C$H_3)_2$, *Ar*N, $^3J_{H\text{-}H}$ = 6.9 Hz), 1.31 (d, 6H, η^2-P(C$H_3)_2$CH_2, $^2J_{H\text{-}P}$ = 9.8 Hz), 4.46 (sept., 2H, 2 C*H*$(CH_3)_2$, *Ar*N, $^3J_{H\text{-}H}$ = 6.5 Hz), 6.85 (d, 1H, *p*-Ph, *Ar*N, $^3J_{H\text{-}H}$ = 7.7 Hz), 6.97 (d, 1H, *m*-Ph, *Ar*N, $^3J_{H\text{-}H}$ = 7.6 Hz). **^{1}H{^{31}P}-NMR** (600 MHz, Benzene-d_6, δ, ppm, selected

signals): -0.32 (s, 1H, η^2-PMe_2CH_2), 1.20 (s, 18H, 2 $P(CH_3)_3$), 1.31 (s, 6H, η^2-$P(CH_3)_2CH_2$). **^{31}P{^{1}H}-NMR** (243 MHz, Benzene-d_6, δ, ppm): -8.36 (d, 2 PMe_3, $^2J_{P\text{-}P}$ = 25.4 Hz), -12.73 (t, PMe_3, $^2J_{P\text{-}P}$ = 17.7 Hz). **^{13}C{^{1}H}-NMR** (151 MHz, Benzene-d_6, δ, ppm): 3.49 (dt, η^2-PMe_2CH_2, $^1J_{P\text{-}C}$ = 18.2 Hz, $^2J_{P\text{-}C}$ = 4.4 Hz), 16.75 (t, 2 $P(CH_3)_3$, $^1J_{P\text{-}C}$ = 11.3 Hz), 20.07 (d, η^2-PMe_2CH_2, $^1J_{P\text{-}C}$ = 11.9 Hz), 23.96 (s, CH_3, *Ar*N), 123.26 (s, *p*-Ph, *Ar*N), 125.09 (s, *m*-Ph, *Ar*N), 145.04 (s, *o*-Ph, *Ar*N), 152.18 (s, *i*-Ph, *Ar*N).

(ArN)Mo(PMe$_3$)$_3$(H)(Br) **^{1}H-NMR** (600 MHz; Benzene-d_6; δ, ppm): 1.19 (s, 12H, CH_3, *Ar*N, $^3J_{H\text{-}H}$ = 6.9 Hz), 1.39 (d, 9H, CH_3, PMe_3, $^2J_{H\text{-}P}$ = 5.9 Hz), 1.49 (overlapped PMe_3 signals with (ArN)Mo(PMe_3)$_2$(η^2-CH_2PMe_2)(Br), found by ^{1}H-^{31}P HSQC), 4.36 (bs, 2 H, C*H*, *Ar*N), 4.88 (dt, 1 H, Mo*H*, $^2J_{H\text{-}P}$ = 44.5 Hz, $^2J_{H\text{-}P}$ = 28.6 Hz), 6.97 (m, *m*-Ph & *o*-Ph, *Ar*N). **^{31}P{^{1}H}-NMR** (243 MHz, Benzene-d_6, δ, ppm): -5.79 (d, 2 PMe_3, $^2J_{P\text{-}P}$ = 18.1 Hz), -22.98 (d, PMe_3, $^2J_{P\text{-}P}$ = 18.5 Hz). **^{13}C{^{1}H}-NMR** (151 MHz, Benzene-d_6, δ, ppm): 18.36 (t, PMe_3, $^1J_{C\text{-}P}$ = 12.0 Hz), 21.68 (d, 2 PMe_3, $^1J_{C\text{-}P}$ = 16.9 Hz), 23.96 (s, CH_3, *Ar*N), 26.39 (bs, *C*H, *Ar*N), 124.88 (s, *m*-Ph, *Ar*N), 143.84 (s, *o*-Ph, *Ar*N).

NMR reaction between (ArN)Mo(PMe$_3$)$_2$(η^2-CH$_2$PMe$_2$)(H) (III-13) and MeI

(ArN)Mo(PMe_3)$_2$(η^2-CH_2PMe_2)(H) (23.0 mg, 0.0475 mmol) was added to an NMR tube as a dark brown C_6D_6 solution. To this MeI (3.00 μL, 0.0475 mmol) was added *via* 10 μL syringe. After 30 minutes at room temperature full conversion to two isomers of the insertion product (ArN)Mo(PMe_3)$_2$(η^2-CH_2PMe_2)(I) (**III-22**) were observed in a 6:1 ratio. Methane was also observed after the reaction went to completion.

^{1}H NMR (600 MHz, Benzene-d_6, δ, ppm): -0.48 (td, 2H, CH_3, η^2-CH_2PMe_2, $^2J_{H\text{-}P}$ = 8.8 Hz, $^1J_{H\text{-}P}$ = 2.2 Hz), 1.23 (bd, 12H, CH_3, *Ar*N, $^3J_{H\text{-}P}$ = 6.7 Hz), 1.26 (vt, 18H, 2 PMe_3, $^2J_{H\text{-}P}$ = 6.5 Hz), 1.30 (d, 6H, CH_3, η^2-CH_2PMe_2, $^2J_{H\text{-}P}$ = 9.9 Hz), 4.45 (bs, 2H, C*H*, *Ar*N), 6.94 (d, 2H, *m*-Ph, $^3J_{H\text{-}H}$ =

7.7 Hz), 7.05 (t, 2H, *o*-Ph, $^{3}J_{H-H}$ = 7.6 Hz). **^{31}P{^{1}H} NMR** (243 MHz, Benzene-d_6, δ, ppm): -13.74 (d, 2 *P*Me$_3$, $^{2}J_{P-P}$ = 25.6 Hz,), -23.34 (t, PMe$_2$CH$_2$, $^{2}J_{P-P}$ = 22.9 Hz,). **^{13}C{^{1}H}-NMR** (151 MHz, Benzene-d_6, δ, ppm): 2.54 (dt, *C*H$_2$, η^2-*C*H$_2$PMe$_2$, $^{1}J_{C-P}$ = 18.2 Hz, $^{2}J_{C-P}$ = 4.0 Hz), 18.18 (t, *C*H$_3$, P*Me*$_3$, $^{1}J_{C-P}$ = 11.7 Hz), 18.85 (d, P*Me*$_3$, $^{1}J_{C-P}$ = 13.0 Hz), 23.89 (bs, *C*H$_3$, *Ar*N), 26.74 (bs, *C*H, *Ar*N), 123.30 (s, *m*-Ph, *Ar*N), 125.22 (s, *p*-Ph, *Ar*N), 152.55 (s, *i*-Ph, *Ar*N).

NMR reaction between (ArN)Mo(PMe$_3$)$_2$(η^2-CH$_2$PMe$_2$)(H) (III-13) and dichloromethane

(ArN)Mo(PMe$_3$)$_2$(η^2-CH$_2$PMe$_2$)(H) (18.2 mg, 0.0364 mmol) was added to an NMR tube as a dark brown C_6D_6 solution. To this CH_2Cl_2 (1.16 μL, 0.0182 mmol) was added *via* 10 μL syringe. After one night at room temperature half of the starting material remained, and full consumption of CH_2Cl_2 was seen. An extra half equivalent of CH_2Cl_2 was added to fully generate (ArN)Mo(PMe$_3$)$_2$(η^2-CH$_2$PMe$_2$)(Cl) (**III-24**) as well as a small amount of (ArN)Mo(PMe$_3$)$_3$Cl$_2$. CH_3Cl and methane were observed as the reaction progressed.

^{1}H NMR (600 MHz, Benzene-d_6, δ, ppm): -0.27 (dt, 2H, CH$_2$, η^2-C*H*$_2$PMe$_2$, $^{3}J_{H-P}$ = 12.2 Hz, $^{2}J_{H-P}$ = 3.3 Hz), 1.16 (vt, 18H, 2 P*Me*$_3$, $^{2}J_{H-P}$ = 6.6 Hz), 1.25 (d, 12 H, C*H*$_3$, *Ar*N, $^{3}J_{H-H}$ = 7.0 Hz), 1.32 (d, 6H, C*H*$_3$, η^2-C*H*$_2$P*Me*$_2$, $^{2}J_{H-P}$ = 9.4 Hz), 4.48 (dsept, 2H, C*H*$_3$, *Ar*N, $^{3}J_{H-H}$ = 6.9 Hz), 7.01 (m, 3H, overlapping peaks of *m*-Ph & *p*-Ph). **^{31}P{^{1}H} NMR** (243 MHz, Benzene-d_6, δ, ppm): -4.71 (d, 2P, *P*Me$_3$, $^{2}J_{P-P}$ = 19.7 Hz), -7.37 (t, 1P, *P*Me$_3$, $^{2}J_{P-P}$ = 19.8 Hz). **^{13}C{^{1}H} NMR** (151 MHz, Benzene-d_6, δ, ppm): 3.57 (dt, *C*H$_2$, η^2-*C*H$_2$PMe$_2$, $^{1}J_{C-P}$ = 18.3 Hz, $^{2}J_{C-P}$ = 4.4 Hz), 16.01 (t, *C*H$_3$, 2 P*Me*$_3$, $^{1}J_{C-P}$ = 11.5 Hz), 20.77 (d, *C*H$_3$, η^2-CH$_2$P*Me*$_2$, $^{1}J_{C-P}$ = 11.1 Hz), 23.98 (s, *C*H$_3$, *Ar*N), 26.32 (s, *C*(CH$_3$)$_3$, *Ar*N), 26.38 (s, *C*(CH$_3$)$_3$, *Ar*N), 123.20 (s, *p*-Ph, *Ar*N), 124.97 (s, *m*-Ph, *Ar*N), 145.32 (s, *o*-Ph, *Ar*N), 151.97 (s, *i*-Ph, *Ar*N).

Reactions of (^{t}BuN)Mo(PMe$_3$)$_2$(η^2-CH$_2$PMe$_2$)Cl with E-H Bonds

Preparation of (^{t}BuN)Mo(PMe$_3$)$_2$(η^2-CH$_2$PMe$_2$)Cl (III-15)

(^{t}BuN)Mo(PMe$_3$)$_3$Cl$_2$ (0.5866 g, 1.262 mmol) was placed in a large Schlenk flask and dissolved in benzene (50 mL). A solution of LiNH(^{t}Bu) (0.1496 g, 1.893 mmol) was added to the Mo solution slowly over a 5 minute period. The solution changed colour from dark purple to opaque brown colour after approximately one hour of stirring at room temperature. After this time the mixture was filtered to give a dark brown filtrate. All volatiles were removed in vacuum and hexanes added (10 mL). In one case, after one week in the - 80 °C freezer brown precipitate was seen and was isolated and dried to give 153.0 mg of pure (^{t}BuN)Mo(PMe$_3$)$_2$(η^2-CH$_2$PMe$_2$)Cl. Yield: 28 %.

^{1}H-NMR (600 MHz, Benzene-d_6, 22 °C, δ, ppm): -0.47 (td, 2H, η^2-C*H*$_2$PMe$_2$, $^3J_{H\text{-}P}$ = 12.5 Hz, $^2J_{H\text{-}P}$ = 3.8 Hz), 1.15 (s, 9H, C*H*$_3$, ^{t}*Bu*N), 1.23 (vt, 18 H, P*Me*$_3$, $^2J_{H\text{-}P}$ = 6.5 Hz), 1.29 (d, 6H, η^2-CH$_2$P*Me*$_2$, $^2J_{H\text{-}P}$ = 9.8 Hz).

^{1}H{^{31}P}-NMR (600 MHz, Benzene-d_6, 22 °C, δ, ppm, selected signals): -0.47 (s, 2H, η^2-C*H*$_2$PMe$_2$), 1.23 (s, 18 H, P*Me*$_3$), 1.29 (s, 6H, η^2-CH$_2$P*Me*$_2$).

^{31}P{^{1}H}-NMR (243.0 MHz, Benzene-d_6, 22 °C, δ, ppm): -2.18 (d, 2P, 2 *P*Me$_3$, $^2J_{P\text{-}P}$ = 19.1 Hz), -6.23 (t, 1P, *P*Me$_3$, $^2J_{P\text{-}P}$ = 19.1 Hz).

General procedure for the *in situ* preparation of (^{t}BuN)Mo(PMe$_3$)$_2$(η^2-CH$_2$PMe$_2$)Cl (III-15)

(^{t}BuN)Mo(PMe$_3$)$_3$Cl$_2$ (21.2 g, 0.0455 mmol) was placed in a small vial and dissolved in C$_6$H$_6$ (0.5 mL). A solution of LiNH(^{t}Bu) (0.5.8 mg, 0.0734 mmol) in C$_6$H$_6$ was directly added to the Mo solution. The solution changed colour from dark purple to opaque brown colour after approximately one hour of stirring at room temperature. All volatiles were removed and product

extracted with hexanes through a medium glass frit in the glove box (1 mL). This was transferred to a separate NMR volatiles removed and C_6D_6 added to give pure (^{t}BuN)Mo(PMe_3)$_2$(η^2-CH_2PMe_2)Cl in almost all cases.

NMR reaction of (^{t}BuN)Mo(PMe_3)$_2$(η^2-CH_2PMe_2)Cl with $PhSiH_3$

Using the general procedure described above or isolated (^{t}BuN)Mo(PMe_3)$_2$(η^2-CH_2PMe_2)Cl (0.0365 mmol) in C_6D_6, $PhSiH_3$ (4.50 μL, 0.0365 mmol) could be directly added and mixed for 2 days at room temperature. After this time NMR showed clean conversion to the silyl chloride complex (^{t}BuN)Mo(PMe_3)$_3$(SiH_2Ph)Cl (**III-32**) with little impurity observed in the NMR.

Preparation of (^{t}BuN)Mo(PMe_3)$_3$(SiH_2Ph)Cl (III-32)

(^{t}BuN)Mo(PMe_3)$_3Cl_2$ (253.1 mg, 0.543 mmol) and LiNH(^{t}Bu) (69.7 mg, 0.881 mmol) were added together in a flask and dissolved in toluene. The mixture was stirred for one hour and volatiles removed in vacuum. (^{t}BuN)Mo(PMe_3)$_2$(η^2-CH_2PMe_2)Cl product was extracted with toluene and filtrate was placed in a separate Schlenk flask. NMR probe showed pure cyclometallated product obtained. To this $PhSiH_3$ (66.9 μL, 0.0365 mmol) was added directly and stirred for 2 hours at room temperature, showing full conversion to the silyl chloride product. All volatiles were removed and a minimum amount of benzene (5 mL) added. This was placed at -78 °C, and benzene sublimed in vacuum to leave a gummy dark red solid which was dried and isolated to give pure (^{t}BuN)Mo(PMe_3)$_3$(SiH_2Ph)Cl (**III-32**). Yield: 167.8 mg, 57.4 %.

^{1}H-NMR (600 MHz, Benzene-d_6, 22 °C, δ, ppm): 0.91 (s, 9H, ^{t}*Bu*N), 1.18 (bd, 9H, 1 P*Me*$_3$, $^2J_{H\text{-}P}$ = 5.9 Hz), 1.39 (vt, 18 H, 2 P*Me*$_3$, $^2J_{H\text{-}P}$ = 6.2 Hz), 5.35 (t, 2 H, Si*H*$_2$Ph, $^3J_{H\text{-}P}$ = 4.9 Hz), 7.22 (d, 1 H, *p*-Ph, SiH_2*Ph*, $^3J_{H\text{-}H}$ = 7.7 Hz), 7.30 (t, 2 H, *m*-Ph, SiH_2*Ph*, $^3J_{H\text{-}H}$ = 7.2 Hz), 8.39 (d, 2 H, *o*-Ph, SiH_2*Ph*). **^{1}H{^{31}P}-NMR** (600 MHz, Benzene-d_6, 22 °C, δ, ppm, selected signals): 1.18 (bs, 9H, 1 P*Me*$_3$), 1.39 (s, 18 H, 2 P*Me*$_3$), 5.35 (s, 2 H, Si*H*$_2$Ph). **^{31}P{^{1}H}-NMR** (243.0 MHz,

Benzene-d_6, 22 °C, δ, ppm): -5.79 (d, 2 P, 2 *P*Me$_3$, $^2J_{P\text{-}P}$ = 20.0 Hz), -13.46 (t, 1 P, *P*Me$_3$, $^2J_{P\text{-}P}$ = 20.5 Hz), **^{29}Si INEPT+** (119 MHz, Benzene-d_6, 22 °C, J = 150 Hz, δ, ppm): -21.32 (tm, *Si*H$_2$Ph, $^1J_{Si\text{-}H}$ = 146.7 Hz).

NMR reaction of (^{t}BuN)Mo(PMe$_3$)$_3$(SiH$_2$Ph)Cl with L-Selectride

(^{t}BuN)Mo(PMe$_3$)$_3$(SiH$_2$Ph)Cl (21.5 mg, 0.040 mmol) was dissolved in C_6D_6 and transferred to an NMR tube. L-Selectride (40.0 μL, 0.040 mmol) was directly added *via* 50 μL syringe. After 1 hour at room temperature, full conversion to the silyl hydride complex (^{t}BuN)Mo(PMe$_3$)$_3$(SiH$_2$Ph)(H) (**III-33**) was observed.

^{1}H-NMR (600 MHz, Benzene-d_6, 22 °C, δ, ppm): -4.49 (dtt, 1 H, Mo*H*, $^2J_{H\text{-}P}$ = 64.0 Hz, $^2J_{H\text{-}P}$ = 32.6 Hz, $^3J_{H\text{-}H}$ = 6.3 Hz), 1.19 (s, 9H, ^{t}*Bu*N), 1.25 (d, 9H, 1 P*Me*$_3$, $^2J_{H\text{-}P}$ = 6.1 Hz), 1.34 (vt, 18 H, 2 P*Me*$_3$, $^2J_{H\text{-}P}$ = 6.1 Hz), 5.38 (tdd, 2 H, Si*H*$_2$Ph, $^3J_{H\text{-}P}$ = 14.3 Hz, $^3J_{H\text{-}H}$ = 6.0 Hz, $^3J_{H\text{-}P}$ = 4.4 Hz), 7.24 (d, 1 H, *p*-Ph, SiH$_2$*Ph*, $^3J_{H\text{-}H}$ = 7.1 Hz), 7.36 (t, 2 H, *m*-Ph, SiH$_2$*Ph*, $^3J_{H\text{-}H}$ = 7.1 Hz), 8.39 (d, 2 H, *o*-Ph, SiH$_2$*Ph*, $^3J_{H\text{-}H}$ = 7.7 Hz). **^{1}H{^{31}P}-NMR** (600 MHz, Benzene-d_6, 22 °C, δ, ppm, selected signals): -4.49 (d, 1 H, Mo*H*, $^3J_{H\text{-}H}$ = 6.3 Hz), 1.5 (bs, 9H, 1 P*Me*$_3$), 1.34 (s, 18 H, 2 P*Me*$_3$), 5.38 (d, 2 H, Si*H*$_2$Ph, $^3J_{H\text{-}H}$ = 6.0 Hz). **^{31}P{^{1}H}-NMR** (243.0 MHz, Benzene-d_6, 22 °C, δ, ppm): 15.94 (t, 1 P, *P*Me$_3$, $^2J_{P\text{-}P}$ = 23.6 Hz), 3.26 (d, 2 P, 2 *P*Me$_3$, $^2J_{P\text{-}P}$ = 23.4 Hz).

Reactions of (ArN)(^{t}BuN)Mo(PMe$_3$)(η^2-C$_2$H$_4$) with Silanes

Preparation of (ArN)(^{t}BuN)Mo(PMe$_3$)(η^2-C$_2$H$_4$) (III-40)

(ArN)(^{t}BuN)MoCl$_2$(DME) (0.5319g, 1.06 mmol) was a placed in a large Schlenk flask with 50 mL of Et$_2$O to give a clear red solution. PMe$_3$ (0.22 mL, 2.12 mmol) was added *via* 1 mL syringe, followed by EtMgBr (0.704 mL, 2.12 mmol, 3 M) as an Et$_2$O solution at room temperature. Immediately, the colour turned murky bright red with the formation of a gummy reddish yellow precipitate. The solution turned dark brown after 10 minutes of intensive stirring

and the mixture was allowed to react for 3 hours at room temperature. After this time all volatiles were removed in vacuum and product was extracted using hexanes (75 mL) or until the solution ran clear. The dark red filtrate was reduced in volume and placed in the -80 °C freezer overnight. After this time red gummy product was observed in the flask and was filtered and washed with cold hexanes (5 mL) to give a gummy red product characterized as (ArN)(^{t}BuN)Mo(PMe$_3$)(η^2-C$_2$H$_4$) (**III-37**) by NMR analysis. Yield: 0.250 g, 50 %.

^{1}H-NMR (600 MHz, Benzene-d_6, 22 °C, δ, ppm): 1.06 (d, 9H, P*Me*$_3$, $^3J_{H-P}$ = 9.2 Hz), 1.29 (d, 6H, (C*H*$_3$)$_2$CH, *Ar*N, $^3J_{H-H}$ = 7.0 Hz), 1.30 (d, 6H, (C*H*$_3$)$_2$CH, *Ar*N, $^3J_{H-H}$ = 6.9 Hz), 1.44 (s, 9H, *tBu*N), 2.22 (td, 1H, C*H*$_2$, η^2-C$_2$H$_4$, $^3J_{H-H}$ = 11.7 Hz, $^2J_{H-H}$ = 4.4 Hz), 2.54 (td, 1H, C*H*$_2$, η^2-C$_2$H$_4$, $^3J_{H-H}$ = 12.2 Hz, $^2J_{H-H}$ = 4.3 Hz), 4.04 (sept, 2H, (CH$_3$)$_2$C*H*, *Ar*N, $^3J_{H-H}$ = 8.3 Hz), 7.08 (overlapping signals, *m*-Ph & *p*-Ph, *Ar*N). **^{31}P{^{1}H}-NMR** (243.0 MHz, Benzene-d_6, 22 °C, δ, ppm): 22.17 (s, *P*Me$_3$). **^{13}C{^{1}H}-NMR** (151 MHz; Benzene-d_6, 22 °C, δ, ppm): 18.04 (d, P*Me*$_3$, $^1J_{C-P}$ = 29.3 Hz), 23.25 (s, (*C*H$_3$)$_2$CH, ArN), 23.67 (s, (*C*H$_3$)$_2$CH, ArN), 26.87 (s, η^2-*C*$_2$H$_4$), 27.76 (s, (CH$_3$)$_2$*C*H, ArN), 35.41 (d, η^2-*C*$_2$H$_4$, $^2J_{C-P}$ = 9.0 Hz), 66.44 (s, (CH$_3$)$_3$*C*N, ^{t}BuN), 122.2 (s, *p*-Ph, *Ar*N), 122.6 (s, *m*-Ph, *Ar*N), 142.2 (s, *o*-Ph, *Ar*N), 153.8 (s, *i*-Ph *Ar*N).

NMR reaction of (ArN)(^{t}BuN)Mo(PMe$_3$)(η^2-C$_2$H$_4$) (III-40) with Me$_2$SiHCl

Me$_2$SiHCl (6.54 μL, 0.059 mmol) was added to a toluene-d$_8$ solution of (ArN)(^{t}BuN)Mo(η^2-C$_2$H$_4$)(PMe$_3$) (26.3 mg, 0.059 mmol) at -55 °C in an NMR tube. Monitoring the reaction at -50 °C showed initial formation of the *β*-agostic silylamido complex (^{t}BuN)Mo(η^3-NAr-SiMe$_2$-H)(η^2-C$_2$H$_4$)(PMe$_3$)(Cl) (**III-45**). Warming the reaction mixture to room temperature shows 50 % conversion to the bis(phosphine) complex (^{t}BuN)Mo(η^3-NAr-SiMe$_2$-H)(PMe$_3$)$_2$(Cl) (**III-44**) and 50 % conversion to the silanimine complex (^{t}BuN)Mo(η^2-NAr-SiMe$_2$)(PMe$_3$)(η^2-C$_2$H$_4$)(Et)(Cl) (**III-43**).

(^{t}BuN)Mo(η^3-NAr-SiMe$_2$-H)(η^2-C$_2$H$_4$)(PMe$_3$)(Cl). **^{1}H-NMR** (600 MHz; Toluene-d$_8$; -15 °C; δ, ppm): 0.46 (s, 3H, Si*Me*), 0.78 (s, 9H, 3 CH$_3$, N^t*Bu*), 0.88 (s, 3H, Si*Me*), 0.94 (d, $^2J_{P\text{-}H}$ = 9.24 Hz, 9H, 3 CH$_3$, PMe$_3$), 1.16 (d, $^3J_{H\text{-}H}$ = 6.6 Hz, 3H, CH$_3$, N*Ar*), 1.23 (d, $^3J_{H\text{-}H}$ = 6.8 Hz, 3H, CH$_3$, N*Ar*), 1.26 (d, $^3J_{H\text{-}H}$ = 7.0 Hz, 3H, CH$_3$, N*Ar*), 1.40 (d, $^3J_{H\text{-}H}$ = 6.7 Hz, 3H, CH$_3$, N*Ar*), 2.43 (ddd, 1H, $^2J_{\text{H-H}}$ = 7.02 Hz, $^3J_{\text{H-Hcis}}$ = 9.6 Hz, $^3J_{\text{H-Htrans}}$ = 12.4 Hz, η^2-C$_2$H$_4$), 2.86 (ddd, $^2J_{\text{H-H}}$ = 7.29 Hz, $^3J_{\text{H-Hcis}}$ = 10.6 Hz, $^3J_{\text{H-Htrans}}$ = 12.1 Hz, 1H, CH$_2$, η^2-C$_2$H$_4$), 3.46, (dd, 1H, $^3J_{H\text{-}H}$ = 10.2 Hz, η^2-C$_2$H$_4$), 3.66 (dd, 1H, $^3J_{H\text{-}H}$ = 11.4 Hz, η^2-C$_2$H$_4$), 3.90 (sept, 1H, $^3J_{\text{H-H}}$ = 6.8 Hz, *Ar*N), 4.27 (sept, 1H, $^3J_{\text{H-H}}$ = 6.7 Hz, *Ar*N), 6.6-7.3 (*Ar*N phenyl peaks overlapped with solvent). **^{31}P{^{1}H}-NMR** (243.0 MHz; Toluene-d$_8$; -15 °C; δ, ppm): -4.22 (s, 1P, *P*Me$_3$). **^{13}C{^{1}H}-NMR** (151 MHz; Toluene-*d*$_8$, -50 °C, δ, ppm): - 1.35 (s, CH$_3$, Si*Me*$_2$), 1.66 (s, CH$_3$, Si*Me*$_2$), 16.07 (d, P*Me*$_3$, $^1J_{\text{C-P}}$ = 27.6 Hz), 24.30 (s, *C*H$_3$, *Ar*N), 25.85 (s, *C*H, *Ar*N), 26.52 (s, *C*H$_3$, *Ar*N), 26.72 (s, *C*H$_3$, *Ar*N), 26.75 (s, *C*H, *Ar*N), 27.21 (s, *C*H$_3$, *Ar*N), 29.20 (s, ^{t}*Bu*N), 50.64 (s, *C*H$_2$, η^2-C$_2$H$_4$), 54.05 (s, *C*H$_2$, η^2-C$_2$H$_4$), 70.27 (s, (CH$_3$)*C*N, ^{t}*Bu*N), 118.3 (s, *p*-Ph, *Ar*N), 122.6 (s, *m*-Ph, *Ar*N), 123.5 (s, *m*-Ph, *Ar*N), 150.0 (s, *i*-Ph, *Ar*N). **^{1}H-^{29}Si HSQC NMR** (119.0 MHz, Toluene-*d*$_8$, -50 °C; *J* = 100 Hz; ^{29}Si projection, δ, ppm): -69.7 (η^3-NAr-*Si*Me$_2$-H). **^{1}H-^{29}Si HSQC JC** (119.0 MHz, Toluene-*d*$_8$; ^{1}H projection, -50 °C, δ, ppm): 1.37 (dd, $^2J_{\text{H-P}}$ = 21.3 Hz, $^1J_{\text{Si-H}}$ = 90.0 Hz, η^3-NAr-SiMe$_2$-*H*).

(^{t}BuN)Mo(η^2-NAr-SiMe$_2$)(η^2-C$_2$H$_4$)(Et)(Cl): **^{1}H-NMR** (600 MHz, Toluene-d$_8$, -15 °C; δ, ppm): 0.10 (s, 3H, Si*Me*), 0.32 (s, 3H, Si*Me*), 0.70 (s, 9H, 3 CH$_3$, N^t*Bu*), 1.18 (d, $^3J_{H\text{-}H}$ = 7.2 Hz, 3H, CH$_3$, N*Ar*), 1.22 (d, $^3J_{H\text{-}H}$ = 7.2 Hz, CH$_3$, N*Ar*), 1.41 (d, $^3J_{H\text{-}H}$ = 7.2 Hz, 3H, CH$_3$, N*Ar*), 1.50 (d, $^3J_{H\text{-}H}$ = 7.2 Hz, 3H, CH$_3$, N*Ar*), 1.74 (ddd, $^2J_{H\text{-}H}$ = 12.3 Hz, $^3J_{H\text{-}H}$ = 4.4 Hz, 1H, CH$_2$, η^2-*C*$_2$*H*$_4$), 2.04 (t, $^3J_{H\text{-}H}$ = 7.4 Hz, 3H, CH$_3$, Et), 2.20 (ddd, $^2J_{H\text{-}H}$ = 12.5 Hz, $^3J_{H\text{-}H}$ = 6.3 Hz, 1H, CH$_2$, η^2-*C*$_2$*H*$_4$), 2.31 (dq, $^2J_{H\text{-}H}$ = 9.9 Hz, $^3J_{H\text{-}H}$ = 7.5 Hz, 1 H, CH$_2$, Et), 2.41 (ddd, $^2J_{H\text{-}H}$ = 12.2 Hz, $^3J_{H\text{-}H}$ = 6.2 Hz, 1H, CH$_2$, η^2-*C*$_2$*H*$_4$), 2.68 (ddd, $^2J_{H\text{-}H}$ = 12.1 Hz, $^3J_{H\text{-}H}$ = 4.7 Hz, 1H, CH$_2$, η^2-*C*$_2$*H*$_4$),

3.36 (dq, $^{2}J_{H\text{-}H}$ = 9.7 Hz, $^{3}J_{H\text{-}H}$ = 7.0 Hz, 1 H, CH_2, Et), 3.53 (sept., $^{3}J_{H\text{-}H}$ = 6.8 Hz, 1H, CH, N*Ar*), 3.79 (sept., $^{3}J_{H\text{-}H}$ = 6.9 Hz, 1H, CH, N*Ar*), 7.02 (d, $^{3}J_{H\text{-}H}$ = 6.6 Hz, 1H, *m*-Ar), 7.07 (t, $^{3}J_{H\text{-}H}$ = 6.2 Hz, 1H, *p*-Ar). **^{1}H-^{13}C HSQC** (151 MHz, Toluene-d_8, ^{13}C projections, -15 °C; δ, ppm): 2.43 (*C*H_3, Si*Me*$_2$), 3.46 (*C*H_3, Si*Me*$_2$), 21.99 (*C*H_3, Et) 23.81, 23.60, 25.56, 26.39 (*C*H_3, *Ar*N), 27.67, 28.01 (Me$_2$*C*H, *Ar*N), 28.93 (CH_3, ^{t}*Bu*N), 39.26 (*C*H_2, η^2-*C*$_2$H$_4$), 39.90 (*C*H_2, Et), 49.28 (*C*H_2, η^2-*C*$_2$H$_4$). **^{1}H-^{29}Si HSQC NMR** (119.0 MHz, Toluene-d_8, -15 °C; *J* = 7 Hz; ^{29}Si projection, δ, ppm): 10.04 (*Si*Me$_2$)

(^{t}BuN)Mo(η^3-NAr-SiMe$_2$-H)(PMe$_3$)$_2$(Cl): **^{1}H-NMR** (600 MHz; tol-d_8; -20 °C; δ, ppm): 0.60 (s, 3H, Si*Me*), 0.87 (d, $^{2}J_{H\text{-}P}$ = 23.6 Hz, $^{1}J_{\text{Si-H}}$ = 91.2 Hz, 1H, Mo*H*Si, found by ^{1}H-^{29}Si – HSQC JC) 0.88 (s, 3H, Si*Me*), 0.95 (d, $^{2}J_{P\text{-}H}$ = 8.4 Hz, 9H, 3 CH_3, PMe_3) 1.12 (d, $^{3}J_{H\text{-}H}$ = 6.8 Hz, 3H, CH_3, N*Ar*), 1.13 (s, 9H, 3 CH_3, N^{t}*Bu*), 1.29 (d, $^{3}J_{H\text{-}H}$ = 6.8 Hz, 3H, CH_3, N*Ar*), 1.32 (d, $^{3}J_{H\text{-}H}$ = 6.8 Hz, 3H, CH_3, N*Ar*), 1.38 (d, $^{2}J_{H\text{-}P}$ = 7.2 Hz, 9H, 3 CH_3, PMe_3), 1.55 (d, $^{3}J_{H\text{-}H}$ = 6.5 Hz, 3H, CH_3, N*Ar*), 3.75 (sept, $^{3}J_{H\text{-}H}$ = 6.7 Hz, 1H, CH, N*Ar*), 4.46 (sept, $^{3}J_{H\text{-}H}$ = 6.7 Hz, 1H, CH, N*Ar*), 7.13 (t, $^{3}J_{H\text{-}H}$ = 7.6 Hz, 1H, *p*-Ar), 7.18 (d, $^{3}J_{H\text{-}H}$ = 7.2 Hz, 1H, *m*-Ar), 7.33 (d, $^{3}J_{H\text{-}H}$ = 7.2 Hz, 1H, *m*-Ar). **^{31}P{^{1}H}-NMR** (243.0 MHz; Toluene-d_8; -20 °C; δ, ppm): -7.38 (d, $^{2}J_{P\text{-}P}$ = 9.4 Hz, *P*Me_3) 3.25 (d, $^{2}J_{P\text{-}P}$ = 9.0 Hz, *P*Me_3). **^{1}H-^{29}Si HSQC NMR** (119.0 MHz, Toluene-d_8, -20 °C; *J* = 100 Hz; ^{29}Si projection, δ, ppm): -64.5 (η^3-NAr-*Si*Me$_2$-*H*). **^{1}H-^{29}Si-HSQC JC** (119.0 MHz; Toluene-d_8; -20 °C; ^{1}H projection, δ, ppm): 0.89 (d, $^{1}J_{Si\text{-}H}$ = 91.2 Hz, η^3-NAr-SiMe$_2$-*H*).

NMR reaction of (ArN)(^{t}BuN)Mo(PMe$_3$)(η^2-C$_2$H$_4$) (III-40) with PhSiH$_3$

(ArN)(^{t}BuN)Mo(η^2-C_2H_4)(PMe_3) (22.8 mg, 0.0511 mmol) was dissolved in C_6D_6 in the glove box and transferred to an NMR tube. $PhSiH_3$ (12.6 μL, 0.102 mmol) was directly added to this NMR tube to give a colour change from dark red to dark brown over an hour period. NMR

analysis at low temperature and room temperature showed foration of the NMR characterized β-agostic silylamido complex (^{t}BuN)Mo(η^3-NAr-SiHPh-H)(SiH$_2$Ph)(PMe$_3$) (**III-46**).

^{1}H-NMR (600 MHz, Benzene-d_6, 22 °C, δ, ppm): 0.52 (d, 3H, C*H*$_3$, *Ar*N, $^3J_{H-H}$ = 6.7 Hz), 0.98 (d, 3H, C*H*$_3$, *Ar*N, $^3J_{H-H}$ = 6.7 Hz), 1.07 (d, 9H, P*Me*$_3$, $^2J_{H-P}$ = 8.6 Hz), 1.11 (d, 3H, C*H*$_3$, *Ar*N, $^3J_{H-H}$ = 6.7 Hz), 1.15 (s, 9H, ^{t}BuN), 1.29 (d, 3H, C*H*$_3$, *Ar*N, $^3J_{H-H}$ = 6.9 Hz), 2.60 (sept, 1H, C*H*, *Ar*N, $^3J_{H-H}$ = 6.8 Hz), 3.46 (sept, 1H, C*H*, *Ar*N, $^3J_{H-H}$ = 6.8 Hz), 3.94 (m, 1H, Si*H*, η^3-NAr-SiHPh-*H*), 5.04 (bs, 1H, Si*H*, η^3-NAr-Si*H*Ph-H), 5.55 (s, 1H, Si*H*, Mo-Si*H*$_2$Ph), 5.72 (d, 1H, Si*H*, Mo-Si*H*$_2$Ph, $^3J_{H-P}$ = 2.2 Hz), 6.93 (m, *m*-Ph, *Ar*N), 7.00 – 7.12 (overlapping multiplets, *m*-Ph & *p*-Ph, *Ar*N; *m*-Ph & *p*-Ph, Si*Ph*), 7.29 (*m*-Ph, Si*Ph*, $^3J_{H-H}$ = 7.4 Hz), 7.65 (d, 1H, *o*-Ph, Si*Ph*, $^3J_{H-H}$ = 7.6 Hz), 8.15 (d, 1H, *o*-Ph, Si*Ph*, $^3J_{H-H}$ = 6.6 Hz). **^{31}P{^{1}H}-NMR** (243.0 MHz, Benzene-d_6, 22 °C, δ, ppm): 12.00 (s, *P*Me$_3$). **^{1}H-^{29}Si HSQC** (119.2 MHz; Benzene-d_6, ^{29}Si projection, 22 °C; δ, ppm): -77.9 (η^3-NAr-*Si*HPh-H), -7.2 (Mo-*Si*H$_2$Ph). **^{1}H-^{13}C HSQC/^{13}C{^{1}H}-DEPT^{135}** (151.0 MHz; Benzene-d_6, ^{13}C projection, 22 °C; δ, ppm): 18.59 (d, PMe$_3$, $^2J_{C-P}$ = 25.9 Hz), 22.40, 22.52, 25.98, 26.21 (s, *C*H$_3$, *Ar*N), 27.18, 27.63, (s, *C*H, *Ar*N), 31.91 (s, *C*H$_3$, ^{t}*Bu*N), 122.4 , 122.5 (s, *m*-Ph, Si*Ph*), 126.81, 126.90 (s, *m*-Ph, Si*Ph*), 135.83, 135.97 (s, *o*-Ph, Si*Ph*).

NMR reaction of (ArN)(^{t}BuN)Mo(PMe$_3$)(η^2-C$_2$H$_4$) with HSiCl$_3$

(ArN)(^{t}BuN)Mo(η^2-C$_2$H$_4$)(PMe$_3$) (22.4 mg, 0.0502 mmol) was dissolved in C$_6$D$_6$ in the glove box and transferred to an NMR tube. PMe$_3$ (10.34 μL, 0.101 mmol) and HSiCl$_3$ (12.6 μL, 0.0502 mmol) were sequentially added and a colour change from red to dark pink was observed. NMR analysis showed formation of the complex (^{t}BuN)Mo(PMe$_3$)$_2$(η^2-C$_2$H$_4$)Cl$_2$ (**III-49**) along with release of the silanimine dimer (ArNSiHCl)$_2$

(^{t}BuN)Mo(PMe$_3$)$_2$(η^2-C$_2$H$_4$)Cl$_2$ **^{1}H-NMR** (600 MHz, Benzene-d_6, 22 °C; δ, ppm): 0.64 (s, 9H, ^{t}*Bu*N), 1.43 (vt, 18H, 2 P*Me*$_3$, $^2J_{H-P}$ = 8.2 Hz), 2.27 (m, 2H, η^2-C$_2$H$_4$, $^3J_{H-H}$ = 10.1 Hz, $^2J_{H-H}$ = 2.6

Hz), 2.62 (m, 2H, η^2-C_2H_4, $^3J_{H-H}$ = 10.7 Hz, $^2J_{H-H}$ = 3.6 Hz) **^{31}P{^{1}H} NMR** (243.0 MHz, Benzene-d_6, 22 °C; δ, ppm): -6.11 (s, 2 *P*Me$_3$). **^{13}C{^{1}H} NMR** (151.0 MHz; Benzene-d_6, 22 °C; δ, ppm): 15.22 (vt, P*Me*$_3$, $^1J_{C-P}$ = 26.1 Hz), 28.66 (s, CH_3, ^{t}*Bu*N), 46.10 (t, *C*H$_2$, η^2-C_2H_4, $^2J_{C-P}$ = 2.7 Hz), 68.77 (s, Me$_3$*C*N, ^{t}*Bu*N).

(ArNSiHCl)$_2$ **^{1}H-NMR** (600 MHz, Benzene-d_6, 22 °C; δ, ppm): 1.12 (d, 24 H, C*H*$_3$, *Ar*N, $^3J_{H-H}$ = 6.7 Hz), 3.40 (sept, 4H, Me$_2$C*H*, *Ar*N, $^3J_{H-H}$ = 6.7 Hz), 5.47 (s, 2H, Si*H*Cl). **^{13}C{^{1}H} NMR** (151.0 MHz; Benzene-d_6, 22 °C; δ, ppm): 24.60 (s, *C*H$_3$, *Ar*N), 28.65 (s, Me$_2$*C*H, *Ar*N), 125.18 (s, *m*-Ph, *Ar*N), 128.57 (s, *p*-Ph, *Ar*N), 132.66 (s, *o*-Ph, *Ar*N), 144.78 (s, *i*-Ph, ArN). **^{29}Si INEPT+** (119.2 MHz, Benzene-d_6, 22 °C; δ, ppm): -19.86 (d, SiHCl, $^1J_{Si-H}$ = 337.0 Hz)**.**

Preparation of (^{t}BuN){μ-^{t}BuN(SiHPh)$_2$}Mo(H)(SiH$_2$Ph)(PMe$_3$)$_2$

A solution of (^{t}BuN)$_2$Mo(PMe$_3$)$_2$ (300.0 mg, 0.769 mmol) in hexanes (12 mL) was precooled to -30 °C using an acetone/CO_2 bath. PhSiH$_3$ (0.19 mL, 1.54) was added in one portion and the mixture stirred for 1 h 20 min at -30 °C. After this time the solution was warmed to 0/-5 °C and all volatiles removed in vacuum to give a light brown powder characterized as (^{t}BuN){μ-^{t}BuN(SiHPh)$_2$}Mo(H)(SiH$_2$Ph)(PMe$_3$)$_2$ (**III-51**). Yield: 0.38 g, 82 %. Alternatively, a similar procedure using complex (^{t}BuN)$_2$Mo(PMe$_3$)(η^2-C_2H_4) with one equivalent of PMe$_3$ in a hexane/toluene (5:1) mixture can be employed resulting in similar yields and purity.

^{1}H-NMR (600 MHz; Toluene-d$_8$; - 28 °C; δ, ppm): 0.62 (s, 9H, ^{t}*Bu*N), 0.99 (d, $^2J_{P-H}$ = 6.0 Hz, 9H, P*Me$_3$*), 1.04 (d, $^2J_{P-H}$ = 7.5 Hz, 9H, P*Me$_3$*), 1.47 (s, 9H, ^{t}*Bu*N), 1.54 (bd, 1H, $^2J_{P-H}$ = 21.0 Hz, Mo*H*), 5.13 (bd, 1H, $^2J_{P-H}$ = 19.6 Hz, Si*H*$_2$Ph), 5.60 (dd, 1H, $^3J_{P-H}$ = 14.9 Hz, $^2J_{H-H}$ = 7.5 Hz, Si*H*$_2$Ph), 6.03 (dd, 1H, $^3J_{P-H}$ = 9.6 Hz, $^3J_{P-H}$ = 3.7 Hz, {(Si*H*Ph)$_2$(*u*-N^{t}Bu)}), 6.67 (ddd, 1H, $^2J_{H-H}$ = 5.9 Hz, $^3J_{P-H}$ = 11.6 Hz, $^3J_{P-H}$ = 17.2 Hz, {(Si*H*Ph)$_2$(*u*-N^{t}Bu)}), 7.26 (m, 2H, *p*-H, Si*Ph*), 7.32 (t, 1H, $^3J_{H-H}$ = 7.5 Hz, *p*-H, Si*Ph*), 7.40 (t, 2H, $^3J_{H-H}$ = 7.5 Hz, *m*-H, Si*Ph*), 7.46 (t, 2H, $^3J_{H-H}$ =

7.5 Hz, *m*-H, Si*Ph*), 7.49 (t, 2H, $^{3}J_{H\text{-}H}$ = 7.5 Hz, *m*-H, Si*Ph*), 8.32 (bs, 2H, *o*-H, Si*Ph*), 8.48 (d, 2H, $^{3}J_{H\text{-}H}$ = 6.6 Hz, *o*-H, Si*Ph*), 8.54 (d, 2H, $^{3}J_{H\text{-}H}$ = 6.7 Hz, *o*-H, Si*Ph*). **^{1}H-NMR** (600 MHz; Toluene-d_8; 22 °C; δ, ppm): 0.61 (s, 9H, ^{t}*Bu*N), 1.05 (d, $^{2}J_{P\text{-}H}$ = 6.4 Hz, P*Me*$_3$), 1.14 (d, 9H, $^{2}J_{P\text{-}H}$ = 7.7 Hz, P*Me*$_3$), 1.39 (s, 9H, ^{t}*Bu*N), 1.50 (bd, 1H, $^{2}J_{P\text{-}H}$ = 21.0 Hz, Mo*H*), 5.05 (d, 1H, $^{3}J_{P\text{-}H}$ = 19.4 Hz, Si*H*$_2$Ph), 5.50 (bddd, 1H, $^{3}J_{P\text{-}H}$ = 15.9 Hz, $^{2}J_{H\text{-}H}$ = 7.4 Hz, Si*H*$_2$Ph), 6.04 (dd, 1H, $^{3}J_{P\text{-}H}$ = 3.7 Hz, $^{3}J_{P\text{-}H}$ = 9.2 Hz, {(Si*H*Ph)$_2$(*u*-N^{t}Bu)}), 6.59 (ddd, 1H, $^{2}J_{H\text{-}H}$ = 5.8 Hz, $^{3}J_{P\text{-}H}$ = 11.6 Hz, $^{3}J_{P\text{-}H}$ = 17.5 Hz, {(Si*H*Ph)$_2$(*u*-N^{t}Bu)}), 7.23 (m, 3H, *p*-H, Si*Ph*), 7.36 (t, 2H, $^{3}J_{H\text{-}H}$ = 7.3 Hz, *m*-H, Si*Ph*), 7.40 (t, 4H, $^{3}J_{H\text{-}H}$ = 7.0 Hz, *m*-H, Si*Ph*), 8.25 (d, 2H, $^{3}J_{H\text{-}H}$ = 7.0 Hz, *o*-H, Si*Ph*), 8.37 (d, 2H, $^{3}J_{H\text{-}H}$ = 7.3 Hz, *o*-H, Si*Ph*), 8.39 (d, 2H, $^{3}J_{H\text{-}H}$ = 7.3 Hz, *o*-H, Si*Ph*). **^{1}H{^{31}P}-NMR** (600 MHz, Toluene-d_8, 22 °C, δ, ppm, selected signals): 6.59 (d, 1H, $^{2}J_{H\text{-}H}$ = 5.9 Hz, {(Si*H*Ph)$_2$(*u*-N^{t}Bu)}), 6.04 (s, 1H, {(Si*H*Ph)$_2$(*u*-N^{t}Bu)}), 5.49 (s, 1H, Si*H*$_2$Ph), 5.05 (s, 1H, Si*H*$_2$Ph), 1.55 (d, 1H, $^{2}J_{H\text{-}H}$ = 5.9 Hz, Mo*H*). **^{31}P{^{1}H}-NMR** (243.0 MHz, Toluene-d_8, -28 °C, δ, ppm): -40.2 (d, $^{2}J_{P\text{-}P}$ = 34.5 Hz, *P*Me$_3$), -16.3 (d, $^{2}J_{P\text{-}P}$ = 34.5 Hz, *P*Me$_3$). **^{31}P{^{1}H}-NMR** (121.5 MHz, Toluene-d_8, 22 °C, δ, ppm): -41.5 (d, $^{2}J_{P\text{-}P}$ = 32.0 Hz, *P*Me$_3$), -17.2 (d, $^{2}J_{P\text{-}P}$ = 34.5 Hz, *P*Me$_3$). **^{29}Si INEPT+** (119.2 MHz, Toluene-d_8, -28 °C, *J* = 180 Hz, δ, ppm): -14.3 (tdd, $^{1}J_{Si\text{-}H}$ = 154.4 Hz, $^{2}J_{Si\text{-}P}$ = 25.0 Hz, $^{2}J_{Si\text{-}P}$ = 28.6 Hz, *Si*H$_2$Ph), -5.0 (d, $^{1}J_{Si\text{-}H}$ = 186.0 Hz, {(*Si*HPh)$_2$(*u*-N^{t}Bu)}), 1.4 (ddd, $^{1}J_{Si\text{-}H}$ = 166.9 Hz, $^{2}J_{Si\text{-}P}$ = 25.0 Hz, $^{2}J_{Si\text{-}P}$ = 20.3 Hz, {(*Si*HPh)$_2$(*u*-N^{t}Bu)}). **^{29}Si RF INEPT NMR** (119.2 MHz, Toluene-d_8, -18 °C, *J* = 180 Hz, δ, ppm): 1.4 (dd, $^{2}J_{Si\text{-}P}$ = 16.7 Hz, $^{2}J_{Si\text{-}P}$ = 28.6 Hz, {(*Si*HPh)$_2$(*u*-N^{t}Bu)}, "up"), -5.1 (d, $^{2}J_{Si\text{-}P}$ = 10.7 Hz, {(*Si*HPh)$_2$(*u*-N^{t}Bu)}, "up"), -14.7 (t, $^{2}J_{Si\text{-}P}$ = 23.8 Hz, *Si*H$_2$Ph, "down"). **^{1}H-^{31}P HSQC JC NMR** (243.0 Hz, Toluene-d_8; -20 °C; *J* = 15 Hz; ^{1}H projection; δ, ppm): 1.6 (d, $^{2}J_{H\text{-}P}$ = 30.0 Hz, {(Si*H*Ph)$_2$(*u*-N^{t}Bu)}). **^{13}C{^{1}H]-NMR** (151 MHz; Toluene-d_8; - 28 °C; δ, ppm): 14.9 (d, $^{1}J_{C\text{-}P}$ = 18.1 Hz, P*Me*$_3$), 19.1 (d, $^{1}J_{C\text{-}P}$ = 24.1 Hz, P*Me*$_3$), 30.3 (s, *C*H$_3$, ^{t}BuN), 31.7 (s, *C*H$_3$, ^{t}*Bu*N), 34.8 (s, *C*H$_3$, ^{t}BuN=Mo), 54.7 (s, *C*(CH$_3$)$_3$,

N^{t}Bu), 127.3 (s, *m*-C, Si*Ph*), 127.5 (s, *m*-C, Si*Ph*), 128.1 (s, *m*-C, Si*Ph*), 128.2 (s, *p*-C, Si*Ph*), 128.4 (s, *p*-C, Si*Ph*), 133.9 (s, *o*-C, Si*Ph*), 137.1 (s, *o*-C, Si*Ph*), 137.8 (s, *o*-C, Si*Ph*), 143.2 (s, *i*-C, Si*Ph*), 147.8 (s, *i*-C, Si*Ph*), 148.8 (s, *i*-C, Si*Ph*). **IR (nujol)**: 1825 cm^{-1} (medium, Mo-H), 1890 cm^{-1} (strong, Si-H), 2037 cm^{-1} (strong, Si-H), 2142 (strong, Si-H). **Elem. Anal.** (%): calc for $C_{32}H_{56}MoN_2P_2Si_3$ (710.945) C 54.06, H 7.94, N 3.94; found C 53.99 H 7.87, N 4.22.

General Procedure for Addition of Silane during VT NMR Study

To a solution of (^{t}BuN)Mo(PMe$_3$)(L) (L = PMe$_3$, η^2-CH$_2$CH$_2$) in toluene-d$_8$, PMe$_3$ was added in one portion at room temperature. The sample was cooled to -196 °C using liquid nitrogen on a Schlenk line and PhSiH$_3$ was directly added. The sample was quickly removed from the liquid nitrogen and inverted once, then immediately placed back. The sample was then placed into a pre-cooled NMR machine at the appropriate temperature and monitored at various temperatures. In some cases, the sample was allowed to react for 2-4 hours at -40 °C, then monitored by NMR at the appropriate temperature.

(^{t}BuN)Mo(η^3-N^{t}Bu-SiHPh-H)(PMe$_3$)$_2$(Et) (III-53)

^{1}H-NMR (600 MHz, Toluene-d_8, -53 °C, δ, ppm): -0.82 (s, 1H, Si-H$_{agostic}$, $^{1}J_{\text{Si-H}}$ = 125.1 Hz, found by ^{1}H-^{29}Si HSQC 1D JC), 1.03 (s, 9H, 3 CH$_3$, ^{t}*Bu*N=Mo), 1.10 (s, 9H, 3 CH$_3$, Mo-N^{t}*Bu*-SiH$_2$Ph), 1.32 (d, 9H, PMe$_3$, $^{2}J_{\text{H-P}}$ = 5.22 Hz), 1.43 (d, 9H, PMe$_3$, $^{2}J_{\text{H-P}}$ = 5.28 Hz), 1.96 (t, 3H, CH$_3$, Mo-CH$_2$-C*H$_3$*, $^{3}J_{\text{H-H}}$ = 7.53 Hz), 2.50 (m, 1H, Mo-C*H$_2$*-CH$_3$), 2.61 (m, 1H, Mo-C*H$_2$*-CH$_3$), 5.66 (s, 1H, Si-*H$_{class}$*, $^{1}J_{\text{Si-H}}$ = 212.0 Hz, found by ^{1}H-^{29}Si HSQC 1D JC), 7.27 (m, 2H, *m*-Ph), 7.96 (d, 2H, *o*-Ph, $^{3}J_{\text{H-H}}$ = 6.9 Hz). **^{31}P{^{1}H}-NMR** (243.0 MHz, Toluene-d_8, -53 °C, δ, ppm): -7.78 (d, 1P, PMe$_3$, $^{2}J_{\text{P-P}}$ = 291.7 Hz), -10.12 (d, 1P, PMe$_3$, $^{2}J_{\text{P-P}}$ = 291.8 Hz). **^{1}H-^{29}Si HSQC NMR** (119.0 MHZ, Toluene-d_8; -53 °C; *J* = 150 Hz; ^{29}Si projection, δ, ppm): -75.4 (Mo-N^{t}Bu-*Si*H$_2$Ph).

(^{t}BuN)Mo(η^3-N^{t}Bu-SiHPh-H)(PMe$_3$)$_2$(SiH$_2$Ph) (III-54)

^{1}H-NMR (600 MHz, Toluene-d_8, -78 °C, δ, ppm): 0.17 (s, 1H, Si-H$_{agostic}$, $^1J_{Si-H}$ = 110.3 Hz, found by ^{1}H-^{29}Si HSQC 1D JC), 1.00 (s, 9H, 3 CH$_3$, ^{t}*Bu*N=Mo), 1.35 (bs, 18H, 2 P*Me$_3$*), 1.37 (s, 9H, 3 CH$_3$, Mo-N^t*Bu*-SiH$_2$Ph), 5.43 (s, 1H, Si-*H$_{class}$*, $^1J_{Si-H}$ = 226.1 Hz, found by ^{1}H-^{29}Si HSQC 1D JC), 5.76 (s, 1H, Mo-Si*H$_2$*Ph), 5.81 (s, 1H, Mo-Si*H$_2$*Ph), 7.23 (t, 2H, *m*-Ph, Mo-N^{t}BuSiH*Ph*, $^3J_{H-H}$ = 7.26 Hz), 7.37 (t, 2H, *m*-Ph, Mo-SiH$_2$*Ph*, $^3J_{H-H}$ = 7.23 Hz), 7.84 (d, 2H, *o*-Ph, Mo-N^{t}BuSiH*Ph*, $^3J_{H-H}$ = 6.84 Hz), 8.22 (d, 2H, *o*-Ph, Mo-SiH$_2$*Ph*, $^3J_{H-H}$ = 6.98 Hz). **^{31}P{^{1}H}-NMR** (243.0 MHz, Toluene-d_8, -72 °C, δ, ppm): -10.9 (d, 1P, PMe$_3$, $^2J_{P-P}$ = 268.2 Hz), -13.0 (d, 1P, PMe$_3$, $^2J_{P-P}$ = 266.8 Hz). **^{1}H-^{29}Si HSQC NMR** (119.0 MHZ, Toluene-d_8; -53 °C; *J* = 150 Hz; ^{29}Si projection, δ, ppm): -8.4 (Mo-*Si*H$_2$Ph), -81.1 (Mo-N^{t}Bu-*Si*H$_2$Ph).

(^{t}BuN)Mo(H)(η^3-PhHSi-N(^{t}Bu)-SiHPh-H)(PMe$_3$)$_2$ (III-52)

^{1}H-NMR (600 MHz, Toluene-d_8, -41 °C, δ, ppm): -4.63 (dd, 1H, $^2J_{H-P}$ = 54.9 Hz, $^2J_{H-P}$ = 19.5 Hz, Mo-*H*, minor isomer), -4.43 (ddd, 1H, $^2J_{H-P}$ = 46.1 Hz, $^2J_{H-P}$ = 16.7 Hz, $^2J_{H-H}$ = 4.4 Hz, Mo-*H*, major isomer), 0.37 (dt, 1H, $^2J_{H-P}$ = 45.5 Hz, $^2J_{H-H}$ = 4.4 Hz, Si*H$_{agostic}$*, major isomer), 0.81 (d, 9H, $^2J_{H-P}$ = 7.3 Hz, P*Me$_3$*, major isomer), 0.88 (d, 9H, $^2J_{H-P}$ = 7.3 Hz, P*Me$_3$*, major isomer), 1.36 (s, 9H, ^{t}*Bu*N=Mo, major isomer), 1.44 (s, 9H, μ-N(*^{t}Bu)*, major isomer), 6.84 (bd, 1H, $^2J_{H-H}$ = 5.3 Hz, Si*H*$_{classical}$, major isomer), 6.92 (bs, 1H, Mo-Si*H*Ph, major isomer), 7.22 (bs, 1H, Mo-Si*H*Ph, minor isomer), 7.23 (t, 1H, $^3J_{H-H}$ = 7.4 Hz, *p*-H, Mo-SiH*Ph*, major isomer), 7.27 (t, 1H, *p*-H, $^3J_{H-H}$ = 7.4 Hz, SiH$_2$*Ph*, major isomer), 7.36 (t, 1H, $^3J_{H-H}$ = 7.1 Hz, *m*-H, Mo-SiH*Ph*, major isomer), 7.43 (t, 2H, *m*-H, SiH$_2$*Ph*, $^3J_{H-H}$ = 7.3 Hz, major isomer), 7.47 (t, 1H, *m*-H, Mo-SiH*Ph*, $^3J_{H-H}$ = 6.9 Hz, major isomer), 8.25 (bd, 1H, *o*-H, Mo-SiH*Ph*, $^3J_{H-H}$ = 6.2 Hz, major isomer), 8.39 (bs, 2H, *o*-H, SiH$_2$*Ph*, $^3J_{H-H}$ = 7.3 Hz, major isomer), 8.56 (bd, 1H, *o*-H, Mo-SiH*Ph*, $^3J_{H-H}$ = 6.3 Hz, major isomer). **^{31}P{^{1}H}-NMR** (243.0 MHz, Toluene-d_8, -25 °C, δ, ppm): 2.4 (d, $^2J_{P-P}$ = 43.7 Hz,

P*Me*$_3$, minor isomer), -0.8 (d, $^2J_{P\text{-}P}$ = 43.7 Hz, *P*Me$_3$, major isomer), -5.1 (d, $^2J_{P\text{-}P}$ = 43.7 Hz, *P*Me$_3$, minor isomer), -7.0 (d, $^2J_{P\text{-}P}$ = 43.7 Hz, *P*Me$_3$, major isomer). **^{29}Si INEPT+** (119 MHz, Toluene-d_8, -40 °C, *J* = 200 Hz, δ, ppm): -19.5 (dd, $^1J_{H\text{-}Si}$ = 37.3 Hz, $^1J_{H\text{-}Si}$ = 199.8 Hz, Si*H*$_2$Ph, minor isomer), -16.2 (dd, $^1J_{H\text{-}Si}$ = 34.9 Hz, $^1J_{H\text{-}Si}$ = 195.6 Hz, *Si*H$_2$Ph, major isomer), 5.2 (d, $^1J_{H\text{-}Si}$ = 172.3 Hz, *Si*HPh, major isomer), 7.5 (d, $^1J_{H\text{-}Si}$ = 182.7 Hz, *Si*HPh, minor isomer). **^{13}C{^{1}H}-NMR** (151 MHz; Toluene-d$_8$; - 40 °C; δ, ppm): 19.89 (d, 3C, P*Me*$_3$, $^1J_{C\text{-}P}$ = 23.8 Hz), 22.65 (d, 3C, P*Me*$_3$, $^1J_{C\text{-}P}$ = 24.8 Hz), 31.35 (s, 3C, *C*H$_3$, ^{t}BuN), 31.97 (s, 3C, *C*H$_3$, ^{t}BuN), 54.54 (s, 1C, *C*(CH$_3$)$_3$, ^{t}BuN), 65.70 (s, 1C, *C*(CH$_3$)$_3$, ^{t}BuN), 127-130 (*p*-Ph, *m*-Ph, overlapped by solvent signals, found by ^{1}H-^{13}C HSQC), 134.0 (*o*-Ph, 2C, MoSiH*Ph*), 137.1 (*o*-Ph, 2C, Si*Ph*), 149.2 (*i*-Ph, 1C, Si*Ph*), 151.0 (*i*-Ph, 1C, Si*Ph*).

(^{t}BuN)Mo{(SiHPh)$_2$(*μ*-N^{t}Bu)}(PMe$_3$)$_2$(H)$_2$ (III-55)

^{1}H-NMR (600 MHz, Toluene-d_8, 0 °C, δ, ppm): 0.80 (s, 9H, 3 CH$_3$, Mo=N^t*Bu*), 1.05 (d, 9H, PMe$_3$, $^2J_{H\text{-}P}$ = 7.7 Hz), 1.10 (d, 9H, PMe$_3$, $^2J_{H\text{-}P}$ = 6.7 Hz), 1.25 (Mo-H, found by ^{1}H-^{1}H COSY and ^{1}H-^{29}Si HSQC (*J* = 7 Hz), partially obscured by complex **3**) 1.39 (s, 9H, 3 CH$_3$, Si-N^t*Bu*-Si), 1.48 (Mo-H, found by ^{1}H-^{1}H COSY and ^{1}H-^{29}Si HSQC (*J* = 7 Hz), partially obscured by complex **3**), 5.92 (ddd, 1H, Si-*H*, $^3J_{H\text{-}H}$ = 3.8 Hz, $^3J_{H\text{-}P}$ = 5.93 Hz, $^2J_{H\text{-}P}$ = 11.57 Hz, $^1J_{Si\text{-}H}$ = 169.2 Hz {found by ^{1}H-^{29}Si HSQC 1D JC}), 6.51 (dt, 1H, Si-*H*, $^3J_{H\text{-}H}$ = 6.1 Hz, $^2J_{H\text{-}P}$ = 6.1 Hz, $^2J_{H\text{-}P}$ = 12.2 Hz, $^1J_{Si\text{-}H}$ = 187.1 Hz {found by ^{1}H-^{29}Si HSQC 1D JC}), 8.33 (d, 2H, *o*-Ph, $^3J_{H\text{-}H}$ = 6.9 Hz). **^{1}H{^{31}P}-NMR** (600 MHz, Toluene-d_8, 0 °C, δ, ppm, selected signals): 6.51 (d, 1H, Si-*H*, $^3J_{H\text{-}H}$ = 6.12 Hz), 5.92 (bd, 1H, Si-*H*, $^3J_{H\text{-}H}$ = 3.7 Hz), 1.10 (s, P*Me*$_3$), 1.05 (s, P*Me*$_3$). **^{31}P{^{1}H}-NMR** (243.0 MHz, Toluene-d_8, 0 °C, δ, ppm): -9.65 (d, 1P, PMe$_3$, $^2J_{P\text{-}P}$ = 31.3 Hz), -34.60 (d, 1P, PMe$_3$, $^2J_{P\text{-}P}$ = 31.1 Hz). **^{31}P{^{1}H}-NMR** (selectively decoupled from methyl group at 1.10 ppm in ^{1}H-NMR, 243.0 MHz, Toluene-d_8, 0 °C, δ, ppm): -9.63 (bt, 1P, PMe$_3$, $^2J_{P\text{-}P}$ = 33.4 Hz), -34.49

(m, 1P, PMe_3, $^3J_{P\text{-}H}$ = 13.0 Hz, $^2J_{P\text{-}P}$ = 27.6 Hz, $^2J_{P\text{-}H}$ = 51.7 Hz). **$^{31}P\{^1H\}$-NMR** (selectively decoupled from methyl group at 1.05 ppm in ^{1}H-NMR, 243.0 MHz, Toluene-d_8, 0 °C, δ, ppm): -9.63 (dd, 1P, PMe_3, $^2J_{P\text{-}P}$ = 33.4 Hz, $^2J_{P\text{-}H}$ = 33.4 Hz), -34.70 (m, 1P, PMe_3). **$^{31}P\{^1H\}$-NMR** (selectively decoupled from hydride at 1.25 ppm in ^{1}H-NMR, 243.0 MHz, Toluene-d_8, 0 °C, δ, ppm): -9.63 (d, 1P, PMe_3, $^2J_{P\text{-}P}$ = 33.4 Hz), -34.60 (m, 1P, PMe_3). **^{29}Si INEPT +** (119 MHz, Toluene-d_8, 0 °C, J = 150 Hz, δ, ppm): 4.05 (d, $^1J_{Si\text{-}H}$ = 170.0 Hz), -2.17 (d, $^1J_{Si\text{-}H}$ = 185.3 Hz).

(^{t}BuN){μ-^{t}BuN(SiHPh)$_2$}Mo(PMe$_3$)$_3$ (III-56)

^{1}H-NMR (600 MHz, Toluene-d_8, 0 °C, δ, ppm): 0.90 (d, 9H, PMe_3, $^2J_{H\text{-}P}$ = 6.78 Hz), 1.06 (s, 9H, 3 CH_3, ^{t}*Bu*N=Mo), 1.26 (d, 9H, PMe_3, $^2J_{H\text{-}P}$ = 6.12 Hz), 1.45 (s, 9H, 3 CH_3, μ-N^t*Bu*), 1.74 (d, 9H, PMe_3, $^2J_{H\text{-}P}$ = 6.90 Hz), 5.36 (ddd, 1H, MoSi*H*Ph, $^1J_{Si\text{-}H}$ = 226.1 Hz, found by ^{1}H-^{29}Si HSQC 1D JC, $^2J_{H\text{-}P}$ = 3.00 Hz, $^2J_{H\text{-}P}$ = 4.98 Hz, $^2J_{H\text{-}P}$ = 7.80 Hz), 7.05 (bd, 1H, MoSi*H*Ph, $^1J_{Si\text{-}H}$ = 226.1 Hz, found by ^{1}H-^{29}Si HSQC 1D JC, partially obscured by solvent peaks), 7.29 (t, 2H, *m*-Ph, $^3J_{H\text{-}H}$ = 7.56 Hz), 7.47 (t, 2H, *m*-Ph, $^3J_{H\text{-}H}$ = 7.47 Hz), 7.96 (d, 2H, *o*-Ph, $^3J_{H\text{-}H}$ = 7.08Hz), 8.27 (d, 2H, *o*-Ph, $^3J_{H\text{-}H}$ = 6.96 Hz). **$^1H\{^{31}P\}$-NMR** (600 MHz, Toluene-d_8, 0 °C, δ, ppm; selected signals): 0.90 (s, 9H, PMe_3), 1.26 (s, 9H, PMe_3), 1.74 (s, 9H, PMe_3), 5.36 (s, 1H, Mo-Si*H*Ph), 7.05 (s, 1H, Mo-Si*H*Ph). **$^{31}P\{^1H\}$-NMR** (243.0 MHz, Toluene-d_8, 0 °C, δ, ppm): 5.66 (t, 1P, PMe_3, $^2J_{P\text{-}P}$ = 22.6 Hz), -7.48 (dd, 1P, PMe_3, $^2J_{P\text{-}Pcis}$ = 18.2 Hz, $^2J_{P\text{-}Ptrans}$ = 91.1 Hz), -13.54 (dd, 1P, PMe_3, $^2J_{P\text{-}Pcis}$ = 27.4 Hz, $^2J_{P\text{-}Ptrans}$ = 91.2 Hz). **^{29}Si INEPT+** (119 MHz, Toluene-d_8, 0 °C, J = 150 Hz, δ, ppm): 41.70 (bd, $^1J_{Si\text{-}H}$ = 169.3 Hz), -10.42 (dddd, Mo-*Si*HPh, $^1J_{Si\text{-}H}$ = 152.0 Hz, $^2J_{Si\text{-}P}$ = 19.3 Hz, $^2J_{Si\text{-}P}$ = 19.3 Hz, $^2J_{Si\text{-}P}$ = 38.3 Hz).

Reactivity of (^{t}BuN)Mo(H)(SiH$_2$Ph){(μ-^{t}BuN)(SiHPh)$_2$}(PMe$_3$)$_2$ (III-51) with Organic Substrates

NMR reaction of (^{t}BuN)Mo(H)(SiH$_2$Ph){(μ-^{t}BuN)(SiHPh)$_2$}(PMe$_3$)$_2$ and benzaldehyde

A light brown solution of (^{t}BuN)Mo(H)(SiH_2Ph){(μ-^{t}BuN)($SiHPh)_2$}($PMe_3)_2$ (15.4 mg, 0.0217 mmol) in C_6D_6 was placed in an NMR tube. Benzaldehyde (4.42 μL, 0.0432 mmol) was added *via* 10 μL syringe directly to the solution. Immediately, the colour changed to dark brown and formation of the hydrosilylation product was seen PhH_2SiOBn as well as decomposition.

NMR reaction of (^{t}BuN)Mo(H)(SiH_2Ph){(μ-^{t}BuN)($SiHPh)_2$}($PMe_3)_2$ and acetophenone

A light brown solution of (^{t}BuN)Mo(H)(SiH_2Ph){(μ-^{t}BuN)($SiHPh)_2$}($PMe_3)_2$ (15.4 mg, 0.0217 mmol) in C_6D_6 was placed in an NMR tube. Benzaldehyde (4.42 μL, 0.0432 mmol) was added *via* 10 μL syringe directly to the solution. Immediately, the colour changed to dark brown and formation of the hydrosilylation product was seen $PhH_2SiOCH(Me)Ph$ as well as decomposition.

NMR reaction of (^{t}BuN)Mo(H)(SiH_2Ph){(μ-^{t}BuN)($SiHPh)_2$}($PMe_3)_2$ and phenylacetylene

A light brown solution of (^{t}BuN)Mo(H)(SiH_2Ph){(μ-^{t}BuN)($SiHPh)_2$}($PMe_3)_2$ (22.5 mg, 0.0316 mmol) in C_6D_6 was placed in an NMR tube. Phenylacetylene (3.48 μL, 0.0316 mmol) was added *via* 10 μL syringe directly to the solution. Immediately, the colour changed to dark brown and formation of the hydrosilylation product was seen $H_2C=C(Ph)SiH_2Ph$ as well as decomposition.

NMR reaction of (^{t}BuN)Mo(H)(SiH_2Ph){(μ-^{t}BuN)($SiHPh)_2$}($PMe_3)_2$ and styrene

A light brown solution of (^{t}BuN)Mo(H)(SiH_2Ph){(μ-^{t}BuN)($SiHPh)_2$}($PMe_3)_2$ (15.8 mg, 0.0222 mmol) in C_6D_6 was placed in an NMR tube. Soon after styrene (2.55 μL, 0.022 mmol) was added *via* 10 μL syringe directly to the solution. The solution remained light brown in colour for a 24 hour period. After 3 days the solution turned dark brown and decomposition of the starting material was observed as well as production of the hydrosilylation product $PhCH(SiH_2Ph)CH_3$.

NMR reaction of (^{t}BuN)Mo(H)(SiH_2Ph){(μ-^{t}BuN)($SiHPh)_2$}($PMe_3)_2$ and ethylene

A light brown solution of (^{t}BuN)Mo(H)(SiH_2Ph){(μ-^{t}BuN)($SiHPh)_2$}($PMe_3)_2$ (15.8 mg, 0.0222 mmol) in C_6D_6 was placed in an NMR tube. The NMR tube was taken out of the glove box and

placed on a Schlenk line and freeze-pump-thawed three times using liquid N_2. Ethylene gas was condensed into the NMR tube and the solution was allowed to react. The solution quickly changed colour once removed from the liquid N_2 bath and a variety of products were observed including the NMR characterized (^{t}BuN)Mo(κ^2-*Si*,*C*-*Si*HPh-N^{t}Bu-SiHPh-*C*H(CH_3))(PMe_3)(η^2-C_2H_4).

^{1}H-NMR (600 MHz, Benzene-d_6, 22 °C, δ, ppm): - 2.12 (d, 3H, C*H*$_3$, $^3J_{H\text{-}H}$ = 6.9 Hz), 0.47 (s, 9H, C*H*$_3$, ^{t}Bu), 0.87 (d, 9H, P*Me*$_3$, $^2J_{H\text{-}P}$ = 7.8 Hz), 1.02 (signal corresponding to CH methine, obscured by other products, found by ^{1}H-^{13}C HSQC and HMBC), 1.82 (s, 9H, C*H*$_3$, ^{t}Bu), 2.37 (ddd, 2H, η^2-C_2*H*$_4$, $^3J_{H\text{-}H}$ = 18.3, $^2J_{H\text{-}H}$ = 6.1 Hz), 2.5 (ddd, 2H, η^2-C_2*H*$_4$, $^3J_{H\text{-}H}$ = 18.4, $^2J_{H\text{-}H}$ = 6.2 Hz), 6.64 (s, 1H, Si*H*Ph), 6.65 (d,1H, Si*H*Ph, $^2J_{H\text{-}P}$ = 7.8 Hz), 7.1 -7.5 (*m*-Ph and *p*-Ph obscured by multiple products), 8.40 (d, 2H, *o*-Ph, SiH*Ph*, $^3J_{H\text{-}H}$ = 7.3 Hz), 8.50 (d, 2H, *o*-Ph, SiH*Ph*, $^3J_{H\text{-}H}$ = 7.9 Hz). **^{1}H{^{31}P}-NMR** (600 MHz, Benzene-d_6, 22 °C, δ, ppm, selected signals): 6.65 (s, 1H, Si*H*Ph). **^{31}P{^{1}H}-NMR** (243.0 MHz, Benzene-d_6, 22 °C, δ, ppm): -5.1 ppm (s, 1P, *P*Me_3). **^{1}H-^{29}Si HSQC** (119 MHz, Benzene-d_6, 22 °C, *J* = 200 Hz, ^{29}Si projections, δ, ppm): 39.8 ppm (*Si*HPh), -9.1 (*Si*HPh) **^{1}H-^{13}C HSQC** (151 MHz; Benzene-d_6, 22 °C; δ, ppm): 1.64 (s, *C*H_3, MoCH*C*H_3), 14.24 (d, *C*H_3, $^1J_{C\text{-}P}$ = 20.1 Hz), 19.78 (d, *C*H, Mo*C*HCH$_3$, $^2J_{C\text{-}P}$ = 7.62 Hz), 30.03 (s, ^{t}*Bu*N), 31.27 (s, η^2-*C*$_2$H$_4$), 33.71 (s, ^{t}*Bu*N).

NMR reaction of (^{t}BuN)Mo(PMe_3)(η^2-C_2H_4) with Ethylene and $PhSiH_3$

(^{t}BuN)$_2$Mo(PMe_3)(η^2-C_2H_4) (24.5 mg, 0.0716 mmol) was dissolved in C_6D_6 in the glove box and transferred to an NMR tube. This was then placed on a Schlenk line and freeze-pump-thawed three times. After this was done ethylene gas was quickly condensed in the NMR tube and thawed back to room temperature showing no reactivity with the starting material. To this $PhSiH_3$ (8.82 μL, 0.0716 mmol) was added to the ethylene atmosphere and allowed to react for 2

hours at room temperature. 2D-NMR experiments showed the production of the ethyl/ethylene β-agostic silylamido complex (^{t}BuN)Mo(η^3-N^{t}Bu-Si(Et)Ph-H)(Et)(η^2-C_2H_4) (**III-57**). This complex slowly decomposes after 2 days at room temperature.

^{1}H-NMR (600 MHz, Benzene-d_6, 22 °C, δ, ppm): 1.13 (CH_2, SiPh*Et*, found by ^{1}H-^{29}Si HSQC (J = 15 Hz) and ^{1}H-^{13}C HMBC), 1.23 (s, 9H, ^{t}*Bu*N), 1.36 (Si-*H*···Mo, found by ^{1}H-^{29}Si HSQC (J = 150 Hz)), 1.64 (s, 9H, ^{t}*Bu*N), 2.17 (t, 3H, CH_3, Et, $^3J_{H-H}$ = 7.7 Hz), 2.52 (ddd, 2H, η^2-C_2H_4, $^3J_{H-H}$ = 11.7, $^2J_{H-H}$ = 6.3 Hz), 2.70 (m, 2H, η^2-C_2H_2), 2.70 (m, 1H, CH_2, Et), 2.83 (m, 3H, overlapping multiplets of CH_2 and η^2-C_2H_2), 7.10 (m, 3H, *m*-Ph & *p*-Ph, SiEt*Ph*), 7.53 (d, 2H, *o*-Ph, $^3J_{H-H}$ = 7.8 Hz). **^{29}Si INEPT+** (119 MHz, Benzene-d_6, 22 °C, J = 150 Hz, δ, ppm): -52.8 (d, PhEt*Si*-H···Mo, $^1J_{Si-H}$ = 149.3 Hz). **^{1}H-^{13}C HSQC** (151 MHz; Benzene-d_6, 22 °C; δ, ppm): 14.0 (*C*H_3, Si*Et*), 21.9 (*C*H_3, *Et*), 28.4 (*C*H_2, Et), 30.1 (^{t}*Bu*N), 34.3 (*C*H_2, η^2-*C*$_2H_2$), 36.9 (^{t}*Bu*N), 39.6 (*C*H_2, η^2-*C*$_2H_2$), 128.2 (*p*-Ph), 129.8 (*m*-Ph), 135.2 (*o*-Ph).

NMR reaction of (^{t}BuN)Mo(PMe$_3$)(η^2-C$_2$H$_4$) with Ethylene, BPh$_3$ and PhSiH$_3$

(^{t}BuN)$_2$Mo(PMe$_3$)(η^2-C_2H_4) (20.4 mg, 0.0596 mmol) and BPh$_3$ (14.5 mg, 0.0599 mmol) were dissolved in C_6D_6 in two separate vials in the glove box, mixed together and transferred to an NMR tube. This was then placed on a Schlenk line and freeze-pump-thawed three times. After this was done ethylene gas was quickly condensed in the NMR tube and thawed back to room temperature showing no reactivity with the starting material. To this PhSiH$_3$ (7.35 μL, 0.0596 mmol) was added to the ethylene atmosphere and allowed to react for 1 hour at room temperature. 2D-NMR experiments showed the production of the ethyl/ethylene non-agostic silylamido complex (^{t}BuN)Mo(N^{t}BuSiH$_2$Ph)(Et)(η^2-C_2H_4) (**III-59**). Adding PMe$_3$ to this solution generates (^{t}BuN)Mo(η^3-N^{t}Bu-Si(Et)Ph-H)(Et)(η^2-C_2H_4) (**III-58**).

^{1}H-NMR (600 MHz, Benzene-d_6, 22 °C, δ, ppm): 1.18 (s, 9H, ^{t}*Bu*N), 1.58 (m, 1H, η^2-C$_2$*H*$_4$), 1.61 (s, 9H, ^{t}*Bu*N), 1.79 (m, 1H, η^2-C$_2$*H*$_4$), 2.17 (t, 3H, C*H*$_3$, Et, $^3J_{H\text{-}H}$ = 7.8 Hz), 2.42 (ddd, 1H, η^2-C$_2$*H*$_4$, $^3J_{H\text{-}H}$ = 11.5 Hz, $^2J_{H\text{-}H}$ = 6.4 Hz), 2.72 (m, 1H, C*H*$_2$, Et), 2.76 (ddd, 1H, η^2-C$_2$*H*$_4$, $^3J_{H\text{-}H}$ = 11.1 Hz, $^2J_{H\text{-}H}$ = 5.0 Hz), 2.85 (m, 1H, C*H*$_2$, Et), 3.08 (d, 1H, Si*H*$_2$Ph, $^2J_{H\text{-}H}$ = 3.4 Hz), 3.44 (d, 1H, Si*H*$_2$Ph, $^2J_{H\text{-}H}$ = 3.4 Hz), 7.09 (d, 1H, p-Ph, Si*Ph*, $^3J_{H\text{-}H}$ = 7.8 Hz), 7.16 (t, 2H, *m*-Ph, Si*Ph*, $^3J_{H\text{-}H}$ = 7.8 Hz), *7*.94 (d, 2H, *o*-Ph, Si*Ph*, $^3J_{H\text{-}H}$ = 7.5 Hz). **^{1}H-^{29}Si HSQC** (119 MHz, Benzene-d_6, 22 °C, *J* = 200 Hz, ^{29}Si projections, δ, ppm): -71.0 Hz (*Si*H$_2$Ph). **^{1}H-^{29}Si HSQC 1D JC** (119 MHz, Benzene-d_6, 22 °C, *J* = 200 Hz, ^{29}Si satellites, δ, ppm): 3.08 (dd, 1H, Si*H*$_2$Ph,$^1J_{Si\text{-}H}$ = 197.8 Hz), 3.44 (dd, 1H, Si*H*$_2$Ph, $^1J_{Si\text{-}H}$ = 188.1 Hz). **^{1}H-^{13}C HSQC** (151 MHz; Benzene-d_6, 22 °C; δ, ppm): 21.5 (*C*H$_3$, Et), 29.0 (*C*H$_2$, Et), 30.1 (^{t}*Bu*N), 33.5 (*C*H$_2$, η^2-*C*$_2$H$_4$), 36.8 (^{t}*Bu*N), 40.2 (*C*H$_2$, η^2-*C*$_2$H$_4$), 128.4 (*p*-Ph), 131.5 (*m*-Ph), 136.0 (*o*-Ph).

NMR reaction of (^{t}BuN)Mo(H)(SiH$_2$Ph){(μ-^{t}BuN)(SiHPh)$_2$}(PMe$_3$)$_2$ and Acetonitrile

(^{t}BuN)Mo(H)(SiH$_2$Ph){(μ-^{t}BuN)(SiHPh)$_2$}(PMe$_3$)$_2$ (17.8 mg, 0.0250 mmol) was dissolved in C$_6$D$_6$ and placed in an NMR tube. Acetonitrile (1.31 μL, 0.0250 mmol) was added *via* 10 μL syringe and the solution allowed to react overnight. After one night at room temperature generation of the acetonitrile complex (^{t}BuN=)Mo{η^2-SiHPh-N^{t}Bu-SiHPh-N=C(Me)}(PMe$_3$)$_2$ (**III-60**) was observed according to NMR in a 4:1 ratio with a minor isomer.

^{1}H-NMR (600 MHz, Benzene-d_6, 22 °C, δ, ppm): 0.44 (d, 9H, P*Me*$_3$, $^2J_{H\text{-}P}$ = 6.6 Hz, minor), 0.76 (d, 9H, P*Me*$_3$, $^2J_{H\text{-}P}$ = 6.4 Hz, major), 1.26 (d, 9H, P*Me*$_3$, $^2J_{H\text{-}P}$ = 6.8 Hz, major), 1.38 (s, 9H, ^{t}*Bu*N, minor), 1.40 (s, 9H, ^{t}*Bu*N, major), 1.76 (s, 9H, ^{t}*Bu*N, major), 1.78 (s, 9H, ^{t}*Bu*N, minor), 2.66 (t, 3H, C*H*$_3$, η^2-N≡C*Me*, $^4J_{H\text{-}P}$ = 2.1 Hz, major), 2.88 (t, 3H, C*H*$_3$, η^2-N≡C*Me*, $^4J_{H\text{-}P}$ = 2.1 Hz, minor), 6.30 (bq, 1H, Si*H*, $^3J_{H\text{-}P}$ = 2.7 Hz, minor), 6.31 (bq, 1H, Si*H*, $^3J_{H\text{-}P}$ = 2.7 Hz, major), 7.13 (d, 1H, Si*H*, $^3J_{H\text{-}P}$ = 7.7 Hz, minor), 7.17 (d, 1H, Si*H*, $^3J_{H\text{-}P}$ = 6.8 Hz, major), 7.29 – 7.33 (m, *p*-

Ph, major & minor, found by ^{1}H-^{13}C HSQC), 7.40 (t, 2H, *m*-Ph, $^{3}J_{H\text{-}H}$ = 7.4 Hz, major), 7.45 (t, 2H, *m*-Ph, $^{3}J_{H\text{-}H}$ = 7.5 Hz, major), 7.51 (t, 2H, *m*-Ph, $^{3}J_{H\text{-}H}$ = 7.5 Hz, minor), 8.05 (d, 2H, *o*-Ph, $^{3}J_{H\text{-}H}$ = 6.9 Hz, major), 8.21 (d, 2H, *o*-Ph, $^{3}J_{H\text{-}H}$ = 6.8 Hz, major), 8.26 (d, 2H, *o*-Ph, $^{3}J_{H\text{-}H}$ = 6.9 Hz, minor), 8.32 (d, 2H, *o*-Ph, $^{3}J_{H\text{-}H}$ = 7.0 Hz, minor). **^{1}H{^{31}P}-NMR** (600 MHz, Benzene-d_6, 22 °C, δ, ppm, selected signals): 2.66 (s, 3H, C*H*$_3$, η^2-N≡C*Me*, major), 2.88 (s, 3H, C*H*$_3$, η^2-N≡C*Me*, minor), 6.30 (s, 1H, Si*H*, minor), 6.31 (d, 1H, Si*H*, $^{4}J_{H\text{-}H}$ = 1.5 Hz, major), 7.13 (s, 1H, Si*H*, minor), 7.17 (d, 1H, Si*H*, $^{4}J_{H\text{-}H}$ = 1.5 Hz, major). **^{31}P{^{1}H}-NMR** (243.0 MHz, Benzene-d_6, 22 °C, δ, ppm): -1.37 (d, 1P, *P*Me$_3$, $^{2}J_{P\text{-}P}$ = 227.8 Hz, minor), -3.04 (d, 1P, *P*Me$_3$, $^{2}J_{P\text{-}P}$ = 228.0 Hz, major), -4.82 (d, 1P, *P*Me$_3$, $^{2}J_{P\text{-}P}$ = 227.7 Hz, minor), -5.81 (d, 1P, *P*Me$_3$, $^{2}J_{P\text{-}P}$ = 228.2 Hz, major). **^{29}Si INEPT+** (119 MHz, Benzene-d_6, 22 °C, δ, ppm): 40.11 (doublet of multiplets, *Si*HPh, $^{1}J_{Si\text{-}H}$ = 151.9 Hz, major), -25.99 (doublet of multiplets, *Si*HPh, $^{1}J_{Si\text{-}H}$ = 222.7 Hz, major), -27.29 (doublet of multiplets, $^{1}J_{Si\text{-}H}$ = 209.2 Hz, minor). **^{13}C{^{1}H} NMR** (151.0 MHz; Benzene-d_6, 22 °C; δ, ppm): 18.41 (d, P*Me*$_3$, $^{1}J_{C\text{-}P}$ = 18.4 Hz, minor), 18.61 (d, P*Me*$_3$, $^{1}J_{C\text{-}P}$ = 17.5 Hz, major), 19.17 (d, P*Me*$_3$, $^{1}J_{C\text{-}P}$ = 18.2 Hz, minor), 19.42 (d, P*Me*$_3$, $^{1}J_{C\text{-}P}$ = 18.5 Hz, major), 29.65 (s, *C*H$_3$, η^2-N≡C*Me*, major), 29.91 (s, *C*H$_3$, η^2-N≡C*Me*, minor), 33.68 (s, (*C*H$_3$)$_3$C, ^{t}*Bu*N, major), 33.69 (s, (*C*H$_3$)$_3$C, ^{t}*Bu*N, minor), 33.84 (s, (*C*H$_3$)$_3$C, ^{t}*Bu*N, minor), 34.37 (s, (*C*H$_3$)$_3$C, ^{t}*Bu*N, major), 37.96 (η^2-N≡*C*Me, found by HMBC, major), 38.83 (η^2-N≡*C*Me, found by HMBC, minor), 54.65 (s, (CH$_3$)$_3$*C*, ^{t}*Bu*N, minor), 54.73 (s, (CH$_3$)$_3$*C*, ^{t}*Bu*N, major), 65.20 (s, (CH$_3$)$_3$*C*, ^{t}*Bu*N, minor), 65.24 (s, (CH$_3$)$_3$*C*, ^{t}*Bu*N, major), 125.65 (s, *p*-Ph, major), 125.72 (s, *p*-Ph, minor), 127.39 (s, *m*-Ph, major), 128.04 (s, *m*-Ph, major), 129.08 (s, *p*-Ph, minor), 129.32 (s, *p*-Ph, major), 132.80 (s, *o*-Ph, major), 133.04 (s, *o*-Ph, minor), 134.36 (s, *o*-Ph, minor), 134.48 (s, *o*-Ph, major), 141.72 (s, *i*-Ph, minor), 142.76 (s, *i*-ph, major), 157.2 (s, *i*-Ph, minor) 158.01 (s, *i*-Ph, major), 256.44 (s, η^2-*C*≡NPh, $^{2}J_{C\text{-}P}$ = 13.5 Hz).

NMR reaction of (^{t}BuN)Mo(H)(SiH$_2$Ph){(μ-^{t}BuN)(SiHPh)$_2$}(PMe$_3$)$_2$ and Benzonitrile

(^{t}BuN)Mo(H)(SiH$_2$Ph){(μ-^{t}BuN)(SiHPh)$_2$}(PMe$_3$)$_2$ (18.1 mg, 0.0254 mmol) was dissolved in C_6D_6 and placed in an NMR tube. PhCN (2.62 μL, 0.0254 mmol) was added *via* 10 μL syringe and the solution allowed to react . After 3 days at room temperature the colour changed to a vibrant dark blue colour and generation of the benzonitrile complex (^{t}BuN=)Mo{η^2-SiHPh-N^{t}Bu-SiHPh-N=C(Ph)}(PMe$_3$)$_2$ (**III-61**) was observed according to NMR in a 4:1 ratio with a minor isomer.

Synthesis of (^{t}BuN=)Mo{η^2-SiHPh-N^{t}Bu-SiHPh-N=C(Ph)}(PMe$_3$)$_2$ (III-61)

(^{t}BuN)Mo(H)(SiH$_2$Ph){(μ-^{t}BuN)(SiHPh)$_2$}(PMe$_3$)$_2$ (326.0 mg, 0.459 mmol) was placed in a Schlenk flask and dissolved in toluene (10 mL). Benzonitrile (47.2 μL, 0.0459 mmol) was directly added to this and stirred for three days. After this time the flask was removed of all volatiles in vacuum and hexanes (5 mL) were added then placed in the -30 °C freezer overnight. After this time, dark blue precipitate was observed and the solution was cold filtered, then washed with 5 mL of cold hexane to leaving a dark blue powder. The product was then dried in vacuum and isolated in the glove box. Yield: 241.0 mg, 70%.

^{1}H-NMR (600 MHz, Benzene-d_6, 22 °C, δ, ppm): 0.37 (d, 9H, P*Me*$_3$, $^2J_{H-P}$ = 7.0 Hz, minor), 0.57 (d, 9H, P*Me*$_3$, $^2J_{H-P}$ = 6.7 Hz, minor), 1.06 (d, 9H, P*Me*$_3$, $^2J_{H-P}$ = 6.7 Hz, major), 1.11 (d, 9H, P*Me*$_3$, $^2J_{H-P}$ = 6.9 Hz, minor), 1.34 (s, 9H, ^{t}*Bu*N, major) , 1.35 (s, 9H, ^{t}*Bu*N, minor), 1.77 (s, 9H, ^{t}*Bu*N, major and minor), 6.42 (bq, 1H, Si*H*, $^3J_{H-P}$ = 1.5 Hz, minor), 6.43 (d, 1H, Si*H*, $^3J_{H-P}$ = 1.5 Hz, major), 7.03 (m, Si*H*, found by ^{1}H-^{29}Si HSQC, major), 7.10 (m, Si*H*, found by ^{1}H-^{29}Si HSQC, minor), 7.15 (*m*-Ph or *p*-Ph, η^2-N≡C*Ph*, found by ^{1}H-^{13}C HSQC, major), 7.20 (m, 4H, *p*-Ph, SiH*Ph*, major), 7.25 (t, 2 H, *m*-Ph, η^2-N≡C*Ph*, $^3J_{H-H}$ = 7.7 Hz), 7.33 (t, 2H, *m*-Ph, SiH*Ph*, $^3J_{H-H}$ = 7.5 Hz), 7.40 (t, 2 H, *m*-Ph, SiH*Ph*, $^3J_{H-H}$ = 7.5 Hz, major), 7.98 (d, 2H, *o*-Ph, η^2-N≡C*Ph*, $^3J_{H-}$

$_H$ = 7.0 Hz, major), 8.02 (d, 2H, *o*-Ph, SiH*Ph*, $^3J_{H-H}$ = 6.7 Hz, minor), 8.14 (d, 2H, *o*-Ph, SiH*Ph*, $^3J_{H-H}$ = 6.7 Hz, minor), 8.27 (d, 2H, *o*-Ph, SiH*Ph*, $^3J_{H-H}$ = 6.7 Hz, major), 8.33 (d, 2H, *o*-Ph, SiH*Ph*, $^3J_{H-H}$ = 6.7 Hz, major). **^{1}H{^{31}P}-NMR** (600 MHz, Benzene-d_6, 22 °C, δ, ppm, selected signals): 6.42 (bs, 1H, Si*H*, minor), 6.43 (bs, 1H, Si*H*, major). **^{31}P{^{1}H}-NMR** (243.0 MHz, Benzene-d_6, 22 °C, δ, ppm): -2.02 (d, 1 P, *P*Me$_3$, $^2J_{P-P}$ = 232.1 Hz, major), -4.12 (d, 1 P, *P*Me$_3$, $^2J_{P-P}$ = 229.5 Hz, minor), -6.25 (d, 1 P, *P*Me$_3$, $^2J_{P-P}$ = 232.1 Hz, major), -6.49 (d, 1 P, *P*Me$_3$, $^2J_{P-P}$ = 229.5 Hz, minor). **^{29}Si INEPT+** (119 MHz, Benzene-d_6, 22 °C, J = 150 Hz, δ, ppm): 37.51 (bd, *Si*HPh, $^1J_{Si-H}$ = 156.8 Hz, minor), 36.28 (bd, *Si*HPh, $^1J_{Si-H}$ = 154.6 Hz, major), -24.89 (bd, *Si*HPh, $^1J_{Si-H}$ = 210.0 Hz, major), -24.98 (bd, *Si*HPh, $^1J_{Si-H}$ = 216.5 Hz, minor). **^{13}C{^{1}H} NMR** (151.0 MHz; Benzene-d_6, 22 °C; δ, ppm): 18.06 (d, P*Me*$_3$, $^1J_{C-P}$ = 19.3 Hz, major), 18.08 (d, P*Me*$_3$, $^1J_{C-P}$ = 18.2 Hz, minor), 18.52 (d, P*Me*$_3$, $^1J_{C-P}$ = 19.0 Hz, major), 18.71 (d, P*Me*$_3$, $^1J_{C-P}$ = 18.9 Hz, minor), 33.80 (s, *C*H$_3$, ^{t}*Bu*N, minor), 33.81 (s, *C*H$_3$, ^{t}*Bu*N, major), 33.96 (s, *C*H$_3$, ^{t}*Bu*N, major), 34.27 (s, *C*H$_3$, ^{t}*Bu*N, minor), 54.81 (s, *C*, ^{t}*Bu*N, minor), 54.87 (s, *C*, ^{t}*Bu*N, major), 56.26 (s, *C*, ^{t}*Bu*N, minor), 65.68 (s, *C*, ^{t}*Bu*N, minor), 125.82, 125.87 (*o*-Ph, SiH*Ph*, major), 127.46, 127.81, 128.87 (*m*-Ph, η^2-C≡N*Ph*, SiH*Ph*, major), 130.35, 133.20, 134.67 (*o*-Ph, η^2-C≡N*Ph*, SiH*Ph*, major), 130.65, 132.84, 134.90 (*o*-Ph, η^2-C≡N*Ph*, SiH*Ph*, minor). 156.68 (*i*-Ph, SiH*Ph*, major), 157.46 (*i*-Ph, SiH*Ph*, major), 258.32 (s, η^2-*C*≡NPh, $^2J_{C-P}$ = 13.1 Hz).

NMR reaction of (^{t}BuN)Mo(H)(SiH$_2$Ph){(μ-^{t}BuN)(SiHPh)$_2$}(PMe$_3$)$_2$ and 4-Methoxybenzonitrile

(^{t}BuN)Mo(H)(SiH$_2$Ph){(μ-^{t}BuN)(SiHPh)$_2$}(PMe$_3$)$_2$ (25.0 mg, 0.0352 mmol) and 4-MeO-PhCN (4.7g, 0.0352 mmol) were dissolved in C_6D_6 in a small separate vials in the glove box. The nitrile solution was added directly to the Mo complex and transferred to an NMR tube where and was added *via* 10 μL syringe and the solution allowed to react. After 3 days at room temperature the colour changed to a vibrant dark blue colour and generation of the benzonitrile complex

(^{t}BuN=)Mo{η^2-SiHPh-N^{t}Bu-SiHPh-N=C(*p*-OMe-Ph)}(PMe_3)$_2$ (**III-62**) was observed according to NMR in a 4:1 ratio with a minor isomer.

Synthesis of (^{t}BuN)Mo{(μ-^{t}BuN)(SiHPh)$_2$}(η^2-N≡C(*p*-OMe-Ph))(PMe_3)$_2$ (III-62)

A solution of (^{t}BuN)Mo(H)(SiH_2Ph){(μ-^{t}BuN)($SiHPh)_2$}(PMe_3)$_2$ (379.0 mg, 0.533 mmol) in benzene (40 mL) was placed in a Schlenk flask. A separate solution of 4-methoxybenzonitrile (71.0 mg, 0.533 mmol) in benzene (10 mL) was directly added to the Mo solution where a colour change was seen to dark purple after stirring one night at room temperature. All volatiles were removed in vacuum and hexanes added (5 mL), then placed in the -30 °C freezer overnight. After this time dark purple powder was observed and was filtered and dried to give 164.3 mg of the (^{t}BuN=)Mo{η^2-SiHPh-N^{t}Bu-SiHPh-N=C(*p*-OMe-Ph)}(PMe_3)$_2$ (**III-62**). Yield: 42 %.

^{1}H-NMR (600 MHz, Benzene-d_6, 22 °C, δ, ppm): 0.42 (d, 9H, P*Me*$_3$, $^2J_{H\text{-}P}$ = 6.9 Hz, major), 0.64 (d, 9H, P*Me*$_3$, $^2J_{H\text{-}P}$ = 6.5 Hz, minor), 1.12 (d, 9H, P*Me*$_3$, $^2J_{H\text{-}P}$ = 7.0 Hz, major), 1.16 (d, 9H, P*Me*$_3$, $^2J_{H\text{-}P}$ = 6.8 Hz, minor), 1.36 (s, 9H, ^{t}*Bu*N, major), 1.37 (s, 9H, ^{t}*Bu*N, minor), 1.66 (s, 9H, ^{t}*Bu*N, minor), 1.68 (s, 9H, ^{t}*Bu*N, major), 3.07 (s, 3H, C*H*$_3$, η^2-N≡C(*p*-O*Me*-Ph), minor), 3.22 (s, 3H, C*H*$_3$, η^2-N≡C(*p*-O*Me*-Ph), major), 6.42 (bq, 1H, Si*H*Ph, $^3J_{H\text{-}P}$ = 1.9 Hz, minor), 6.45 (d, 1H, Si*H*Ph, $^3J_{H\text{-}P}$ = 2.9 Hz, major), 6.62 (d, 2H, *m*-Ph, η^2-N≡C(*p*-OMe-*Ph*), $^3J_{H\text{-}H}$ = 8.8 Hz, minor), 6.81 (d, 2H, *m*-Ph, η^2-N≡C(*p*-OMe-*Ph*), $^3J_{H\text{-}H}$ = 8.8 Hz, major), 7.08 (dd, 1H, Si*H*Ph, $^3J_{H\text{-}P}$ = 8.2 Hz, $^3J_{H\text{-}P}$ = 2.9 Hz, major), 7.22 (quart, 2 H, *p*-Ph, SiH*Ph*, $^3J_{H\text{-}H}$ = 7.4 Hz, major), 7.36 (t, 2H, *m*-Ph, SiH*Ph*, $^3J_{H\text{-}H}$ = 7.6 Hz, major), 7.43 (t, 2H, *m*-Ph, SiH*Ph*, $^3J_{H\text{-}H}$ = 7.6 Hz, major), 7.55 (d, 2H, *o*-Ph, η^2-N≡C(*p*-OMe-*Ph*), $^3J_{H\text{-}H}$ = 7.8 Hz, minor), 7.95 (d, 2H, *m*-Ph, η^2-N≡C(*p*-OMe-*Ph*), $^3J_{H\text{-}H}$ = 8.6 Hz, major), 8.05 (d, 2H, *o*-Ph, SiH*Ph*, $^3J_{H\text{-}H}$ = 8.0 Hz, minor), 8.18 (d, 2H, *o*-Ph, SiH*Ph*, $^3J_{H\text{-}H}$ = 7.8 Hz, minor), 8.31 (d, *o*-Ph, SiH*Ph*, $^3J_{H\text{-}H}$ = 7.6 Hz, major), 8.36 (d, *o*-Ph, SiH*Ph*, $^3J_{H\text{-}H}$ = 7.6 Hz, major). **^{1}H{^{31}P}-NMR** (600 MHz, Benzene-d_6, 22 °C, δ, ppm, selected signals): 6.42

(bs, 1H, Si*H*Ph, minor), 6.45 (bs, 1H, Si*H*Ph, major), 7.08 (bs, 1H, Si*H*Ph). **^{31}P{^{1}H}-NMR** (243.0 MHz, Benzene-d_6, 22 °C, δ, ppm): -1.45 (d, 1 P, *P*Me$_3$, $^2J_{P\text{-}P}$ = 234.9 Hz, major), -3.63 (d, 1 P, *P*Me$_3$, $^2J_{P\text{-}P}$ = 228.3 Hz, minor), -5.75 (d, 1 P, *P*Me$_3$, $^2J_{P\text{-}P}$ = 235.6 Hz, major), -5.98 (d, 1 P, *P*Me$_3$, $^2J_{P\text{-}P}$ = 233.1 Hz, minor). **^{29}Si INEPT+** (119 MHz, Benzene-d_6, 22 °C, J = 150 Hz, δ, ppm): 37..93 (bd, *Si*HPh, $^1J_{Si\text{-}H}$ = 163.6 Hz, minor), 36.68 (bd, *Si*HPh, $^1J_{Si\text{-}H}$ = 154.0 Hz, major), -25.24 (bd, *Si*HPh, $^1J_{Si\text{-}H}$ = 209.3 Hz, major), -25.41 (bd, *Si*HPh, $^1J_{Si\text{-}H}$ = 221.6 Hz, minor). **^{13}C{^{1}H} NMR** (151.0 MHz; Benzene-d_6, 22 °C; δ, ppm): 18.18 (d, P*Me*$_3$, $^1J_{C\text{-}P}$ = 18.7 Hz, major), 18.21 (d, P*Me*$_3$, $^1J_{C\text{-}P}$ = 18.4 Hz, minor), 18.62 (d, P*Me*$_3$, $^1J_{C\text{-}P}$ = 18.7 Hz, major), 18.89 (d, P*Me*$_3$, $^1J_{C\text{-}P}$ = 18.7 Hz, minor), 33.84 (s, *C*H$_3$, ^{t}*Bu*N, minor), 33.85 (s, *C*H$_3$, ^{t}*Bu*N, major), 33.96 (s, *C*H$_3$, ^{t}*Bu*N, major), 34.27 (s, *C*H$_3$, ^{t}*Bu*N, minor), , 54.49 (s, *C*H$_3$, η^2-N≡C(*p*-O*Me*-Ph), minor), 54.65 (s, *C*H$_3$, η^2-N=C(*p*-O*Me*-Ph), major), 54.78 (s, *C*, ^{t}*Bu*N, minor), 54.84 (s, *C*, ^{t}*Bu*N, major), 65.48 (s, *C*, ^{t}*Bu*N, major and minor), 113.91 (s, *m*-Ph, η^2-N=C(*p*-OMe-*Ph*), minor), 114.14 (s, *m*-Ph, η^2-N≡C(*p*-OMe-*Ph*), major), 125.80 (s, *p*-Ph, SiH*Ph*, major), 127.47 (s, *m*-Ph, SiH*Ph*, major), 127.90 (s, *m*-Ph, SiH*Ph*, major), 132.22 (s, *o*-Ph, η^2-N≡C(*p*-OMe-*Ph*), major), 132.87 (s, *o*-Ph, SiH*Ph*, minor), 133.22 (s, *o*-Ph, SiH*Ph*, major), 134.66 (s, *o*-Ph, SiH*Ph*, major), 134.92 (s, *o*-Ph, SiH*Ph*, minor), 142.41 (s, *i*-Ph, SiH*Ph*, major), 157.07 (s, *i*-Ph, SiH*Ph*, major), 161.09 (s, *i*-Ph, η^2-N≡C(*p*-OMe-*Ph*), major), 260.12 (s, η^2-*C*≡NPh, $^2J_{C\text{-}P}$ = 12.5 Hz)

NMR reaction of (^{t}BuN)Mo(PMe$_3$)(η^2-C$_2$H$_4$) with Benzonitrile, PhSiH$_3$ and PMe$_3$

PhCN (6.26 μL, 0.0608 mmol) and PhSiH$_3$ (7.49 μL, 0.0608 mmol) were sequentially added to a small vial containing (^{t}BuN)$_2$Mo(PMe$_3$)(η^2-C$_2$H$_4$) (20.8 mg, 0.0608 mmol) dissolved in C$_6$D$_6$ in the glove box. The solution was quickly transferred to an NMR tube and PMe$_3$ (6.29 μL, 0.608 mmol) added on Schlenk line. This was allowed to react for 1.5 hours where clean conversion to (^{t}BuN)Mo(N(^{t}Bu)SiH$_2$Ph)(PMe$_3$)(Et)(η^2-N≡CPh) (**III-63**). After 3 hours conversion to the

(^{t}BuN=)Mo{η^2-SiHPh-N^{t}Bu-SiHPh-N=C(Ph)}(PMe_3)$_2$ (**III-61**) product was observed along with decomposition products.

(^{t}BuN)Mo(N(^{t}Bu)SiH$_2$Ph)(PMe$_3$)(Et)(N≡CPh): **^{1}H-NMR** (600 MHz; Benzene-d_6; δ, ppm): 1.00 (d, $^2J_{P\text{-}H}$ = 12.42 Hz, 9H, PMe_3), 1.15 (s, 9H, ^{t}*Bu*N=Mo), 1.50 (s, 9H, ^{t}*Bu*N-SiMe_2Ph), 2.20 (t, 3H, $^3J_{H\text{-}H}$ = 7.47 Hz, CH_3, Et), 2.52 (m, 2H, CH_2, Et), 5.98 (d, 2H, $^4J_{H\text{-}P}$ = 1.8 Hz, Si*H$_2$*), 7.06 (bt, 1H, $^3J_{H\text{-}H}$ = 7.77 Hz, *p-Ph*-Si), 7.06 (bt, 1H, $^3J_{H\text{-}H}$ = 7.77 Hz, *p-Ph*-CN), 7.19 (d, $^3J_{H\text{-}H}$ = 7.38 Hz, *m-Ph*-Si), 7.90 (d, $^3J_{H\text{-}H}$ = 6.36 Hz, *o-Ph*-Si), 7.98 (d, $^3J_{H\text{-}H}$ = 7.98 Hz, *o-Ph*-CN).

^{13}C NMR (151 MHz; Benzene-d_6; δ, ppm): 11.42 (d, $^2J_{C\text{-}P}$ = 53.5 Hz, PMe_3), 20.51 (s, CH_2, Et), 22.97 (s, CH_3, Et) 32.05 (s, 3 Me, ^{t}BuN=Mo), 33.72 (s, 3 Me, ^{t}*Bu*N-SiH_2Ph), 49.15 (s, Ph*C*≡N), 64.6 (s, Mo=N*C*$(Me)_3$), 65.8 (s, SiN*C*$(Me)_3$) 126.76 (s, *o*-Ph-CN), 124.08 (s, *p*-Ph-CN), 127.83 (s, *p*-Ph-Si), 129.23 (s, *m*-Ph-Si), 135.28 (s, *o*-Ph-Si), 138.57 (s, *i*-Ph-Si). **^{31}P{^{1}H}-NMR** (243.0 MHz; Benzene-d_6 ; δ, ppm): 20.9 (s, PMe_3). **^{29}Si INEPT + NMR** (119.2 MHz; Benzene-d_6; *J* = 200 Hz, δ, ppm): -37.8 (tt, $^1J_{Si\text{-}H}$ = 199.6 Hz, $^3J_{Si\text{-}P}$ = 5.56 Hz, SiH_2Ph).

VI. Appendix

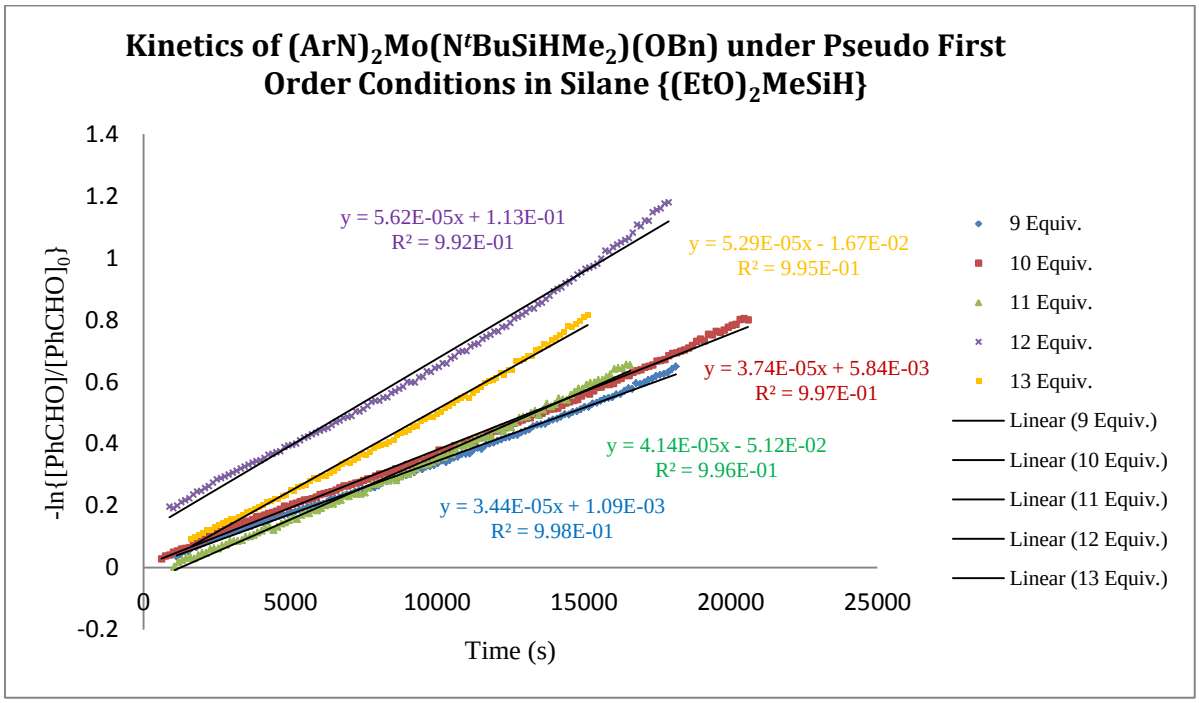

Figure 17 - *ln*{[PhCHO]/[PhCHO]$_0$}/time dependence for reactions of **III-6** with (EtO)$_2$MeSiH under pseudo 1st order conditions using excess silane.

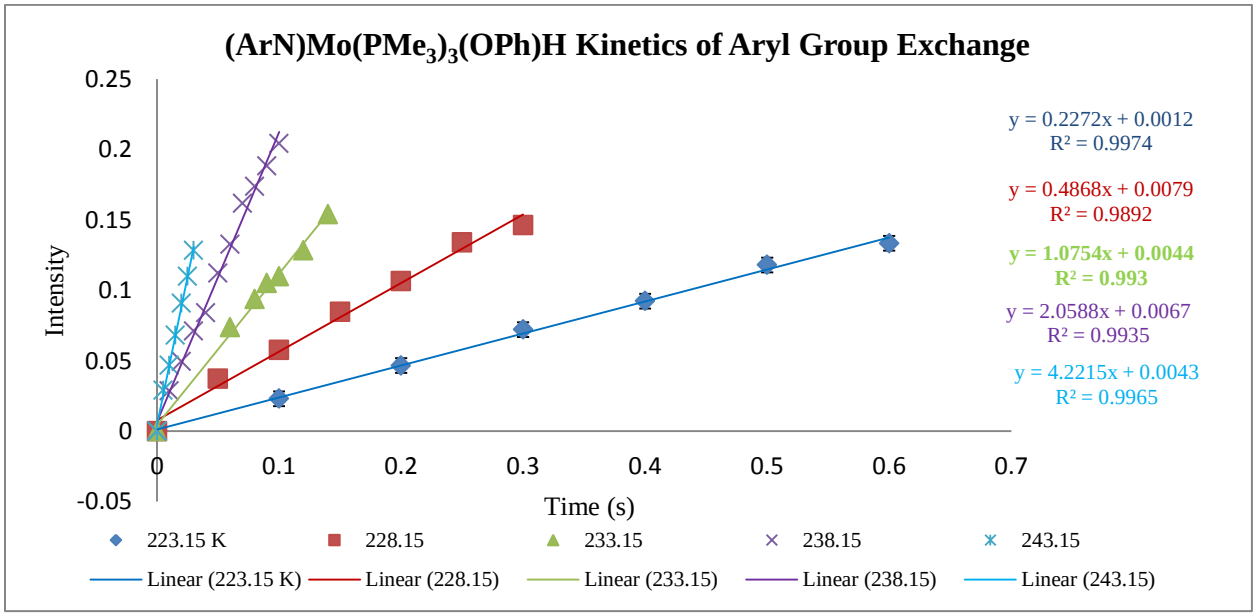

Figure 18 – Intensity vs. Time (s) plot for the exchange between isopropyl methines for complex **III-27** determined by 1D-EXSY NMR.

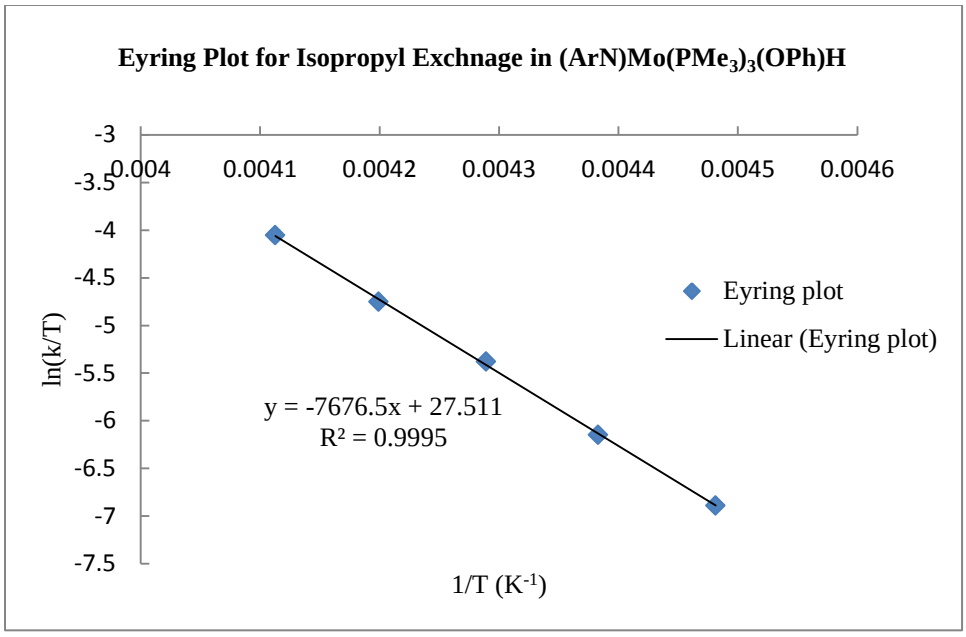

Figure 19 – Eyring Plot for exchange between isopropyl methines in complex **III-27**.

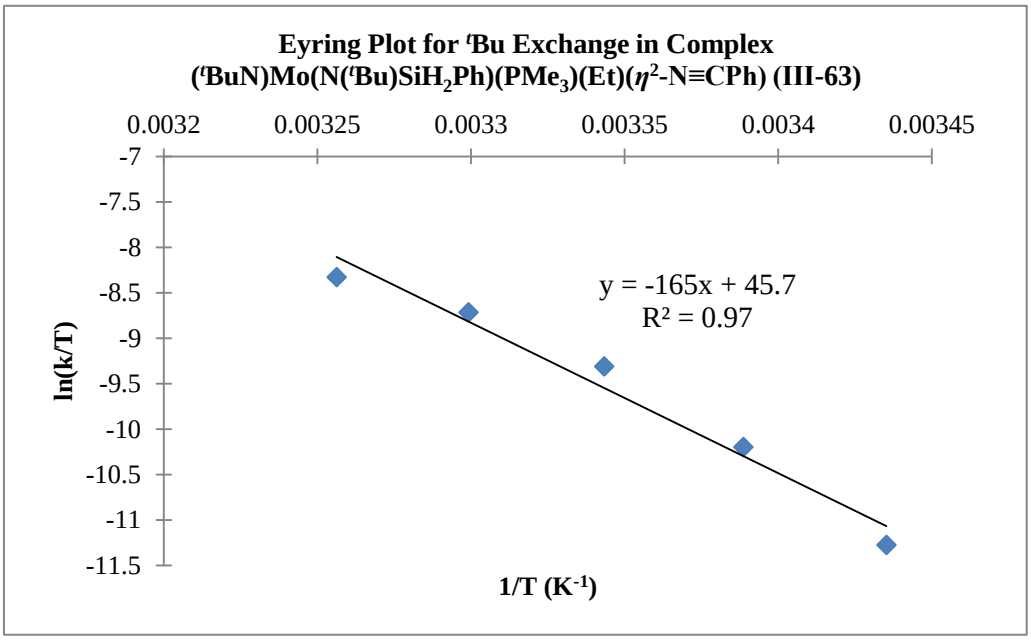

Figure 20 – Eyring Plot for the ^{t}Bu exchange between imido groups in complex **III-63**.

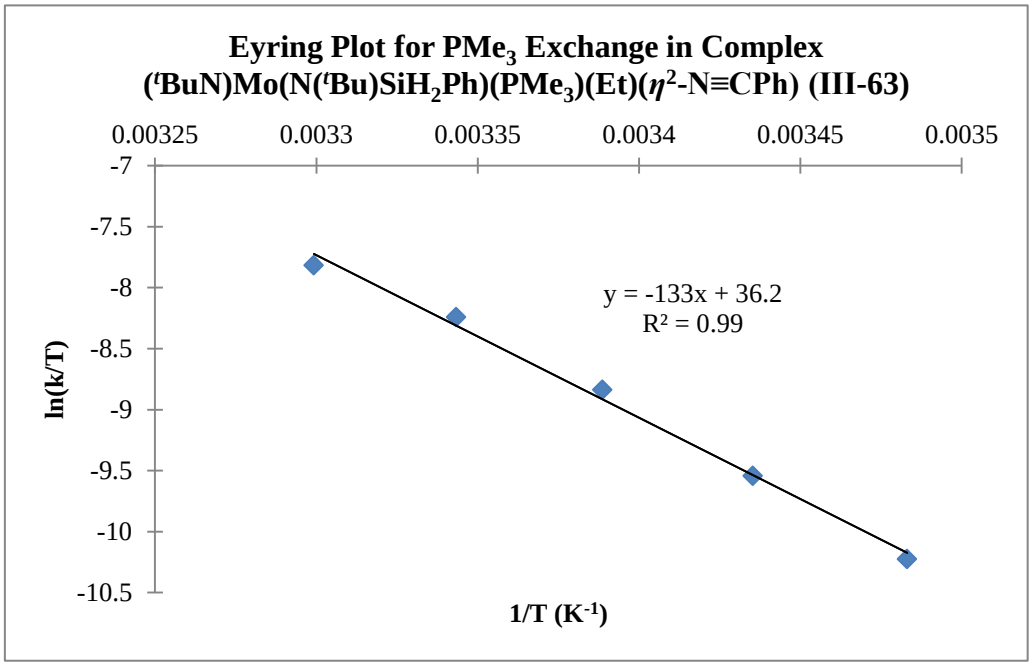

Figure 21- Eyring Plot for the PMe_3 exchange between free and coordinated phsophine in complex **III-63**.

Table 6 - Crystal structure determination parameters for **III-30**.

Empirical formula	C84 H110 Mo2 N2 P8	
Formula weight	1587.37	
Temperature	200(2) K	
Wavelength	0.71073 Å	
Crystal system	Triclinic	
Space group	P -1	
Unit cell dimensions	a = 12.9821(10) Å	α = 105.676(4)°.
	b = 16.4559(14) Å	β = 103.090(4)°.
	c = 20.8367(15) Å	γ = 90.836(5)°.
Volume	4160.8(6) $Å^3$	
Z	2	
Density (calculated)	1.267 Mg/m^3	
Absorption coefficient	0.498 mm^{-1}	
F(000)	1664	
Crystal size	0.180 x 0.100 x 0.080 mm^3	
Theta range for data collection	1.874 to 24.713°.	
Index ranges	-15<=h<=14, -19<=k<=18, 0<=l<=24	
Reflections collected	35024	
Independent reflections	13890	
Completeness to theta = 25.242°	91.6 %	
Absorption correction	Semi-empirical from equivalents	
Max. and min. transmission	0.745688 and 0.551553	
Refinement method	Full-matrix least-squares on F^2	
Data / restraints / parameters	13890 / 518 / 926	
Goodness-of-fit on F^2	1.026	
Final R indices [I>2sigma(I)]	R1 = 0.0800, wR2 = 0.1853	
R indices (all data)	R1 = 0.1395, wR2 = 0.2247	
Largest diff. peak and hole	1.480 and -1.167 $e.Å^{-3}$	

Table 7 - Crystal structure determination parameters for **III-39**.

Empirical Formula	$C_{23}H_{50}MoNOP_3$
Formula Weight	547.22
Temperature, K	200(2)
Wavelength, Å	0.71073
Crystal System	Orthorhombic
Space Group	Pnma
Volume, $Å^3$	3079.48
Unit cell dimensions	a = 16.161(3) Å α = 90.00 °
	b = 13.814(2) Å β = 90.00 °
	c = 13.794(2) Å γ = 90.00 °
Z	4
Calculated Density, g/cm^3	0.618
Absorption coefficient, mm^{-1}	0.274
F(000)	630
Crystal Size	0.19 x 0.15 x 0.12
Radiation, (lambda, Å)	Graphite MoK/a
Theta Range, deg	1.94 to 28.30
Limiting indicies	$-21 \leq h \leq 20$, $-18 \leq k \leq 18$, $-18 \leq l \leq 18$
Reflections collected/unique	36605/3971
Completeness to theta = 28.30 °	99.6 %
Reflections with I>2sigma(I)	3663
Min. and Max. transmission	0.9498 and 0.9679
Solution Method	Direct method (SHELXS-97)
Refinement method	Full-matrix least-squares on F^2 (SHELXS-97)
Data/restraints/parameters	3971/0/157
Goodness-of-fit on F^2	1.095
Final R indicies [I>2sigma(I)]	R1 = 0.0213, wR2 = 0.0554
R indices (all data)	R1 = 0.0245. wR2 = 0.0579
Largest diff. peak and hole, $e/Å^3$	0.298 and -0.339

VII. References

(1) Kubas, G. J. In *Metal Dihydrogen and σ-Bond Complexes*; Springer US: 2001, p 17.
(2) Corey, J. Y. *Chem. Rev.* **2011**, *111*, 863.
(3) Nikonov, G. I. In *Advances in Organometallic Chemistry*; Robert West, A. F. H., Stone, F. G. A., Eds.; Academic Press: 2005; Vol. Volume 53, p 217.
(4) Kubas, G. J.; Ryan, R. R.; Swanson, B. I.; Vergamini, P. J.; Wasserman, H. J. *J. Am. Chem. Soc.* **1984**, *106*, 451.
(5) Kubas, G. J. *J. Organomet. Chem.* **2001**, *635*, 37.
(6) Nikonov, G. I. *J. Organomet. Chem.* **2001**, *635*, 24.
(7) Lachaize, S.; Sabo-Etienne, S. *Eur. J. Inorg. Chem.* **2006**, *2006*, 2115.
(8) Procopio, L. J.; Carroll, P. J.; Berry, D. H. *J. Am. Chem. Soc.* **1991**, *113*, 1870.
(9) Nikonov, G. I.; Mountford, P.; Ignatov, S. K.; Green, J. C.; Leech, M. A.; Kuzmina, L. G.; Razuvaev, A. G.; Rees, N. H.; Blake, A. J.; Howard, J. A. K.; Lemenovskii, D. A. *J. Chem. Soc., Dalton Trans.* **2001**, 2903.
(10) Ignatov, S. K.; Rees, N. H.; Dubberley, S. R.; Razuvaev, A. G.; Mountford, P.; Nikonov, G. I. *Chem. Commun.* **2004**, 952.
(11) Ignatov, S. K.; Khalimon, A. Y.; Rees, N. H.; Razuvaev, A. G.; Mountford, P.; Nikonov, G. I. *Inorg. Chem.* **2009**, *48*, 9605.
(12) Khalimon, A. Y.; Simionescu, R.; Kuzmina, L. G.; Howard, J. A. K.; Nikonov, G. I. *Angew. Chem. Int. Ed.* **2008**, *47*, 7701.
(13) Peterson, E.; Khalimon, A. Y.; Simionescu, R.; Kuzmina, L. G.; Howard, J. A. K.; Nikonov, G. I. *J. Am. Chem. Soc.* **2008**, *131*, 908.
(14) Khalimon, A. Y.; Shirobokov, O. G.; Peterson, E.; Simionescu, R.; Kuzmina, L. G.; Howard, J. A. K.; Nikonov, G. I. *Inorg. Chem.* **2012**, *51*, 4300.
(15) Khalimon, A. Y.; Ignatov, S. K.; Okhapkin, A. I.; Simionescu, R.; Kuzmina, L. G.; Howard, J. A. K.; Nikonov, G. I. *Chem. Eur. J.* **2013**, *19*, 8573.
(16) Marciniec, B. *Comprehensive handbook on hydrosilylation*; Pergamon Press, 1992.
(17) Hoyano, J.; Elder, M.; Graham, W. A. G. *J. Am. Chem. Soc.* **1969**, *91*, 4568.
(18) Graham, W. A. G. *J. Organomet. Chem.* **1986**, *300*, 81.
(19) Graham, W. A. G.; Jetz, W. *Inorg. Chem.* **1971**, *10*, 1159.
(20) Schubert, U. In *Advances in Organometallic Chemistry*; Stone, F. G. A., Robert, W., Eds.; Academic Press: 1990; Vol. Volume 30, p 151.
(21) Schubert, U.; Scholz, G.; Müller, J.; Ackermann, K.; Wörle, B.; Stansfield, R. F. D. *J. Organomet. Chem.* **1986**, *306*, 303.
(22) La Placa, S. J.; Hamilton, W. C.; Ibers, J. A.; Davison, A. *Inorg. Chem.* **1969**, *8*, 1928.
(23) Rankin, D. W. H.; Robertson, A. *J. Organomet. Chem.* **1976**, *105*, 331.
(24) Schubert, U.; Ackermann, K.; Woerle, B. *J. Am. Chem. Soc.* **1982**, *104*, 7378.
(25) Colomer, E.; Corriu, R. J. P.; Marzin, C.; Vioux, A. *Inorg. Chem.* **1982**, *21*, 368.
(26) Lichtenberger, D. L.; Rai-Chaudhuri, A. *J. Am. Chem. Soc.* **1989**, *111*, 3583.
(27) Lichtenberger, D. L.; Rai-Chaudhuri, A. *Organometallics* **1990**, *9*, 1686.
(28) Nikonov, G. I. *Organometallics* **2003**, *22*, 1597.
(29) Bent, H. A. *Chem. Rev.* **1961**, *61*, 275.
(30) Sadow, A. D.; Tilley, T. D. *J. Am. Chem. Soc.* **2003**, *125*, 9462.
(31) Burckhardt, U.; Casty, G. L.; Gavenonis, J.; Tilley, T. D. *Organometallics* **2002**, *21*, 3108.

(32) Schubert, U.; Bahr, K.; Müller, J. *J. Organomet. Chem.* **1987**, *327*, 357.
(33) Herrmann, W. A.; Huber, N. W.; Behm, J. *Chem. Ber.* **1992**, *125*, 1405.
(34) Airoldi, C.; Bradley, D. C.; Chudzynska, H.; Hursthouse, M. B.; Malik, K. M. A.; Raithby, P. R. *J. Chem. Soc., Dalton Trans.* **1980**, 2010.
(35) Bradley, D. C.; Chudzynska, H.; Backer-Dirks, J. D. J.; Hursthouse, M. B.; Ibrahim, A. A.; Motevalli, M.; Sullivan, A. C. *Polyhedron* **1990**, *9*, 1423.
(36) Procopio, L. J.; Carroll, P. J.; Berry, D. H. *J. Am. Chem. Soc.* **1994**, *116*, 177.
(37) Herrmann, W. A.; Eppinger, J.; Spiegler, M.; Runte, O.; Anwander, R. *Organometallics* **1997**, *16*, 1813.
(38) Klimpel, M. G.; Görlitzer, H. W.; Tafipolsky, M.; Spiegler, M.; Scherer, W.; Anwander, R. *J. Organomet. Chem.* **2002**, *647*, 236.
(39) Meermann, C.; Gerstberger, G.; Spiegler, M.; Törnroos, K. W.; Anwander, R. *Eur. J. Inorg. Chem.* **2008**, *2008*, 2014.
(40) Nagl, I.; Scherer, W.; Tafipolsky, M.; Anwander, R. *Eur. J. Inorg. Chem.* **1999**, *1999*, 1405.
(41) Speier, J. L.; Webster, J. A.; Barnes, G. H. *J. Am. Chem. Soc.* **1957**, *79*, 974.
(42) Karstedt, B.; Google Patents: 1973.
(43) Ojima, I.; Kogure, T.; Nihonyanagi, M.; Nagai, Y. *Bull. Chem. Soc. Jpn.* **1972**, *45*, 3506.
(44) Ojima, I.; Nihonyanagi, M.; Nagai, Y. *J. Chem. Soc., Chem. Commun.* **1972**, 938a.
(45) Chalk, A. J.; Harrod, J. F. *J. Am. Chem. Soc.* **1965**, *87*, 16.
(46) A. Schroeder, M.; S. Wrighton, M. *J. Organomet. Chem.* **1977**, *128*, 345.
(47) Marciniec, B. *Coord. Chem. Rev.* **2005**, *249*, 2374.
(48) Marciniec, B. *Appl. Organomet. Chem.* **2000**, *14*, 527.
(49) Marciniec, B. In *Hydrosilylation*; Marciniec, B., Ed.; Springer Netherlands: 2009; Vol. 1, p 3.
(50) Zheng, G. Z.; Chan, T. H. *Organometallics* **1995**, *14*, 70.
(51) Carter, M. B.; Schiott, B.; Gutierrez, A.; Buchwald, S. L. *J. Am. Chem. Soc.* **1994**, *116*, 11667.
(52) Yun, J.; Buchwald, S. L. *J. Am. Chem. Soc.* **1999**, *121*, 5640.
(53) Ison, E. A.; Trivedi, E. R.; Corbin, R. A.; Abu-Omar, M. M. *J. Am. Chem. Soc.* **2005**, *127*, 15374.
(54) Bullock, R. M.; Voges, M. H. *J. Am. Chem. Soc.* **2000**, *122*, 12594.
(55) Du, G.; Fanwick, P. E.; Abu-Omar, M. M. *J. Am. Chem. Soc.* **2007**, *129*, 5180.
(56) Dioumaev, V. K.; Bullock, R. M. *Nature* **2000**, *424*, 530.
(57) Junge, K.; Schroder, K.; Beller, M. *Chem. Commun.* **2011**, *47*, 4849.
(58) Chakraborty, S.; Guan, H. *Dalton Trans.* **2010**, *39*, 7427.
(59) Schwarz, G. *Cell. Mol. Life Sci.* **2005**, *62*, 2792.
(60) Keinan, E.; Perez, D. *J. Org. Chem.* **1987**, *52*, 2576.
(61) Frost, C. G.; Hartley, B. C. *Org. Lett.* **2007**, *9*, 4259.
(62) Fuchikami, T.; Ubukata, Y.; Tanaka, Y. *Tetrahedron Lett.* **1991**, *32*, 1199.
(63) Schmidt, T. *Tetrahedron Lett.* **1994**, *35*, 3513.
(64) Fernandes, A. C.; Fernandes, R.; Romao, C. C.; Royo, B. *Chem. Commun.* **2005**, 213.
(65) Costa, P. J.; Romão, C. C.; Fernandes, A. C.; Royo, B.; Reis, P. M.; Calhorda, M. J. *Chem. Eur. J.* **2007**, *13*, 3934.
(66) Drees, M.; Strassner, T. *Inorg. Chem.* **2007**, *46*, 10850.
(67) Fernandes, A. C.; Romão, C. C. *J. Mol. Catal. A-Chem.* **2006**, *253*, 96.

(68) Fernandes, A. C.; Romão, C. C. *Tetrahedron Lett.* **2005**, *46*, 8881.
(69) Fernandes, A. C.; Romão, C. C. *J. Mol. Catal. A-Chem.* **2007**, *272*, 60.
(70) Cabrita, I.; Sousa, S. C. A.; Fernandes, A. C. *Tetrahedron Lett.* **2010**, *51*, 6132.
(71) Nolin, K. A.; Krumper, J. R.; Pluth, M. D.; Bergman, R. G.; Toste, F. D. *J. Am. Chem. Soc.* **2007**, *129*, 14684.
(72) Shirobokov, O. G.; Kuzmina, L. G.; Nikonov, G. I. *J. Am. Chem. Soc.* **2011**, *133*, 6487.
(73) Shirobokov, O. G.; Gorelsky, S. I.; Simionescu, R.; Kuzmina, L. G.; Nikonov, G. I. *Chem. Commun.* **2010**, *46*, 7831.
(74) Albrecht, M. *Chem. Rev.* **2009**, *110*, 576.
(75) Mohr, F.; Privér, S. H.; Bhargava, S. K.; Bennett, M. A. *Coord. Chem. Rev.* **2006**, *250*, 1851.
(76) Shilov, A. E.; Shul'pin, G. B. *Chem. Rev.* **1997**, *97*, 2879.
(77) Herrmann, W. A.; Böhm, V. P. W.; Reisinger, C.-P. *J. Organomet. Chem.* **1999**, *576*, 23.
(78) van der Boom, M. E.; Milstein, D. *Chem. Rev.* **2003**, *103*, 1759.
(79) Bedford, R. B.; Cazin, C. S. J.; Holder, D. *Coord. Chem. Rev.* **2004**, *248*, 2283.
(80) Parshall, G. W. *J. Am. Chem. Soc.* **1968**, *90*, 1669.
(81) Bennett, M. A.; Milner, D. L. *Chem. Commun.* **1967**, 581.
(82) Keim, W. *J. Organomet. Chem.* **1968**, *14*, 179.
(83) Brookhart, M.; Green, M. L. H.; Wong, L.-L. In *Progress in Inorganic Chemistry*; John Wiley & Sons, Inc.: 2007, p 1.
(84) Crabtree, R. H.; Hamilton, D. G. In *Advances in Organometallic Chemistry*; Stone, F. G. A., Robert, W., Eds.; Academic Press: 1988; Vol. Volume 28, p 299.
(85) Chatt, J.; Davidson, J. M. *J. Chem. Soc.* **1965**, 843.
(86) Green, M. L. H.; Parkin, G.; Mingqin, C.; Prout, K. *J. Chem. Soc., Chem. Commun.* **1984**, 1400.
(87) Hajela, S.; Bercaw, J. E. *Organometallics* **1994**, *13*, 1147.
(88) Schore, N. E.; Hope, H. *J. Am. Chem. Soc.* **1980**, *102*, 4251.
(89) Hofmann, P.; Stauffert, P.; Schore, N. E. *Chem. Ber.* **1982**, *115*, 2153.
(90) Choukroun, R.; Gervais, D. *J. Chem. Soc., Chem. Commun.* **1985**, 224.
(91) Blandy, C.; Locke, S. A.; Young, S. J.; Schore, N. E. *J. Am. Chem. Soc.* **1988**, *110*, 7540.
(92) Young, S. J.; Olmstead, M. M.; Knudsen, M. J.; Schore, N. E. *Organometallics* **1985**, *4*, 1432.
(93) Choukroun, R.; Basso-Bert, M.; Gervais, D. *J. Chem. Soc., Chem. Commun.* **1986**, 1317.
(94) Raoult, Y.; Choukroun, R.; Blandy, C. *Organometallics* **1992**, *11*, 2443.
(95) Gibson, V. C.; Grebenik, P. D.; Green, M. L. H. *J. Chem. Soc., Chem. Commun.* **1983**, 1101.
(96) Steinborn, D.; Neumann, O.; Bruhn, C.; Rüffer, T.; Boese, R.; Heinemann, F. W. *Chem. Eur. J.* **1998**, *4*, 2204.
(97) Cloke, F. G. N.; Green, M. L. H. *J. Chem. Soc., Dalton Trans.* **1981**, 1938.
(98) Cloke, F. G. N.; Cox, K. P.; Green, M. L. H.; Bashkin, J.; Prout, K. *J. Chem. Soc., Chem. Commun.* **1982**, 393.
(99) Brookhart, M.; Cox, K.; Cloke, F. G. N.; Green, J. C.; Green, M. L. H.; Hare, P. M.; Bashkin, J.; Derome, A. E.; Grebenik, P. D. *J. Chem. Soc., Dalton Trans.* **1985**, 423.
(100) Rabinovich, D.; Zelman, R.; Parkin, G. *J. Am. Chem. Soc.* **1992**, *114*, 4611.
(101) Sattler, A.; Parkin, G. *Chem. Commun.* **2011**, *47*, 12828.

(102) Green, M. L. H.; Parkin, G.; Chen, M.; Prout, K. *J. Chem. Soc., Dalton Trans.* **1986**, 2227.
(103) Murphy, V. J.; Rabinovich, D.; Hascall, T.; Klooster, W. T.; Koetzle, T. F.; Parkin, G. *J. Am. Chem. Soc.* **1998**, *120*, 4372.
(104) Green, M. L. H.; Parkin, G.; Moynihan, K. J.; Prout, K. *J. Chem. Soc., Chem. Commun.* **1984**, 1540.
(105) Rabinovich, D.; Zelman, R.; Parkin, G. *J. Am. Chem. Soc.* **1990**, *112*, 9632.
(106) Hascall, T.; Murphy, V. J.; Parkin, G. *Organometallics* **1996**, *15*, 3910.
(107) Kelly, B. V.; Tanski, J. M.; Janak, K. E.; Parkin, G. *Organometallics* **2006**, *25*, 5839.
(108) Zhu, G.; Parkin, G. *Inorg. Chem.* **2005**, *44*, 9637.
(109) Buccella, D.; Parkin, G. *J. Am. Chem. Soc.* **2006**, *128*, 16358.
(110) Buccella, D.; Parkin, G. *Chem. Commun.* **2009**, 289.
(111) Sattler, A.; Parkin, G. *J. Am. Chem. Soc.* **2011**, *133*, 3748.
(112) Janak, K. E.; Tanski, J. M.; Churchill, D. G.; Parkin, G. *J. Am. Chem. Soc.* **2002**, *124*, 4182.
(113) Zhu, G.; Pang, K.; Parkin, G. *J. Am. Chem. Soc.* **2008**, *130*, 1564.
(114) Li, J.; Yoshizawa, K. *Chem. Eur. J.* **2012**, *18*, 783.
(115) Miscione, G. P.; Carvajal, M. A.; Bottoni, A. *Organometallics* **2011**, *30*, 4924.
(116) Liu, Y.; Zhang, D.; Gao, J.; Liu, C. *Chem. Eur. J.* **2012**, *18*, 15537.
(117) van der Eide, E. F.; Piers, W. E.; Parvez, M.; McDonald, R. *Inorg. Chem.* **2006**, *46*, 14.
(118) Kuiper, D. S.; Wolczanski, P. T.; Lobkovsky, E. B.; Cundari, T. R. *Inorg. Chem.* **2008**, *47*, 10542.
(119) Baker, R. T.; Calabrese, J. C.; Harlow, R. L.; Williams, I. D. *Organometallics* **1993**, *12*, 830.
(120) Filippou, A. C.; Weidemann, N.; Philippopoulos, A. I.; Schnakenburg, G. *Angew. Chem. Int. Ed.* **2006**, *45*, 5987.
(121) Filippou, A. C.; Weidemann, N.; Schnakenburg, G. *Angew. Chem. Int. Ed.* **2008**, *47*, 5799.
(122) Rathke, J. W.; Muetterties, E. L. *J. Am. Chem. Soc.* **1975**, *97*, 3272.
(123) Karsch, H. H.; Klein, H. F.; Schmidbaur, H. *Angew. Chem., Int. Ed. Engl.* **1975**, *14*, 637.
(124) Karsch, H. H.; Klein, H.-F.; Schmidbaur, H. *Chem. Ber.* **1977**, *110*, 2200.
(125) Karsch, H. H. *Chem. Ber.* **1977**, *110*, 2213.
(126) Jones, W. D.; Foster, G. P.; Putinas, J. M. *Inorg. Chem.* **1987**, *26*, 2120.
(127) Antberg, M. D., Lutz *Z. Naturforsch., B: Chem. Sci.* **1987**, *42*, 435
(128) Werner, H.; Werner, R. *J. Organomet. Chem.* **1981**, *209*, C60.
(129) Werner, H.; Gotzig, J. *Organometallics* **1983**, *2*, 547.
(130) Desrosiers, P. J.; Shinomoto, R. S.; Flood, T. C. *J. Am. Chem. Soc.* **1986**, *108*, 1346.
(131) Field, L. D.; Jurd, P. M.; Magill, A. M.; Bhadbhade, M. M. *Organometallics* **2013**, *32*, 636.
(132) Gotzig, J.; Werner, R.; Werner, H. *J. Organomet. Chem.* **1985**, *290*, 99.
(133) Holland, A. W.; Bergman, R. G. *Organometallics* **2002**, *21*, 2149.
(134) Al-Jibori, S.; Crocker, C.; McDonald, W. S.; Shaw, B. L. *J. Chem. Soc., Dalton Trans.* **1981**, 1572.
(135) Fryzuk, M. D.; Joshi, K.; Chadha, R. K.; Rettig, S. J. *J. Am. Chem. Soc.* **1991**, *113*, 8724.
(136) Arndtsen, B. A.; Bergman, R. G. *Science* **1995**, *270*, 1970.
(137) Hinderling, C.; Plattner, D. A.; Chen, P. *Angew. Chem., Int. Ed. Engl.* **1997**, *36*, 243.

(138) Hinderling, C.; Feichtinger, D.; Plattner, D. A.; Chen, P. *J. Am. Chem. Soc.* **1997**, *119*, 10793.
(139) Luecke, H. F.; Bergman, R. G. *J. Am. Chem. Soc.* **1997**, *119*, 11538.
(140) Niu, S.; Hall, M. B. *J. Am. Chem. Soc.* **1998**, *120*, 6169.
(141) Bresciani, N.; Calligaris, M.; Delise, P.; Nardin, G.; Randaccio, L. *J. Am. Chem. Soc.* **1974**, *96*, 5642.
(142) Bresciani-Pahor, N. *Acta Crystallogr., Sect. B: Struct. Sci.* **1977**, *33*, 3214.
(143) Bresadola, S.; Longato, B.; Morandini, F. *J. Organomet. Chem.* **1977**, *128*, C5.
(144) Bresadola, S.; Bresciani-Pahor, N.; Longato, B. *J. Organomet. Chem.* **1979**, *179*, 73.
(145) van der Sluis, M.; Beverwijk, V.; Termaten, A.; Bickelhaupt, F.; Kooijman, H.; Spek, A. L. *Organometallics* **1999**, *18*, 1402.
(146) Robinson, R.; Clarkson, J. M.; Moody, M. A.; Sharp, P. R. *Organometallics* **2011**, *30*, 1730.
(147) Schrock, R. R.; Murdzek, J. S.; Bazan, G. C.; Robbins, J.; DiMare, M.; O'Regan, M. *J. Am. Chem. Soc.* **1990**, *112*, 3875.
(148) McConville, D. H.; Wolf, J. R.; Schrock, R. R. *J. Am. Chem. Soc.* **1993**, *115*, 4413.
(149) Wigley, D. E. In *Progress in Inorganic Chemistry*; John Wiley & Sons, Inc.: 2007, p 239.
(150) Dyer, P. W.; Gibson, V. C.; Howard, J. A. K.; Whittle, B.; Wilson, C. *J. Chem. Soc., Chem. Commun.* **1992**, 1666.
(151) Dyer, P. W.; Gibson, V. C.; Howard, J. A. K.; Wilson, C. *J. Organomet. Chem.* **1993**, *462*, C15.
(152) Radius, U.; Sundermeyer, J.; Pritzkow, H. *Chem. Ber.* **1994**, *127*, 1827.
(153) Green, M. L. H.; Konidaris, P. C.; Mountford, P.; Simpson, S. J. *J. Chem. Soc., Chem. Commun.* **1992**, 256.
(154) Khalimon, A. Y.; Simionescu, R.; Nikonov, G. I. *J. Am. Chem. Soc.* **2011**, *133*, 7033.
(155) Procopio, L. J.; Carroll, P. J.; Berry, D. H. *Organometallics* **1993**, *12*, 3087.
(156) Marciniec, B. In *Hydrosilylation*; Marciniec, B., Ed.; Springer Netherlands: 2009; Vol. 1, p 289.
(157) Bheeter, L. P.; Henrion, M.; Brelot, L.; Darcel, C.; Chetcuti, M. J.; Sortais, J.-B.; Ritleng, V. *Adv. Synth. Catal.* **2012**, *354*, 2619.
(158) Postigo, L.; Royo, B. *Adv. Synth. Catal.* **2012**, *354*, 2613.
(159) Fontaine, F.-G.; Nguyen, R.-V.; Zargarian, D. *Can. J. Chem.* **2003**, *81*, 1299.
(160) Chakraborty, S.; Krause, J. A.; Guan, H. *Organometallics* **2008**, *28*, 582.
(161) Tran, B. L.; Pink, M.; Mindiola, D. J. *Organometallics* **2009**, *28*, 2234.
(162) Constable, D. J. C.; Dunn, P. J.; Hayler, J. D.; Humphrey, G. R.; Leazer, J. J. L.; Linderman, R. J.; Lorenz, K.; Manley, J.; Pearlman, B. A.; Wells, A.; Zaks, A.; Zhang, T. Y. *Green Chem.* **2007**, *9*, 411.
(163) Nikonov, G. I.; Mountford, P.; Dubberley, S. R. *Inorg. Chem.* **2002**, *42*, 258.
(164) Kennedy-Smith, J. J.; Nolin, K. A.; Gunterman, H. P.; Toste, F. D. *J. Am. Chem. Soc.* **2003**, *125*, 4056.
(165) Cantrell, G. K.; Meyer, T. Y. *Organometallics* **1997**, *16*, 5381.
(166) Cantrell, G. K.; Meyer, T. Y. *J. Am. Chem. Soc.* **1998**, *120*, 8035.
(167) K. Cantrell, G.; Y. Meyer, T. *Chem. Commun.* **1997**, 1551.
(168) Jolly, M.; Mitchell, J. P.; Gibson, V. C. *J. Chem. Soc., Dalton Trans.* **1992**, 1329.
(169) Hartwig, J. F. *Organotransition metal chemistry : from bonding to catalysis / John F. Hartwig*; Sausalito, Calif. : University Science Books, c2010., 2010.

(170) Khalimon, A. Y.; Peterson, E.; Lorber, C.; Kuzmina, L. G.; Howard, J. A. K.; van der Est, A.; Nikonov, G. I. *Eur. J. Inorg. Chem.* **2013**, *2013*, 2205.
(171) Hartwig, J. F. *Organotransition metal chemistry: from bonding to catalysis*; Univ. Science Books, 2010.
(172) Chisholm, M. H.; Hammond, C. E.; Huffman, J. C. *Polyhedron* **1989**, *8*, 1419.
(173) Dyer, P. W.; Gibson, V. C.; Howard, J. A. K.; Whittle, B.; Wilson, C. *Polyhedron* **1995**, *14*, 103.
(174) Templeton, J. L.; Ward, B. C. *J. Am. Chem. Soc.* **1980**, *102*, 3288.
(175) Dixon, J. T.; Green, M. J.; Hess, F. M.; Morgan, D. H. *J. Organomet. Chem.* **2004**, *689*, 3641.
(176) Castro, A.; Galakhov, M. V.; Gómez, M.; Gómez-Sal, P.; Martín, A.; Sánchez, F. *J. Organomet. Chem.* **2000**, *595*, 36.
(177) Cundari, T. R. *J. Am. Chem. Soc.* **1992**, *114*, 7879.
(178) Marinescu, S. C.; Singh, R.; Hock, A. S.; Wampler, K. M.; Schrock, R. R.; Müller, P. *Organometallics* **2008**, *27*, 6570.
(179) Rothwell, I. P. *Accounts Chem. Res.* **1988**, *21*, 153.
(180) Bell, A.; Clegg, W.; Dyer, P. W.; Elsegood, M. R. J.; Gibson, V. C.; Marshall, E. L. *J. Chem. Soc., Chem. Commun.* **1994**, 2247.
(181) Copley, R. C. B.; Dyer, P. W.; Gibson, V. C.; Howard, J. A. K.; Marshall, E. L.; Wang, W.; Whittle, B. *Polyhedron* **1996**, *15*, 3001.
(182) Bell, A.; Clegg, W.; Dyer, P. W.; Elsegood, M. R. J.; Gibson, V. C.; Marshall, E. L. *J. Chem. Soc., Chem. Commun.* **1994**, 2547.
(183) Dyer, P. W.; Gibson, V. C.; Clegg, W. *J. Chem. Soc., Dalton Trans.* **1995**, 3313.
(184) Dubberley, S. R.; Ignatov, S. K.; Rees, N. H.; Razuvaev, A. G.; Mountford, P.; Nikonov, G. I. *J. Am. Chem. Soc.* **2002**, *125*, 642.
(185) Khalimon, A. Y.; Ignatov, S. K.; Simionescu, R.; Kuzmina, L. G.; Howard, J. A. K.; Nikonov, G. I. *Inorg. Chem.* **2011**, *51*, 754.
(186) Khalimon, A. Y. *PhD Thesis* **2011**.
(187) Berry, D. H.; Chey, J.; Zipin, H. S.; Carroll, P. J. *Polyhedron* **1991**, *10*, 1189.
(188) Nikonov, G. I.; Vyboishchikov, S. F.; Kuzmina, L. G.; Howard, J. A. K. *Chem. Commun.* **2002**, 568.
(189) Campion, B. K.; Falk, J.; Tilley, T. D. *J. Am. Chem. Soc.* **1987**, *109*, 2049.
(190) Elsner, F. H.; Tilley, T. D.; Rheingold, A. L.; Geib, S. J. *J. Organomet. Chem.* **1988**, *358*, 169.
(191) Campion, B. K.; Heyn, R. H.; Tilley, T. D. *J. Am. Chem. Soc.* **1990**, *112*, 2011.
(192) Casty, G. L.; Tilley, T. D.; Yap, G. P. A.; Rheingold, A. L. *Organometallics* **1997**, *16*, 4746.
(193) Robert, P.; Le Bozec, H.; Dixneuf, P. H.; Hartstock, F.; Taylor, N. J.; Carty, A. J. *Organometallics* **1982**, *1*, 1148.
(194) Robert, P.; Demerseman, B.; Dixneuf, P. H. *Organometallics* **1984**, *3*, 1771.
(195) Sattler, A.; Parkin, G. *Nature* **2010**, *463*, 523.